DE GRUYTER REFERENCE

Tharwat F. Tadros

HANDBOOK OF COLLOID AND INTERFACE SCIENCE

VOLUME 4: INDUSTRIAL APPLICATIONS: AGROCHEMICALS, PAINTS, COATINGS AND FOOD SYSTEMS

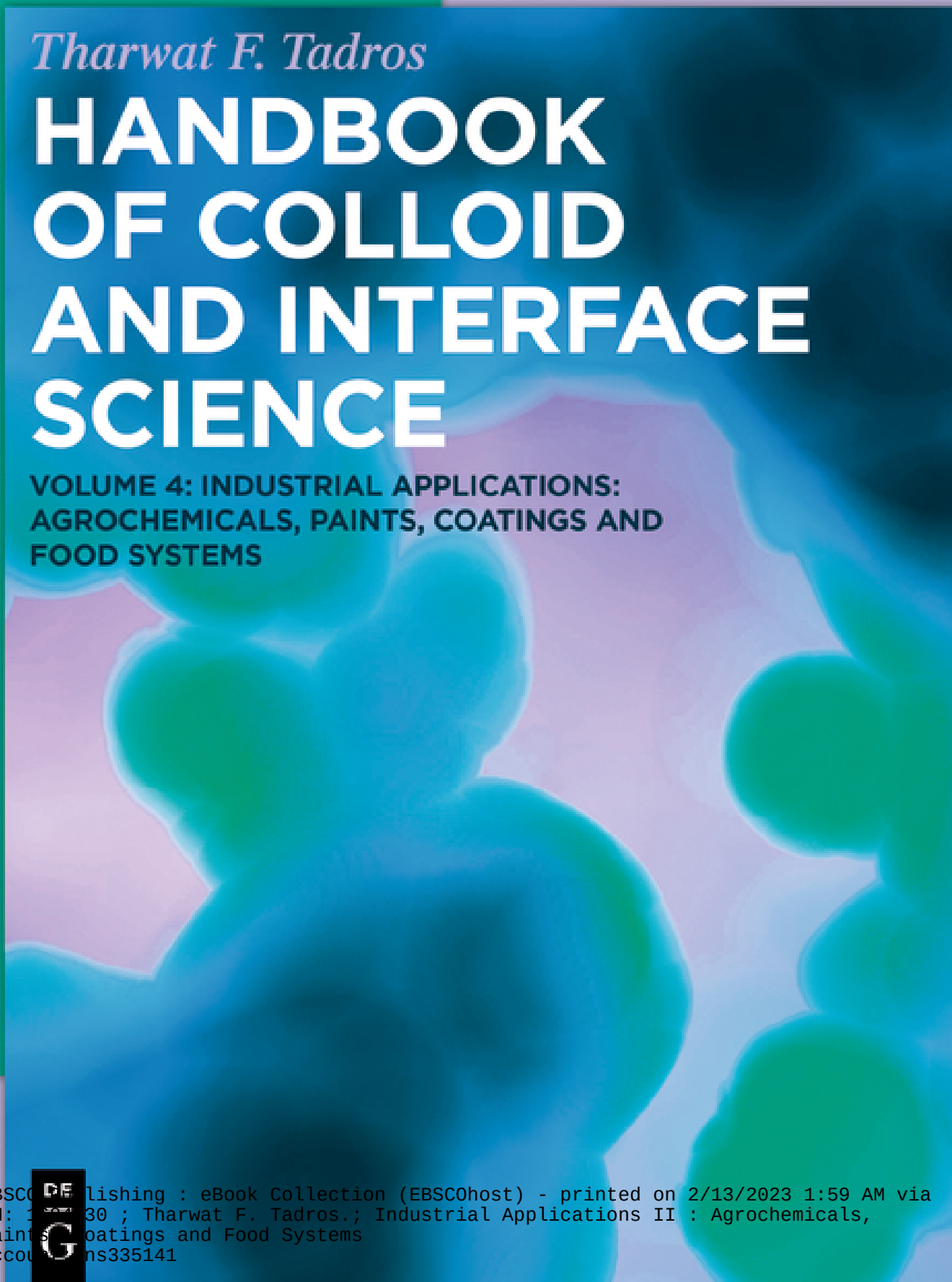

Tharwat F. Tadros

Handbook of Colloid and Interface Science

De Gruyter Reference

Also of Interest

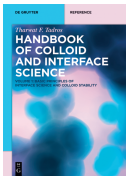

Handbook of Colloid and Interface Science.
Volume 1: Basic Principles of Interface Science and Colloid Stability
Tadros, 2017
ISBN 978-3-11-053990-5, e-ISBN 978-3-11-054089-5

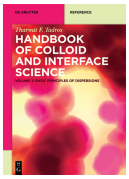

Handbook of Colloid and Interface Science.
Volume 2: Basic Principles of Dispersions
Tadros, 2017
ISBN 978-3-11-053991-2, e-ISBN 978-3-11-054195-3

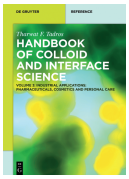

Handbook of Colloid and Interface Science.
Volume 3: Industrial Applications:
Pharmaceuticals, Cosmetics and Personal Care
Tadros, 2017
ISBN 978-3-11-055409-0, e-ISBN 978-3-11-055525-7

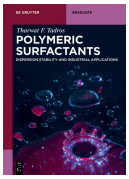

Polymeric Surfactants.
Dispersion Stability and Industrial Applications
Tadros, 2017
ISBN 978-3-11-048722-0, e-ISBN 978-3-11-048728-2

Emulsions.
Formation, Stability, Industrial Applications
Tadros, 2016
ISBN 978-3-11-045217-4, e-ISBN 978-3-11-045224-2

Tharwat F. Tadros

Handbook of Colloid and Interface Science

Volume 4:
Industrial Applications:
Agrochemicals, Paints, Coatings and Food Systems

DE GRUYTER

Author
Prof. Tharwat F. Tadros
89 Nash Grove Lane
Workingham RG40 4HE
Berkshire, UK
tharwattadros3@gmail.com

ISBN 978-3-11-057803-4
e-ISBN (PDF) 978-3-11-057899-7
e-ISBN (EPUB) 978-3-11-057833-1
Set-ISBN 978-3-11-057906-2

Library of Congress Cataloging-in-Publication Data
A CIP catalog record for this book has been applied for at the Library of Congress.

Bibliographic information published by the Deutsche Nationalbibliothek
The Deutsche Nationalbibliothek lists this publication in the Deutsche Nationalbibliografie; detailed bibliographic data are available on the Internet at http://dnb.dnb.de.

Cover image: satori13/iStock/Getty Images Plus
Typesetting: PTP-Berlin, Protago-TEX-Production GmbH, Berlin
Printing and binding: CPI Books GmbH, Leck
♾ Printed on acid-free paper
Printed in Germany

www.degruyter.com

Preface

The field of colloid and interface science plays a major role in most industrial systems. This is particularly the case with most formulations consisting of disperse systems. In all formulations consisting of suspensions, emulsions, foams, gels, etc., the structure of the interfacial region determines their colloidal properties. The topics of colloid and interface science can be conveniently subdivided under two main headings, namely disperse systems and interfacial phenomena. This subdivision does not imply any separation for the following reasons. All disperse systems involve an interface. Many interfacial phenomena are precursors for formation of disperse systems, e.g. nucleation and growth, emulsification, etc. The main objectives of the present handbook, namely Volume 4, are to illustrate how the basic principles that are involved in interfacial phenomena (described in detail in Volumes 1 and 2) are applied in agrochemicals, paints and coatings and food systems. Particular emphasis will be given to the formation of colloidal dispersions and their stabilization. The colloid stability/instability of any disperse system is determined by the property of the interfacial region. In actual fact colloid and interface science are one individual subject.

The field of colloid and interface science has no boundary since chemists, physicists, engineers, biologists, mathematicians can all be engaged in the field. For successful applications in industry, multidisciplinary teams are required. Understanding the basic principles of colloid and interface science will enable industry to develop many complex systems in shorter periods of time. Most colloidal systems used in industry are multiphase and complex formulations. They may contain more than one disperse phase, e.g. suspension/emulsion systems (suspoemulsions).

Three applications of colloid and interface science – in agrochemicals, paints and coating and food systems – are given in this volume. Part I deals with the application of colloid and interface science phenomena in agrochemical formulations. Chapter 1 describes the various surfactants that can be used in agrochemical formulations as well as their solution properties and phase behaviour. Chapter 2 describes the method of preparation of emulsion concentrates (EWs) and the methods that can be applied for selection of the emulsifiers. The major breakdown processes of emulsions are described with the methods that can be applied to stabilize the emulsion against each of these processes. Chapter 3 describes the process of formulation of suspension concentrates (SCs) with particular reference to the role of wetting/dispersing agents. The methods that can be applied for control of the physical stability of SCs are described. Chapter 4 deals with formulation of suspoemulsions (mixtures of suspensions and emulsions) and the various possible interactions between the particles and droplets. The methods that can be applied to reduce homo- and heteroflocculation as well as emulsion coalescence are described. Chapter 6 lists the main advantages for formulating the agrochemical as a microemulsion. The main advantages are the thermodynamic stability of the system as well as the possibility of enhancing its biological

https://doi.org/10.1515/9783110578997-001

efficacy. Chapter 7 describes the various methods that can be applied for controlled release of the active ingredient. These range from the use of microencapsulation as well as the use of grains and granules. Chapter 8 gives a detailed account of the interfacial aspects of agrochemical spray formulations. The processes of droplet impaction and adhesion, wetting and spreading and spray retention are described at a fundamental level. The role of surfactants in penetration of the active ingredient is also described.

Part II describes the application of colloid and interface science in paints and coatings. Chapter 9 gives a general introduction on the main constituents of a paint formulation and the main requirements for application. Chapter 10 deals with the subject of preparation of polymer colloids that are used as film formers, by emulsion and dispersion polymerization. Particular attention is given to the use of polymeric surfactants in both processes. Chapter 11 describes the process of pigment dispersion with particular reference to the role of surfactants in wetting and breaking of segregates. Chapter 12 deals with the process of dispersion of aggregates and agglomerates into single particles, as well as the process of size reduction by bead milling. Chapter 13 describes the flow properties (rheology) of paints. The various methods that can be applied to study the rheology of a paint are described. This is followed by giving some examples of the flow properties of some commercial paints.

Part III discusses the application of colloid and interface science principles in food colloids. Chapter 14 describes the interaction between food-grade surfactants and water, with particular reference to the various liquid crystalline structures produced. Both binary and tertiary phase diagrams are described. Chapter 15 emphasizes the use of proteins as emulsifiers for food products. The structure of proteins and their interfacial properties are described. This is followed by sections on protein-polysaccharide and surfactant-polysaccharide interactions. Chapter 16 gives an account of the surfactant association structures, microemulsions and emulsions in food. Particular attention is paid to the use of lamellar liquid crystalline structures for stabilizing emulsions against coalescence. Chapter 17 describes the flow characteristics (rheology) of food emulsions. Both interfacial and bulk rheological properties are described. Particular attention is given to the correlation of interfacial viscosity and elasticity with emulsion stability. Chapter 18 deals with the application of rheological methods for assessment of mouth feel and texture of food products. Newtonian and non-Newtonian systems as well as microgels are presented in order to describe the correlation of rheological parameters with mouth feel and texture of food products.

This text gives a number of examples illustrating the applications of colloid and interface science principles to agrochemicals, paints and coatings and food systems. The handbook will be valuable for formulation scientists and chemical engineers involved in formulating the above mentioned industrial systems. It can also be valuable for research scientists and postgraduate students involved in these research areas.

Tharwat Tadros — April 2017

Contents

Part I: **Colloid and interface science in agrochemical formulations**

1 Surfactants used in agrochemical formulations and their solution properties

1.1 General classification of surfactants

A simple classification of surfactants based on the nature of the hydrophilic group is commonly used. Three main classes may be distinguished, namely anionic, cationic and amphoteric [1, 2]. A useful technical reference is McCutcheon [3], which is produced annually to update the list of available surfactants. A recent text by van Os et al. [4] listing the physicochemical properties of selected anionic, cationic and nonionic surfactants has been published by Elsevier. Another useful text is the Handbook of Surfactants by Porter [5]. It should also be mentioned that a fourth class of surfactants, usually referred to as polymeric surfactants, has been used for many years for the preparation of EWs (emulsion concentrates) and SCs (suspension concentrates) and their stabilization.

Anionic surfactants are the most widely used class of surfactants in agrochemical applications [5, 6]. This is due to their relatively low cost of manufacture and they are used in practically every type of formulation. Linear chains are preferred since they are more effective and more degradable than the branched chains. The most commonly used hydrophilic groups are carboxylates, sulphates, sulphonates and phosphates. A general formula may be ascribed to anionic surfactants as follows:

- Carboxylates: $C_nH_{2n+1}COO^-X$
- Sulphates: $C_nH_{2n+1}OSO_3^-X$
- Sulphonates: $C_nH_{2n+1}SO_3^-X$
- Phosphates: $C_nH_{2n+1}OPO(OH)O^-X$
  with n being the range 8–16 atoms and the counterion X is usually Na^+.

Several other anionic surfactants are commercially available such as sulphosuccinates, isethionates and taurates and these are sometimes used for special applications.

Carboxylates are perhaps the earliest known surfactants, since they constitute the earliest soaps, e.g. sodium or potassium stearate, $C_{17}H_{35}COONa$, sodium myristate, $C_{14}H_{29}COONa$. The alkyl group may contain unsaturated portions, e.g. sodium oleate, which contains one double bond in the C_{17} alkyl chain. Most commercial soaps will be a mixture of fatty acids obtained from tallow, coconut oil, palm oil, etc. The main attraction of these simple soaps is their low cost, their ready biodegradability and low toxicity. Their main disadvantage is their ready precipitation in water containing bivalent ions such as Ca^{2+} and Mg^{2+}. To avoid their precipitation in hard water, the carboxylates are modified by introducing some hydrophilic chains, e.g. ethoxy carboxylates with the general structure $RO(CH_2CH_2O)_nCH_2COO^-$, ester carboxylates con-

https://doi.org/10.1515/9783110578997-002

taining hydroxyl or multi-COOH groups, sarcosinates which contain an amide group with the general structure $RCON(R')COO^-$.

The addition of the ethoxylated groups results in increased water solubility and enhanced chemical stability (no hydrolysis). The modified ether carboxylates are also more compatible with electrolytes. They are also compatible with other nonionic, amphoteric and sometimes even cationic surfactants. The ester carboxylates are very soluble in water, but they suffer from the problem of hydrolysis. The sarcosinates are not very soluble in acid or neutral solutions but they are quite soluble in alkaline media. They are compatible with other anionics, nonionics and cationics. The phosphate esters have very interesting properties being intermediate between ethoxylated nonionics and sulphated derivatives. Sulphates are the largest and most important class of synthetic surfactants, which were produced by reaction of an alcohol with sulphuric acid, i.e. they are esters of sulphuric acid. In practice sulphuric acid is seldom used and chlorosulphonic or sulphur dioxide/air mixtures are the most common methods of sulphating the alcohol. However, due to their chemical instability (hydrolysing to the alcohol, particularly in acid solutions), they are now overtaken by the sulphonates which are chemically stable.

The properties of sulphate surfactants depend on the nature of the alkyl chain and the sulphate group. The alkali metal salts show good solubility in water, but they tend to be affected by the presence of electrolytes. The most common sulphate surfactant is sodium dodecyl sulphate (abbreviated as SDS and sometimes referred to as sodium lauryl sulphate) which at room temperature ($\approx 25\,°C$) is quite soluble and 30 % aqueous solutions are fairly fluid (low viscosity). However, below 25 °C, the surfactant may separate out as a soft paste as the temperature falls below its Krafft point (the temperature above which the surfactant shows a rapid increase in solubility with further increase of temperature). The latter depends on the distribution of chain lengths in the alkyl chain, the wider the distribution the lower the Krafft temperature. Thus, by controlling this distribution one may achieve a Krafft temperature of $\approx 10\,°C$. As the surfactant concentration is increased to 30–40 % (depending on the distribution of chain length in the alkyl group), the viscosity of the solution increases very rapidly and may produce a gel. The critical micelle concentration (cmc) of SDS (the concentration above which the properties of the solution show abrupt changes) is 8×10^{-3} mol dm^{-3} (0.24 %).

As with the carboxylates, the sulphate surfactants are also chemically modified to change their properties. The most common modification is to introduce some ethylene oxide units in the chain, usually referred to as alcohol ether sulphates. For example, sodium dodecyl 3-mole ether sulphate, which is essentially dodecyl alcohol reacted with 3 mol EO, is sulphated and neutralized by NaOH. The presence of PEO confers improved solubility when compared with the straight alcohol sulphates. In addition, the surfactant becomes more compatible with electrolytes in aqueous solution. The ether sulphates are also more chemically stable than the alcohol sulphates. The cmc of the ether sulphates is also lower than the corresponding surfactant without the EO units.

With sulphonates, the sulphur atom is directly attached to the carbon atom of the alkyl group and this gives the molecule stability against hydrolysis, when compared with the sulphates (where the sulphur atom is indirectly linked to the carbon of the hydrophobe via an oxygen atom). The alkyl aryl sulphonates are the most common type of these surfactants (for example sodium alkyl benzene sulphonate) and these are usually prepared by reaction of sulphuric acid with alkyl aryl hydrocarbons, e.g. dodecyl benzene. A special class of sulphonate surfactants are the naphthalene and alkyl naphthalene sulphonates, which are commonly used as dispersants for SCs.

As with the sulphates, some chemical modification is achieved by introducing ethylene oxide units, e.g. sodium nonyl phenol 2-mole ethoxylate ethane sulphonate $C_9H_{19}C_6H_4(OCH_2CH_2)_2SO_3^-Na^+$.

The linear alkyl benzene sulphonates (LABS) are manufactured from alkyl benzene and the alkyl chain length can vary from C_8 to C_{15} and their properties are mainly influenced by the average molecular weight and the spread of carbon number of the alkyl side chain. The cmc of sodium dodecyl benzene sulphonate is 5×10^{-3} mol dm^{-3} (0.18 %).

Another class of sulphonates is the α-olefin sulphonates which are prepared by reacting linear α-olefin with sulphur trioxide, typically yielding a mixture of alkene sulphonates (60–70 %), 3- and 4-hydroxyalkane sulphonates (≈ 30 %) and some disulphonates and other species. The two main α-olefin fractions used as starting material are C_{12}–C_{16} and C_{16}–C_{18}.

A special class of sulphonates are sulphosuccinates which are esters of sulphosuccinic acid,

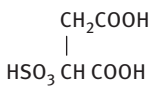

Both mono- and diesters are produced. A widely used diester in many formulations is sodium di(2-ethylhexyl)sulphosuccinate (that is sold commercially under the trade name Aerosol OT). This is an excellent wetting agent for agrochemical powders in water, which is essential for the preparation of SCs. The diesters are soluble both in water and in many organic solvents. They are particularly useful for preparing water-in-oil (W/O) microemulsions.

Both alkyl phosphates and alkyl ether phosphates are made by treating the fatty alcohol or alcohol ethoxylates with a phosphorylating agent, usually phosphorous pentoxide, P_4O_{10}. The reaction yields a mixture of mono- and diesters of phosphoric acid. The ratio of the two esters is determined by the ratio of the reactants and the amount of water present in the reaction mixture. The physicochemical properties of the alkyl phosphate surfactants depend on the ratio of the esters. Phosphate surfactants are used in the metal working industry due to their anticorrosive properties.

The most common cationic surfactants are the quaternary ammonium compounds [8, 9] with the general formula $R'R''R'''R''''N^+X^-$, where X^- is usually a chloride ion and R represents alkyl groups. A common class of cationics is the alkyl trimethyl ammonium chlorides, where R contains 8–18 C atoms, e.g. dodecyl trimethyl ammonium chloride, $C_{12}H_{25}(CH_3)_3NCl$. Another cationic surfactant class is that containing two long chain alkyl groups, i.e. dialkyl dimethyl ammonium chloride, with the alkyl groups having a chain length of 8–18 C atoms. These dialkyl surfactants are less soluble in water than the monoalkyl quaternary compounds, but they are sometimes used in agrochemical formulations as adjuvants and/or rheology modifiers. A special cationic surfactant is alkyl dimethyl benzyl ammonium chloride (sometimes referred to as benzalkonium chloride), which may also be used in some formulations as an adjuvant. Imidazolines can also form quaternaries, the most common product being the ditallow derivative quaternized with dimethyl sulphate.

Cationic surfactants can also be modified by incorporating polyethylene oxide chains, e.g. dodecyl methyl polyethylene oxide ammonium chloride.

Cationic surfactants are generally water soluble when there is only one long alkyl group. They are generally compatible with most inorganic ions and hard water. Cationics are generally stable to pH changes, both acid and alkaline. They are incompatible with most anionic surfactants, but they are compatible with nonionics. These cationic surfactants are insoluble in hydrocarbon oils. In contrast, cationics with two or more long alkyl chains are soluble in hydrocarbon solvents, but they become only dispersible in water (sometimes forming bilayer vesicle type structures). They are generally chemically stable and can tolerate electrolytes. The cmc of cationic surfactants is close to that of anionics with the same alkyl chain length.

Amphoteric (zwitterionic) surfactants contain both cationic and anionic groups [10]. The most common amphoterics are the N-alkyl betaines which are derivatives of trimethyl glycine $(CH_3)_3NCH_2COOH$ (that was described as betaine). An example of betaine surfactant is lauryl amido propyl dimethyl betaine $C_{12}H_{25}CON(CH_3)_2CH_2COOH$. These alkyl betaines are sometimes described as alkyl dimethyl glycinates.

The main characteristic of amphoteric surfactants is their dependency on the pH of the solution in which they are dissolved. In acid pH solutions, the molecule acquires a positive charge and it behaves like a cationic, whereas in alkaline pH solutions they become negatively charged and behave like an anionic. A specific pH can be defined at which both ionic groups show equal ionization (the isoelectric point of the molecule. This can be described by the following scheme,

$N^+...COOH$	⟷	$N^+...COO^-$	⟷	$NH...COO^-$
acid, pH < 3		isoelectric		pH > 6, alkaline

Amphoteric surfactants are sometimes referred to as zwitterionic molecules. They are soluble in water, but the solubility shows a minimum at the isoelectric point. Amphoterics show excellent compatibility with other surfactants, forming mixed micelles.

They are chemically stable both in acids and alkalis. The surface activity of amphoterics varies widely and it depends on the distance between the charged groups and they show a maximum in surface activity at the isoelectric point.

Another class of amphoteric are the N-alkyl amino propionates having the structure $R–NHCH_2CH_2COOH$. The NH group is reactive and can react with another acid molecule (e.g. acrylic) to form an amino dipropionate $R–N(CH_2CH_2COOH)_2$. Alkyl imidazoline-based product can also be produced by reacting alkyl imidazoline with a chloro acid. However, the imidazoline ring breaks down during the formation of the amphoteric.

The change in charge with pH of amphoteric surfactants affects their properties, such as wetting, foaming, etc. At the isoelectric point, the properties of amphoterics resemble those of nonionics very closely. Below and above the IEP, the properties shift towards those of cationic and anionic surfactants respectively. Zwitterionic surfactants have excellent dermatological properties and they also exhibit low eye irritation.

The most common nonionic surfactants are those based on ethylene oxide, referred to as ethoxylated surfactants [11–13]. Several classes can be distinguished: alcohol ethoxylates, alkyl phenol ethoxylates, fatty acid ethoxylates, monoalkaolamide ethoxylates, sorbitan ester ethoxylates, fatty amine ethoxylates and ethylene oxide–propylene oxide copolymers (sometimes referred to as polymeric surfactants).

Another important class of nonionics are the multihydroxy products such as glycol esters, glycerol (and polyglycerol) esters, glucosides (and polyglucosides) and sucrose esters. Amine oxides and sulphinyl surfactants represent nonionics with a small head group.

Alcohol ethoxylates are generally produced by ethoxylation of a fatty chain alcohol such as dodecanol. Several generic names are given to this class of surfactants such as ethoxylated fatty alcohols, alkyl polyoxyethylene glycol, monoalkyl polyethylene oxide glycol ethers, etc. A typical example is dodecyl hexaoxyethylene glycol monoether with the chemical formula $C_{12}H_{25}(OCH_2CH_2O)_6OH$ (sometimes abbreviated as $C_{12}E_6$). In practice, the starting alcohol will have a distribution of alkyl chain lengths and the resulting ethoxylate will have a distribution of ethylene oxide chain length. Thus the numbers listed in the literature refer to average numbers.

The cmc of nonionic surfactants is about two orders of magnitude lower than the corresponding anionics with the same alkyl chain length. The solubility of the alcohol ethoxylates depend both on the alkyl chain length and the number of ethylene oxide units in the molecule. Molecules with an average alkyl chain length of 12 C atoms and containing more than 5 EO units are usually soluble in water at room temperature. However, as the temperature of the solution is gradually raised, the solution becomes cloudy (as a result of dehydration of the PEO chain) and the temperature at which this occurs is referred to as the cloud point (CP) of the surfactant. At a given alkyl chain length, the CP increases with increasing EO chain length of the molecule. The CP changes with changing concentration of the surfactant solution and the trade literature usually quotes the CP of a 1 % solution. The CP is also affected by the presence of

electrolyte in the aqueous solution. Most electrolytes lower the CP of a nonionic surfactant solution. Nonionics tend to have maximum surface activity near to the cloud point. The CP of most nonionics increases markedly on the addition of small quantities of anionic surfactants. The surface tension of alcohol ethoxylate solutions decreases with decreasing EO units of the chain. The viscosity of a nonionic surfactant solution increases gradually with increasing its concentration, but at a critical concentration (which depends on the alkyl and EO chain lengths) its viscosity shows a rapid increase and ultimately a gel-like structure appears. This results from the formation of liquid crystalline structure of the hexagonal type. In many cases, the viscosity reaches a maximum after which it shows a decrease due to the formation of other structures (e.g. lamellar phases) (see Chapter 3).

Alkyl phenol ethoxylates are prepared by the reaction of ethylene oxide with the appropriate alkyl phenol. The most common surfactants of this type are those based on nonyl phenol. These surfactants are cheap to produce, but they suffer from the problem of biodegradability and potential toxicity (the by-product of degradation is nonyl phenol, which has considerable toxicity). In spite of these problems, nonyl phenol ethoxylates are still used in many agrochemical formulations, due to their advantageous properties, such as their solubility both in aqueous and nonaqueous media, their good emulsification and dispersion properties, etc.

Fatty acid ethoxylates are produced by the reaction of ethylene oxide with a fatty acid or a polyglycol and they have the general formula $RCOO–(CH_2CH_2O)_nH$. When a polyglycol is used, a mixture of mono- and diesters ($RCOO–(CH_2CH_2O)_n–OCOR$) is produced. These surfactants are generally soluble in water provided there are enough EO units and the alkyl chain length of the acid is not too long. The mono-esters are much more soluble in water than the diesters. In the latter case, a longer EO chain is required to render the molecule soluble. The surfactants are compatible with aqueous ions, provided there is not much unreacted acid. However, these surfactants undergo hydrolysis in highly alkaline solutions.

The sorbitan esters and their ethoxylated derivatives (Spans and Tweens) are perhaps one of the most commonly used nonionics. The sorbitan esters are produced by reaction of sorbitol with a fatty acid at a high temperature (> 200 °C). The sorbitol dehydrates to 1,4-sorbitan and then esterification takes place. If one mole of fatty acid is reacted with one mole of sorbitol, one obtains a mono-ester (some diester is also produced as a by-product). Thus, sorbitan mono-ester has the following general formula,

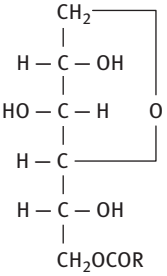

The free OH groups in the molecule can be esterified, producing di- and tri-esters. Several products are available depending on the nature of the alkyl group of the acid and whether the product is a mono-, di- or tri-ester. Some examples are given below,

- Sorbitan monolaurate – Span 20
- Sorbitan monopalmitate – Span 40
- Sorbitan monostearate – Span 60
- Sorbitan monooleate – Span 80
- Sorbitan tristearate – Span 65
- Sorbitan trioleate – Span 85

The ethoxylated derivatives of Spans (Tweens) are produced by reaction of ethylene oxide on any hydroxyl group remaining on the sorbitan ester group. Alternatively, the sorbitol is first ethoxylated and then esterified. However, the final product has different surfactant properties to the Tweens. Some examples of Tween surfactants are given below,

- Polyoxyethylene (20) sorbitan monolaurate – Tween 20
- Polyoxyethylene (20) sorbitan monopalmitate – Tween 40
- Polyoxyethylene (20) sorbitan monostearate – Tween 60
- Polyoxyethylene (20) sorbitan monooleate – Tween 80
- Polyoxyethylene (20) sorbitan tristearate – Tween 65
- Polyoxyethylene (20) sorbitan tri-oleate – Tween 85

The sorbitan esters are insoluble in water, but soluble in most organic solvents (low HLB number surfactants). The ethoxylated products are generally soluble in water and they have relatively high HLB numbers. One of the main advantages of the sorbitan esters and their ethoxylated derivatives is their approval as food additives. They are also widely used in cosmetics and some pharmaceutical preparations.

Ethoxylated fats and oils are useful for application in agrochemical formulations, e.g. as solubilizers.

Amine ethoxylates are prepared by addition of ethylene oxide to primary or secondary fatty amines. With primary amines, both hydrogen atoms on the amine group react with ethylene oxide and therefore the resulting surfactant has the structure,

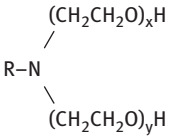

The above surfactants acquire a cationic character if the EO units are small in number and if the pH is low. However, at high EO levels and neutral pH they behave very similarly to nonionics. At low EO content, the surfactants are not soluble in water, but

become soluble in an acid solution. At high pH, the amine ethoxylates are water soluble provided the alkyl chain length of the compound is not long (usually a C_{12} chain is adequate for reasonable solubility at sufficient EO content).

Several surfactants have been synthesized starting from mono- or oligosaccharides by reaction with the multifunctional hydroxyl groups. The technical problem is one of joining a hydrophobic group to the multihydroxyl structure. Several surfactants have been made, e.g. esterification of sucrose with fatty acids or fatty glycerides to produce sucrose esters. The most interesting sugar surfactants are the alkyl polyglucosides (APG). These molecules are produced from starch or glucose; first by reaction with butanol in the presence of an acid catalyst to produce butyl oligoglycosides intermediate, which are then reacted with a fatty alcohol such as dodecanol (acid catalyst) to produce dodecyl polyglucoside with a low degree of polymerization n (1.1–3)

The basic raw materials are glucose and fatty alcohols (which may be derived from vegetable oils) and hence these surfactants are sometimes referred to as "environmentally friendly". A product with $n = 2$ has two glucose residues with four OH groups on each molecule (i.e. total of 8 OH groups). The chemistry is more complex and commercial products are mixtures with $n = 1.1$ to 3. The properties of APG surfactants depend on the alkyl chain length and the average degree of polymerization. APG surfactants have good solubility in water and they have high cloud points (> 100 °C). They are stable in neutral and alkaline solutions but are unstable in strong acid solutions. APG surfactants can tolerate high electrolyte concentrations and they are compatible with most types of surfactants.

Speciality surfactant, namely fluorocarbon and silicone surfactants can lower the surface tension of water to values below 20 mN m^{-1} (most surfactants described above lower the surface tension of water to values above 20 mN m^{-1}, typically in the region of 25–27 mN m^{-1}). The fluorocarbon and silicone surfactants are sometimes referred to as superwetters as they cause enhanced wetting and spreading of their aqueous solution. However, they are much more expensive than conventional surfactants and they are only applied for specific applications in which the low surface tension is a desirable property.

Fluorocarbon surfactants have been prepared with various structures consisting of perfluoroalkyl chains and anionic, cationic, amphoteric and polyethylene oxide polar groups. These surfactants have good thermal and chemical stability and they are excellent wetting agents for low energy surfaces.

Silicone surfactants, sometimes referred to as organosilicones are those with polydimethyl silixane backbone. The silicone surfactants are prepared by the incorporation of a water-soluble or hydrophilic group into a siloxane backbone. The latter can also be modified by incorporation of a paraffinic hydrophobic chain at the end or along the polysiloxane backbone. The most common hydrophilic groups are EO/PO and the structures produced are rather complex and most manufacturers of silicone surfactants do not reveal the exact structure. The mechanism by which these molecules

lower the surface tension of water to low values is far from being well understood. The surfactants are widely applied as spreading agents on many hydrophobic surfaces.

Incorporating organophilic groups into the backbone of the polydimethyl siloxane backbone can give products that exhibit surface active properties in organic solvents.

The most common polymeric surfactants used in agrochemical formulation are the ethylene oxide-propylene oxide copolymers (EO/PO). These surfactants are sold under the trade name Pluronics (BASF, Germany). Two types may be distinguished: those prepared by reaction of polyoxypropylene glycol (difunctional) with EO or mixed EO/PO, giving block copolymers with the structure,

$$HO(CH_2CH_2O)_n\text{–}(CH_2\underset{\displaystyle CH_3}{\underset{|}{C}}HO)_m\text{–}(CH_2CH_2)_nOH, \text{ abbreviated } (EO)_n(PO)_m(EO)_n$$

Various molecules are available, where n and m are varied systematically.

The second type of EO/PO copolymers are prepared by reaction of polyethylene glycol (difunctional) with PO or mixed EO/PO. These will have the structure $(PO)_n(EO)_m(PO)_n$ and they are referred to as reverse Pluronics.

Trifunctional products are also available where the starting material is glycerol. These have the structure,

$$\begin{array}{l} CH_2 - (PO)_m(EO)_n \\ | \\ CH - (PO)_n(EO)_n \\ | \\ CH_2 - \ PO\ _m\ EO\ _n \end{array}$$

Tetrafunctional products are available where the starting material is ethylene diamine. These have the structures,

$$\begin{array}{ccc} (EO)_n & & (EO)_n \\ \quad\backslash & & /\quad \\ & NCH_2CH_2N & \\ \quad/ & & \backslash\quad \\ (EO)_n & & (EO)_n \end{array}$$

$$\begin{array}{ccc} (EO)_n(PO)_m & & (PO)_m(EO)_n \\ \quad\backslash & & /\quad \\ & NCH_2CH_2N & \\ \quad/ & & \backslash\quad \\ (EO)_n(PO)_m & & (PO)_m(EO)_n \end{array}$$

The recent development of speciality polymeric surfactants of the graft type ("comb" structures) has enabled one to obtain specific applications in dispersions. An example of such molecules is the graft copolymer of polymethyl methacrylate backbone with several PEO side chains (sold under the trade name Atlox 4913), which has excellent dispersing and stabilizing properties for concentrated dispersions of hydrophobic particles in water. Using such a dispersant, one can obtain highly stable concentrated suspensions. These surfactants have been modified in several ways to produce molecules that are suitable as emulsifiers, dispersants in extreme conditions such as high or low pH values, high electrolyte concentrations, temperatures etc. Other polymeric surfactants that are suitable for dispersing agrochemical particles in nonaqueous media have also been prepared in which the side chains were made oil soluble, such as polyhydroxystearic acid.

1.2 Properties of solutions of surfactants

The physical properties of surface active agents differ from those of smaller or nonamphipathic molecules in one major aspect, namely the abrupt changes in their properties above a critical concentration [2, 14, 15]. This is illustrated in Fig. 1.1, in which a number of physical properties (osmotic pressure, turbidity, solubilization, magnetic resonance, surface tension, equivalent conductivity and self-diffusion) are plotted as a function of concentration for an ionic surfactant [2, 14].

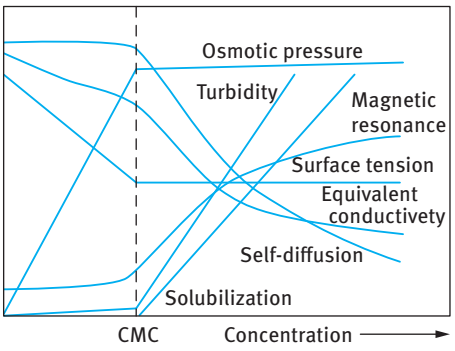

Fig. 1.1: Variation of solution properties with concentration for surfactants.

At low concentrations, most properties are similar to those of a simple electrolyte. One notable exception is the surface tension, which decreases rapidly with increasing surfactant concentration. However, all the properties (interfacial and bulk) show an abrupt change at a particular concentration that is consistent with the fact that at and above this concentration, surface active ions or molecules in solution associate to form larger units. These associated units are called micelles (self-assembled structures) and the first-formed aggregates are generally approximately spherical in shape.

The concentration at which this association phenomenon occurs is known as the critical micelle concentration (cmc). Each surfactant molecules has a characteristic cmc value at a given temperature and electrolyte concentration. The most common technique for measuring the cmc is surface tension, γ, which shows a break at the cmc, after which γ remains virtually constant with any further increase in concentration. However, other techniques such as self-diffusion measurements, NMR and fluorescence spectroscopy can be applied. A compilation of cmc values was given in 1971 by Mukerjee and Mysels [16], which is clearly not an up-to-date text, but is an extremely valuable reference. As an illustration, the cmc values of a number of surface active agents are given in Tab. 1.1, to show some of the general trends [2, 14, 15]. Within any class of surface active agent, the cmc decreases with increasing chain length of the hydrophobic portion (alkyl group). As a general rule, the cmc decreases by a factor of 2 for ionics (without added salt) and by a factor of 3 for nonionics on adding one methylene group to the alkyl chain. With nonionic surfactants, increasing the length of the hydrophilic group (polyethylene oxide) causes an increase in cmc.

In general, nonionic surfactants have lower cmc values than their corresponding ionic surfactants of the same alkyl chain length. Incorporation of a phenyl group in the alkyl group increases its hydrophobicity to a much smaller extent than increasing its chain length with the same number of carbon atoms. The valency of the counterion in ionic surfactants has a significant effect on the cmc. For example, increasing the valency of the counterion from 1 to 2 causes a reduction of the cmc by roughly a factor of 4.

Tab. 1.1: Critical micelle concentration of surfactant classes.

Surface active agent	cmc (mol dm^{-3})
(A) *Anionic*	
Sodium octyl-l-sulphate	1.30×10^{-1}
Sodium decyl-l-sulphate	3.32×10^{-2}
Sodium dodecyl-l-sulphate	8.39×10^{-3}
Sodium tetradecyl-l-sulphate	2.05×10^{-3}
(B) *Cationic*	
Octyl trimethyl ammonium bromide	1.30×10^{-1}
Decetryl trimethyl ammonium bromide	6.46×10^{-2}
Dodecyl trimethyl ammonium bromide	1.56×10^{-2}
Hexactecyltrimethyl ammonium bromide	9.20×10^{-4}
(C) *Nonionic*	
Octyl hexaoxyethylene glycol monoether C_8E_6	9.80×10^{-3}
Decyl hexaoxyethylene glycol monoether $C_{10}E_6$	9.00×10^{-4}
Decyl nonaoxyethylene glycol monoether $C_{10}E_9$	1.30×10^{-3}
Dodecyl hexaoxyethylene glycol monoether $C_{12}E_6$	8.70×10^{-5}
Octylphenyl hexaoxyethylene glycol monoether C_8E_6	2.05×10^{-4}

The cmc for ionic surfactants is, to a first approximation, independent of temperature. The cmc varies in a non-monotonic way by ca. 10–20 % over a wide temperature range. However, nonionic surfactants of the ethoxylate type show a monotonic decrease [17, 18] in cmc with increasing temperature.

The effect of adding of cosolutes, e.g. electrolytes and nonelectrolytes, on the cmc can be very striking. For example, addition of 1 : 1 electrolyte to a solution of anionic surfactant gives a dramatic lowering of the cmc, which may amount to one order of magnitude. The effect is moderate for short-chain surfactants, but is much larger for long-chain ones. At high electrolyte concentrations, the reduction in cmc with increasing number of carbon atoms in the alkyl chain is much stronger than without added electrolyte. This rate of decrease at high electrolyte concentrations is comparable to that of nonionics. The effect of added electrolyte also depends on the valency of the added counterions. In contrast, for nonionics, addition of electrolytes causes only small variation in the cmc.

Non-electrolytes such as alcohols can also cause a decrease in the cmc. The alcohols are less polar than water and are distributed between the bulk solution and the micelles. The more preference they have for the micelles, the more they stabilize them. A longer alkyl chain leads to a less favourable location in water and a more favourable location in the micelles.

The presence of micelles can account for many of the unusual properties of solutions of surface active agents. For example, it can account for the near constant surface tension value above the cmc (see Fig. 1.1). It also accounts for the reduction in molar conductance of the surface active agent solution above the cmc, which is consistent with the reduction in mobility of the micelles as a result of counterions. The presence of micelles also accounts for the rapid increase in light scattering or turbidity above the cmc.

The presence of micelles was originally suggested by McBain [19], who suggested that below the cmc most of the surfactant molecules are unassociated, whereas in the isotropic solutions immediately above the cmc, micelles and surfactant ions (molecules) are thought to co-exist, the concentration of the latter changing very slightly as more surfactant is dissolved. However, the self-association of an amphiphile occurs in a stepwise manner with one monomer added to the aggregate at a time. For a long chain amphiphile, the association is strongly cooperative up to a certain micelle size where counteracting factors became increasingly important. Typically, the micelles have a closely spherical shape in a rather wide concentration range above the cmc. Originally, it was suggested by Adam [20] and Hartley [21] that micelles are spherical in shape and have the following properties:

(i) the association unit is spherical with a radius approximately equal to the length of the hydrocarbon chain;
(ii) the micelle contains about 50–100 monomeric units – the aggregation number generally increases with increasing alkyl chain length;

(iii) with ionic surfactants, most counterions are bound to the micelle surface, thus significantly reducing the mobility from the value to be expected from a micelle with non-counterion bonding;
(iv) micellization occurs over a narrow concentration range as a result of the high association number of surfactant micelles;
(v) the interior of the surfactant micelle has essentially the properties of a liquid hydrocarbon. This is confirmed by the high mobility of the alkyl chains and the ability of the micelles to solubilize many water-insoluble organic molecules, e.g. dyes and agrochemicals.

To a first approximation, micelles can, over a wide concentration range above the cmc, be viewed as microscopic liquid hydrocarbon droplets covered with polar head groups, which interact strongly with water molecules. It appears that the radius of the micelle core constituted of the alkyl chains is close to the extended length of the alkyl chain, i.e. in the range 1.5030 nm. As we will see later, the driving force for micelle formation is the elimination of the contact between the alkyl chains and water. The larger a spherical micelle, then the more efficient this is, since the volume-to-area ratio increases. It should be noted that the surfactant molecules in the micelles are not all extended. Only one molecule needs to be extended to satisfy the criterion that the radius of the micelle core is close to the extended length of the alkyl chain. The majority of surfactant molecules are in a disordered state. In other words, the interior of the micelle is close to that of the corresponding alkane in a neat liquid oil. This explains the large solubilization capacity of the micelle towards a broad range of nonpolar and weakly polar substances.

At the surface of the micelle, associated counterions (in the region of 50–80 % of the surfactant ions) are present. However, simple inorganic counterions are very loosely associated with the micelle. The counterions are very mobile (see below) and there is no specific complex formed with a definite counterion-head group distance. In other words, the counterions are associated by long-range electrostatic interactions.

A useful concept for characterizing micelle geometry is the critical packing parameter, CPP [15]. The aggregation number N is the ratio between the micellar core volume, V_{mic}, and the volume of one chain, v,

$$N = \frac{V_{\mathrm{mic}}}{v} = \frac{(4/3)\pi R_{\mathrm{mic}}^3}{v}, \tag{1.1}$$

where R_{mic} is the radius of the micelle.

The aggregation number, N, is also equal to the ratio of the area of a micelle, A_{mic}, to the cross-sectional area, a, of one surfactant molecule,

$$N = \frac{A_{\mathrm{mic}}}{a} = \frac{4\pi R_{\mathrm{mic}}^2}{a}. \tag{1.2}$$

Combining equations (1.1) and (1.2),

$$\frac{v}{R_{\text{mic}}a} = \frac{1}{3}. \tag{1.3}$$

Since R_{mic} cannot exceed the extended length of a surfactant alkyl chain, l_{max},

$$l_{\text{max}} = 1.5 + 1.265n_{\text{c}}. \tag{1.4}$$

This means that for a spherical micelle,

$$\frac{v}{l_{\text{max}}a} \leq \frac{1}{3}. \tag{1.5}$$

The ratio $v/(l_{\text{max}}$ a) is denoted as the critical packing parameter (CPP).

Although, the spherical micelle model accounts for many of the physical properties of solutions of surfactants, a number of phenomena remain unexplained unless other shapes are considered. For example, McBain [22] suggested the presence of two types of micelles, spherical and lamellar, in order to account for the drop in molar conductance of surfactant solutions. The lamellar micelles are neutral and hence they account for the reduction in the conductance. Later, Harkins et al. [23] used McBain's model of lamellar micelles to interpret his X-ray results in soap solutions. Moreover, many modern techniques such as light scattering and neutron scattering indicate that in many systems the micelles are not spherical. For example, Debye and Anacker [24] proposed a cylindrical micelle to explain that light scattering results of hexadecyl trimethyl ammonium bromide in water. Evidence for disc-shaped micelles has also been obtained under certain conditions. A schematic representation of the spherical, lamellar and rod-shaped micelles, suggested by McBain, Hartley and Debye is given in Fig. 1.2.

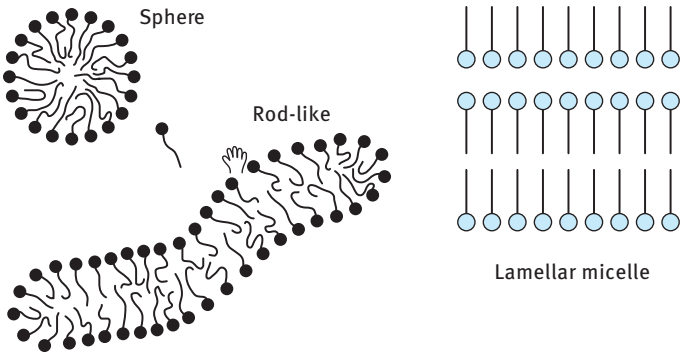

Fig. 1.2: Shape of micelles.

1.3 Solubility–temperature relationship for surfactants

Many ionic surfactants show dramatic temperature-dependent solubility [1]. The solubility may be very low at low temperatures and then increases by orders of magnitude in a relatively narrow temperature range. This is illustrated in Fig. 1.3, which shows the change of solubility and cmc of sodium decyl sulphonate with temperature. This phenomenon is generally denoted as the Krafft phenomenon, with the temperature for the onset of increasing solubility being known as the Krafft temperature. The cmc increases slowly with temperature and at the Krafft temperature the solubility is equal to the cmc. At this temperature there is an equilibrium between hydrated surfactant solid, micelles and monomers (triple point). The Krafft temperature may vary dramatically with subtle changes in the surfactant chemical structure. In general, the Krafft temperature increases rapidly as the alkyl chain length of the surfactant increases. It decreases with increasing alkyl chain distribution of the surfactant. It also depends on the head group and counterion. Addition of electrolytes causes an increase in the Krafft temperature.

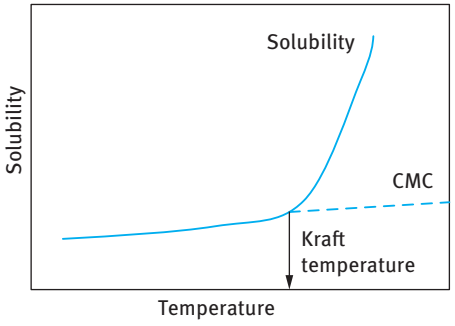

Fig. 1.3: Variation of solubility and critical micelle concentration (cmc) with temperature.

With nonionic surfactants of the ethoxylate type, an increase in temperature for a solution at a given concentration causes dehydration of the polyethylene oxide (PEO) chains and at a critical temperature the solution become cloudy. This is illustrated in Fig. 1.4, which shows the phase diagram of $C_{12}E_6$. Below the cloud point (CP) curve one can identify different liquid crystalline phases: hexagonal – cubic – lamellar, which are schematically shown in Fig. 1.5.

1.4 Thermodynamics of micellization

As mentioned above, the process of micellization is one of the most important characteristics of surfactant solutions and hence it is essential to understand its mechanism (the driving force for micelle formation). This requires analysis of the dynamics of the

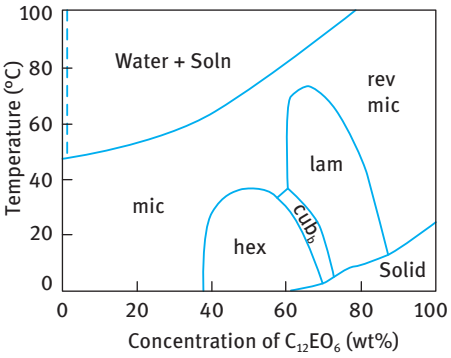

Fig. 1.4: Phase diagram of nonionic surfactants.

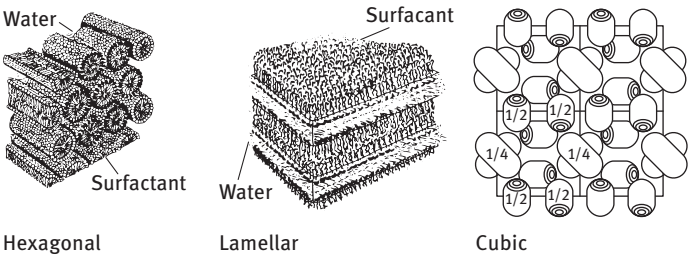

Fig. 1.5: Schematic picture of liquid crystalline phases.

process (i.e. the kinetic aspects) as well as the equilibrium aspects, where the laws of thermodynamics may be applied to obtain the free energy, enthalpy and entropy of micellization.

Micellization is a dynamic phenomenon in which n monomeric surfactant molecules associate to form a micelle S_n, i.e.,

$$nS \Leftrightarrow S_n. \tag{1.6}$$

Hartley [21] envisaged a dynamic equilibrium in which surface active agent molecules are constantly leaving the micelles whilst other molecules from solution enter the micelles. The same applies to the counterions with ionic surfactants, which can exchange between the micelle surface and bulk solution.

Experimental investigations using fast kinetic methods such as stop flow, temperature and pressure jumps, and ultrasonic relaxation measurements have shown that there are two relaxation processes for micellar equilibrium [25–31] characterized by relaxation times τ_1 and τ_2. The first relaxation time, τ_1, is of the order of 10^{-7} s (10^{-8} to 10^{-3} s) and represents the lifetime of a surface active molecule in a micelle, i.e. it represents the association and dissociation rate (represented by association and dissociation rate constants k^+ and k^- respectively) for a single molecule entering and leaving the micelle, which may be represented by the equation,

$$S + S_{n-1} \underset{k^-}{\overset{k^+}{\rightleftarrows}} S_n. \tag{1.7}$$

The slower relaxation time τ_2 corresponds to a relatively slow process, namely the micellization dissolution process represented by equation (1.1). The value of τ_2 is of the order of milliseconds (10^{-3}–1 s) and hence can be conveniently measured by stopped flow methods. The fast relaxation time τ_1 can be measured using various techniques depending on its range. For example, τ_1 values in the range of 10^{-8}–10^{-7} s are accessible to ultrasonic absorption methods, whereas τ_1 in the range of 10^{-5}–10^{-3} s can be measured by pressure jump methods. The value of τ_1 depends on surfactant concentration, chain length and temperature. τ_1 increases with increasing chain length of surfactants, i.e. the residence time increases with increasing chain length.

The above discussion emphasizes the dynamic nature of micelles and it is important to realize that these molecules are in continuous motion and that there is a constant interchange between micelles and solution. The dynamic nature also applies to the counterions, which exchange rapidly with lifetimes in the range 10^{-9}–10^{-8} s. Furthermore, the counterions appear to be laterally mobile and not to be associated with (single) specific groups on the micelle surfaces [15].

Two general approaches have been employed in tackling the problem of the equilibrium aspects of micelle formation. The first and most simple approach treats micelles as a single phase, and this is referred to as the phase separation model. In this model, micelle formation is considered as a phase separation phenomenon and the cmc is then the saturation concentration of the amphiphile in the monomeric state whereas the micelles constitute the separated pseudophase. Above the cmc, a phase equilibrium exists with a constant activity of the surfactant in the micellar phase. The Krafft point is viewed as the temperature at which solid hydrated surfactant, micelles and a solution saturated with undissociated surfactant molecules are in equilibrium at a given pressure.

In the second approach, micelles and single surfactant molecules or ions are considered to be in association–dissociation equilibrium. In its simplest form, a single equilibrium constant is used to treat the process represented by equation (1.1). The cmc is merely a concentration range above which any added surfactant appears in solution in a micellar form. Since the solubility of the associated surfactant is much greater than that of the monomeric surfactant, the solubility of the surfactant as a whole will not increase markedly with temperature until it reaches the cmc region. Thus, in the mass action approach, the Krafft point represents the temperature at which the surfactant solubility equals the cmc.

Consider an anionic surfactant, in which n surfactant anions, S^-, and n counterions M^+ associate to form a micelle, i.e.,

$$nS^- + nM^+ \leftrightarrow S_n. \tag{1.8}$$

The micelle is simply a charged aggregate of surfactant ions plus an equivalent number of counterions in the surrounding atmosphere and is treated as a separate phase.

The chemical potential of the surfactant in the micellar state is assumed to be constant, at any given temperature, and this may be adopted as the standard chemical potential, μ_m^0, by analogy to a pure liquid or a pure solid. Considering the equilibrium between micelles and monomer, then,

$$\mu_m^0 = \mu_1^0 + RT \ln a, \tag{1.9}$$

where μ_1 is the standard chemical potential of the surfactant monomer and a_1 is its activity which is equal to $f_1 x_1$, where f_1 is the activity coefficient and x_1 the mole fraction. Therefore, the standard free energy of micellization per mol of monomer, ΔG_m^0, is given by,

$$\Delta G_m^0 = \mu_m^0 - \mu_1^0 = RT \ln a_1 \approx RT \ln x_1, \tag{1.10}$$

where f_1 is taken as unity (a reasonable value in very dilute solution). The cmc may be identified with x_1 so that

$$\Delta G_m^0 = RT \ln[\text{cmc}]. \tag{1.11}$$

In equation (1.11), the cmc is expressed as a mole fraction, which is equal to $C/(55.5 + C)$, where C is the concentration of surfactant in mol dm^{-3}, i.e.,

$$\Delta G_m^0 = RT \ln C - RT \ln(55.5 + C). \tag{1.12}$$

It should be stated that ΔG^0 should be calculated using the cmc expressed as a mole fraction as indicated by equation (1.12). However, most cmc quoted in the literature are given in mol dm^{-3} and, in many cases of ΔG^0 values have been quoted, when the cmc was simply expressed in mol dm^{-3}. Strictly speaking, this is incorrect, since ΔG^0 should be based on x_1 rather than on C. The value of ΔG^0, when the cmc is expressed in mol dm^{-3} is substantially different from the ΔG^0 value when the cmc is expressed in mole fraction. For example, dodecyl hexaoxyethylene glycol, the quoted cmc value is 8.7×10^{-5} mol dm^{-3} at 25 °C. Therefore,

$$\Delta G^0 = RT \ln \frac{8.7 \times 10^{-5}}{55.5 + 8.7 \times 10^{-5}} = -33.1 \text{ kJ mol}^{-1}, \tag{1.13}$$

when the mole fraction scale is used. On the other hand,

$$\Delta G^0 = RT \ln 8.7 \times 10^{-5} = -23.2 \text{ kJ mol}^{-1}, \tag{1.14}$$

when the molarity scale is used.

The phase separation model has been questioned for two main reasons. Firstly, according to this model a clear discontinuity in the physical property of a surfactant solution, such as surface tension, turbidity, etc. should be observed at the cmc. This is not always found experimentally and the cmc is not a sharp breakpoint. Secondly, if two phases actually exist at the cmc, then equating the chemical potential of the surfactant molecule in the two phases would imply that the activity of the surfactant

in the aqueous phase would be constant above the cmc. If this were the case, the surface tension of a surfactant solution should remain constant above the cmc. However, careful measurements have shown that the surface tension of a surfactant solution decreases slowly above the cmc, particularly when using purified surfactants.

The mass action model assumes a dissociation-association equilibrium between surfactant monomers and micelles and an equilibrium constant can be calculated. For a nonionic surfactant, where charge effects are absent, this equilibrium is simply represented by equation (1.1) which assumes a single equilibrium. In this case, the equilibrium constant K_m is given by the equation,

$$K_m = \frac{[S_n]}{[S]^n}. \tag{1.15}$$

The standard free energy per monomer is then given by,

$$-\Delta G_m^0 = -\frac{\Delta G}{n} = \frac{RT}{n} \ln K_m = \frac{RT}{n} \ln[S_n] - RT \ln[S]. \tag{1.16}$$

For many micellar systems, $n > 50$ and, therefore, the first term on the right-hand side of equation (1.16) may be neglected, resulting in the following expression for ΔG_m^0,

$$\Delta G_m^0 = RT \ln[S] = RT \ln[\text{cmc}], \tag{1.17}$$

which is identical to the equation derived using the phase separation model.

The mass action model allows a simple extension to be made to the case of ionic surfactants, in which micelles attract a substantial proportion of counterions, into an attached layer. For a micelle made up of n surfactant ions, where $n - p$ charges are associated with counterions, i.e. having a net charge of p units and degree of dissociation p/n, the following equilibrium may be established (for an anionic surfactant with Na^+ counterions),

$$nS^- + (n-p)Na^+ \leftrightarrow S_n^{p^-}, \tag{1.18}$$

$$K_m = \frac{[S_n^{p^-}]}{[S^-]^n [Na^+]^{(n-p)}}. \tag{1.19}$$

A convenient solution for relating ΔG_m to [cmc] was given by Phillips [21] who arrived at the following expression,

$$\Delta G_m^0 = \{2 - (p/n)\} RT \ln[\text{cmc}] \tag{1.20}$$

For many ionic surfactants, the degree of dissociation (p/n) is ≈ 0.2 so that,

$$\Delta G_m^0 = 1.8 RT \ln[\text{cmc}]. \tag{1.21}$$

Comparison with equation (1.18) clearly shows that for similar ΔG_m, the [cmc] is about two orders of magnitude higher for ionic surfactants when compared with nonionic surfactant of the same alkyl chain length (see Tab. 1.1).

In the presence of excess added electrolyte, with mole fraction x, the free energy of micellization is given by the expression,

$$\Delta G_{\mathrm{m}}^{0} = RT \ln[\mathrm{cmc}] + \{1 - (p/n)\} \ln x. \tag{1.22}$$

Equation (1.22) shows that as x increases, the [cmc] decreases.

It is clear from equation (1.22) that as $p \to 0$, i.e. when most charges are associated with counterions,

$$\Delta G_{\mathrm{m}}^{0} = 2RT \ln[\mathrm{cmc}], \tag{1.23}$$

whereas when $p \approx n$, i.e. the counterions are bound to micelles,

$$\Delta G_{\mathrm{m}}^{0} = RT \ln[\mathrm{cmc}], \tag{1.24}$$

which is the same equation for nonionic surfactants.

Although the mass action approach could account for a number of experimental results, such as small change in the properties around the cmc, it has not escaped criticism. For example, the assumption that surfactants exist in solution in only two forms, namely single ions and micelles of uniform size is debatable. Analysis of various experimental results has shown that micelles have a size distribution which is narrow and concentration dependent. Thus, the assumption of a single aggregation number is an oversimplification and in reality there is a micellar size distribution.

The enthalpy of micellization can be calculated from the variation of cmc with temperature. This follows from,

$$-\Delta H^{0} = RT^{2} \frac{\mathrm{d} \ln[\mathrm{cmc}]}{\mathrm{d}T}. \tag{1.25}$$

The entropy of micellization can then be calculated from the relationship between ΔG^{0} and ΔH^{0}, i.e.,

$$\Delta G^{0} = \Delta H^{0} - T\Delta S^{0}. \tag{1.26}$$

Therefore ΔH^{0} may be calculated from the surface tension–log C plots at various temperatures. Unfortunately, the errors in locating the cmc (which in many cases is not a sharp point) leads to a large error in the value of ΔH^{0}. A more accurate and direct method of obtaining ΔH^{0} is microcalorimetry. As an illustration, the thermodynamic parameters, ΔG^{0}, ΔH^{0}, and $T\Delta S^{0}$ for octylhexaoxyethylene glycol monoether (C_8E_6) are given in Tab. 1.2.

Tab. 1.2: Thermodynamic quantities for micellization of octylhexaoxyethylene glycol monoether.

Temp. (°C)	ΔG^{0} (kJ mol^{-1})	ΔH^{0} (kJ mol^{-1}) (from cmc)	ΔH^{0} (kJ mol l^{-1}) (from calorimetry)	$T\Delta S^{0}$ (kJ mol^{-1})
25	−21.3 + 2.1	8.0 ± 4.2	20.1 ± 0.8	41.8 ± 1.0
40	−23.4 + 2.1		14.6 ± 0.8	38.0 ± 1.0

It can be seen from Tab. 1.2 that ΔG^0 is large and negative. However, ΔH^0 is positive, indicating that the process is endothermic. In addition, $T\Delta S^0$ is large and positive which implies that in the micellization process there is a net increase in entropy. As we will see in the next section, this positive enthalpy and entropy point to a different driving force for micellization to that encountered in many aggregation processes.

The influence of alkyl chain length of the surfactant on the free energy, enthalpy and entropy of micellization, was demonstrated by Rosen [32] who listed these parameters as a function of alkyl chain length for sulphoxide surfactants. The results showed that the standard free energy of micellization becomes increasingly negative as the chain length increases. This is to be expected since the cmc decreases with increasing alkyl chain length. However, ΔH^0 becomes less positive and $T\Delta S$ becomes more positive with increasing chain length of the surfactant. Thus, the large negative free energy of micellization is made up of a small positive enthalpy (which decreases slightly with increasing chain length of the surfactant) and a large positive entropy term $T\Delta S^0$, which becomes more positive as the chain is lengthened. These results can be accounted for in terms of the hydrophobic effect as described below.

Until recently, the formation of micelles was regarded primarily as an interfacial energy process, analogous to the process of coalescence of oil droplets in an aqueous medium. If this were the case, micelle formation would be a highly exothermic process, as the interfacial free energy has a large enthalpy component. As mentioned above, experimental results have clearly shown that micelle formation involves only a small enthalpy change and is often endothermic. The negative free energy of micellization is the result of a large positive entropy. This led to the conclusion that micelle formation must be predominantly entropy driven process. Two main sources of entropy have been suggested. The first is related to the so-called "hydrophobic effect". This effect was first established from a consideration of the free energy enthalpy and entropy of transfer of hydrocarbon from water to a liquid hydrocarbon. To account for this large positive entropy of transfer several authors [32, 33] suggest that the water molecules around a hydrocarbon chain are ordered, forming "clusters" or "icebergs". On transfer of an alkane from water to a liquid hydrocarbon, these clusters are broken thus releasing water molecules which now have a higher entropy. This accounts for the large entropy of transfer of an alkane from water to a hydrocarbon medium. This effect is also reflected in the much higher heat capacity change on transfer, ΔC_p^0, when compared with the heat capacity in the gas phase, C_p^0.

The above effect is also operative on transfer of surfactant monomer to a micelle during the micellization process. The surfactant monomers will also contain "structured" water around their hydrocarbon chain. On transfer of such monomers to a micelle, these water molecules are released and they have a higher entropy.

The second source of entropy increase on micellization may arise from the increase in flexibility of the hydrocarbon chains on their transfer from an aqueous to a hydrocarbon medium [34, 35]. The orientations and bending of an organic chain are likely to be more restricted in an aqueous phase compared to an organic phase.

It should be mentioned that with ionic and zwitterionic surfactants, an additional entropy contribution, associated with the ionic head groups, must be considered. Upon partial neutralization of the ionic charge by the counterions when aggregation occurs, water molecules are released. This will be associated with an entropy increase which should be added to the entropy increase resulting from the hydrophobic effect mentioned above. However, the relative contribution of the two effects is difficult to assess in a quantitative manner.

1.5 Micellization in surfactant mixtures (mixed micelles)

In most agrochemical formulations, more than one surfactant molecule is used in the system. It is, therefore, necessary to predict the type of possible interactions and whether these lead to some synergistic effects. Two general cases may be considered: Surfactant molecules with no net interaction (with similar head groups) and systems with net interaction.

The case of surfactant mixtures with no net interaction is exemplified by mixing two surfactants with the same head group but with different chain lengths. In analogy with the hydrophilic-lipophilic balance (HLB) for surfactant mixtures, one can also assume the cmc of a surfactant mixture (with no net interaction) to be an average of the two cmc's of the single components [2],

$$\mathrm{cmc} = x_1 \mathrm{cmc}_1 + x_2 \mathrm{cmc}_2, \tag{1.27}$$

where x_1 and x_2 are the mole fractions of the respective surfactants in the system. However, the mole fractions should not be those in the whole system, but those inside the micelle. This means that equation (1.27) should be modified,

$$\mathrm{cmc} = x_1^{\mathrm{m}} \mathrm{cmc}_1 + x_2^{\mathrm{m}} \mathrm{cmc}_2. \tag{1.28}$$

The superscript 'm' indicates that the values are inside the micelle. If x_1 and x_2 are the solution composition, then,

$$\frac{1}{\mathrm{cmc}} = \frac{x_1}{\mathrm{cmc}_1} + \frac{x_2}{\mathrm{cmc}_2}. \tag{1.29}$$

The molar composition of the mixed micelle is given by,

$$x_1^{\mathrm{m}} = \frac{x_1 \mathrm{cmc}_2}{x_1 \mathrm{cmc}_2 + x_2 \mathrm{cmc}_1}. \tag{1.30}$$

Fig. 1.6 shows the cmc as a function of molar composition of the solution and in the micelles for a mixture of SDS and nonylphenol with 10 mol ethylene oxide (NP–E_{10}). If the molar composition of the micelles is used as the x-axis, the cmc is more or less the arithmetic mean of the cmc's of the two surfactants. If, on the other hand, the molar composition in the solution is used as the x-axis (which at the cmc is equal to the total

molar concentration), then the cmc of the mixture shows a dramatic decrease at low fractions of NP–E_{10}. This decrease is due to the preferential absorption of NP–E_{10} in the micelle. This higher absorption is due to the higher hydrophobicity of the NP–E_{10} surfactant when compared with SDS.

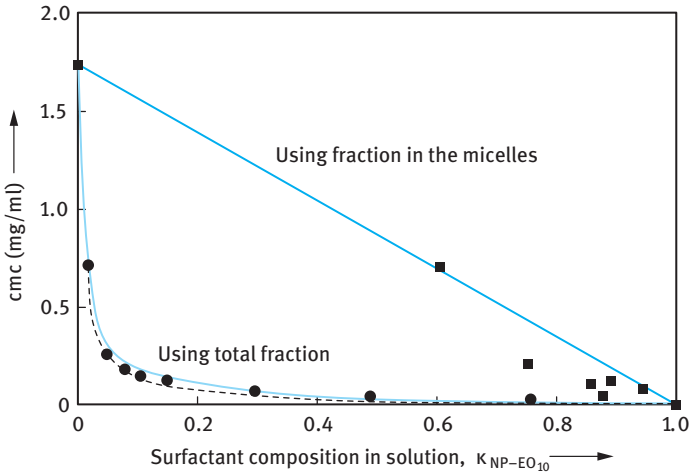

Fig. 1.6: cmc as a function of surfactant composition, x_1, or micellar surfactant composition, x_1^m for the system SDS + NP–E_{10}.

With many agrochemical formulations, different kinds of surfactants are mixed together, for example anionics and nonionics, and in this case one must consider the net interaction between the surfactant molecules. The nonionic surfactant molecules shield the repulsion between the negative head groups in the micelle and hence there will be a net interaction between the two types of molecules. Another example is the case when anionic and cationic surfactants are mixed, whereby very strong interaction will take place between the oppositely charged surfactant molecules. To account for this interaction, equation (1.28) has to be modified by introducing activity coefficients of the surfactants, f_1^m and f_2^m in the micelle,

$$\mathrm{cmc} = x_1^m f_1^m \mathrm{cmc}_1 + x_2^m f_2^m \mathrm{cmc}_2. \tag{1.31}$$

An expression for the activity coefficients can be obtained using the regular solutions theory,

$$\ln f_1^m = (x_2^m)^2 \beta, \tag{1.32}$$

$$\ln f_2^m = (x_2^m)^2 \beta, \tag{1.33}$$

where β is an interaction parameter between the surfactant molecules in the micelle. A positive β value means that there is a net repulsion between the surfactant molecules in the micelle, whereas a negative β value means a net attraction.

The cmc of the surfactant mixture and the composition x_1 are given by the following equations,

$$\frac{1}{\text{cmc}} = \frac{x_1}{f_1^{\text{m}}\text{cmc}_1} + \frac{x_2}{f_2^{\text{m}}\text{cmc}_2}, \tag{1.34}$$

$$x_1^{\text{m}} = \frac{x_1 f_2^{\text{m}}\text{cmc}_2}{x_1 f_2^{\text{m}}\text{cmc}_2 + x_2 f_2^{\text{m}}\text{cmc}_1}. \tag{1.35}$$

As β becomes more negative, the cmc of the mixture decreases. β values in the region of –2 are typical for anionic/nonionic mixtures, whereas values in the region of –10 to –20 are typical of anionic/cationic mixtures. With increasing the negative value of β, the mixed micelles tend towards a mixing ratio of 50 : 50, which reflects the mutual electrostatic attraction between the surfactant molecules.

The predicted cmc and micellar composition depend both on the ratio of the cmc's as well as the value of β. When the cmc's of the single surfactants are similar, the predicted value of the cmc is very sensitive to small variation in β. On the other hand, when the ratio of the cmc's is large, the predicted value of the mixed cmc and the micellar composition are insensitive to variation of the β parameter. For mixtures of nonionic and ionic surfactants, the β decreases with increasing electrolyte concentration. This is due to the screening of the electrostatic repulsion on addition of electrolyte. With some surfactant mixtures, the β decreases with increasing temperature, i.e. the net attraction decreases with increasing temperature.

1.6 Surfactant–polymer interaction

Mixtures of surfactants and polymers are very common in many agrochemical formulations. With many suspension and emulsion systems stabilized with surfactants, polymers are added for a number of reasons. For example, polymers are added as suspending agents ("thickeners") to prevent sedimentation or creaming of these systems. The interaction between surfactants and water-soluble polymers result in some synergistic effects, e.g. enhancing the surface activity, stabilizing suspensions and emulsions, etc. It is therefore important to study the interaction between surfactants and water-soluble polymers in a systematic way.

One of the earliest studies of surfactant/polymer interaction came from surface tension measurements. Fig. 1.7 shows some typical results for the effect of addition of polyvinylpyrrolidone (PVP) on the γ–log C curves of SDS [36].

In a system of fixed polymer concentration and varying surfactant concentrations, two critical concentrations appear, denoted by T_1 and T_2. T_1 represents the concentration at which interaction between the surfactant and polymer first occurs. This is sometimes termed the critical aggregation concentration (CAC), i.e. the onset of association of surfactant to the polymer. Because of this there is no further increase in surface activity and thus no lowering of surface tension. T_2 represents the concentration at which the polymer becomes saturated with surfactant. Since T_1 is generally

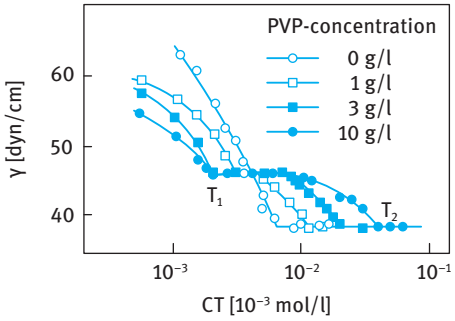

Fig. 1.7: γ–log C curves for SDS solutions in the presence of different concentrations of PVP.

lower than the cmc of the surfactant in the absence of polymer, then "adsorption" or "aggregation" of SDS on or with the polymer is more favourable than normal micellization. As the polymer is saturated with surfactant (i.e. beyond T_2) the surfactant monomer concentration and the activity start to increase again and there is a lowering of γ until the monomer concentration reaches the cmc, after which γ remains virtually constant and normal surfactant micelles begin to form.

The above picture is confirmed if the association of surfactant is directly monitored (e.g. by using surfactant selective electrodes, by equilibrium dialysis or by some spectroscopic technique). At low surfactant concentration, there is no significant interaction. At the CAC, a strongly cooperative binding is indicated and at higher concentrations a plateau is reached. A further increase in surfactant concentration produces "free" surfactant molecules until the surfactant activity or concentration joins the curve obtained in the absence of polymer. The binding isotherms show the strong analogy with micelle formation and the interpretation of these isotherms in terms of a depression of the cmc [39].

Several factors influence the interaction between surfactant and polymer and these are summarized as follows.

(i) Temperature; an increase in temperature generally increases the CAC, i.e. the interaction becomes less favourable.

(ii) Addition of electrolyte; this generally decreases the CAC, i.e. it increases the binding.

(iii) Surfactant chain length; an increase in the alkyl chain length decreases the CAC, i.e. it increases association. A plot of log CAC versus the number of carbon atoms, n, is linear (similar to the log cmc–n relationship obtained for surfactants alone).

(iv) Surfactant structure; alkyl benzene sulphonates are similar to SDS, but introduction of EO groups in the chain weakens the interaction.

(v) Surfactant classes; weaker interaction is generally observed with cationics when compared to anionics. However, the interaction can be promoted by using a strongly interacting counterion for the cationic (e.g. CNS^-). Interaction between ethoxylated surfactants and nonionic polymers is weak but the interaction is stronger with alkyl phenol ethoxylates.

(vi) Polymer molecular weight; a minimum molecular weight of ≈ 4000 for PEO and PVP is required for "complete" interaction.
(vii) Amount of polymer; the CAC seems to be insensitive to (or slightly lower with) increasing polymer concentration. T_2 increases linearly with increasing polymer concentration.
(viii) Polymer structure and hydrophobicity; several uncharged polymers such as PEO, PVP and polyvinyl alcohol (PVOH) interact with charged surfactants. Many other uncharged polymers interact weakly with charged surfactants, e.g. hydroxyethyl cellulose (HEC), dextran and polyacrylamide (PAAm).

For anionic surfactants, the following order of increased interaction has been listed: PVOH < PEO < MEC (methyl cellulose) < PVAc (partially hydrolyzed polyvinyl acetate) < PPO ≈ PVP. For cationic surfactants, the following order was listed: PVP < PEO < PVOH < MEC < PVAc < PPO. The position of PVP can be explained by the slight positive charge on the chain, which causes repulsion with cations and attraction with anionics.

The driving force for polymer/surfactant interaction is the same as that for the process of micellization (see above). As with micelles, the main driving force is the reduction of hydrocarbon/water contact area of the alkyl chain of the dissolved surfactant. A delicate balance between several forces is responsible for the surfactant/polymer association [40–42]. For example, aggregation is resisted by the crowding of the ionic head groups at the surface of the micelle. Packing constraints also resist association. Molecules that screen the repulsion between the head groups, e.g. electrolytes and alcohol, promote association. A polymer molecule with hydrophobic and hydrophilic segments (which is also flexible) can enhance association by ion-dipole association between the dipole of the hydrophilic groups and the ionic head groups of the surfactant. In addition, contact between the hydrophobic segments of the polymer and the exposed hydrocarbon areas of the micelles can enhance association. With SDS/PEO and SDS/PVP, the association complexes are approximately three monomer units per molecule of aggregated surfactant.

Generally speaking, there are two alternative pictures of mixed surfactant/polymer solutions, one describing the interaction in terms of a strongly cooperative association or binding of the surfactant to the polymer chain and one in terms of a micellization of surfactant on or in the vicinity of the polymer chain. For polymers with hydrophobic groups the binding approach is preferred, whereas for hydrophilic homopolymers the micelle formation picture is more likely. The latter picture has been suggested by Cabane [37, 40] who proposed a structure in which the aggregated SDS is surrounded by macromolecules in a loopy configuration.

The consequences of the above model are:
(i) More favourable free energy of association (CAC < cmc) and increased ionic dissociation of the aggregates.
(ii) An altered environment of the CH_2 groups of the surfactant near the head group.

The micelle sizes are similar with polymer present and without, and the aggregation numbers are typically similar or slightly lower than those of the micelles forming in the absence of a polymer. In the presence of a polymer, the surfactant chemical potential is lowered with respect to the situation without polymer [38, 39].

Water-soluble polymers are modified by grafting a low amount of hydrophobic groups (of the order of 1% of the monomers reacted in a typical molecule) resulting in the formation of "associative structures". These molecules are referred to as associative thickeners and are used as rheology modifiers in many agrochemical formulations. An added surfactant will interact strongly with the hydrophobic groups of the polymer, leading to a strengthened association between the surfactant molecules and the polymer chain. A schematic picture for the interaction between SDS and hydrophobically modified hydroxyethyl cellulose (HM-HEC) is shown in Fig. 1.8, which shows the interaction at various surfactant concentrations [1].

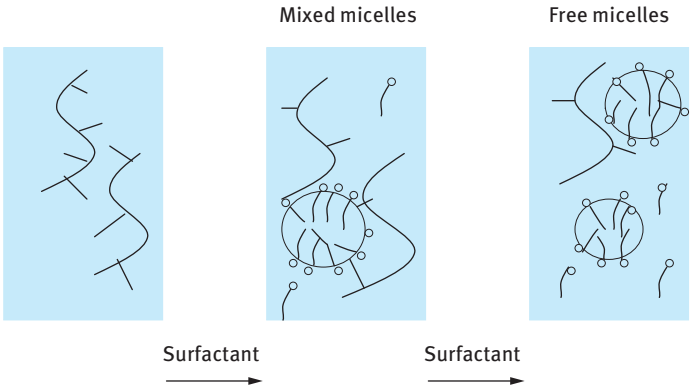

Fig. 1.8: Schematic representation of the interaction between surfactant and HM polymer.

Initially, the surfactant monomers interact with the hydrophobic groups of the HM polymer and at some surfactant concentration (CAC), the micelles can crosslink the polymer chains. At higher surfactant concentrations, the micelles, which are now abundant, will no longer be shared between the polymer chains, i.e. the crosslinks are broken. These effects are reflected in the variation of viscosity with surfactant concentration for HM polymer as illustrated in Fig. 1.9. The viscosity of the polymer increases with increasing surfactant concentration, reaching a maximum at an optimum concentration (maximum crosslinks) and then decreasing with any further increase of surfactant concentration. For the unmodified polymer, the changes in viscosity are relatively small.

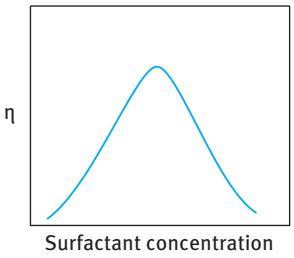

Fig. 1.9: Viscosity–surfactant concentration relationship for HM modified polymer solutions.

References

[1] Tadros T. Applied surfactants. Weinheim: Wiley-VCH; 2005.
[2] Holmberg K, Jonsson B, Kronberg B, Lindman B. Surfactants and polymers in aqueous solution. 2nd edition. John Wiley & Sons, USA; 2003.
[3] McCutcheon. Detergents and Emulsifiers. New Jersey: Allied Publishing Co.; published annually.
[4] van Os NM, Haak JR, Rupert LAM. Physico-chemical properties of selected anionic, cationic and nonionic surfactants. Amsterdam: Elsevier Publishing Co.; 1993.
[5] Porter MR. Handbook of surfactants. Blackie, USA; Chapman and Hall; 1994.
[6] Linfield WM, editor. Anionic surfactants. New York: Marcel Dekker; 1967.
[7] Lucassen-Reynders EH. Anionic surfactants – Physical chemistry of surfactant action. New York: Marcel Dekker; 1981.
[8] Jungermana E. Cationic surfactants. New York: Marcel Dekker; 1970.
[9] Rubingh N, Holland PM, editors. Cationic surfactants – Physical chemistry. New York: Marcel Dekker; 1991.
[10] Buestein BR, Hiliton CL. Amphoteric surfactants. New York: Marcel Dekker; 1982.
[11] Schick MJ, editor. Nonionic surfactants. New York: Marcel Dekker; 1966.
[12] Schick MJ, editor. Nonionic surfactants: Physical chemistry. New York: Marcel Dekker; 1987.
[13] Schonfeldt N. Surface active ethylene oxide adducts. USA: Pergamon Press; 1970.
[14] Lindman B. In: Tadros TF, editor. Surfactants. London: Academic Press; 1984.
[15] Israelachvili JN. Intermolecular and surface forces, with special applications to colloidal and biological systems. London: Academic Press; 1985. p. 251.
[16] Mukerjee P, Mysels KJ. Critical micelle concentrations of aqueous surfactant systems. Washington DC: National Bureau of Standards Publication; 1971.
[17] Elworthy PH, Florence AT, Macfarlane CB. Solubilization by surface active agents. London: Chapman and Hall; 1968.
[18] Shinoda K, Nagakawa T, Tamamushi BI, Isemura T. Colloidal surfactants, some physicochemical properties. London: Academic Press; 1963.
[19] McBain JW. Trans Faraday Soc. 1913;9:99.
[20] Adam NK. J Phys Chem. 1925;29:87.
[21] Hartley GS. Aqueous solutions of paraffin chain salts. Paris: Hermann and Cie; 1936.
[22] McBain JW. Colloid science. Boston: Heath; 1950.
[23] Harkins WD, Mattoon WD, Corrin ML. J Amer Chem Soc. 1946;68:220. J Colloid Sci. 1946;1:105.
[24] Debye P, Anaker EW. J Phys Colloid Chem. 1951;55:644.
[25] Anainsson EAG, Wall SN. J Phys Chem. 1974;78:1024. 1975;79:857.
[26] Anainsson EAG, Wall SN, Almagren M, Hoffmann H, Kielmann I, Ulbricht W, Zana R, Lang J, Tondre C. J Phys Chem. 1976;80:905.

[27] Rassing J, Sams PJ, Wyn-Jones E. J Chem Soc. Faraday II, 1974;70:1247.
[28] Jaycock MJ, Ottewill RH, Fourth Int. Congress Surface Activity. 1964;2:545.
[29] Okub T, Kitano H, Ishiwatari T, Isem N. Proc Royal Soc. 1979;A36:81.
[30] Phillips JN. Trans Faraday Soc. 1955;51:561.
[31] Kahlweit M, Teubner M. Adv Colloid Interface Sci. 1980;13:1.
[32] Rosen ML. Surfactants and interfacial phenomena. New York: Wiley-Interscience; 1978.
[33] Tanford C. The hydrophobic effect. 2nd edition. New York: Wiley; 1980.
[34] Stainsby G, Alexander AE. Trans Faraday Soc. 1950;46:587.
[35] Arnow RH, Witten L. J Phys Chem. 1960;64:1643.
[36] Robb ID. Chemistry and Industry. 1972:530–535.
[37] Cabane B, Duplessix R. J Phys (Paris). 1982;43:1529.
[38] Nagaarajan R. Colloids and Surfaces. 1885;13:1.
[39] Gilyani T, Wolfram E. Colloids and Surfaces. 1981;3:181.
[40] Cabane B. J Phys Chem. 1977;81:1639.
[41] Evans DF, Winnerstrom H. The colloidal domain. Where physics, chemistry, biology and technology meet. New York: John Wiley and Sons Inc. VCH; 1994. p. 312.
[42] Goddard ED. Colloids and Surfaces. 1986;19:301.

2 Emulsion concentrates (EWs)

2.1 Introduction

Many agrochemicals are formulated as oil-in-water (O/W) emulsion concentrates (EWs) [1]. These systems offer many advantages over the more traditionally used emulsifiable concentrates (ECs). By using an O/W system one can reduce the amount of oil in the formulation since in most cases a small proportion of oil is added to the agrochemical oil (if this has a high viscosity) before emulsification. In some cases, if the agrochemical oil has a low to medium viscosity one can emulsify the active ingredient directly into water. With many agrochemicals with low melting point, which are not suitable for the preparation of a suspension concentrate, one can dissolve the active ingredient in a suitable oil and the oil solution is then emulsified into water. EWs that are aqueous based produce less hazard to the operator reducing any skin irritation. In addition, in most cases EWs are less phytotoxic to plants when compared with ECs. The O/W emulsion is convenient for incorporation of water-soluble adjuvants (mostly surfactants). EWs can also be less expensive when compared to ECs since a lower surfactant concentration is used to produce the emulsion and also one replaces a great proportion of oil by water. The only drawback of EWs when compared to ECs is the need to use high speed stirrers and/or homogenizers to obtain the required droplet size distribution. In addition, EWs require control and maintenance of their physical stability. As will be discussed later, EWs are only kinetically stable and one has to control the breakdown processes that occur on storage, such as creaming or sedimentation, flocculation, Ostwald ripening, coalescence and phase inversion.

In this chapter I will start with the principles of formation of emulsions and the role of the surfactants. This is followed by a section on the procedures that can be applied to select the emulsifiers. The third section will deal to the breakdown processes that may occur on storage and methods of their prevention. The last section will deal with the assessment and prediction of the long-term physical stability of EWs.

2.2 Formation of emulsions

Consider a system in which an oil is represented by a large drop 2 of area A_1 immersed in a liquid 2, which is now subdivided into a large number of smaller droplets [1] with total area A_2 ($A_2 \gg A_1$) as shown in Fig. 2.1 The interfacial tension γ_{12} is the same for the large and smaller droplets since the latter are generally in the region of 0.1 to few μm. The change in free energy in going from state I to state II is made from two contributions: A surface energy term (that is positive) that is equal to $\Delta A\gamma_{12}$ (where $\Delta A = A_2 - A_1$). An entropy of dispersions term which is also positive (since producing a large number of droplets is accompanied by an increase in configurational entropy) which is equal to $T\Delta S^{\text{conf}}$.

https://doi.org/10.1515/9783110578997-003

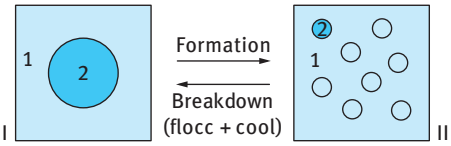

Fig. 2.1: Schematic representation of emulsion formation and breakdown.

From the second law of thermodynamics,

$$\Delta G^{\text{form}} = \Delta A \gamma_{12} - T\Delta S^{\text{conf}}. \tag{2.1}$$

In most cases $\Delta A \gamma_{12} \gg T\Delta S^{\text{conf}}$, which means that ΔG^{form} is positive, i.e. the formation of emulsions is non-spontaneous and the system is thermodynamically unstable. In the absence of any stabilization mechanism, the emulsion will break by flocculation, coalescence, Ostwald ripening or a combination of all these processes. This is illustrated in Fig. 2.2 which shows several paths for emulsion breakdown processes.

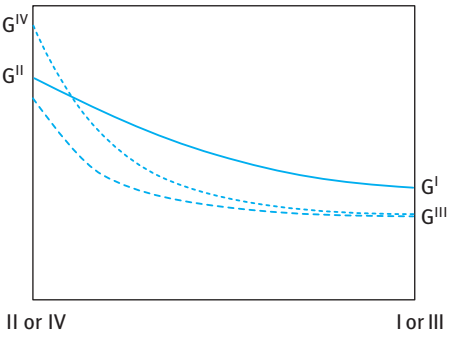

Fig. 2.2: Free energy path in emulsion breakdown: —, flocc. + coal.; ---, flocc. + coal. + sed.; ···, flocc. + coal. + sed. + Ostwald ripening.

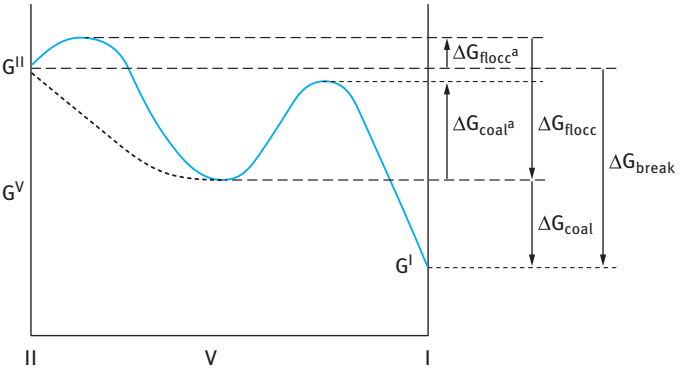

Fig. 2.3: Schematic representation of free energy path for breakdown (flocculation and coalescence) for systems containing an energy barrier.

In the presence of a stabilizer (surfactant and/or polymer), an energy barrier is created between the droplets and therefore the reversal from state II to state I becomes non-continuous as a result of the presence of these energy barriers. This is illustrated in Fig. 2.3. In the presence of the above energy barriers, the system becomes kinetically stable [1]. The energy barrier can be created by electrostatic and/or steric repulsion which will overcome the everlasting van der Waals attraction.

2.3 Mechanism of emulsification

To prepare an emulsion oil, water, surfactant and energy are needed [2, 3]. This can be understood from a consideration of the energy required to expand the interface, $\Delta A\gamma$ (where ΔA is the increase in interfacial area when the bulk oil with area A_1 produces a large number of droplets with area A_2; $A_2 \gg A_1$, γ is the interfacial tension). Since γ is positive, the energy to expand the interface is large and positive. This energy term cannot be compensated by the small entropy of dispersion $T\Delta S$ (which is also positive) and as discussed before, the total free energy of formation of an emulsion, ΔG is positive.

Thus, emulsion formation is non-spontaneous and energy is required to produce the droplets. The formation of large droplets (few μm), as is the case for macroemulsions, is fairly easy and hence high speed stirrers such as the Ultra-Turrax or Silverson mixer are sufficient to produce the emulsion. In contrast, the formation of small drops (submicron as is the case with nanoemulsions) is difficult and this requires a large amount of surfactant and/or energy. The high energy required for formation of nanoemulsions can be understood from a consideration of the Laplace pressure p (the difference in pressure between inside and outside the droplet [2, 3],

$$\Delta p = \gamma\left(\frac{1}{R_1} + \frac{1}{R_2}\right), \tag{2.2}$$

where R_1 and R_2 are the principal radii of curvature of the drop.

For a spherical drop, $R_1 = R_2 = R$ and,

$$\Delta p = \frac{\gamma}{2R}. \tag{2.3}$$

To break up a drop into smaller ones, it must be strongly deformed and this deformation increases p [1, 2]. Surfactants play major roles in the formation of emulsions: By lowering the interfacial tension, p is reduced and hence the stress needed to break up a drop is reduced [2, 3]. Surfactants prevent coalescence of newly formed drops.

To describe emulsion formation one has to consider two main factors: hydrodynamics and interfacial science. To assess emulsion formation, one usually measures the droplet size distribution, using for example laser diffraction techniques. A useful average diameter d is,

$$d_{nm} = \left(\frac{S_m}{S_n}\right)^{1/(n-m)}. \tag{2.4}$$

In most cases d_{32} (the volume/surface average or Sauter mean) is used. The width of the size distribution can be given as the variation coefficient c_m, which is the standard deviation of the distribution weighted with d^m divided by the corresponding average d. Generally, C_2 will be used which corresponds to d_{32}.

An alternative way to describe the emulsion quality is to use the specific surface area A (surface area of all emulsion droplets per unit volume of emulsion),

$$A = \pi s^2 = \frac{6\phi}{d_{32}}, \tag{2.5}$$

where ϕ is the volume fraction of the emulsion.

2.4 Methods of emulsification

Several procedures [3, 4] may be applied for emulsion preparation, these range from simple pipe flow (low agitation energy, L), static mixers and general stirrers (low to medium energy, L–M), high speed mixers such as the Ultra-Turrax (M), colloid mills and high pressure homogenizers (high energy, H), ultrasound generators (M–H). The method of preparation can be continuous (C) or batchwise (B): Pipe flow and static mixers – C; stirrers and Ultra-Turrax – B, C; colloid mill and high pressure homogenizers – C; ultrasound – B, C.

In all methods, there is liquid flow [5, 6]; unbounded and strongly confined flow. In unbounded flow any droplet is surrounded by a large amount of flowing liquid (the confining walls of the apparatus are far away from most of the droplets). The forces can be frictional (mostly viscous) or inertial. Viscous forces cause shear stresses to act on the interface between the droplets and the continuous phase (primarily in the direction of the interface). The shear stresses can be generated by laminar flow (LV) [13] or turbulent flow (TV) [7].

Within each regime, an essential variable is the intensity of the forces acting:

$$\text{viscous stress during laminar flow} = \eta G, \tag{2.6}$$

where G is the velocity gradient.

The intensity in turbulent flow [5, 6] is expressed by the power density ε (the amount of energy dissipated per unit volume per unit time),

$$\varepsilon = \eta G^2. \tag{2.7}$$

The viscosity of the oil plays an important role in the break-up of droplets; the higher the viscosity, the longer it will take to deform a drop. The deformation time τ_{def} is given by the ratio of oil viscosity to the external stress acting on the drop,

$$\tau_{\text{def}} = \frac{\eta_{\text{D}}}{\sigma_{\text{ext}}}. \tag{2.8}$$

The viscosity of the continuous phase η_C plays an important role in some regimes. For the turbulent viscous regime, larger η_C leads to smaller droplets. For the laminar viscous regime, the effect is even stronger.

2.5 Role of surfactants in emulsion formation

Surfactants lower the interfacial tension γ and this causes a reduction in droplet size. The latter decreases with decreasing γ. For a turbulent regime, the droplet diameter is proportional to $\gamma^{3/5}$.

The amount of surfactant required to produce the smallest drop size will depend on its activity a (concentration) in the bulk which determines the reduction in γ, as given by the Gibbs adsorption equation,

$$-\mathrm{d}\gamma = RT\,\Gamma\,\mathrm{d}\ln a, \tag{2.9}$$

where R is the gas constant, T is the absolute temperature and Γ is the surface excess (number of moles adsorbed per unit area of the interface). Γ increases with increasing surfactant concentration and eventually it reaches a plateau value (saturation adsorption).

The value of γ obtained depends on the nature of the oil and surfactant used. Small molecules such as nonionic surfactants lower γ more than polymeric surfactants such as PVA. Another important role of the surfactant is its effect on the interfacial dilational modulus ε [8–10],

$$\varepsilon = \frac{\mathrm{d}\gamma}{\mathrm{d}\ln A}. \tag{2.10}$$

During emulsification an increase in the interfacial area A takes place and this causes a reduction in Γ. The equilibrium is restored by adsorption of surfactant from the bulk, but this takes time (shorter times occur at higher surfactant activity). Thus ε is small at small a and also at large a. Because of the lack or slowness of equilibrium with polymeric surfactants, ε will not be the same for expansion and compression of the interface.

In practice, surfactant mixtures are used and these have pronounced effects on γ and ε. Some specific surfactant mixtures give lower γ values than either of the two individual components [5, 6]. The presence of more than one surfactant molecule at the interface tends to increase ε at high surfactant concentrations. The various components vary in surface activity. Those with the lowest γ tend to predominate at the interface, but if present at low concentrations, it may take a long time before reaching the lowest value. Polymer-surfactant mixtures may show some synergetic surface activity.

Apart for their effect on reducing γ, surfactants play major roles in deformation and break-up of droplets [5, 6]. Surfactants allow the existence of interfacial tension

gradients which are crucial for the formation of stable droplets. In the absence of surfactants (clean interface), the interface cannot withstand a tangential stress; the liquid motion will be continuous. If a liquid flows along the interface with surfactants, the latter will be swept downstream causing an interfacial tension gradient. The interface will then drag some of the bordering liquid with it (the Marangoni effect).

Interfacial tension gradients [5, 6] are very important in stabilizing the thin liquid film between the droplets, which is very important during the beginning of emulsification (films of the continuous phase may be drawn through the disperse phase and collision is very large). The magnitude of the γ-gradients and of the Marangoni effect depends on the surface dilational modulus ε.

Another important role of the emulsifier is to prevent coalescence during emulsification. This is certainly not due to the strong repulsion between the droplets, since the pressure at which two drops are pressed together is much greater than the repulsive stresses. The counteracting stress must be due to the formation of γ-gradients.

Closely related to the above mechanism is the Gibbs–Marangoni effect. The depletion of surfactant in the thin film between approaching drops results in a γ-gradient without liquid flow being involved. This results in an inward flow of liquid that tends to drive the drops apart [5, 6].

The Gibbs–Marangoni effect also explains the Bancroft rule which states that the phase in which the surfactant is most soluble forms the continuous phase. If the surfactant is in the droplets, a γ-gradient cannot develop and the drops would be prone to coalescence. Thus, surfactants with HLB > 7 tend to form O/W emulsions and those with HLB < 7 tend to form W/O emulsions. The Gibbs–Marangoni effect also explains the difference between surfactants and polymers for emulsification. Polymers give larger drops when compared with surfactants. Polymers give a smaller value of ε at small concentrations when compared to surfactants.

Various other factors should also be considered for emulsification, including the disperse phase volume fraction ϕ. An increase in ϕ leads to an increase in droplet collision and hence coalescence during emulsification. With increasing ϕ, the viscosity of the emulsion increases and could change the flow from being turbulent to being laminar.

The presence of many particles results in a local increase in velocity gradients. This means that G increases. In turbulent flow, an increase in ϕ will induce turbulence depression. This will result in larger droplets. Depressing turbulence by adding polymers tends to remove the small eddies, resulting in the formation of larger droplets.

If the mass ratio of surfactant to continuous phase is kept constant, an increase in ϕ results in a decrease in surfactant concentration and hence an increase in γ_{eq}. This results in larger droplets. If the mass ratio of surfactant to disperse phase is kept constant, the above changes are reversed.

2.6 Selection of emulsifiers

2.6.1 The hydrophilic-lipophilic balance (HLB) concept

The selection of different surfactants in the preparation of either O/W or W/O emulsions is often still made on an empirical basis. A semi-empirical scale for selecting surfactants is the hydrophilic-lipophilic balance (HLB number) developed by Griffin [11, 12]. This scale is based on the relative percentage of hydrophilic to lipophilic (hydrophobic) groups in the surfactant molecule(s). For an O/W emulsion droplet, the hydrophobic chain resides in the oil phase whereas the hydrophilic head group resides in the aqueous phase. For a W/O emulsion droplet, the hydrophilic group(s) reside in the water droplet, whereas the lipophilic groups reside in the hydrocarbon phase. A summary of HLB ranges and their application is given in Tab. 2.1.

Tab. 2.1 gives a guide to the selection of surfactants for a particular application. The HLB number depends on the nature of the oil [8, 9]. As an illustration, Tab. 2.2 gives the required HLB numbers to emulsify various oils.

The relative importance of the hydrophilic and lipophilic groups was first recognized when using mixtures of surfactants containing varying proportions of low and high HLB number [11, 12]. The efficiency of any combination (as judged by phase separation) was found to pass a maximum when the blend contained a particular proportion of the surfactant with the higher HLB number. This is illustrated in Fig. 2.4, which shows the variation in emulsion stability, droplet size and interfacial tension as a function of percentage surfactant with high HLB number.

Tab. 2.1: Summary of HLB ranges and their applications.

HLB range	Application
3–6	W/O emulsifier
7–9	Wetting agent
8–18	O/W emulsifier
13–15	Detergent
15–18	Solubilizer

Tab. 2.2: Required HLB numbers to emulsify various oils.

Oil	W/O emulsion	O/W emulsion
Paraffin oil	4	10
Beeswax	5	9
Lanolin, anhydrous	8	12
Cyclohexane	—	15
Toluene	—	15

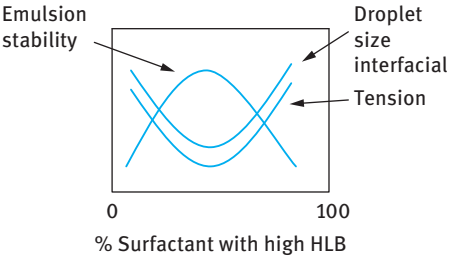

Fig. 2.4: Variation of emulsion stability, droplet size and interfacial tension with percentage surfactant with high HLB number.

The average HLB number may be calculated from additivity,

$$\mathrm{HLB} = x_1\mathrm{HLB}_1 + x_2\mathrm{HLB}_2. \tag{2.11}$$

x_1 and x_2 are the weight fractions of the two surfactants with HLB_1 and HLB_2.

Griffin [11, 12] developed simple equations for calculating the HLB number of relatively simple nonionic surfactants. For a polyhydroxy fatty acid ester

$$\mathrm{HLB} = 20\left(1 - \frac{S}{A}\right). \tag{2.12}$$

S is the saponification number of the ester and A is the acid number. For a glyceryl monostearate, $S = 161$ and $A = 198$; The HLB is 3.8 (suitable for W/O emulsion). For a simple alcohol ethoxylate, the HLB number can be calculated from the weight percent of ethylene oxide (E) and polyhydric alcohol (P),

$$\mathrm{HLB} = \frac{E + P}{5}. \tag{2.13}$$

If the surfactant contains PEO as the only hydrophilic group, the contribution from one OH group can be neglected,

$$\mathrm{HLB} = \frac{E}{5}. \tag{2.14}$$

For a nonionic surfactant $C_{12}H_{25}$–O–$(CH_2$–CH_2–$O)_6$, the HLB is 12 (suitable for O/W emulsion).

The above simple equations cannot be used for surfactants containing propylene oxide or butylene oxide, nor can they be applied for ionic surfactants. Davies [13] devised a method for calculating the HLB number for surfactants from their chemical formulae, using empirically determined group numbers. A group number is assigned to various component groups. A summary of the group numbers for some surfactants is given in Tab. 2.3.

The HLB is given by the following empirical equation,

$$\mathrm{HLB} = 7 + \sum(\text{hydrophilic group numbers}) - \sum(\text{lipohilic group numbers}). \tag{2.15}$$

Davies [13] has shown that the agreement between HLB numbers calculated from the above equation and those determined experimentally is quite satisfactory.

Tab. 2.3: HLB group numbers.

	Group number
Hydrophilic	
$-SO_4Na^+$	38.7
$-COO^-$	21.2
–COONa	19.1
N(tertiary amine)	9.4
Ester (sorbitan ring)	6.8
–O–	1.3
CH–(sorbitan ring)	0.5
Lipophilic	
(–CH–), ($-CH_2-$), CH_3	0.475
Derived	
$-CH_2-CH_2-O$	0.33
$-CH_2-CH_2-CH_2-O-$	0.11

Various other procedures have been developed to obtain a rough estimate of the HLB number. Griffin found good correlation between the cloud point of 5 % solution of various ethoxylated surfactants and their HLB number.

Davies [13] attempted to relate the HLB values to the selective coalescence rates of emulsions. Such correlations were not realized, since it was found that the emulsion stability and even its type depend to a large extent on the method of dispersing the oil into the water and vice versa. At best the HLB number can only be used as a guide for selecting optimum compositions of emulsifying agents.

One may take any pair of emulsifying agents that fall at opposite ends of the HLB scale, e.g. Tween 80 (sorbitan monooleate with 20 mol EO, HLB = 15) and Span 80 (sorbitan monooleate, HLB = 5) and use them in various proportions to cover a wide range of HLB numbers. The emulsions should be prepared in the same way, with a few percent of the emulsifying blend. The stability of the emulsions is then assessed at each HLB number from the rate of coalescence or qualitatively by measuring the rate of oil separation. In this way one may be able to find the optimum HLB number for a given oil. Having found the most effective HLB value, various other surfactant pairs are compared at this HLB value, to find the most effective pair.

2.6.2 The phase inversion temperature (PIT) concept

This concept which has been developed by Shinoda [14, 15] is closely rated to the HLB balance concept described above. Shinoda and co-workers found that many O/W emulsions stabilized with nonionic surfactants undergo a process of inversion at a critical temperature (PIT). The PIT can be determined by following the emul-

sion conductivity (small amount of electrolyte is added to increase the sensitivity) as a function of temperature. The conductivity of the O/W emulsion increases with increasing temperature until the PIT is reached, above which there will be a rapid reduction in conductivity (W/O emulsion is formed).

Shinoda and co-workers [14, 15] found that the PIT is influenced by the HLB number of the surfactant. The size of the emulsion droplets was found to depend on the temperature and HLB number of the emulsifiers. The droplets are less stable towards coalescence close to the PIT. However, by rapid cooling of the emulsion a stable system may be produced. Relatively stable O/W emulsions were obtained when the PIT of the system was 20–65 °C higher than the storage temperature. Emulsions prepared at a temperature just below the PIT followed by rapid cooling generally have smaller droplet sizes. This can be understood if one considers the change of interfacial tension with temperature. The interfacial tension decreases with increasing temperature reaching a minimum close to the PIT, after which it increases. Thus, the droplets prepared close to the PIT are smaller than those prepared at lower temperatures. These droplets are relatively unstable towards coalescence near the PIT, but by rapid cooling of the emulsion one can retain the smaller size. The above procedure may be applied to prepare mini-(nano)emulsions.

The optimum stability of the emulsion was found to be relatively insensitive to changes in the HLB value or the PIT of the emulsifier, but instability was very sensitive to the PIT of the system. It is essential, therefore to measure the PIT of the emulsion as a whole (with all other ingredients). At a given HLB value, stability of the emulsions against coalescence increases markedly as the molar mass of both the hydrophilic and lipophilic components increases.

The enhanced stability using high molecular weight surfactants (polymeric surfactants) can be understood from a consideration of the steric repulsion which produces more stable films. Films produced using macromolecular surfactants resist thinning and disruption, thus reducing the possibility of coalescence.

The emulsions showed maximum stability when the distribution of the PEO chains was broad. The cloud point is lower but the PIT is higher than in the corresponding case for narrow sized distributions. The PIT and HLB number are directly related parameters.

Addition of electrolytes reduces the PIT and hence an emulsifier with a higher HLB value is required when preparing emulsions in the presence of electrolytes. Electrolytes cause dehydration of the PEO chains and in effect this reduces the cloud point of the nonionic surfactant. One needs to compensate for this effect by using a surfactant with higher HLB. The optimum PIT of the emulsifier is fixed if the storage temperature is fixed. In view of the above correlation between PIT and HLB and the possible dependency of the kinetics of droplet coalescence on the HLB number, it has been suggested that PIT measurements can be used as a rapid method for assessing emulsion stability. However, one should be careful in using such methods for assessing the long-term stability since the correlations were based on a very limited

number of surfactants and oils. Measuring the PIT can at best be used as a guide for the preparation of stable emulsions. Assessment of the stability should be evaluated by following the droplet size distribution as a function of time using a Coulter Counter or light diffraction techniques. Following the rheology of the emulsion as a function of time and temperature may also be used for assessing the stability against coalescence. Care should be taken in analysing the rheological results. Coalescence results in an increase in droplet size and this is usually followed by a reduction in the viscosity of the emulsion. This trend is only observed if the coalescence is not accompanied by flocculation of the emulsion droplets (which results in an increase in the viscosity). Ostwald ripening can also complicate the analysis of the rheological data.

2.6.3 The cohesive energy (CER) concept for emulsifier selection

Beerbower and Hills [16] considered the dispersing tendency of the oil and water interfaces of the surfactant or emulsifier in terms of the ratio of the cohesive energies of the mixtures of oil with the lipophilic portion of the surfactant, and the water with the hydrophilic portion. They used the Winsor R_0 concept which is the ratio of the intermolecular attraction of oil molecules (O) and lipophilic portion of surfactant (L), C_{LO}, to that of water (W) and hydrophilic portion (H), C_{HW},

$$R_0 = \frac{C_{LO}}{C_{HW}}. \tag{2.16}$$

Several interaction parameters may be identified at the oil and water sides of the interface. One can identify at least nine interaction parameters, as illustrated in Fig. 2.5.

C_{LL}, C_{OO}, C_{LO} (at oil side)

C_{HH}, C_{WW}, C_{HW} (at water side)

C_{LW}, C_{HO}, C_{LH} (at the interface)

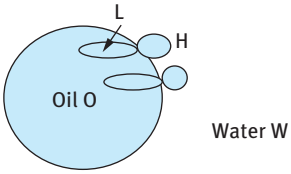

Fig. 2.5: Schematic representation of interaction parameters.

In the absence of emulsifier, there will be only three interaction parameters: C_{OO}, C_{WW}, C_{OW}; if $C_{OW} \ll C_{WW}$, the emulsion breaks.

The above interaction parameters may be related to the Hildebrand solubility parameter δ [17] (at the oil side of the interface) and the Hansen [18] nonpolar, hydrogen bonding and polar contributions to δ at the water side of the interface. The solubility

parameter of any component is related to its heat of vaporization ΔH by the expression,

$$\delta_2 = \frac{\Delta H - RT}{V_M}, \tag{2.17}$$

where V_M is the molar volume.

Hansen [18] considered δ (at the water side of the interface) to consist of three main contributions: a dispersion contribution, δ_d, a polar contribution, δ_p and a hydrogen bonding contribution, δ_h. These contributions have different weighting factors,

$$\delta^2 = \delta_d^2 + \delta_p^2 + \delta_h^2. \tag{2.18}$$

Beerbower and Hills [16] used the following expression for the HLB number,

$$HLB = 20\frac{M_H}{M_L + M_H} = 20\frac{V_H\rho_H}{V_L\rho_L + V_H\rho_H}, \tag{2.19}$$

where M_H and M_L are the molecular weights of the hydrophilic and lipophilic portions of the surfactants. V_L and V_H are their corresponding molar volumes whereas ρ_H and ρ_L are the densities respectively.

The cohesive energy ratio was originally defined by Winsor, equation (2.16). When $C_{LO} > C_{HW}$, $R > 1$ and a W/O emulsion forms. If $C_{LO} < C_{HW}$, $R < 1$ and an O/W emulsion forms. If $C_{LO} = C_{HW}$, $R = 1$ and a planer system results; this denotes the inversion point.

R_0 can be related to V_L, δ_L and V_H, δ_H by the expression,

$$R_0 = \frac{V_L\delta_L^2}{V_H\delta_H^2}. \tag{2.20}$$

Using equation (2.19),

$$R_0 = \frac{V_L(\delta_d^2 + 0.25\delta_p^2 + 0.25\delta_h^2)_L}{V_H(\delta_d^2 + 0.25\delta_p^2 + 0.25\delta_h^2)_H}. \tag{2.21}$$

Combining equations (2.20) and (2.21), one obtains the following general expression for the cohesive energy ratio,

$$R_0 = \left(\frac{20}{HLB} - 1\right)\frac{\rho_H(\delta_d^2 + 025\delta_p^2 + 0.25\delta_h^2)_L}{\rho_L(\delta_d^2 + 0.25\delta_p^2 + 0.25\delta_p^2)_L}. \tag{2.22}$$

For O/W systems, HLB = 12–15 and $R_0 = 0.58–0.29$ ($R_0 < 1$). For W/O systems, HLB = 5–6 and $R_0 = 2.3–1.9$ ($R_0 > 1$). For a planer system, HLB = 8–10 and $R_0 = 1.25–0.85$ ($R_0 \approx 1$).

The R_0 equation combines both the HLB and cohesive energy densities. It gives a more quantitative estimate of emulsifier selection. R_0 considers HLB, molar volume and chemical match. The success of the above approach depends on the availability of data on the solubility parameters of the various surfactant portions. Some values are tabulated in the book by Barton [19].

2.6.4 The critical packing parameter (CPP) for emulsifier selection

The critical packing parameter (CPP) is a geometric expression relating the hydrocarbon chain volume (v) and length (l) and the interfacial area occupied by the head group (a) [20],

$$\text{CPP} = \frac{v}{l_c a_0}. \tag{2.23}$$

a_0 is the optimal surface area per head group, l_c is the critical chain length.

Regardless of the shape of any aggregated structure (spherical or cylindrical micelle, or a bilayer), no point within the structure can be farther from the hydrocarbon–water surface than l_c. The critical chain length, l_c, is roughly equal to but less than the fully extended length of the alkyl chain.

The CPP for any micelle shape can be calculated from simple packing constrains. Consider a spherical micelle,

$$\text{volume of the micelle} = \left(\frac{4}{3}\right)\pi r^3 = nv, \tag{2.24}$$

$$\text{area of the micelle} = 4\pi r^2 = na. \tag{2.25}$$

v is the volume of the hydrocarbon chain and n is the aggregation number.

The cross-sectional area of the hydrocarbon chain,

$$a_0 = \frac{v}{l_c}. \tag{2.26}$$

From equations (2.25) and (2.26)

$$a = \frac{3v}{r}. \tag{2.27}$$

Since r has to be less than l_c, packing constrains imply that $a > 3a_0$ or $a_0/a < 1/3$. Thus, the CPP for a spherical micelle is $< 1/3$.

Surfactants that form spherical micelles with the above packing constraints are more suitable for O/W emulsions.

For a cylindrical micelle,

$$\text{volume} = \pi r^2 l = nv, \tag{2.28}$$

$$\text{area} = 2\pi r\, l = na, \tag{2.29}$$

$$a = \frac{2v}{r}, \tag{2.30}$$

Since r has to be less than the extended length of the hydrocarbon chain l_c, then packing constraints imply that $a > 2a_0$ or $a_0/a < 1/2$. Thus the CPP for a cylindrical micelle is $< 1/2$.

When the CPP exceeds 1/2, but is less than 1, spherical bilayers (vesicles) can be produced. When the CPP is ≈ 1, the bilayers may remain planer.

When the CPP > 1, inverted micelles are produced. Surfactants that produce these structures are suitable for formation of W/O emulsions.

2.7 Emulsion stability

Several breakdown processes may occur on storage depending on:

(i) Particle size distribution and density difference between the droplets and the medium.
(ii) Magnitude of the attractive versus repulsive forces which determines flocculation.
(iii) Solubility of the disperse droplets and the particle size distribution which determines Ostwald ripening.
(iv) Stability of the liquid film between the droplets that determines coalescence.
(v) Phase Inversion.

The various breakdown processes are illustrated in the Fig. 2.6. This is followed by a description of each of the breakdown processes and methods that can be applied to prevent such instability.

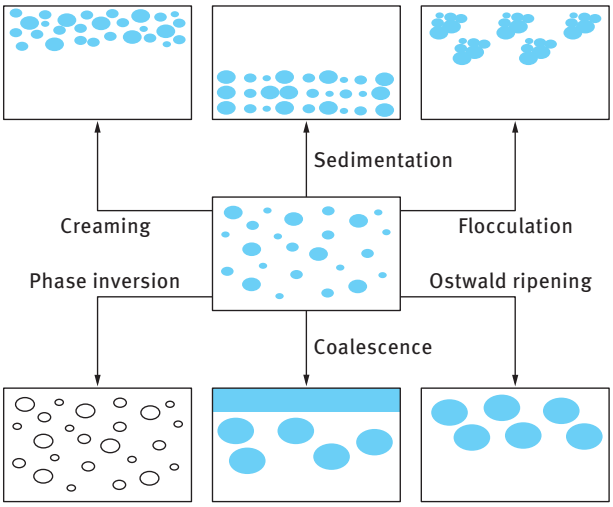

Fig. 2.6: Schematic representation of the various breakdown processes in emulsions.

It should be mentioned that understanding each of these breakdown processes at a molecular lever is far from being achieved at present. This is due to the fact that the breakdown processes can occur simultaneously. In addition, preparation of model emulsions that are monodisperse is difficult. Also the adsorption and conformation of surfactants and polymers at the O/W interface involves various interactions with the oil and continuous phases and it is difficult to understand such interactions at a molecular level.

2.7.1 Creaming or sedimentation of emulsions

This is the result of gravity, when the density of the droplets and the medium are not equal. Fig. 2.7 and 2.8 and give a schematic picture for creaming or sedimentation for three cases [1].

Case (a) represents the situation for small droplets (< 0.1 μ, i.e. nanoemulsions) in which the Brownian diffusion kT (where k is the Boltzmann constant and T is the absolute temperature) exceeds the force of gravity (mass × acceleration due to gravity g),

$$kT \ll \frac{4}{3}\pi R^3 \Delta\rho g L, \tag{2.31}$$

where R is the droplet radius, $\Delta\rho$ is the density difference between the droplets and the medium and L is the height of the container.

Case (b) represents emulsions consisting of "monodisperse" droplets with a radius >1 μm. In this case, the emulsion separates into two distinct layers with the droplets forming a cream or sediment leaving a clear supernatant liquid. This situation is seldom observed in practice.

Case (c) is that for a polydisperse (practical) emulsion, in which case the droplets will cream or sediment at various rates. In this last case, a concentration gradient

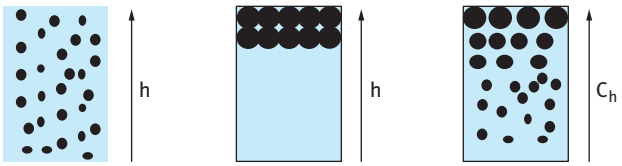

Fig. 2.7: Schematic representation of emulsion creaming.

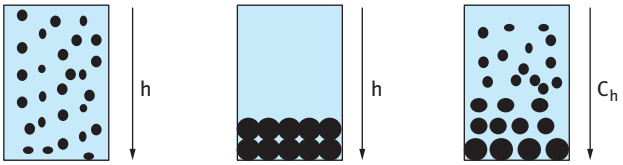

Fig. 2.8: Schematic representation of sedimentation of emulsions.

builds up with the larger droplets staying at the top of the cream layer or the bottom,

$$C(h) = C_0 \exp\left(-\frac{mgh}{kT}\right), \tag{2.32}$$

$$m = \frac{4}{3}\pi R^3 \Delta\rho g. \tag{2.33}$$

$C(h)$ is the concentration (or volume fraction ϕ) of droplets at height h, whereas C_0 is the concentration at top or bottom of the container.

The creaming or sedimentation rate of the emulsion depends on the volume fraction ϕ of the system. For very dilute emulsions ($\phi < 0.01$), the rate could be calculated using Stokes' law which balances the hydrodynamic force with gravity force,

$$\text{hydrodynamic force} = 6\pi\eta R v_0, \tag{2.34}$$

$$\text{gravity force} = \frac{4}{3}\pi R^3 \Delta\rho g, \tag{2.35}$$

$$v_0 = \frac{2}{9}\frac{\Delta\rho g R^2}{\eta_0}. \tag{2.36}$$

v_0 is the Stokes velocity and η_0 is the viscosity of the medium.

For an O/W emulsion with $\Delta\rho = 0.2$ in water ($\eta_0 \approx 10^{-3}$ Pa s), the rate of creaming or sedimentation is $\approx 4.4 \times 10^{-5}$ m s^{-1} for 10 µm droplets and $\approx 4.4 \times 10^{-7}$ m s^{-1} for 1 µm droplets. This means that in a 0.1 m container creaming or sedimentation of the 10 µm droplets is complete in ≈ 0.6 hour and for the 1 µm droplets this takes ≈ 60 hours.

For moderately concentrated emulsions ($0.2 > \phi > 0.1$) one has to take into account the hydrodynamic interaction between the droplets, which reduces the Stokes velocity to a value v given by the following expression,

$$v = v_0(1 - k\phi), \tag{2.37}$$

where k is a constant that accounts for hydrodynamic interaction. k is of the order of 6.5, which means that the rate of creaming or sedimentation is reduced by about 65 %.

For concentrated emulsions ($\phi > 0.2$), the rate of creaming or sedimentation becomes a complex function of ϕ as is illustrated in Fig. 2.9, which also shows the change of relative viscosity η_r with ϕ. As can be seen from Fig. 2.9, v decreases with increasing ϕ and ultimately it approaches zero when ϕ exceeds a critical value, ϕ_p, which is the so-called "maximum packing fraction".

The value of ϕ_p for monodisperse "hard spheres" ranges from 0.64 (for random packing) to 0.74 for hexagonal packing. The value of ϕ_p exceeds 0.74 for polydisperse systems. Also for emulsions which are deformable, ϕ_p can be much larger than 0.74.

The above figure also shows that when ϕ approaches ϕ_p, η_r approaches ∞. In practice most emulsions are prepared at ϕ values well below ϕ_p, usually in the range 0.2–0.5, and under these conditions creaming or sedimentation is the rule rather than the exception.

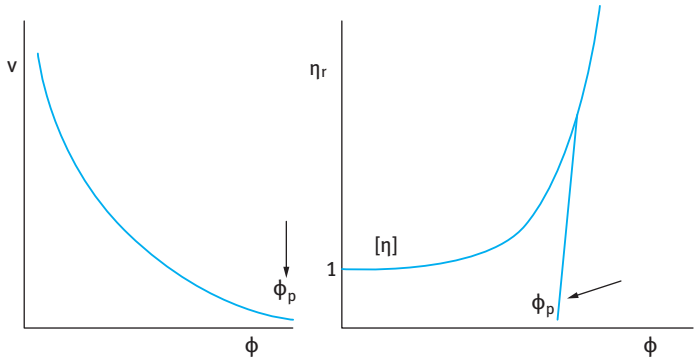

Fig. 2.9: Variation of v and η_r with ϕ.

Several procedures may be applied to reduce or eliminate creaming or sedimentation:

(i) Matching density of oil and aqueous phases. Clearly if $\Delta\rho = 0$, $v = 0$; however, this method is seldom practical. Density matching, if possible, only occurs at one temperature.

(ii) Reduction of droplet size. Since the gravity force is proportional to R^3, then if R is reduced by a factor of 10, the gravity force is reduced by 1000. Below a certain droplet size (which also depends on the density difference between oil and water), the Brownian diffusion may exceed gravity and creaming or sedimentation is prevented. This is the principle of formulation of nanoemulsions (with size range 50–200 nm) which may show very little or no creaming or sedimentation. The same applies for microemulsions (size range 5–50 nm).

(iii) Use of "thickeners" that are high molecular weight polymers, natural or synthetic such as xanthan gum, hydroxyethyl cellulose, alginates, carrageenans, etc. To understand the role of these "thickeners", let us consider the gravitational stresses exerted during creaming or sedimentation,

$$\text{stress} = \text{mass of drop} \times \text{acceleration of gravity} = \frac{4}{3}\pi R^3 \Delta\rho g. \tag{2.38}$$

To overcome such stress one needs a restoring force,

$$\text{restoring force} = \text{area of drop} \times \text{stress of drop} = 4\pi R^2 \sigma_p. \tag{2.39}$$

Thus, the stress exerted by the droplet σ_p is given by,

$$\sigma_p = \frac{\Delta\rho R g}{3}. \tag{2.40}$$

Simple calculation shows that σ_p is in the range 10^{-3}–10^{-1} Pa, which implies that for predicting creaming or sedimentation one needs to measure the viscosity at such low stresses. This can be obtained by using constant stress or creep measurements.

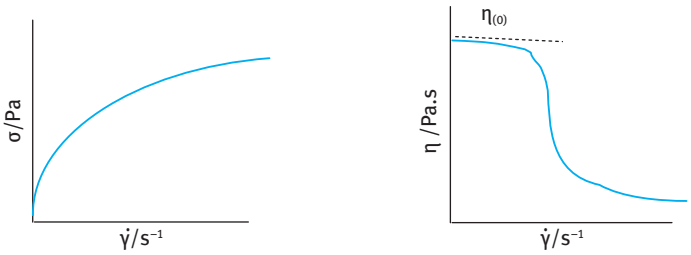

Fig. 2.10: Variation of (stress) σ and viscosity η with shear rate γ.

The above described "thickeners" satisfy the criteria for obtaining very high viscosities at low stresses or shear rates. This can be illustrated from plots of shear stress τ and viscosity η versus shear rate (or shear stress), as shown in Fig. 2.10.

These systems are described as "pseudoplastic" or shear thinning. The low shear (residual or zero shear rate) viscosity $\eta(0)$ can reach several thousand Pa s and such high values prevent creaming or sedimentation.

The above behaviour is obtained above a critical polymer concentration (C^*) which can be located from plots of log η versus log C as illustrated in Fig. 2.11. Below C^* the log η–log C curve has a slope in the region of 1, whereas above C^* the slope of the line exceeds 3.

(iv) Controlled flocculation. The total energy–distance of separation curve for electrostatically stabilized particles shows a shallow minimum (secondary minimum) at relatively long distance of separation between the droplets. By addition of small amounts of electrolyte, such a minimum can be made sufficiently deep for weak flocculation to occur. The same applies for sterically stabilized emulsions, which show only one minimum, whose depth can be controlled by reducing the thickness of the adsorbed layer. This can be obtained by reducing the molecular weight of the stabilizer and/or addition of a nonsolvent for the chains (e.g. electrolyte).

The above phenomenon of weak flocculation may be applied to reduce creaming or sedimentation, although in practice this is not easy since one has also to control the droplet size.

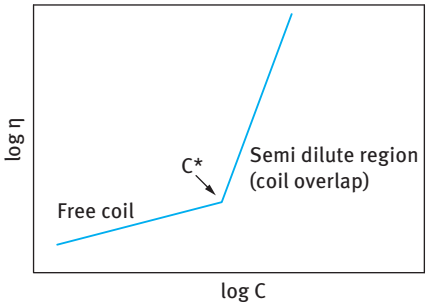

Fig. 2.11: log η–log C for polymer solutions.

(v) Depletion flocculation obtained by addition of "free" (nonadsorbing) polymer in the continuous phase [21, 22]. At a critical concentration, or volume fraction of free polymer, ϕ_p^+, weak flocculation occurs, since the free polymer coils become "squeezed out" from between the droplets. This is illustrated in Fig. 2.12 which shows the situation when the polymer volume fraction exceeds the critical concentration.

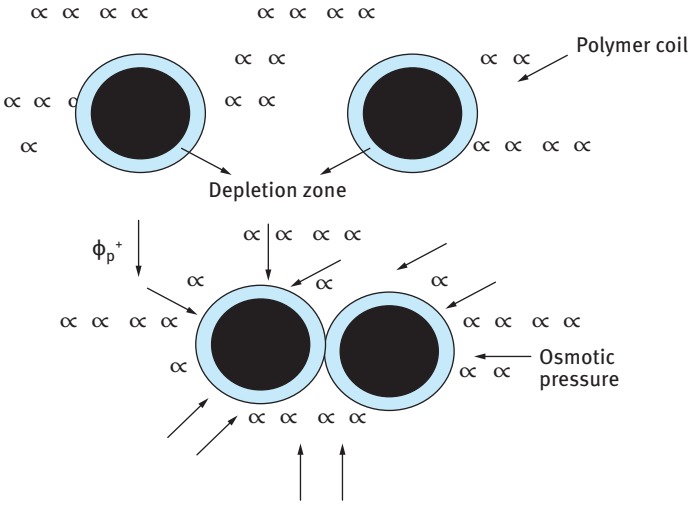

Fig. 2.12: Schematic representation of depletion flocculation.

The osmotic pressure outside the droplets is higher than in between the droplets and this results in attraction whose magnitude depends on the concentration of the free polymer and its molecular weight, as well as the droplet size and ϕ. The value of ϕ_p^+ decreases with increasing molecular weight of the free polymer. It also decreases as the volume fraction of the emulsion increases.

The above weak flocculation can be applied to reduce creaming or sedimentation although it suffers from the following drawbacks: Temperature dependency; as the temperature increases, the hydrodynamic radius of the free polymer decreases (due to dehydration) and hence more polymer will be required to achieve the same effect at lower temperatures. If the free polymer concentration is increased above a certain limit, phase separation may occur and the flocculated emulsion droplets may cream or sediment faster than in the absence of the free polymer.

2.7.2 Flocculation of emulsions

Flocculation is the result of van der Waals attraction that is universal for all disperse systems. The van der Waals attraction G_A is inversely proportional to the droplet-

droplet distance of separation h and it depends on the effective Hamaker constant A of the emulsion system. One way to overcome the van der Waals attraction is by electrostatic stabilization using ionic surfactants which results in the formation of electrical double layers that introduce a repulsive energy that overcomes the attractive energy. Emulsions stabilized by electrostatic repulsion become flocculated at intermediate electrolyte concentrations. The second and most effective method of overcoming flocculation is by "steric stabilization" using nonionic surfactants or polymers. Stability may be maintained in electrolyte solutions (as high as 1 mol dm^{-3} depending on the nature of the electrolyte) and up to high temperatures (in excess of 50 °C) provided the stabilizing chains (e.g. PEO) are still in better than θ-conditions ($\chi < 0.5$).

For charge-stabilized emulsions, e.g. using ionic surfactants, the most important criterion is to make G_{max} as high as possible; this is achieved by three main conditions: high surface or zeta potential, low electrolyte concentration and low valency of ions.

For sterically stabilized emulsions, four main criteria are necessary in this case:

(i) Complete coverage of the droplets by the stabilizing chains.
(ii) Firm attachment (strong anchoring) of the chains to the droplets.

This requires the chains to be insoluble in the medium and soluble in the oil. However, this is incompatible with stabilization which requires a chain that is soluble in the medium and strongly solvated by its molecules. These conflicting requirements are solved by the use of A–B, A–B–A block or BA_n graft copolymers (B is the "anchor" chain and A is the stabilizing chain(s))

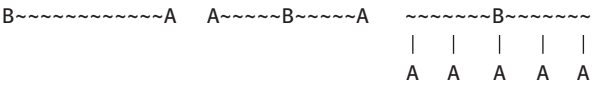

Examples for the B chains for O/W emulsions are polystyrene, polymethylmethacrylate, polypropylene oxide and alkyl polypropylene oxide. For the A chain(s), polyethylene oxide (PEO) or polyvinyl alcohol are good examples.

(iii) Thick adsorbed layers. The adsorbed layer thickness should be in the region of 5–10 nm. This means that the molecular weight of the stabilizing chains could be in the region of 1000–5000.
(iv) The stabilizing chain should be maintained in good solvent conditions ($\chi < 0.5$) under all conditions of temperature changes on storage.

2.7.3 Ostwald ripening

The driving force for Ostwald ripening is the difference in solubility between the small and large droplets (the smaller droplets have higher Laplace pressure and higher solubility than the larger ones). This is illustrated Fig. 2.13 where r_1 decreases and r_2 increases as a result of diffusion of molecules from the smaller to the larger droplets.

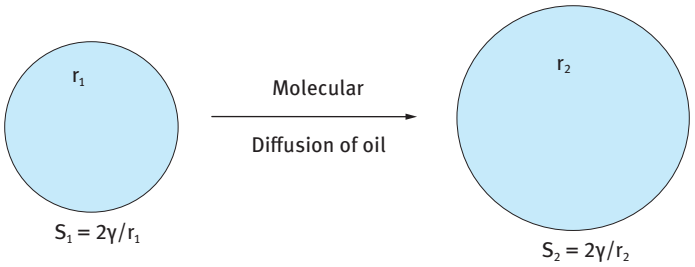

Fig. 2.13: Schematic representation of Ostwald ripening.

The difference in chemical potential between different sized droplets was given by Lord Kelvin [23],

$$S(r) = S(\infty)\exp\left(\frac{2\gamma V_m}{rRT}\right), \tag{2.41}$$

where $S(r)$ is the solubility surrounding a particle of radius r, $S(\infty)$ is the bulk solubility, V_m is the molar volume of the dispersed phase, R is the gas constant and T is the absolute temperature. The quantity $(2\gamma V_m/RT)$ is termed the characteristic length. It has an order of ≈ 1 nm or less, indicating that the difference in solubility of a 1 µm droplet is of the order of 0.1 % or less. Theoretically, Ostwald ripening should lead to condensation of all droplets into a single drop [23]. This does not occur in practice since the rate of growth decreases with increasing droplet size.

For two droplets with radii r_1 and r_2 ($r_1 < r_2$),

$$\frac{RT}{V_m}\ln\left[\frac{S(r_1)}{S(r_2)}\right] = 2\gamma\left[\frac{1}{r_1} - \frac{1}{r_2}\right]. \tag{2.42}$$

Equation (2.42) shows that the larger the difference between r_1 and r_2, the higher the rate of Ostwald ripening.

Ostwald ripening can be quantitatively assessed from plots of the cube of the radius versus time t [24–26],

$$r^3 = \frac{8}{9}\left[\frac{S(\infty)\gamma V_m D}{\rho RT}\right]t. \tag{2.43}$$

D is the diffusion coefficient of the disperse phase in the continuous phase.

Several methods may be applied to reduce Ostwald ripening:

(i) Addition of a second disperse phase component which is insoluble in the continuous medium (e.g. squalane) [24]. In this case partitioning between different droplet sizes occurs, with the component having low solubility expected to be concentrated in the smaller droplets. During Ostwald ripening in a two component system, equilibrium is established when the difference in chemical potential between different size droplets (which results from curvature effects) is balanced by the difference in chemical potential resulting from partitioning of the two components. This effect reduces further growth of droplets.

(ii) Modification of the interfacial film at the O/W interface. According to equation (2.43) a reduction in γ results in reduction of Ostwald ripening rate. By using surfactants that are strongly adsorbed at the O/W interface (i.e. polymeric surfactants) and which do not desorb during ripening (by choosing a molecule that is insoluble in the continuous phase) the rate could be significantly reduced [27].

An increase in the surface dilational modulus ε (= $\mathrm{d}\gamma/\mathrm{d}\ln A$) and decrease in γ would be observed for the shrinking drop and this tends to reduce further growth. A–B–A block copolymers such as PHS–PEO–PHS (which is soluble in the oil droplets but insoluble in water) can be used to achieve the above effect. This polymeric emulsifier enhances the Gibbs elasticity and causes reduction of γ to very low values.

2.7.4 Coalescence of emulsions

When two emulsion droplets come in close contact in a floc or creamed layer or during Brownian diffusion, thinning and disruption of the liquid film may occur, resulting in eventual rupture. On close approach of the droplets, film thickness fluctuations may occur. Alternatively, the liquid surfaces undergo some fluctuations forming surface waves, as illustrated in Fig. 2.14.

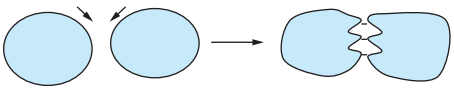

Fig. 2.14: Schematic representation of surface fluctuations.

The surface waves may grow in amplitude and the apices may join as a result of the strong van der Waals attraction (at the apex, the film thickness is the smallest). The same applies if the film thins to a small value (critical thickness for coalescence).

A very useful concept was introduced by Deryaguin [28] who suggested that a "disjoining pressure" $\pi(h)$ is produced in the film which balances the excess normal pressure,

$$\pi(h) = P(h) - P_0, \tag{2.44}$$

where $P(h)$ is the pressure of a film with thickness h and P_0 is the pressure of a sufficiently thick film such that the net interaction free energy is zero.

$\pi(h)$ may be equated to the net force (or energy) per unit area acting across the film,

$$\pi(h) = -\frac{\mathrm{d}G_\mathrm{T}}{\mathrm{d}h}, \tag{2.45}$$

where G_T is the total interaction energy in the film.

$\pi(h)$ is made up of three contributions due to electrostatic repulsion (π_E), steric repulsion (π_S) and van der Waals attraction (π_A),

$$\pi(h) = \pi_E + \pi_S + \pi_A. \tag{2.46}$$

To produce a stable film, $\pi_E + \pi_S > \pi_A$ and this is the driving force for prevention of coalescence which can be achieved by two mechanisms and their combination:

(i) Increased repulsion both electrostatic and steric.
(ii) Dampening of the fluctuation by enhancing the Gibbs elasticity.

In general, smaller droplets are less susceptible to surface fluctuations and hence coalescence is reduced. This explains the high stability of nanoemulsions. Several methods may be applied to achieve the above effects:

(i) Use of mixed surfactant films. In many cases using mixed surfactants, say anionic and nonionic or long chain alcohols can reduce coalescence as a result of several effects: High Gibbs elasticity; high surface viscosity; hindered diffusion of surfactant molecules from the film.
(ii) Formation of lamellar liquid crystalline phases at the O/W interface. This mechanism was investigated by Friberg and co-workers [29], who suggested that surfactant or mixed surfactant film can produce several bilayers that "wrap" the droplets. As a result of these multilayer structures, the potential drop is shifted to longer distances, thus reducing the van der Waals attraction.

A schematic representation of the role of liquid crystals is shown in Fig. 2.15, which illustrates the difference between having a monomolecular layer and a multilayer as is the case with liquid crystals. For coalescence to occur, these multilayers have to be removed "two-by-two" and this forms an energy barrier, preventing coalescence.

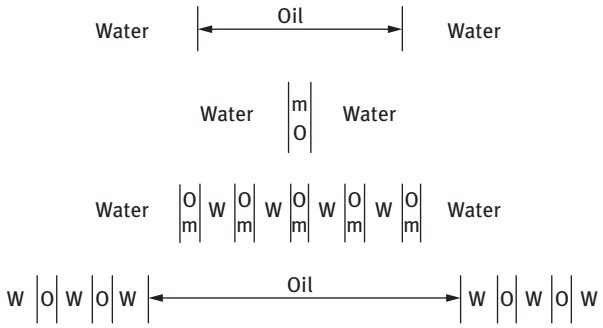

Upper part monomolecular layer

Lower part presence of liquid crystalline phases

Fig. 2.15: Schematic representation of the role of liquid crystalline phases.

Since film drainage and rupture is a kinetic process, coalescence is also a kinetic process. If one measures the number of particles n (flocculated or not) at time t,

$$n = n_t + n_v m, \tag{2.47}$$

where n_t is the number of primary particles remaining, n is the number of aggregates consisting of m separate particles.

For studding emulsion coalescence, one should consider the rate constant of flocculation and coalescence. If coalescence is the dominant factor, then the rate K follows a first order kinetics,

$$n = \frac{n_0}{Kt}[1 + \exp -(Kt)], \tag{2.48}$$

which shows that a plot of log n versus t should give a straight line from which K can be calculated.

2.7.5 Phase inversion

Phase inversion of emulsions can be one of two types: Transitional inversion induced by changing factors which affect the HLB of the system, e.g. temperature and/or electrolyte concentration or catastrophic inversion, which is induced by increasing the volume fraction of the disperse phase [1].

Catastrophic inversion is illustrated in Fig. 2.16, which shows the variation of viscosity and conductivity with the oil volume fraction ϕ. As can be seen, inversion occurs at a critical ϕ, which may be identified with the maximum packing fraction. At ϕ_{cr}, η suddenly decreases; the inverted W/O emulsion has a much lower volume fraction. κ also decreases sharply at the inversion point since the continuous phase is now oil, which has very low conductivity.

Earlier theories of phase inversion were based on packing parameters. When ϕ exceeds the maximum packing (≈ 0.64 for random packing and ≈ 0.74 for hexagonal packing of monodisperse spheres; for polydisperse systems, the maximum packing exceeds 0.74) inversion occurs. However, these theories are not adequate, since

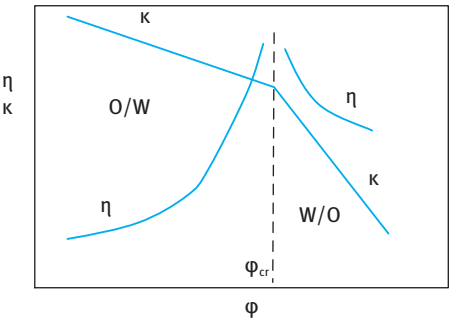

Fig. 2.16: Variation of viscosity (η) and conductivity (κ) with oil volume fraction.

many emulsions invert at ϕ values well below the maximum packing as a result of the change in surfactant characteristics with variation of conditions. For example, when using a nonionic surfactant based on PEO, the latter chain changes its solvation with increasing temperature and/or addition of electrolyte. Many emulsions show phase inversion at a critical temperature (the phase inversion temperature) that depends on the HLB number of the surfactant as well as the presence of electrolytes. By increasing temperature and/or addition of electrolyte, the PEO chains become dehydrated and finally they become more soluble in the oil phase. Under these conditions the O/W emulsion will invert to a W/O emulsion. This dehydration effect amounts to a decrease in the HLB number and when the latter reaches a value that is more suitable for W/O emulsion inversion will occur. At present, there is no quantitative theory that accounts for phase inversion of emulsions.

2.8 Experimental methods for assessing emulsion stability

Several methods may be applied to assess the creaming or sedimentation of emulsions:

(i) Measurement of the rate by direct observation of emulsion separation using graduated cylinders that are placed at constant temperature. This method allows one to obtain the rate as well as the equilibrium cream or sediment volume.
(ii) Turbidity measurements as a function of height at various times, using for example the Turboscan (that measures turbidity from the back scattering of near IR light).
(iii) Ultrasonic velocity and absorption at various heights in the cream or sedimentation tubes.

Centrifugation may be applied to accelerate the rate of creaming or sedimentation and this method is sometimes used for the prediction of emulsion stability. The assumption is made that by increasing the g force the rate of sedimentation or creaming is significantly increased and this could be applied to predict the process from measurements at short time periods.

In a centrifuge, the gravity force is given by,

$$g = \omega^2 x, \tag{2.49}$$

where x is the mean distance of the centrifuge tube from the axis of rotation and ω is the angular velocity ($\omega = 2\pi\nu$, where ν is the number of revolutions per second). Note that if the centrifuge tube is not small compared to x, then the applied centrifugal field cannot be considered to be uniform over the length of the tube.

Modern analytical ultracentrifuges allow one to follow the separation of emulsions in a quantitative manner. With typical O/W emulsions, three layers are generally observed: A clear aqueous phase, an opaque phase consisting of distorted polyhedral

oil droplets and a clear separated oil phase, resulting from coalescence of the polyhedra. The degree of emulsion stability may be taken as the volume of the opaque phase remaining after time t. Alternatively, one may use the volume of oil separated at infinite time as an index for stability.

A simple expression may be used to treat the data in a quantitative manner,

$$\frac{t}{V} = \frac{1}{bV_\infty} + \frac{t}{V_\infty}, \tag{2.50}$$

where V is the volume of oil separated at time t, V_∞ is the extrapolated volume at infinite time and b is a constant. A plot of t/V versus t should give a straight line from which b and V_∞ may be calculated. These two parameters may be taken as indices for emulsion stability.

A more rigorous procedure to study emulsion stability using the ultracentrifuge is to observe the system at various speeds of rotation. At relatively low centrifuge speeds one may observe the expected opaque cream layer. At sufficiently high centrifuge speeds, one may observe a coalesced oil layer and a cream layer which are separated by an extra layer of deformed oil droplets. This deformed layer looks like a "foam", i.e. it consists of oil droplets separated by thin aqueous films.

For certain emulsions, one may find that by increasing the centrifuge speed, the "foam"/cream layer boundary does not move. Under conditions where there is an equilibrium between the "foam"/cream layer, one may conclude that there is no barrier to be overcome in forming the foam layer from the cream layer. This implies that in the foam layer, the aqueous film separating two oil droplets thins to a "black" film under the action of van der Waals forces. The boundary between the foam layer and the coalesced layer is associated with a force (or pressure) barrier. One may observe the minimum centrifuge speed that is necessary to produce a visible amount of coalesced oil after say 30 minutes of centrifugation. This centrifuge speed may be used to calculate the "critical pressure" that needs to be applied to induce coalescence.

For assessing flocculation of emulsions (which may be obtained by carefully diluting the concentrate in the supernatant liquid), the rate can be determined by measuring turbidity, τ, as a function of time,

$$\tau = An_0V_1^2(1 + n_0kt), \tag{2.51}$$

where A is an optical constant, n_0 is the number of droplets at time $t = 0$, V_1 is the volume of the droplets and k is the rate constant of flocculation.

Thus, a plot of τ versus t gives a straight line, in the initial time of flocculation, and k can be calculated from the slope of the line. Flocculation of emulsions can also be assessed by direct droplet counting using optical microscopy (with image analysis), using the Coulter Counter and light diffraction techniques (e.g. using the Mastersizer, Malvern, UK).

The flocculation of emulsion concentrate can be followed using rheological methods. In the absence of any Ostwald ripening and/or coalescence flocculation of the

emulsion concentrates is accompanied by an increase in its viscosity, yield value or elastic modulus. These rheological parameters can be easily measured using rotational viscometers. Clearly if Ostwald ripening and/or coalescence occurs at the same time as emulsion flocculation the viscosity, yield value or elastic modulus will show a complex dependence of these parameters on time and this makes the analysis of the rheological results very difficult.

The best procedure to follow Ostwald ripening is to plot r^3 versus time, following equation (2.43). This gives a straight line from which the rate of Ostwald ripening can be calculated. In this way one can assess the effect of the various additives that may reduce Ostwald ripening, e.g. addition of highly insoluble oil and/or an oil-soluble polymeric surfactant.

The rate of coalescence is measured by following the droplet number n or average droplet size d (diameter) as a function of time. Plots of log droplet number or average diameter versus time give straight lines (at least in the initial stages of coalescence) from which the rate of coalescence K can be estimated using equation (2.48). In this way one can compare the different stabilizers, e.g. mixed surfactant films, liquid crystalline phase and macromolecular surfactant.

The most common procedure to assess phase inversion is to measure the conductivity or the viscosity of the emulsion as a function of ϕ, increase of temperature and/or addition of electrolyte. For example, for an O/W emulsion, phase inversion to W/O is accompanied by a rapid decrease in conductivity and viscosity.

References

[1] Tadros T. Emulsions. Berlin: De Gruyter; 2016.
[2] Walstra P, Smolders PEA. In: Binks BP, editor. Modern aspects of emulsions. Cambridge: The Royal Society of Chemistry; 1998.
[3] Stone HA. Ann Rev Fluid Mech. 1994;226:95.
[4] Wierenga JA, ven Dieren F, Janssen JJM, Agterof WGM. Trans Inst Chem Eng. 1996;74-A:554.
[5] Levich VG. Physicochemical hydrodynamics. Englewood Cliffs: Prentice-Hall; 1962.
[6] Davis JT. Turbulent phenomena. London: Academic Press; 1972.
[7] Lucassen-Reynders EH. In: Becher P, editor. Encyclopedia of emulsion technology. New York: Marcel Dekker; 1996.
[8] Lucassen-Reynders EH. Colloids and Surfaces. 1994;A91:79.
[9] Lucassen J. In: Lucassen-Reynders EH, editor. Anionic surfactants. New York: Marcel Dekker; 1981.
[10] van den Tempel M. Proc Int Congr Surf Act. 1960;2:573.
[11] Griffin WC. J Cosmet Chemists. 1949;1:311; 1954;5:249.
[12] Becher P. In: Schick MJ, editor. Nonionic surfactants: Physical chemistry. New York: Marcel Dekker; 1987.
[13] Davies JT. Proc Int Congr Surface Activity, Vol. 1. 1959, p. 426. Davies JT, Rideal EK. Interfacial phenomena. New York: Academic Press; 1961.
[14] Shinoda K. J Colloid Interface Sci. 1967;25:396.
[15] Shinoda K, Saito H. J Colloid Interface Sci. 1969;30:258.

[16] Beerbower A, Hill MW. Amer Cosmet Perfum. 1972;87:85.
[17] Hildebrand JH. Solubility of non-electrolytes. 2nd edition. New York: Reinhold; 1936.
[18] Hansen CM. J Paint Technol. 1967;39:505.
[19] Barton AFM. Handbook of solubility parameters and other cohesive parameters. New York: CRC Press; 1983.
[20] Israelachvili JN, Mitchell DJ, Ninham BW. J Chem Soc Faraday Trans II. 1976;72:1525.
[21] Asakura A, Oosawa F. J Polymer Sci. 1958;93:183.
[22] Fleer GJ, Scheutjens JMHM, Vincent B. ACS Symposium Series. 1984:240;245.
[23] Thompson W (Lord Kelvin). Phil Mag. 1871;42:448.
[24] Kabalnov AS, Schukin ED. Adv Colloid Interface Sci. 1992;38:69. Kabalanov AS. Langmuir. 1994;10:680.
[25] Lifshitz EM, Slesov VV. Soviet Physics JETP. 1959;35:331.
[26] Wagner C. Z Electrochem. 1961;35:581.
[27] Walstra P. In: Becher P, editor. Encyclopedia of emulsion technology, Vol. 4. New York: Marcel Dekker; 1996.
[28] Deryaguin BV, Scherbaker RL. Kolloid Zh. 1961;23:33.
[29] Friberg S, Jansson PO, Cederberg E. J Colloid Interface Sci. 1976;55:614.

3 Suspension concentrates (SCs)

3.1 Introduction

The formulation of agrochemicals as dispersions of solids in aqueous solution (to be referred to as suspension concentrates or SCs) has attracted considerable attention in recent years. Such formulations are a natural replacement to wettable powders (WPs). The latter are produced by mixing the active ingredient with a filler (usually a clay material) and a surfactant (dispersing and wetting agent). These powders are dispersed into the spray tank to produce a coarse suspension which is applied to the crop. Although wettable powders are simple to formulate they are not the most convenient for the farmer. Apart from being dusty (and occupying a large volume due to their low bulk density), they tend to settle fast in the spray tank and they do not provide optimum biological efficiency as a result of the large particle size of the system. In addition, one cannot incorporate the necessary adjuvants (mostly surfactants) in the formulation. These problems are overcome by formulating the agrochemical as an aqueous SC.

Several advantages may be quoted for SCs. Firstly, one may control the particle size by controlling the milling conditions and proper choice of the dispersing agent. Secondly, it is possible to incorporate high concentrations of surfactants in the formulation which is sometimes essential for enhancing wetting, spreading and penetration (see Chapter 8). Stickers may also be added to enhance adhesion and in some cases to provide slow release.

In recent years there has been considerable research into the factors that govern the stability of suspension concentrates [1–3]. The theories of colloid stability could be applied to predict the physical states of these systems on storage. In addition, analysis of the problem of sedimentation of SCs at a fundamental level has been undertaken [4]. Since the density of the particles is usually larger than that of the medium (water), SCs tend to separate as a result of sedimentation. The sedimented particles tend to form a compact layer at the bottom of the container (sometimes referred to as clay or cake), which is very difficult to redisperse. It is, therefore, essential to reduce sedimentation and formation of clays by incorporating an antisettling agent.

The chapter will start with a section on the preparation of suspension concentrates and the role of surfactants (dispersing agents). This is followed by a section on the control of the physical stability of suspensions. The problem of Ostwald ripening (crystal growth) will also be briefly described and particular attention will be paid to the role of surfactants. The next section will deal with the problem of sedimentation and prevention of claying. The various methods that may be applied to reduce sedimentation and prevention of the formation of hard clays will be summarized. The last section in this chapter will deal with the methods that may be applied for the assessment of the physical stability of SCs. For the assessment of flocculation and crystal growth, particle size analysis techniques are commonly applied. The bulk properties

https://doi.org/10.1515/9783110578997-004

of the suspension, such as sedimentation and separation, and redispersion on dilution may be assessed using rheological techniques. The latter will be summarized with particular emphasis on their application in predicting the long-term physical stability of suspension concentrates.

3.2 Preparation of suspension concentrates and the role of surfactants/dispersing agents

Suspension concentrates are usually formulated using a wet milling process which requires the addition of a surfactant/dispersing agent. The latter should satisfy the following criteria:

(i) A good wetting agent for the agrochemical powder (both external and internal surfaces of the powder aggregates or agglomerates must be spontaneously wetted).
(ii) A good dispersing agent to break such aggregates or agglomerates into smaller units and subsequently help in the milling process (one usually aims at a dispersion with a volume mean diameter of 1–2 μm).
(iii) It should provide good stability in the colloid sense (this is essential for maintaining the particles as individual units once formed).

Powerful dispersing agents are particularly important for the preparation of highly concentrated suspensions (sometimes require for seed dressing). Any flocculation will cause a rapid increase in the viscosity of the suspension and this makes the wet milling of the agrochemical a difficult process.

Dry powders of organic compounds usually consist of particles of various degrees of complexity, depending on the isolation stages and the drying process. Generally, the particles in a dry powder form aggregates (in which the particles are joined together by their crystal faces) or agglomerates (in which the particles touch at edges or corners) forming a looser more open structure. It is essential in the dispersion process to wet the external as well as the internal surfaces and displace the air entrapped between the particles. This is usually achieved by the use of surface active agents of the ionic or nonionic type. In some cases, macromolecules or polyelectrolytes may be efficient in this wetting process. This may be the case since these polymers contain a very wide distribution of molecular weights and the low molecular weight fractions may act as efficient wetting agents. For efficient wetting, the molecules should lower the surface tension of water (see below) and they should diffuse fast in solution and become quickly adsorbed at the solid/solution interface.

Wetting of a solid is usually described in terms of the equilibrium contact angle θ and the appropriate interfacial tensions. This is illustrated in Fig. 3.1.

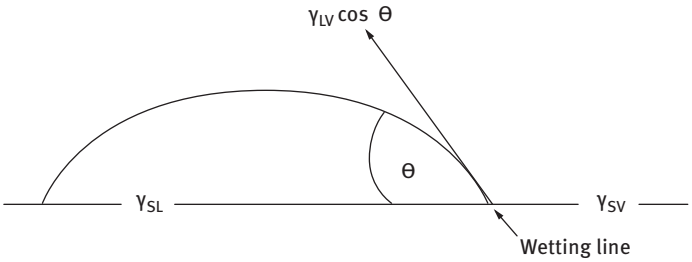

Fig. 3.1: Schematic representation of the contact angle and wetting line.

Using the classic Young's equation,

$$\gamma_{SV} - \gamma_{SL} = \gamma_{LV} \cos\theta, \tag{3.1}$$

or

$$\cos\theta = \frac{(\gamma_{SV} - \gamma_{SL})}{\gamma_{LV}}, \tag{3.2}$$

where γ represents the interfacial tension and the symbols S, L and V refer to the solid, liquid and vapour respectively. It is clear from equation (3.2) that if $\theta < 90°$, a reduction in γ_{LV} improves wetting. Hence the use of surfactants which reduce both γ_{LV} and γ_{SL} to aid wetting is clear. However, the process of wetting of particulate solids is more complex and it involves at least three distinct types of wetting [5, 6], namely adhesional wetting, spreading wetting and immersional wetting. All these processes are determined by the liquid surface tension and the contact angle. The difference between γ_{SV} and γ_{SL} or $\gamma_{LV} \cos\theta$ is referred to as the adhesion or wetting tension.

Let us consider an agrochemical powder with surface area A. Before the powder is dispersed in the liquid it has a surface tension γ_{SV} and after immersion in the liquid it has a surface tension γ_{SL}. The work of dispersion W_d is simply given by the difference in adhesion or wetting tension of the SL and SV,

$$W_d = A(\gamma_{SL} - \gamma_{SV}) = -A\gamma_{LV} \cos\theta. \tag{3.3}$$

It is clear from equation (3.3) that if $\theta < 90°$, $\cos\theta$ is positive and W_d is negative, i.e. wetting of the powder is spontaneous. Since surfactants are added in sufficient amounts ($\gamma_{dynamic}$ is lowered sufficiently) spontaneous dispersion is the rule rather than the exception.

Wetting of the internal surface requires penetration of the liquid into channels between and inside the agglomerates. The process is similar to forcing a liquid through fine capillaries. To force a liquid through a capillary with radius r, a pressure p is required that is given by,

$$p = -\frac{2\gamma_{LV} \cos\theta}{r} = \left[\frac{-2(\gamma_{SV} - \gamma_{SL})}{r\gamma_{LV}}\right]. \tag{3.4}$$

γ_{SL} has to be made as small as possible; rapid surfactant adsorption to the solid surface, low θ. When $\theta = 0$, $p \propto \gamma_{LV}$. Thus for penetration into pores one requires a high γ_{LV}. Thus, wetting of the external surface requires low contact angle θ and low surface tension γ_{LV}. Wetting of the internal surface (i.e. penetration through pores) requires low θ but high γ_{LV}. These two conditions are incompatible and a compromise has to be made: $\gamma_{SV} - \gamma_{SL}$ must be kept at a maximum. γ_{LV} should be kept as low as possible, but not too low.

The next stage to be considered is the wetting of the internal surface, which implies penetration of the liquid into channels between and inside the agglomerates. This is more difficult to define precisely. However, one may make use of the equation derived for capillary phenomena as discussed by Rideal and Washburn [7, 8] who considered the penetration of liquids in capillaries. For horizontal capillaries (gravity neglected), the depth of penetration l in time t is given by the Rideal–Washburn equation [7, 8],

$$l = \left[\frac{rt\gamma_{LV} \cos\theta}{2\eta} \right]^{1/2}. \tag{3.5}$$

To enhance the rate of penetration, γ_{LV} has to be made as high as possible, θ as low as possible and η as low as possible.

For dispersion of powders into liquids one should use surfactants that lower θ while not reducing γ_{LV} too much. The viscosity of the liquid should also be kept at a minimum. Thickening agents (such as polymers) should not be added during the dispersion process. It is also necessary to avoid foam formation during the dispersion process.

For a packed bed of particles, r may be replaced by K, which contains the effective radius of the bed r and a tortuosity factor k ($K = r/k^2$), which takes into account the complex path formed by the channels between the particles, i.e.,

$$l^2 = \frac{kt\gamma_{LV} \cos\theta}{2\eta}. \tag{3.6}$$

Thus a plot of l^2 versus t gives a straight line and from the slope of the line one can obtain θ.

The Rideal–Washburn equation can be applied to obtain the contact angle of liquids (and surfactant solutions) in powder beds. K should first be obtained using a liquid that produces zero contact angle. A packed bed of powder is prepared, say in a tube fitted with a sintered glass at the end (to retain the powder particles). It is essential to pack the powder uniformly in the tube (a plunger may be used in this case). The tube containing the bed is immersed in a liquid that gives spontaneous wetting (e.g. a lower alkane), i.e. the liquid gives a zero contact angle and $\cos\theta = 1$. By measuring the rate of penetration of the liquid (this can be carried out gravimetrically using for example a microbalance or a Kruss instrument) one can obtain K. The tube is then removed from the lower alkane liquid and left to stand for evaporation of the liquid.

It is then immersed in the liquid in question and the rate of penetration is measured again as a function of time. Using equation (3.6), one can calculate $\cos\theta$ and hence θ.

Thus, in summary, the dispersion of a powder in a liquid depends on three main factors, namely the energy of wetting of the external surface, the pressure involved in the liquid penetrating inside and between the agglomerates and the rate of penetration of the liquid into the powder. All these factors are related to two main parameters, namely γ_{LV} and θ. In general, the process is likely to be more spontaneous the lower the θ and the higher γ_{LV}. Since these two factors tend to operate in opposite directions, the choice of the proper surfactant (dispersing agent) can be a difficult task.

For the dispersion of aggregates and agglomerates into smaller units one requires high speed mixing, e.g. a Silverson mixer. In some cases the dispersion process is easy and the capillary pressure may be sufficient to break up the aggregates and agglomerates into primary units. The process is aided by the surfactant which becomes adsorbed on the particle surface. However, one should be careful during the mixing process not to entrap air (foam), which causes an increase in the viscosity of the suspension and prevents easy dispersion and subsequent grinding. If foam formation becomes a problem, one should add antifoaming agents such as polysiloxane antifoaming agents.

After completion of the dispersion process, the suspension is transferred to a ball or bead mill for size reduction. Milling or comminution (the generic term for size reduction) is a complex process and there is little fundamental information on its mechanism. For the breakdown of single crystals into smaller units, mechanical energy is required. This energy in a bead mill, for example, is supplied by impaction of the glass beads with the particles. As a result, permanent deformation of the crystals and crack initiation result. This will eventually lead to the fracture of the crystals into smaller units. However, since the milling conditions are random, it is inevitable that some particles receive impacts that are far in excess of those required for fracture, whereas others receive impacts that are insufficient for fracture them. This makes the milling operation grossly inefficient and only a small fraction of the applied energy is actually used in comminution. The rest of the energy is dissipated as heat, vibration, sound, inter-particulate friction, friction between the particles and beads, and elastic deformation of unfractured particles. For these reasons, milling conditions are usually established by a trial and error procedure. Of particular importance is the effect of various surface active agents and macromolecules on the grinding efficiency. The role played by these agents in the comminution process is far from being understood, although Rehbinder and collaborators [9–11] have given this problem particular consideration. As a result of adsorption of surfactants at the solid/liquid interface, the surface energy at the boundary is reduced and this facilitates the process of deformation or destruction. The adsorption of the surfactant at the solid/solution interface in cracks facilitates their propagation. This is usually referred to as the "Rehbinder effect" [10]. The surface energy manifests itself in destructive processes on solids, since the generation and growth of cracks and separation of one part of a body from another

is directly connected with the development of new free surface. Thus, as a result of adsorption of surface active agents at structural defects in the surface of the crystals, fine grinding is facilitated. In the extreme case where there is a very great reduction in surface energy at the sold/liquid boundary, spontaneous dispersion may take place with the result of the formation of colloidal particles (< 1 μm). Rehbinder [10] has developed a theory for such spontaneous dispersion.

3.3 Effect of surfactant adsorption

Surfactants lower the surface tension of water, γ, and they adsorb at the solid/liquid interface. A plot of γ_{LV} versus log C (where C is the surfactant concentration) results in a gradual reduction in γ_{LV} followed by a linear decrease of γ_{LV} with log C (just below the critical micelle concentration, cmc) and when the cmc is reached, γ_{LV} remains virtually constant. From the slope of the linear portion of the γ–log C curve (just below the cmc), one can obtain the surface excess (number of moles of surfactant per unit area at the L/A interface). Using the Gibbs adsorption isotherm,

$$\frac{d\gamma}{d \log C} = -2.303RT\Gamma, \tag{3.7}$$

where Γ is the surface excess (mol m^{-2}), R is the gas constant and T the absolute temperature.

From Γ one can obtain the area per molecule,

$$\text{area per molecule} = \frac{1}{\Gamma N_{av}} (\text{m}^2) = \frac{10^{18}}{\Gamma N_{av}} (\text{nm}^2). \tag{3.8}$$

Most surfactants produce a vertically oriented monolayer just below the cmc. The area/molecule is usually determined by the cross-sectional area of the head group. For ionic surfactants containing say $-OSO_3^-$ or $-SO_3^-$ head group, the area per molecule is in the region of 0.4 nm^2. For nonionic surfactants containing several moles of ethylene oxide [12–14], the area per molecule can be much larger (1–2 nm^2). Surfactants will also adsorb at the solid/liquid interface. For hydrophobic surfaces, the main driving force for adsorption is by hydrophobic bonding. This results in lowering of the contact angle of water on the solid surface. For hydrophilic surfaces, adsorption occurs via the hydrophilic group, e.g. cationic surfactants on silica. Initially, the surface becomes more hydrophobic and the contact angle θ increases with increasing surfactant concentration. However, at higher cationic surfactant concentration, a bilayer is formed by hydrophobic interaction between the alkyl groups and the surface becomes more and more hydrophilic and eventually the contact angle reaches zero at high surfactant concentrations.

Smolders [15] suggested the following relationship for change of θ with C,

$$\frac{d\gamma_{LV} \cos\theta}{d \ln C} = \frac{d\gamma_{SV}}{d \ln C} - \frac{d\gamma_{SL}}{d \ln C}. \tag{3.9}$$

Using the Gibbs equation,

$$\sin\theta\left(\frac{\mathrm{d}\gamma}{\mathrm{d}\ln C}\right) = RT(\Gamma_{SV} - \Gamma_{SL} - \gamma_{LV}\cos\theta), \tag{3.10}$$

since $\gamma_{LV}\sin\theta$ is always positive, then $(\mathrm{d}\theta/\mathrm{d}\ln C)$ will always have the same sign as the RHS of equation (3.9). Three cases may be distinguished:

- $(\mathrm{d}\theta/\mathrm{d}\ln C) < 0$; $\Gamma_{SV} < \Gamma_{SL} + \Gamma_{LV}\cos\theta$; addition of surfactant improves wetting.
- $(\mathrm{d}\theta/\mathrm{d}\ln C) = 0$; $\Gamma_{SV} = \Gamma_{SL} + \Gamma_{LV}\cos\theta$; surfactant has no effect on wetting.
- $(\mathrm{d}\theta/\mathrm{d}\ln C) > 0$; $\Gamma_{SV} > \Gamma_{SL} + \Gamma_{LV}\cos\theta$; surfactant causes dewetting.

3.4 Control of the physical stability of suspension concentrates

When considering the stability of suspension concentrates one must distinguish between colloid stability and overall physical stability. Colloid stability implies absence of an aggregation between the particles which requires the presence of an energy barrier that is produced by electrostatic, steric repulsion or a combination of the two (electrosteric). Physical stability implies absence of any sedimentation and/or separation, ease of dispersion on shaking and/or dilution in the spray tanks. To achieve overall physical stability one may apply controlled and reversible flocculation methods and/or using a rheology modifier.

To distinguish between colloid stability/instability and physical stability one must consider the state of the suspension on standing, as schematically illustrated in Fig. 3.2.

The above states are determined by:

(i) magnitude and balance of the various interaction forces, electrostatic repulsion, steric repulsion and van der Waals attraction;
(ii) particle size and shape distribution;
(iii) density difference between disperse phase and medium which determines the sedimentation characteristics;
(iv) conditions and prehistory of the suspension, e.g. agitation which determines the structure of the flocs formed (chain aggregates, compact clusters, etc.);
(v) presence of additives, e.g. high molecular weight polymers that may cause bridging or depletion flocculation.

These states may be described in terms of three different energy–distance curves may:

(a) Electrostatic, produced for example by the presence of ionogenic groups on the surface of the particles, or adsorption of ionic surfactants.
(b) Steric, produced for example by adsorption of nonionic surfactants or polymers.
(c) Electrostatic + steric (electrosteric) as for example produced by polyelectrolytes.

These are illustrated in Fig. 3.3.

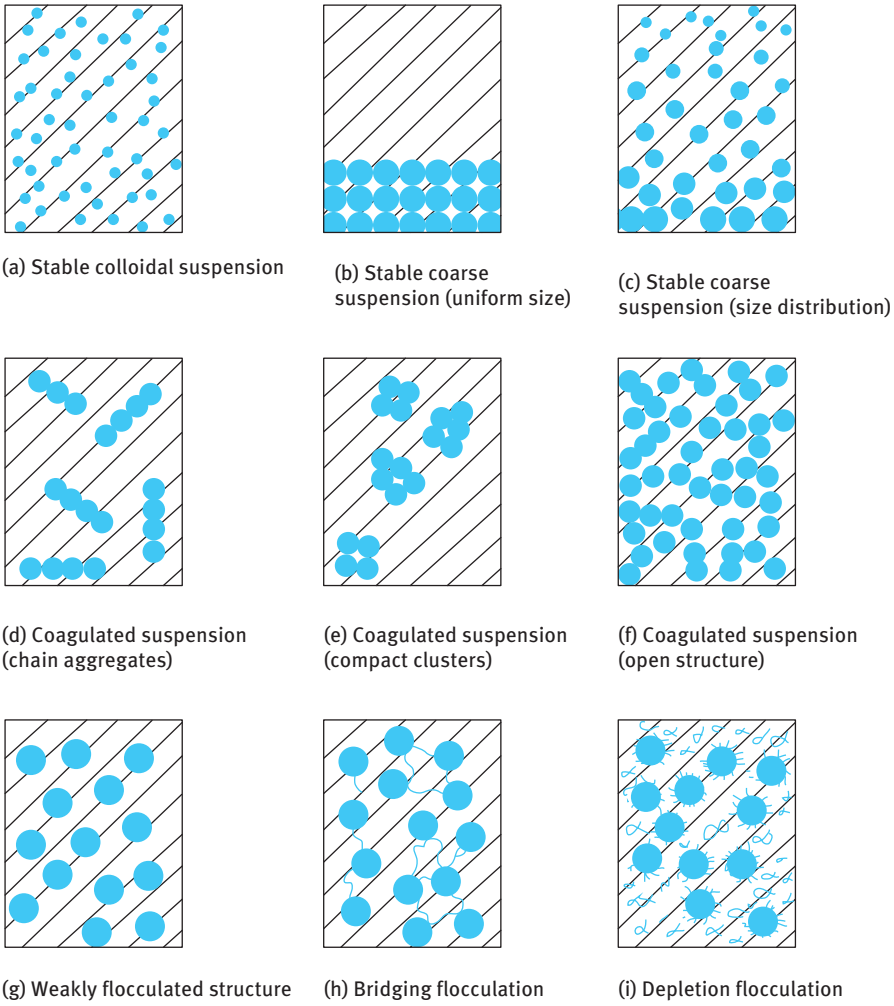

Fig. 3.2: States of the suspension.

A brief description of the various states shown in Fig. 3.2 is given below:

States (a)–(c) correspond to a suspension that is stable in the colloid sense. The stability is obtained as a result of net repulsion due to the presence of extended double layers (i.e. at low electrolyte concentration), the result of steric repulsion producing adsorption of nonionic surfactants or polymers, or the result of a combination of double layer and steric repulsion (electrosteric). State (a) represents the case of a suspension with small particle size (submicron) whereby Brownian diffusion overcomes the gravity force producing uniform distribution of the particles in the suspension, i.e.

$$kT > (4/3)\pi R^3 \Delta\rho g h, \tag{3.11}$$

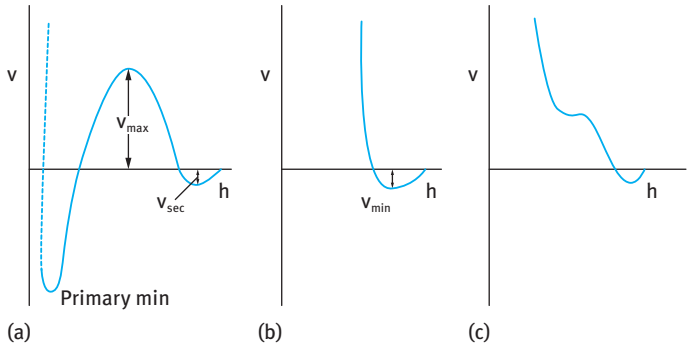

Fig. 3.3: Energy–distance curves for three stabilization mechanisms.

where k is the Boltzmann constant, T is the absolute temperature, R is the particle radius, $\Delta\rho$ is the buoyancy (difference in density between the particles and the medium), g is the acceleration due to gravity and h is the height of the container.

A good example of the above case is a nanosuspension with particle size well below 1 µm that is stabilized by an ionic surfactant or nonionic surfactant or polymer. This suspension will show no separation on storage for long periods of time.

States (b) and (c) represent the case of suspensions in which the particle size range is outside the colloid range (> 1 µm). In this case, the gravity force exceeds Brownian diffusion. With state (b), the particles are uniform and they will settle under gravity forming a hard sediment (technically referred to as "clay" or "cake"). The repulsive forces between the particles allow them to move past each other until they reach small distances of separation (that are determined by the location of the repulsive barrier). Due to the small distances between the particles in the sediment, it is very difficult to redisperse the suspension by simple shaking. With case (c), consisting of a wide distribution of particle sizes, the sediment may contain larger proportions of the larger size particles, but still a hard "clay" is produced. These "clays" are dilatant (i.e. shear thickening) and they can be easily detected by inserting a glass rod into the suspension. Penetration of the glass rod into these hard sediments is very difficult.

States (d)–(f) represent the case for coagulated suspensions which either have a small repulsive energy barrier or in which it is completely absent. State (d) represents the case of coagulation under no stirring conditions in which case chain aggregates are produced that will settle under gravity forming a relatively open structure. State (e) represents the case of coagulation under stirring conditions where compact aggregates are produced that will settle faster than the chain aggregates and the sediment produced is more compact. State (f) represents the case of coagulation at high volume fraction of the particles, ϕ. In this case whole particles will form a "one-floc" structure that is formed from chains and cross-chains that extend from one wall to the other in the container. Such a coagulated structure may undergo some compression (consolidation) under gravity leaving a clear supernatant liquid layer at the top of the

container. This phenomenon is referred to as syneresis. State (g) represents the case of weak and reversible flocculation. This occurs when the secondary minimum in the energy distance curve (Fig. 3.3 (a)) is deep enough to cause flocculation. This can occur at moderate electrolyte concentrations, in particular with larger particles. The same occurs with sterically and electrosterically stabilized suspensions (Fig. 3.3 (b) and (c)). This occurs when the adsorbed layer thickness is not very large, particularly with large particles. The minimum depth required for causing weak flocculation depends on the volume fraction of the suspension. The higher the volume fraction, the lower the minimum depth required for weak flocculation. This flocculation is weak and reversible, i.e. on shaking the container redispersion of the suspension occurs. On standing, the dispersed particles aggregate to form a weak "gel". This process (referred to as sol–gel transformation) leads to reversible time dependency of viscosity (thixotropy). On shearing the suspension, the viscosity decreases and when the shear is removed, the viscosity is recovered.

State (h) represents the case in which the particles are not completely covered by the polymer chains. In this case, simultaneous adsorption of one polymer chain on more than one particle occurs, leading to bridging flocculation. If the polymer adsorption is weak (low adsorption energy per polymer segment), the flocculation could be weak and reversible. In contrast, if the adsorption of the polymer is strong, tough flocs are produced and the flocculation is irreversible.

Case (i) represents a phenomenon, referred to as depletion flocculation, produced by addition of "free" nonadsorbing polymer [16]. In this case, the polymer coils cannot approach the particles to a distance Δ (that is determined by the radius of gyration of free polymer R_G), since the reduction of entropy on close approach of the polymer coils is not compensated by an adsorption energy. The suspension particles will be surrounded by a depletion zone with thickness Δ. Above a critical volume fraction of the free polymer, ϕ_p^+, the polymer coils are "squeezed out" from between the particles and the depletion zones begin to interact. The interstices between the particles are now free from polymer coils and hence an osmotic pressure is exerted outside the particle surface (the osmotic pressure outside is higher than in between the particles) resulting in weak flocculation [16]. A schematic representation of depletion flocculation is shown in Fig. 3.4.

The magnitude of the depletion attraction free energy, G_{dep}, is proportional to the osmotic pressure of the polymer solution, which in turn is determined by ϕ_p and molecular weight M. The range of depletion attraction is proportional to the thickness of the depletion zone, Δ, which is roughly equal to the radius of gyration, R_G, of the free polymer. A simple expression for G_{dep} is [16],

$$G_{dep} = \frac{2\pi R\Delta^2}{V_1}(\mu_1 - \mu_1^0)\left(1 + \frac{2\Delta}{R}\right), \tag{3.12}$$

where V_1 is the molar volume of the solvent, μ_1 is the chemical potential of the solvent in the presence of free polymer with volume fraction ϕ_p and μ_1^0 is the chemical

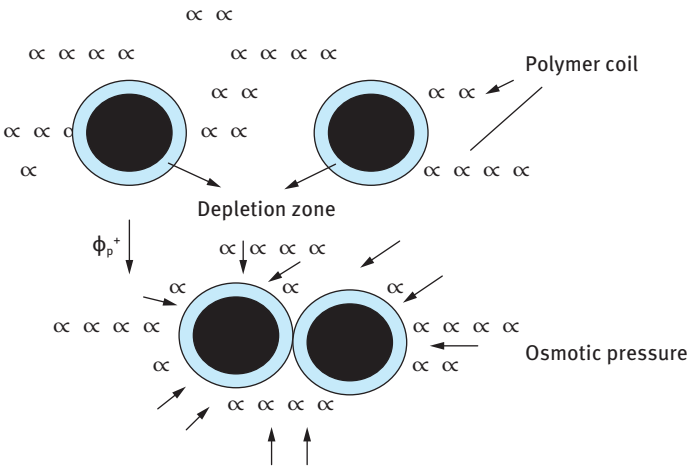

Fig. 3.4: Schematic representation of depletion flocculation.

potential of the solvent in the absence of free polymer. $(\mu_1 - \mu_1^0)$ is proportional to the osmotic pressure of the polymer solution.

The control of stability against irreversible flocculation (where the particles are held together into aggregates that cannot be redispersed by shaking or on dilution) is achieved by the use of powerful dispersing agents, e.g. surfactants of the ionic or nonionic type, nonionic polymers or polyelectrolytes. These dispersing agents must be strongly adsorbed onto the particle surfaces and fully cover them. With ionic surfactants, irreversible flocculation is prevented by the repulsive force generated from the presence of an electrical double layer at the particle-solution interface. Depending on the conditions, this repulsive force can be made sufficiently large to overcome the ubiquitous van der Waals attraction between the particles at intermediate distances of separation. With nonionic surfactants and macromolecules, repulsion between the particles is ensured by the steric interaction of the adsorbed layers on the particle surfaces. With polyelectrolytes, both electrostatic and steric repulsion exist.

Ionic surfactants such as sodium dodecyl benzene sulphonate (NaDBS) or cetyl trimethyl ammonium chloride (CTACl) adsorb on hydrophobic particles of agrochemicals as a result of the hydrophobic interaction between the alkyl group of the surfactant and the particle surface. As a result, the particle surface will acquire a charge that is compensated by counterions (Na^+ in the case of NaDBS and Cl^- in the case of CTACl) forming an electrical double layer.

The adsorption of ionic surfactants at the solid/solution interface is of vital importance in determining the stability of suspension concentrates. The adsorption of ionic surfactants on solid surfaces can be directly measured by equilibrating a known amount of solid (with known surface area) with surfactant solutions of various concentrations. After reaching equilibrium, the solid particles are removed (for exam-

ple by centrifugation) and the concentration of surfactant in the supernatant liquid is analytically determined. From the difference between the initial and final surfactant concentrations (C_1 and C_2 respectively) the number of moles of surfactant adsorbed, Γ, per unit area of solid is determined and the results may be fitted to a Langmuir isotherm,

$$\Gamma = \frac{\Delta C}{mA} = \frac{abC_2}{1 + bC_2}, \tag{3.13}$$

where $\Delta C = C_1 - C_2$, m is the mass of the solid with surface area A, a is the saturation adsorption and b is a constant that is related to the free energy of adsorption, ΔG ($b \propto \exp \Delta G/RT$). From a, the area per surfactant ion on the surface can be calculated (area per surfactant ion = $1/aN_{\text{av}}$).

Results on the adsorption of ionic surfactants on pesticides are scarce. However, Tadros [17] obtained some results on the adsorption of NaDBS and CTABr on a fungicide, namely ethirimol. For NaDBS, the shape of the isotherm was of a Langmuir type, giving an area/DBS^- at saturation of $\approx 0.14\ \text{nm}^2$. The adsorption of CTA^+ showed a two-step isotherm with areas/CTA^+ of 0.27 and $0.14\ \text{nm}^2$ respectively. These results suggest full saturation of the surface with surfactant ions which are vertically oriented.

The above discussion shows that ionic surfactants can be used to stabilize agrochemical suspensions by producing sufficient electrostatic repulsion. When two particles with adsorbed surfactant layers approach each other to a distance where the electrical double layers begin to overlap, strong repulsion occurs, preventing any particle aggregation. The energy–distance curve for such electrostatically stabilized dispersions is schematically shown in Fig. 3.3 (a). This shows an energy maximum, which if high enough ($> 25kT$) prevents particle aggregation into the primary minimum. However, ionic surfactants are the least attractive dispersing agents for the following reasons. Adsorption of ionic surfactants is seldom strong enough to prevent some desorption resulting in the production of "bare" patches which may induce particle aggregation. The system is also sensitive to ionic impurities which are present in the water used for suspension preparation. In particular, the system will be sensitive to bivalent ions (Ca^{2+} or Mg^{2+}) which produce flocculation at relatively low concentrations.

Nonionic surfactants of the ethoxylate type, e.g. $R(CH_2CH_2O)_nOH$ or $RC_6H_5(CH_2CH_2O)_2OH$, provide a better alternative provided the molecule contains sufficient hydrophobic groups to ensure their adsorption and enough ethylene oxide units to provide an adequate energy barrier. The origin of steric repulsion arises from two main effects. The first effect arises from the unfavourable mixing of the poly(ethylene oxide) chains which are in good solvent conditions (water as the medium). This effect is referred to as mixing or osmotic repulsion. The second effect arises from the loss in configurational entropy of the chains when these are forced to overlap on approach of the particles. This is referred to as the elastic or volume restriction effect. The energy–distance curve for such systems (Fig. 3.3 (b)) clearly demonstrates the attraction of steric stabilization. Apart from a small attractive energy minimum (which can be reasonably shallow with sufficiently long poly(ethylene oxide) chains), strong repulsion

occurs and there is no barrier to overcome. A better option is to use block and graft copolymers (polymeric surfactants) consisting of A and B units combined together in A–B, A–B–A or BA_n fashion. B represents units with high affinity for the particle surface and basically insoluble in the continuous medium, thus providing strong adsorption ("anchoring units"). A, on the other hand, represents units with high affinity to the medium (high chain-solvent interaction) and little or no affinity to the particle surface. An example of such a powerful dispersant is a graft copolymer of polymethyl methacrylate-methacrylic acid (the anchoring portion) and methoxy polyethylene oxide (the stabilizing chain) methacrylate [17]. Adsorption measurements of such a polymer on a pesticide, namely ethirimol (a fungicide) showed a high affinity isotherm with no desorption. Using such a macromolecular surfactant, a suspension of high volume fractions could be prepared.

The third class of dispersing agents which is commonly used in SC formulations is that of polyelectrolytes. Of these, sulphonated naphthalene-formaldehyde condensates and lignosulphonates are the most commonly used is agrochemical formulations. These systems show a combined electrostatic and steric repulsion and the energy–distance curve is schematically illustrated in Fig. 3.3 (c). It shows a shallow minimum and maximum at intermediate distances (characteristic of electrostatic repulsion) as well as strong repulsion at relatively short distances (characteristic of steric repulsion). The stabilization mechanism of polyelectrolytes is sometimes referred to as electrosteric. These polyelectrolytes offer some versatility in SC formulations. Since the interaction is fairly long-range in nature (due to the double layer effect), one does not obtain the "hard-sphere" type behaviour which may lead to the formation of hard sediments. The steric repulsion ensures colloid stability and prevents any aggregation on storage.

3.5 Ostwald ripening (crystal growth)

There are several ways in which crystals can grow in an aqueous suspension. One of the most familiar is the phenomenon of "Ostwald ripening", which occurs as a result of the difference in solubility between the small and large crystals [18],

$$\frac{RT}{M}\ln\frac{S_1}{S_2} = \frac{2\sigma}{\rho}\left(\frac{1}{r_1} - \frac{1}{r_2}\right), \tag{3.14}$$

where S_1 and S_2 are the solubilities of crystals with radii r_1 and r_2 respectively, σ is the specific surface energy, ρ is the density and M is the molecular weight of the solute molecules, R is the gas constant and T the absolute temperature. Since r_1 is smaller than r_2, then S_1 is larger than S_2. Another mechanism for crystal growth is related to polymorphic changes in solutions, and again the driving force is the difference in solubility between the two polymorphs. In other words, the less soluble form grows at the expense of the more soluble phase. This is sometimes also accompanied by changes

in the crystal habit. Different faces of the crystal may have different surface energies and deposition may preferentially take place on one of the crystal faces, modifying its shape. Other important factors are the presence of crystal dislocations, kinks, surface impurities, etc.

The crystal growth in suspension concentrates may create undesirable changes. As a result of the drastic change in particle size distribution, the settling of the particles may be accelerated leading to caking and cementing together of some particles in the sediment. Moreover, an increase in particle size may lead to a reduction in biological efficiency. Thus, prevention of crystal growth or at least reducing it to an acceptable level is essential in most suspension concentrates. Surfactants affect crystal growth in a number of ways. The surfactant may affect the rate of dissolution by affecting the rate of transport away from the boundary layer at the crystal solution interface. On the other hand, if the surfactant forms micelles that can solubilize the solute, crystal growth may be enhanced as a result of increasing the concentration gradient. Thus by proper choice of dispersing agent, one may reduce crystal growth of suspension concentrates. This has been demonstrated by Tadros [17] for terbacil suspensions. When using Pluronic P75 (polyethylene oxide–polypropylene oxide block copolymer) crystal growth was significant. By replacing the Pluronic surfactant with polyvinyl alcohol the rate of crystal growth was greatly reduced and the suspension concentrate was acceptable.

It should be mentioned that many surfactants and polymers may act as crystal growth inhibitors if they adsorb strongly on the crystal faces, thus preventing solute deposition. However, the choice of an inhibitor is still an art and there are not many rules that can be used for selecting crystal growth inhibitors.

3.6 Stability against claying or caking

Once a dispersion that is stable in the colloid sense has been prepared, the next task is to eliminate claying or caking. This is the consequence of the colloidally stable suspension particles settling. The repulsive forces necessary to ensure this colloid stability allow the particles to move past each other forming a dense sediment which is very difficult to redisperse. Such sediments are dilatant (shear thickening, see section on rheology) and hence the SC becomes unusable.

The sedimentation velocity v_0 of a very dilute suspension of rigid noninteracting particles with radius a can be determined by equating the gravitational force with the opposing hydrodynamic force as given by Stokes' law, i.e.,

$$\frac{4}{3}\pi a^3(\rho - \rho_0)g = 6\pi\eta_0 a v_0, \tag{3.15}$$

$$v_0 = \frac{2a^2(\rho - \rho_0)}{9\eta_0}, \tag{3.16}$$

where ρ is the density of the particles, ρ_0 that of the medium, η_0 is the viscosity of the medium and g is the acceleration due to gravity. Equation (3.16) predicts a sedimentation rate for particles with radius 1 μm in a medium with a density difference of 0.2 g cm^{-3} and a viscosity of 1 mPa s (i.e. water at 20 °C) of 4.4×10^{-7} m s^{-1}. Such particles will sediment to the bottom of a 0.1 m container in about 60 hours. For 10 μm particles, the sedimentation velocity is 4.4×10^{-5} m s^{-1} and such particles will sediment to the bottom of a 0.1 m container in about 40 minutes.

The above treatment using Stokes' law applies only to very dilute suspensions (volume fraction $\phi < 0.01$). For more concentrated suspensions, the particles no longer sediment independently of each other and one has to take into account both the hydrodynamic interaction between the particles (which applies for moderately concentrated suspensions) and other higher order interactions at relatively high volume fractions. A theoretical relationship between the sedimentation velocity v of non-flocculated suspensions and particle volume fraction has been derived by Batchelor [19, 20]. Such theories apply to relatively low volume fractions (< 0.1) and they show that the sedimentation velocity v at a volume fraction ϕ is related to that at infinite dilution v_0 (the Stokes velocity) by an equation of the form,

$$v = v_0(1 - k\phi), \tag{3.17}$$

where k is a constant in the region of 5–6. Batchelor [19, 20] derived a rigorous theory for sedimentation in a relatively dilute dispersion of spheres. He considered that the reduction in Stokes' velocity with increasing particle number concentration could arise from hydrodynamic interactions. The value of k in equation (3.17) was calculated and found to be equal to 6.55. This theory applies up to a volume fraction of 0.1. At higher volume fractions, the sedimentation velocity becomes a complex function of ϕ and only empirical equations are available to describe the variation of v with ϕ. For example, Reed and Anderson [21] developed a virial expansion technique to describe the settling rate of concentrated suspensions. They derived the following expression for the average velocity, v_{av},

$$v_{av} = v_0 \frac{1 - 1.83\phi}{1 + 4.70\phi}. \tag{3.18}$$

Good agreement between experimental settling rates and those calculated using equation (3.18) was obtained up to $\phi = 0.4$.

More recently, Buscall et al. [22] measured the rate of settling of polystyrene latex particles with $a = 1.55$ μm in 10^{-3} mol dm^{-3} up to $\phi = 0.5$. The results are shown in Fig. 3.5. It can be seen that v/v_0 decreases exponentially with increasing ϕ, approaching zero at $\phi > 0.5$, i.e. in the region of close packing. An empirical equation for the relative settling rate has been derived using the Dougherty–Krieger equation [23] for the relative viscosity, η_r (= η/η_0),

$$\eta_r = \left(1 - \frac{\phi}{\phi_p}\right)^{-[\eta]\phi_p}, \tag{3.19}$$

where $[\eta]$ is the intrinsic viscosity (that is equal to 2.5 for hard spheres) and ϕ_p is the maximum packing fraction (which is close to 0.6). Assuming that $v/v_0 = \alpha(\eta_0/\eta)$, it is easy to derive the following empirical relationship for the relative sedimentation velocity, v_r (= v/v_0),

$$v_r = \left(1 - \frac{\phi}{\phi_p}\right)^{\alpha[\eta]\phi_p} = \left(1 - \frac{\phi}{\phi_p}\right)^{k\phi_p}. \tag{3.20}$$

By allowing the latex to settle completely and then determining the volume concentration of the packed bed, a value of 0.58 was obtained for ϕ_p (close to random packing). Using this value and $k = 5.4$, the relative rate of sedimentation was calculated and this gave the full line shown in Fig. 3.5, whereas the circles represent the experimental points. Thus, agreement between the calculations using the empirical equation and the experimental results is reasonable.

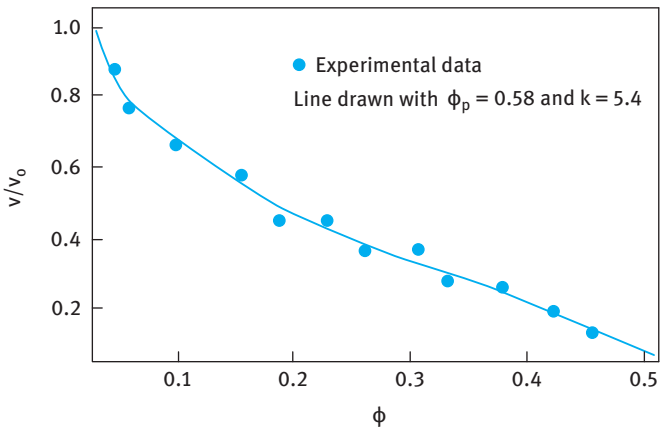

Fig. 3.5: Variation of sedimentation rate with volume fraction for polystyrene dispersions.

It seems from the above discussion that there is a correlation between the reduction in sedimentation rate and the increase in relative viscosity of the suspension as the volume fraction of the suspension is increased. This is schematically shown in Fig. 3.6, which shows that $v \to 0$ and $\eta_r \to \infty$ as $\phi \to \phi_p$. This implies that suspension concentrates with volume fractions approaching the maximum packing do not show any appreciable settling.

However, such dense suspensions have extremely high viscosities and are not a practical solution for reducing settling. In most cases one prepares a suspension concentrate at practical volume fractions (0.2–0.4) and then uses an antisettling agent to reduce settling. Most of the antisettling agents used in practice are high molecular weight polymers. These materials show an increase in the viscosity of the medium as their concentration increases. However, at a critical polymer concentration (which

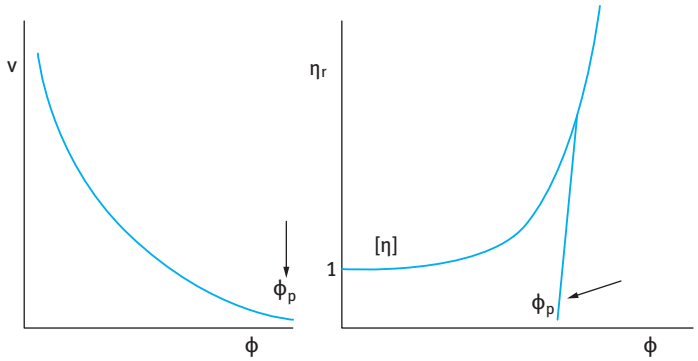

Fig. 3.6: Variation of v and η_r with ϕ.

depends on the nature of the polymer and its molecular weight) they show a very rapid increase in viscosity with a further increase in their concentration. This critical concentration (sometimes denoted by C^*) represents the situation where the polymer coils or rods begin to overlap. Under these conditions the solutions become significantly non-Newtonian (viscoelastic, see section on rheology) and they produce stresses that are sufficient to overcome the stress exerted by the particles. The settling of suspensions in these non-Newtonian fluids is not simple since one has to consider the non-Newtonian behaviour of these polymer solutions. This problem has been addressed by Buscall et al. [22]. In order to adequately describe the settling of particles in non-Newtonian fluids one needs to know how the viscosity of the medium changes with shear rate or shear stress. Most of these viscoelastic fluids show a gradual increase of viscosity with decreasing shear rate or shear stress, but below a critical stress or shear rate they show a Newtonian region with a limiting high viscosity that is denoted as the residual (or zero shear) viscosity. This is illustrated in Fig. 3.7, which shows the variation of the viscosity with shear stress for a number of solutions of ethyl hydroxyethyl cellulose at various concentrations. It can be seen that the viscosity increases with decreasing stress and the limiting value, i.e. the residual viscosity $\eta(0)$, increases rapidly with increasing polymer concentration. The shear thinning behaviour of these polymer solutions is clearly shown, since above a critical stress value the viscosity decreases rapidly with an increase in shear stress. The limiting value of the viscosity is reached at low stresses (< 0.2 Pa).

It is now important to calculate the stress exerted by the particles. This stress is equal to $a\Delta\rho g/3$. For polystyrene latex particles with radius 1.55 μm and density 1.05 g cm^{-3}, this stress is equal to 1.6×10^{-4} Pa. Such stress is lower than the critical stress for most EHEC solutions. In this case one would expect a correlation between the settling velocity and the zero shear viscosity. This is illustrated in Fig. 3.8 where v/a^2 is plotted versus $\eta(0)$. As is clear, a linear relationship between $\log(v/a^2)$ and $\log \eta(0)$ is obtained, with a slope of –1, over three decades of viscosity. This indicates that the

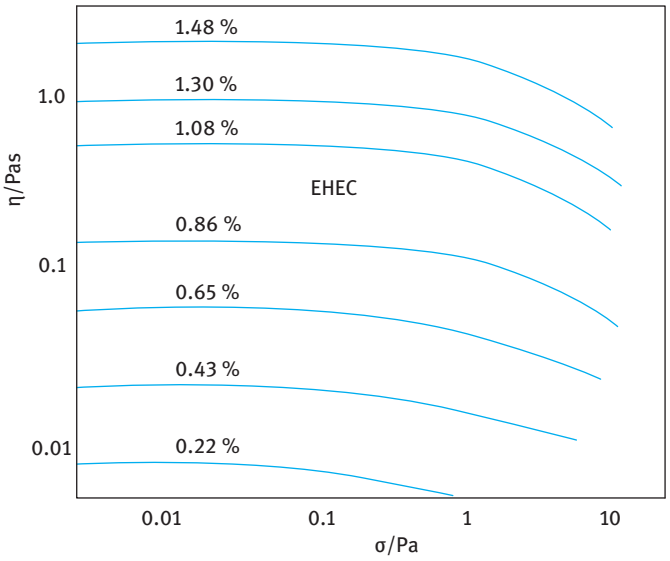

Fig. 3.7: Constant stress (creep) measurements for PS latex dispersions as a function of EHEC concentration.

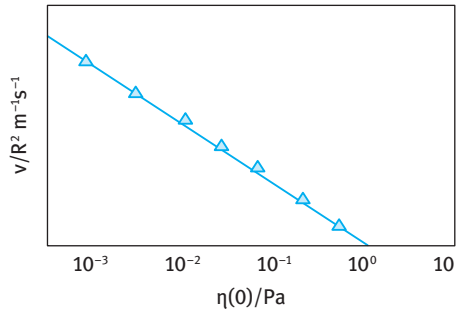

Fig. 3.8: Sedimentation rate versus $\eta(0)$.

settling rate is proportional to $[\eta(0)]^{-1}$. Thus, the settling rate of isolated spheres in non-Newtonian (pseudoplastic) polymer solutions is determined by the zero shear viscosity in which the particles are suspended. As we will see in the section on rheological measurements, determining the zero shear viscosity is not straightforward and requires the use of constant stress rheometers.

The above correlation applies to the simple case of relatively dilute suspensions. For more concentrated suspensions, other parameters should be taken into consideration, such as the bulk (elastic) modulus. It is also clear that the stress exerted by the particles depends not only on the particle size but the density difference between the particle and the medium. Many suspension concentrates have particles with radii up to 10 µm and density difference of more than 1 g cm^{-3}. However, the stress exerted

by such particles will seldom exceed 10^{-2} Pa and most polymer solutions will reach their limiting viscosity value at higher stresses than this value. Thus, in most cases the correlation between settling velocity and zero shear viscosity is justified, at least for relatively dilute systems. For more concentrated suspensions, an elastic network is produced in the system which encompasses the suspension particles as well as the polymer chains. In this case settling of individual particles may be prevented. However, in this case the elastic network may collapse under its own weight and some liquid is squeezed out from between the particles.

This is manifested in a clear liquid layer at the top of the suspension, a phenomenon usually referred to as syneresis. If such separation is not significant, it may not cause any problem on application since by shaking the container the whole system redisperses. However, significant separation is not acceptable since it becomes difficult to homogenize the system. In addition, such extensive separation is cosmetically unacceptable and the formulation rheology should be controlled to reduce such separation to a minimum.

Several methods are applied in practice to control the settling and prevent the formation of dilatant clays: (i) Balance of the density of disperse phase and medium. This is obviously the simplest method for retarding settling, since it is clear from equation (3.16) that if $\rho = \rho_0$, then $v_0 = 0$. However, this method is of limited application and can only be applied to systems where the difference in density between the particle and the medium is not too large. For example, with many organic solids with densities between 1.1 and 1.3 g cm^{-3} suspended in water, some soluble substances such as sugar or electrolytes may be added to the continuous phase to increase the density of the medium to a level that is equal to that of the particles. However, one should be careful that the added substance does not cause any flocculation for the particles. This is particularly the case when using electrolytes, where one should avoid any "salting-out" materials which cause the medium to be a poor solvent for the stabilizing chains. It should also be mentioned that density matching can only be achieved at one temperature. Liquids usually have larger thermal expansion coefficients than solids and if the density is matched, say at room temperature, settling may occur at higher temperatures. Thus, one has to be careful when applying the density matching method, particularly if the formulation is subjected to large temperature changes. (ii) Use of high molecular weight polymers ("thickeners"). High molecular weight materials such as natural gums, hydroxyethyl cellulose or synthetic polymers such as poly(ethylene oxide) may be used to reduce settling of suspension concentrates. The most commonly used material in agrochemical formulations is xanthan gum (produced by converting waste sugar into a high molecular weight material using a micro-organism and sold under the trade names Kelzan or Rhodopol) which is effective at relatively low concentrations (of the order of 0.1–0.2 % depending on the formulation). As mentioned above, these high molecular weight materials produce viscoelastic solutions above a critical concentration. This viscoelasticity produces sufficient residual viscosity to stop the settling of individual particles. The solutions also give enough elasticity to

overcome separation of the suspension. However, one cannot rule out the interaction of these polymers with the suspension particles which may result in "bridging" and hence the role by which such molecules reduce settling and prevent the formation of clays may be complex. To arrive at the optimum concentration and molecular weight of the polymer necessary for preventing settling and claying, one should study the rheological characteristics of the formulation as a function of the variables of the system such as its volume fraction, concentration and molecular weight of the polymer and temperature. (iii) Use of "inert" fine particles. It has long been known that fine inorganic materials such as swellable clays and finely divided oxides (silica or alumina), when added to the dispersion medium of coarser suspensions, can eliminate claying or caking. These fine inorganic materials form a "three-dimensional" network in the continuous medium, which by virtue of its elasticity prevents sedimentation and claying. With swellable clays such as sodium montmorillonite, the gel arises from the interaction of the plate-like particles in the medium. The plate-like particles of sodium montmorillonite consist of an octahedral alumina sheet sandwiched between two tetrahedral silica sheets [24]. In the tetrahedral sheets, tetravalent Si may be replaced by trivalent Al, whereas in the octahedral sheet there may be replacement of trivalent Al with divalent Mg, Fe, Cr or Zn. This replacement is usually referred to as isomorphic substitution [24], i.e. an atom of higher valency is replaced by one of lower valency. This results in a deficit of positive charges or excess of negative charges. Thus, the faces of the clay platelets become negatively charged and these negative charges are compensated by counterions such as Na^+ or Ca^{2+}. As a result, a double layer is produced with a constant charge (that is independent of the pH of the solution). However, at the edges of the platelets, some disruption of the bonds occurs resulting in the formation of an oxide-like layer, e.g. –Al–OH, which undergoes dissociation giving a negative (–Al–O^-) or positive (–Al–OH_2^+) depending on the pH of the solution. An isoelectric point may be identified for the edges (usually between pH 7–9). This means that the double layer at the edges is different from that at the faces and the surface charges can be positive or negative depending on the pH of the solution. For that reason, van Olphen [24] suggested an edge-to-face association of clay platelets (which he termed the "house of cards" structure) and this was assumed to be the driving force for gelation of swellable clays. However, Norrish [25] suggested that clay gelation is caused simply by the interaction of the expanded double layers. This is particularly the case in dilute electrolyte solutions in which the double layer thickness can be several orders of magnitude higher than the particle dimensions.

With oxides, such as finely divided silica, gel formation is caused by formation of chain aggregates, which interact forming a three-dimensional network that is elastic in nature. Clearly, the formation of such networks depends on the nature and particle size of the silica particles. For effective gelation, one should choose silicas with very small particles and highly solvated surfaces. (iv) Use of mixtures of polymers and finely divided solids. Mixtures of polymers, such as hydroxyethyl cellulose or xanthan gum with finely divided solids such as sodium montmorillonite or silica, offer one of

the most robust antisettling systems. By optimizing the ratio of the polymer to the solid particles, one can arrive at the right viscosity and elasticity to reduce settling and separation. Such systems are more shear thinning than the polymer solutions and hence they are more easily dispersed in water on application. The most likely mechanism by which these mixtures produce viscoelastic network is probably through bridging or depletion flocculation. The polymer-particulate mixtures also show less temperature dependency of viscosity and elasticity than the polymer solutions and hence they ensure the long-term physical stability at high temperatures. (v) Controlled flocculation. For systems where the stabilizing mechanism is electrostatic in nature, for example those stabilized by surfactants or polyelectrolytes, the energy–distance curve (Fig. 3.3 (a)) shows a secondary minimum at larger particle separations. Such a minimum can be quite deep (few tens of kT units), particularly for large (> 1 μm) and asymmetric particles. The depth of the minimum also depends on electrolyte concentration. Thus, by adding small amounts of electrolyte, weak flocculation may be obtained. The weakly flocculated systems may produce a gel network (self-structured system) which has sufficient elasticity to reduce settling and eliminate claying. This has been demonstrated by Tadros [17] for ethirimol suspensions stabilized with phenol formaldehyde sulphonated condensate (a polyelectrolyte with modest molecular weight). By increasing NaCl concentration, the depth of the secondary minimum increases, reaching $\approx 50kT$ at the highest electrolyte concentration. By using electrolytes of higher valency such as $CaCl_2$ or $AlCl_3$, such deep minima are produced at much lower electrolyte concentrations. Thus, by controlling electrolyte concentration and valency, one can reach a sufficiently deep secondary minimum for producing a gel with enough elasticity to reduce settling and eliminate claying. For systems stabilized by nonionic surfactants or macromolecules, the energy–distance curve also shows a minimum (Fig. 3.3 (b)) whose depth depends on particle size, Hamaker constant and the thickness of the adsorbed layer, which in turn depends on the molecular weight of the polymer. As the molecular weight of the polymer is reduced below a certain value, the depth of the minimum becomes sufficiently high for weak flocculation to occur. The gel network structure of these weakly flocculated suspensions prevents sedimentation. (vi) Depletion flocculation. The addition of "free" (nonadsorbing) polymer can induce weak flocculation of the suspension when the concentration or volume fraction of the free polymer (ϕ_p) exceeds a critical value that is denoted by ϕ_p^+. The first quantitative analysis of the phenomenon was reported by Asakura and Oosawa [16]. They showed that when two particles approach to a distance of separation that is smaller than the diameter of the free coil, exclusion of the polymer molecules from the interstices between the particles takes place, leading to the formation a polymer-free zone (depletion zone). This was illustrated in Fig. 3.4, which shows the situation below and above ϕ_p^+. As a result of this process, an attractive force, associated with the lower osmotic pressure in the region between the particles, is produced. This weak flocculation process can be applied to prevent sedimentation and formation of clays. This has been illustrated by using ethirimol suspensions stabilized by a graft copolymer

containing poly(ethylene oxide) (PEO) side chains (with $M = 750$) to which free HEC with various molecular weights was added. Above a critical volume fraction of the free polymer (which decreased with increasing molecular weight) weak flocculation occurred, which increased with a further increase in free polymer concentration. This structure may have a sufficient yield value or modulus, G^*, that prevents particle sedimentation. This is illustrated in Fig. 3.9, which shows the variation of G^* with ϕ_p of HEC (with three different molecular weights) for ethirimol suspensions. G^* shows a rapid increase with increasing ϕ_p when the latter is higher than ϕ_p^+. As predicted, the higher the molecular weight of HEC the lower the value of ϕ_p^+.

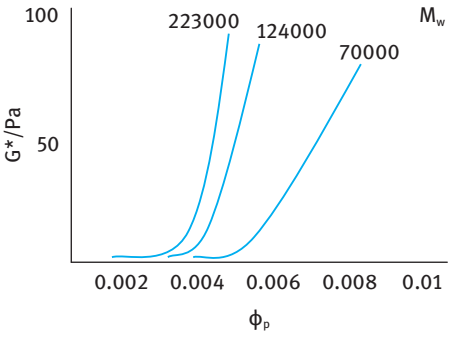

Fig. 3.9: Variation of G^* with ϕ_p for an ethirimol suspension flocculated by HEC.

3.7 Characterization of suspension concentrates and assessment of their long-term physical stability

For the full assessment of the properties of suspension concentrates, three main types of investigations are needed:

(i) Fundamental investigation of the system at a molecular level.
(ii) Investigations into the state of the suspension on standing.
(iii) Bulk properties of the suspension.

All these investigations require a number of sophisticated techniques such as zeta potential measurements, surfactant and polymer adsorption and their conformation at the solid/liquid interface, measurement of the rate of flocculation and crystal growth, and several rheological measurements.

Apart from these practical methods which are present in most industrial laboratories, more fundamental information can be obtained using modern sophisticated techniques such as small angle X-ray and neutron scattering measurements, ultrasonic absorption techniques, etc. Several other modern techniques are also now available for investigating the state of the suspension: Freeze fracture and electron microscopy, atomic force microscopy, scanning tunnelling microscopy and confocal laser microscopy.

In all the above methods, care should be taken in sampling the suspension, which should cause as little disturbance as possible to the "structure" to be investigated. For example, when one investigates the flocculation of a concentrated suspension, dilution of the system for microscopic investigation may lead to a breakdown of the flocs and a false assessment is obtained. The same applies when one investigates the rheology of a concentrated suspension, since transfer of the system from its container to the rheometer may lead to a breakdown of the structure.

For the above reasons one must establish well-defined procedures for every technique and this requires a great deal of skill and experience. It is advisable in all cases to develop standard operation procedures for the above investigations.

The main procedure that may be applied to investigate the charge at the solid/liquid interface (e.g. when using ionic surfactants or polyelectrolytes), which is important in the assessment of electrostatic stabilization, is to measure the zeta potential. The zeta potential is obtained from the measured electrophoretic mobility, provided information is available on particle size and electrolyte concentration. If the above information is not available (as is the case with many practical systems), one should use the electrophoretic mobility for relative comparison between various systems; the assumption can be made that the higher the mobility, the higher the surface charge and the more likely the system is to be stable against flocculation, if the charge is the main stabilizing factor.

Clearly, for systems stabilized by nonionic surfactants and polymers, electrophoretic mobility measurements are less informative. However, zeta potential measurements can be qualitatively used to obtain information on the adsorbed layer thickness for nonionic surfactants and polymers. When a nonionic surfactant or polymer adsorbs at the solid/liquid interface, a shift in the shear plane occurs and this results in a reduction in the zeta potential. If the zeta potential of the particles is measured in the presence and absence of nonionic surfactant or polymer, then the adsorbed layer thickness can be roughly estimated from the reduction in zeta potential.

For measuring surfactant and polymer adsorption, a representative sample of the solid with known mass m and surface area A per gram is equilibrated with a surfactant or polymer with concentration C_1. After equilibrium is reached (at a given constant temperature), the solid is removed by centrifugation and the equilibrium concentration C_2 is determined analytically.

The amount of adsorption Γ in mol m^{-2} is given by,

$$\Gamma = \frac{(C_1 - C_2)}{mA} = \frac{\Delta C}{mA}. \tag{3.21}$$

In most cases (particularly with surfactants) a plot of Γ versus C_2 gives a Langmuir type isotherm. The data can be fitted using the Langmuir equation,

$$\Gamma = \frac{\Gamma_\infty b C_2}{(1 + bC_2)}, \tag{3.22}$$

where b is a constant that is related to the free energy of adsorption,

$$b \propto \left(-\frac{\Delta G_{\text{ads}}}{RT}\right). \tag{3.23}$$

Most polymers (particularly those with high molecular weight) give a high affinity isotherm, indicating irreversibility of adsorption.

Two general techniques may be applied for measuring the rate of flocculation of suspensions, both of which can only be applied for dilute systems. The first method is based on measuring the scattering of light by the particles. For monodisperse particles with a radius that is less than $\lambda/20$ (where λ is the wavelength of light), one can apply the Rayleigh equation in which the turbidity τ_0 is given by,

$$\tau_0 = A' n_0 V_1^2, \tag{3.24}$$

where A' is an optical constant (which is related to the refractive index of the particle and medium and the wavelength of light) and n_0 is the number of particles, each with a volume V_1.

By combining the Rayleigh theory with the Smoluchowski–Fuchs theory of flocculation kinetics [26], one can obtain the following expression for the variation of turbidity with time,

$$\tau = A' n_0 V_1^2 (1 + 2 n_0 k t), \tag{3.25}$$

where k is the rate constant of flocculation.

The second method for obtaining the rate constant of flocculation is by direct particle counting as a function of time. For this purpose, optical microscopy or image analysis may be used, provided the particle size is within the resolution limit of the microscope. Alternatively, the particle number may be determined using electronic devices such as the Coulter Counter or the flow ultramicroscope.

The rate constant of flocculation is determined by plotting $1/n$ versus t, where n is the number of particles after time t, i.e.,

$$\left(\frac{1}{n}\right) = \left(\frac{1}{n_0}\right) + kt. \tag{3.26}$$

The rate constant k of slow flocculation is usually related to the rapid rate constant k_0 (the Smoluchowski rate) by the stability ratio W,

$$W = \left(\frac{k}{k_0}\right). \tag{3.27}$$

One usually plots $\log W$ versus $\log C$ (where C is the electrolyte concentration) to obtain the critical coagulation concentration (CCC), which is the point at which $\log W = 0$.

For sterically stabilized suspensions, flocculation (referred to as incipient flocculation) occurs when the medium for the chains becomes a θ-solvent. This occurs, for example, on heating an aqueous suspension stabilized with poly(ethylene oxide)

(PEO) or poly(vinyl alcohol) chains. Above a certain temperature (the θ-temperature) that depends on electrolyte concentration, flocculation of the suspension occurs. The temperature at which this occurs is defined as the critical flocculation temperature (CFT).

This process of incipient flocculation can be followed by measuring the turbidity of the suspension as a function of temperature. Above the CFT, the turbidity of the suspension rises very sharply.

For the above purpose, the cell in the spectrophotometer that is used to measure the turbidity is placed in a metal block that is connected to a temperature programming unit (which allows one to increase the temperature at a controlled rate).

As discussed above, Ostwald ripening is the result of the difference in solubility S between small and large particles. The smaller particles have larger solubility than the larger particles,

$$S \propto \frac{2\sigma}{r}, \tag{3.28}$$

where σ is the solid/liquid interfacial tension and r is the particle radius.

For two particles with radii r_1 and r_2,

$$\frac{RT}{M} \ln\left(\frac{S_1}{S_2}\right) = \left(\frac{2\sigma}{\rho}\right)\left(\frac{1}{r_1} - \frac{1}{r_2}\right), \tag{3.29}$$

where R is the gas constant, T is the absolute temperature, M is the molecular weight and ρ is the density of the particles.

To obtain a measure of the rate of crystal growth, the particle size distribution of the suspension is followed as a function of time, using either a Coulter counter, a Mastersizer or an optical disc centrifuge. One usually plots the cube of the average radius versus time, which gives a straight line from which the rate of crystal growth can be determined (the slope of the linear curve).

The bulk properties of suspension concentrates can be investigated by measuring the equilibrium sediment volume (or height) and redispersion. For a "structured" suspension, obtained by "controlled" flocculation or addition of "thickeners" (such polysaccharides, clays or oxides), the "flocs" sediment at a rate dependent on their size and the porosity of the aggregated mass. After this initial sedimentation, compaction and rearrangement of the floc structure occurs, a phenomenon referred to as consolidation.

Normally in sediment volume measurements, one compares the initial volume V_0 (or height H_0) with the ultimately reached value V (or H). A colloidally stable suspension gives a "close-packed" structure with relatively small sediment volume (dilatant sediment referred to as clay). A weakly flocculated or structured suspension gives a more open sediment and hence a higher sediment volume. Thus by comparing the relative sediment volume V/V_0 or height H/H_0, one can distinguish between a clayed and a flocculated suspension.

Three different rheological measurements may be applied to investigate the stability/instability of SCs:

(i) Steady state shear stress–shear rate measurements (using a controlled shear rate instrument).
(ii) Constant stress (creep) measurements (carried out using a constant stress instrument).
(iii) Dynamic (oscillatory) measurements (preferably carried out using a constant strain instrument).

These rheological techniques can be used to assess sedimentation and flocculation of suspensions.

As discussed before, the rate of sedimentation decreases with increasing volume fraction of the disperse phase, ϕ, and ultimately it approaches zero at a critical volume fraction ϕ_p (the maximum packing fraction). However, at $\phi \approx \phi_p$, the viscosity of the system approaches ∞. Thus, for most practical suspensions, the system is prepared at ϕ values below ϕ_p and then "thickeners" are added to reduce sedimentation. As mentioned above, these "thickeners" are usually high molecular weight polymers (such as xanthan gum, hydroxyethyl cellulose or associative thickeners), finely divided inert solids (such as silica or swelling clays) or a combination of the two. In all cases, a "gel" network is produced in the continuous phase which is shear thinning (i.e. its viscosity decreases with increasing shear rate) and viscoelastic (i.e. it has viscous and elastic components of the modulus). If the viscosity of the elastic network, at shear stresses (or shear rates) comparable to those exerted by the particles exceeds a certain value, then sedimentation is completely eliminated.

The shear stress, σ_p, exerted by a particle (force/area) can be simply calculated,

$$\sigma_p = \frac{(4/3)\pi R^3 \Delta\rho g}{4\pi R^2} = \frac{\Delta\rho R g}{3}. \tag{3.30}$$

For a 10 μm radius particle with density difference $\Delta\rho = 0.2$, σ_p is equal to,

$$\sigma_p = \frac{0.2 \times 10^3 \times 10 \times 10^{-6} \times 9.8}{3} \approx 6 \times 10^{-3}. \tag{3.31}$$

For smaller particles, smaller stresses are exerted.

Thus, to predict sedimentation, one has to measure the viscosity at very low stresses (or shear rates). These measurements can be carried out using a constant stress rheometer (Carrimed, Bohlin, Rheometrics or Physica). A constant stress σ (using for example a drag cup motor that can apply very small torques and using an air bearing system to reduce the frictional torque) is applied on the system (which may be placed in the gap between two concentric cylinders or a cone-plate geometry) and the deformation (strain γ or compliance $J = \gamma/\sigma = \text{Pa}^{-1}$) is followed as a function of time [27].

For a viscoelastic system, the compliance shows a rapid elastic response J_0 at $t \to 0$ (instantaneous compliance $J_0 = 1/G_0$, where G_0 is the instantaneous modulus that is a measure of the elastic (i.e. "solid-like") component). At $t > 0$, J increases

slowly with time and this corresponds to the retarded response ("bonds" are broken and reformed but not at the same rate). Above a certain time period (that depends on the system), the compliance shows a linear increase with time (i.e. the system reaches a steady state with constant shear rate). If, after the steady state is reached, the stress is removed, elastic recovery occurs and the strain changes sign. This above behaviour (usually referred to as "creep") is schematically represented in Fig. 3.10.

Creep is the sum of a constant value $J_e\sigma_0$ (elastic part) and a viscous contribution $\sigma_0 t/\eta_0$

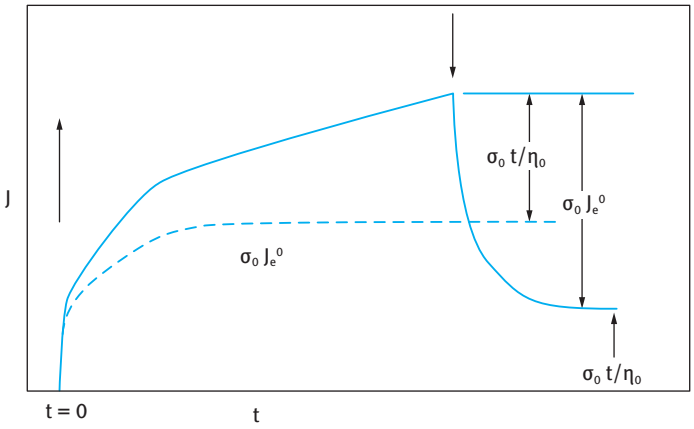

Fig. 3.10: Creep curve for a viscoelastic liquid.

The slope of the linear part of the creep curve gives the value of the viscosity at the applied stress, η_σ,

$$\frac{J}{t} = \frac{\mathrm{Pa}^{-1}}{\mathrm{s}} = \frac{1}{\mathrm{Pa\,s}} = \eta_\sigma. \tag{3.32}$$

The recovery curve will only give the elastic component, which if superimposed on the ascending part of the curve will give the viscous component.

Thus, one measures creep curves as a function of the applied stress (starting from a very small stress of the order of 0.01 Pa). This is illustrated in Fig. 3.11.

The viscosity η_σ (which is equal to the reciprocal of the slope of the straight portion of the creep curve) is plotted as a function of the applied stress. This is schematically shown in Fig. 3.12. Below a critical stress, σ_{cr}, the viscosity reaches a limiting value, $\eta_{(0)}$ namely the residual (or zero shear) viscosity. σ_{cr} may be denoted as the "true yield stress" of the suspension, i.e. the stress above which the "structure" of the system is broken down. Above σ_{cr}, η_σ decreases rapidly with a further increase of shear stress (the shear thinning regime). It reaches another Newtonian value η_∞, which is the high shear limiting viscosity.

Creep measurements (Constant stress) can be used to obtain the residual or zero shear viscosity

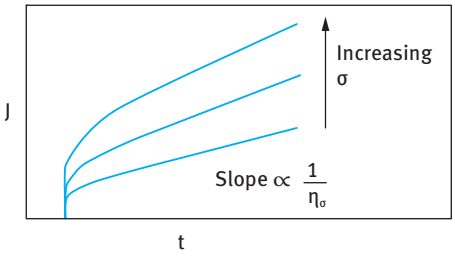

Fig. 3.11: Creep curves at increasing applied stress.

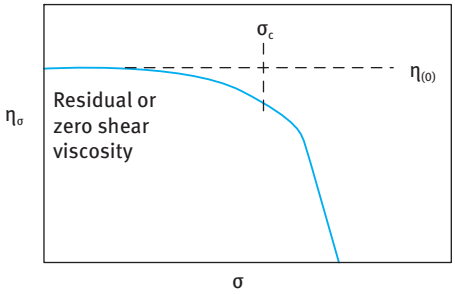

Critical stress is a useful parameter (related to yield stress) as denotes the stress at which stucture "breaks down"

Fig. 3.12: Variation of viscosity with applied stress.

$\eta_{(0)}$ could be several orders of magnitudes (10^4–10^8) higher than η_∞. Usually one obtains good correlation between the rate of sedimentation v and the residual viscosity $\eta_{(0)}$ [22]. This was illustrated in Fig. 3.8.

Above a certain value of $\eta_{(0)}$, v becomes equal to 0. Clearly, to minimize sedimentation one has to increase $\eta_{(0)}$; an acceptable level for the high shear viscosity η_∞ must be achieved, depending on the application. In some cases, a high $\eta_{(0)}$ may be accompanied by a high η_∞ (which may not be acceptable for the application, for example if spontaneous dispersion on dilution is required). If this is the case, the formulation chemist should look for an alternative thickener.

Another problem encountered with many suspensions is that of "syneresis", i.e. the appearance of a clear liquid film at the top of the suspension. "Syneresis" occurs with most "flocculated" and/or "structured" (i.e. those containing a thickener in the continuous phase) suspensions. "Syneresis" may be predicted from measuring the yield value (using steady state measurements of shear stress as a function of shear rate) as a function of time or using oscillatory techniques (whereby the storage and loss modulus are measured as a function of strain amplitude and frequency of oscillation). It is sufficient to state in this section that when a network of the suspension

particles (either alone or combined with the thickener) is produced, the gravity force will cause some contraction of the network (which behaves as a porous plug), thus causing some separation of the continuous phase which is entrapped between the droplets in the network.

As mentioned before, flocculation of suspensions is the result of the long-range van der Waals attraction. Flocculation can be weak (and reversible) or strong, depending on the magnitude of the net attractive forces. Weak flocculation may result in reversible time dependency of the viscosity, i.e. on shearing the suspension at a given shear rate, the viscosity decreases and on standing the viscosity recovers to its original value. This phenomenon is referred to as thixotropy (sol–gel transformation).

Rheological techniques are most convenient to assess suspension flocculation without the need for any dilution (which in most cases results in a breakdown of the floc structure). In steady state measurements the suspension is carefully placed in the gap between concentric cylinder or cone-and-plate platens. For the concentric cylinder geometry, the gap width should be at least 10× larger than the largest particle size (a gap width that is greater than 1 mm is usually used). For the cone-and-plate geometry, a cone angle of 4° or smaller is usually used.

A controlled rate instrument is usually used for the above measurements; the inner (or outer) cylinder, the cone (or the plate) is rotated at various angular velocities (which allow one to obtain the shear rate γ) and the torque is measured on the other element (this allows one to obtain the stress σ).

For a Newtonian system (such as the case of a dilute suspension, with a volume fraction ϕ less than 0.1), σ is related to γ by the equation,

$$\sigma = \eta\gamma, \tag{3.33}$$

where η is the Newtonian viscosity (that is independent of the applied shear rate).

For most practical suspensions (with $\phi > 0.1$ and containing thickeners to reduce sedimentation), a plot of σ versus γ is not linear (i.e. the viscosity depends on the applied shear rate). The most common flow curve is shown in Fig. 3.13 (usually described as a pseudoplastic or shear thinning system). In this case, the viscosity decreases with

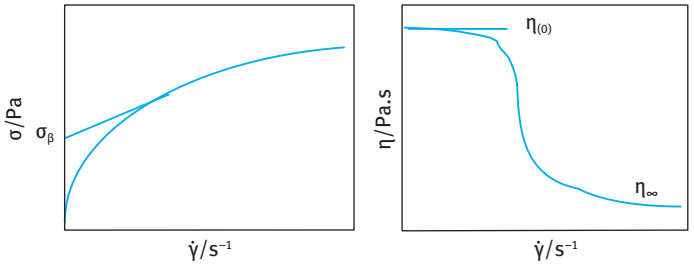

Fig. 3.13: Shear stress and viscosity versus shear rate for a pseudoplastic system.

increasing shear rate, reaching a Newtonian value above a critical shear rate. Several models may be applied to analyse the results of Fig. 3.13.

(i) Power law model,

$$\sigma = k\gamma^n, \tag{3.34}$$

where k is the consistency index of the suspension and n is the power (shear thinning) index ($n < 1$); the lower the value of n the more shear thinning the suspension is. This is usually the case with weakly flocculated suspensions or those to which a "thickener" has been added.

By fitting the results of Fig. 3.13 to equation (3.34) (this is usually done in the software of the computer connected to the rheometer) one can obtain the viscosity of the suspension at a given shear rate,

$$\eta(\text{at a given shear rate}) = \frac{\sigma}{\gamma} = k\gamma^{n-1}. \tag{3.35}$$

(ii) Bingham model,

$$\sigma = \sigma_\beta + \eta_{\text{pl}}\dot{\gamma}, \tag{3.36}$$

where σ_β is the extrapolated yield value (obtained by extrapolation of the shear stress-shear rate curve to $\gamma = 0$). Again this is provided in the software of the rheometer. η_{pl} is the slope of the linear portion of the σ–γ curve (usually referred to as the plastic viscosity).

Both σ_β and η_{pl} may be related to the flocculation of the suspension. At any given volume fraction of the emulsion and at a given particle size distribution, the higher the value of σ_β and η_{pl} the more the flocculated the suspension is. Thus, if one stores a suspension at any given temperature and makes sure that the particle size distribution remains constant (i.e. no Ostwald ripening occurred), an increase in the above parameters indicates flocculation of the suspension on storage. Clearly, if Ostwald ripening occurs simultaneously, σ_β and η_{pl} may change in a complex manner with storage time. Ostwald ripening results in a shift of the particle size distribution to higher diameters; this has the effect of reducing σ_β and η_{pl}. If flocculation occurs simultaneously (having the effect of increasing these rheological parameters), the net effect may be an increase or decrease in the rheological parameters.

The above trend depends on the extent of flocculation relative to Ostwald ripening. Therefore, following σ_β and η_{pl} with storage time requires knowledge of Ostwald ripening and/or coalescence. Only in the absence of this latter breakdown process, one can use rheological measurements as a guide of assessment of flocculation.

(iii) Herschel–Buckley model [27].

In many cases, the shear stress–shear rate curve may not show a linear portion at high shear rates. In this case, the data may be fitted with a Hershel–Buckley model,

$$\sigma = \sigma_\beta + k\gamma^n. \tag{3.37}$$

(iv) Casson's model [27].

This is another semi-empirical model that may be used to fit the data of Fig. 3.13,

$$\sigma^{1/2} = \sigma_C^{1/2} + \eta_C^{1/2}\gamma^{1/2}. \tag{3.38}$$

Note that σ_β is not equal to σ_C.

Equation (3.38) shows that a plot of $\sigma^{1/2}$ versus $\gamma^{1/2}$ gives a straight line from which σ_C and η_C can be evaluated.

In all the above analyses, the assumption was made that a steady state was reached. In other words, no time effects occurred during the duration of the flow experiment. However, many suspensions (particularly those that are weakly flocculated or "structured" to reduce sedimentation) show time effects during flow. At any given shear rate, the viscosity of the suspension continues to decrease with increasing the time of shear; on stopping the shear, the viscosity recovers to its initial value. This reversible decrease of viscosity is referred to as thixotropy.

The most common procedure for studying thixotropy is to apply a sequence of shear stress-shear rate regimes within controlled periods. If the flow curve is carried out within a very short time (say increasing the rate from 0 to say 500 s^{-1} in 30 s and then reducing it again from 500 to 0 s^{-1} within the same period), one finds that the descending curve is below the ascending one.

The above behaviour can be explained from a consideration of the structure of the system. If, for example the suspension is weakly flocculated, then on applying a shear force on the system, this flocculated structure is broken down (and this is the cause of the shear thinning behaviour). On reducing the shear rate back to zero, the structure builds up only in part within the duration of the experiment (30 s).

The ascending and descending flow curves show hysteresis that is usually referred to as the "thixotropic loop". If now the same experiment is repeated within a longer experimental time (say 120 s for the ascending and 120 s for the descending curves), the hysteresis decreases, i.e. the "thixotropic loop" becomes smaller.

The above study may be used to investigate the state of flocculation of a suspension. Weakly flocculated suspensions usually show thixotropy and the change in thixotropy with applied time may be used as an indication of the strength of this weak flocculation.

The above analysis is only qualitative and one cannot use the results in a quantitative manner. This is due to the possible breakdown of the structure on transferring the suspension to the rheometer and also during the uncontrolled shear experiment.

A very important point that must be considered during rheological measurements is the possibility of "slip" during the measurements. This is particularly the case with highly concentrated suspensions, in which the flocculated system may form a "plug" in the gap of the platens leaving a thin liquid film at the walls of the concentric cylinder or cone-and-plate geometry. To reduce "slip" one should use roughened walls for the platens.

Strongly flocculated suspensions usually show much less thixotropy than weakly flocculated systems. Again one must be careful in drawing definite conclusions without other independent techniques (e.g. microscopy).

The second method for investigating flocculation is to use constant stress or creep measurements. This method has been described in detail in the section on sedimentation. Basically, a constant stress σ is applied on the system and the compliance J (Pa^{-1}) is plotted as a function of time as was illustrated in Fig. 3.10 (creep curve).

The above experiment is repeated several times increasing the stress from the smallest possible value (that can be applied by the instrument), increasing the stress in small increments. A set of creep curves are produced at various applied stresses as was illustrated in Fig. 3.11. From the slope of the linear portion of the creep curve (after the system reaches a steady state), the viscosity at each applied stress, η_σ, is calculated. A plot of η_σ versus σ (as illustrated in Fig. 3.13) allows one to obtain the limiting (or zero shear) viscosity $\eta_{(0)}$ and the critical stress σ_{cr} (which may be identified with the "true" yield stress of the system).

The values of $\eta_{(0)}$ and σ_{cr} may be used to assess the flocculation of the suspension on storage. If flocculation occurs on storage (without any Ostwald ripening), the values of $\eta_{(0)}$ and σ_{cr} may show a gradual increase with increasing storage time.

As discussed in the previous section (on steady state measurements), the trend becomes complicated if Ostwald ripening occurs simultaneously (both have the effect of reducing $\eta_{(0)}$ and σ_{cr}). Thus, these measurements should be supplemented by particle size distribution measurements of the diluted suspension (making sure that no flocs are present after dilution) to assess the extent of Ostwald ripening.

Another complication may arise from the nature of the flocculation. If the latter occurs in an irregular way (producing strong and tight flocs), $\eta_{(0)}$ may increase, while σ_{cr} may show some decrease and this complicates the analysis of the results.

In spite of the above complications, constant stress measurements may provide valuable information on the state of the suspension on storage. Carrying out creep experiments and ensuring that a steady state is reached can be time consuming. One usually carries out a stress sweep experiment, where the stress is gradually increased (within a predetermined time period to ensure that one is not too far from reaching the steady state) and plots of η_σ versus σ are established.

The above experiments are carried out at various storage times (say every two weeks) and temperatures. From the change of $\eta_{(0)}$ and σ_{cr} with storage time and temperature, one may obtain information on the degree and the rate of flocculation of the system.

One main problem in carrying the above experiments is sample preparation. When a flocculated emulsion is removed from the container, care should be taken not to cause too much disturbance to that structure (minimum shear should be applied on transferring the emulsion to the rheometer). It is also advisable to use separate containers for assessing flocculation. A relatively large sample is prepared and this is then transferred to a number of separate containers.

Dynamic (oscillatory) measurements are by far the most commonly used method to obtain information on the flocculation of a suspension. A strain is applied in a sinusoidal manner, with an amplitude γ_0 and a frequency ν (cycles/s or Hz) or ω (rad s^{-1}). In a viscoelastic system (such as the case with a flocculated suspension), the stress oscillates with the same frequency, but out of phase from the strain. From measuring the time shift between strain and stress amplitudes (Δt) one can obtain the phase angle shift δ,

$$\delta = \Delta t \omega. \tag{3.39}$$

A schematic representation of the variation of strain and stress with ε is shown in Fig. 3.14.

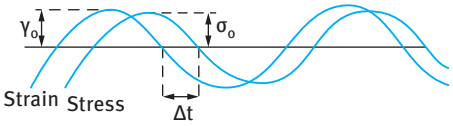

Δt = time shift for sine waves of stress and strain
Δt ω = δ, phase angle shift
ω = frequency in radian s^{-1}
ω = 2 π ν

Perfectly elasic solid	δ = 0
Perfectly viscous liquid	δ = 90°
Viscoelastic system	0 < δ < 90°

Fig. 3.14: Stress–strain relationship for a viscoelastic system.

From the amplitudes of stress and strain and the phase angle shift, one can obtain the various viscoelastic parameters: the complex modulus G^*, the storage modulus (the elastic component of the complex modulus) G', the loss modulus (the viscous component of the complex modulus) G'', tan δ and the dynamic viscosity η'.

$$\text{complex modulus } |G^*| = \frac{\sigma_0}{\gamma_0}, \tag{3.40}$$

$$\text{storage modulus } G' = |G^*| \cos \delta, \tag{3.41}$$

$$\text{loss modulus } G'' = |G^*| \sin \delta \tag{3.42}$$

$$\tan \delta = \frac{G''}{G'} \tag{3.43}$$

$$\text{dynamic viscosity } \eta' = \frac{G''}{\omega}. \tag{3.44}$$

G' is a measure of the energy stored in a cycle of oscillation. G'' is a measure of the energy dissipated as viscous flow in a cycle of oscillation. tan δ is a measure of the relative magnitudes of the viscous and elastic components. Clearly, the smaller the value of tan δ, the more elastic the system is and vice versa.

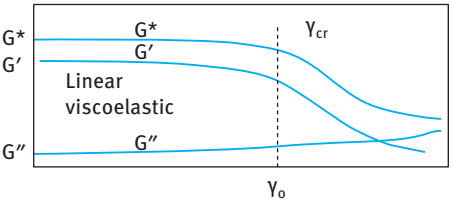

Linear viscoelastic region
G*, G′ and G″ are independent of strain amplitude
γ_{cr} is the critical strain above which systems shows non-linear response (break down of structure)

Fig. 3.15: Strain sweep results.

η', the dynamic viscosity, shows a decrease with increasing frequency ω. η' reaches a limiting value as $\omega \to 0$. The value of η' in this limit is identical to the residual (or zero shear) viscosity $\eta_{(0)}$.

In oscillatory measurements one carries out two sets of experiments: (i) Strain sweep measurements. In this case, the oscillation is fixed (say at 0.1 or 1 Hz) and the viscoelastic parameters are measured as a function of strain amplitude. This allows one to obtain the linear viscoelastic region. In this region all moduli are independent of the applied strain amplitude and become only a function of time or frequency. This is illustrated in Fig. 3.15, which shows a schematic representation of the variation of G^*, G' and G'' with strain amplitude (at a fixed frequency).

It can be seen from Fig. 3.15 that G^*, G' and G'' remain virtually constant up to a critical strain value, γ_{cr}. This region is the linear viscoelastic region. Above γ_{cr}, G^* and G' starts to fall, whereas G'' starts to increase. This is the nonlinear region. The value of γ_{cr} may be identified with the minimum strain above which the "structure" of the suspension starts to break down (for example breakdown of flocs into smaller units and/or breakdown of a "structuring" agent).

From γ_{cr} and G', one can obtain the cohesive energy E_c (J m^{-3}) of the flocculated structure [27],

$$E_c = \int_0^{\gamma_{cr}} \sigma \, d\gamma = \int_0^{\gamma_{cr}} G'\gamma \, d\gamma = \frac{1}{2} G'\gamma_{cr}^2. \tag{3.45}$$

E_c may be used in a quantitative manner as a measure of the extent and strength of the flocculated structure in a suspension. The higher the value of E_c the more flocculated the structure is. Clearly E_c depends on the volume fraction of the suspension as well as the particle size distribution (which determines the number of contact points in a floc). Therefore, for quantitative comparison between various systems, one has to make sure that the volume fraction of the disperse particles is the same and the suspensions have very similar particle size distribution.

E_c also depends on the strength of the flocculated structure, i.e. the energy of attraction between the particles. This depends on whether the flocculation is in the primary or secondary minimum. Flocculation in the primary minimum is associated

with a large attractive energy and this leads to higher values of E_c when compared with the values obtained for secondary minimum flocculation. For a weakly flocculated suspension, such as the case with secondary minimum flocculation of an electrostatically stabilized suspension, the deeper the secondary minimum, the higher the value of E_c (at any given volume fraction and particle size distribution of the suspension).

With a sterically stabilized suspension, weak flocculation can also occur when the thickness of the adsorbed layer decreases. Again, the value of E_c can be used as a measure of the flocculation; the higher the value of E_c, the stronger the flocculation. If incipient flocculation occurs (on reducing the solvency of the medium for the change to worse than θ-condition) a much deeper minimum is observed and this is accompanied by a much larger increase in E_c.

To apply the above analysis, one must have an independent method for assessing the nature of the flocculation. Rheology is a bulk property that can give information on the interdroplet interaction (whether repulsive or attractive) and to apply it in a quantitative manner one must know the nature of these interaction forces. However, rheology can be used in a qualitative manner to follow the change in the suspension on storage. Providing the system does not undergo any Ostwald ripening, the change of the moduli with time and in particular the change of the linear viscoelastic region may be used as an indication of flocculation. Strong flocculation is usually accompanied by a rapid increase in G' and this may be accompanied by a decrease in the critical strain above which the "structure" breaks down. This may be used as an indication for the formation of "irregular" flocs which become sensitive to the applied strain. The floc structure will entrap a large amount of the continuous phase and this leads to an apparent increase in the volume fraction of the suspension and hence an increase in G'.

(ii) Oscillatory sweep. In this case, the strain amplitude is kept constant in the linear viscoelastic region (one usually takes a point far from γ_{cr} but not too low, i.e. in the midpoint of the linear viscoelastic region) and measurements are carried out as a function of frequency. This is schematically represented in Fig. 3.16 for a viscoelastic liquid system.

Both G^* and G' increase with increasing frequency and ultimately, above a certain frequency, they reach a limiting value and show little dependency on frequency. G'' is higher than G' in the low frequency regime; it also increases with increasing frequency and at a certain characteristic frequency ω^* (that depends on the system) it becomes equal to G' (usually referred to as the crossover point), after which it reaches a maximum and then shows a reduction with a further increase in frequency.

In the low frequency regime, i.e. below ω^*, $G'' > G'$, this regime corresponds to longer times (remember that the time is reciprocal of frequency) and under these conditions the response is more viscous than elastic. In the high frequency regime, i.e. above ω^*, $G' > G''$, this regime corresponds to shorter times and under these conditions the response is more elastic than viscous.

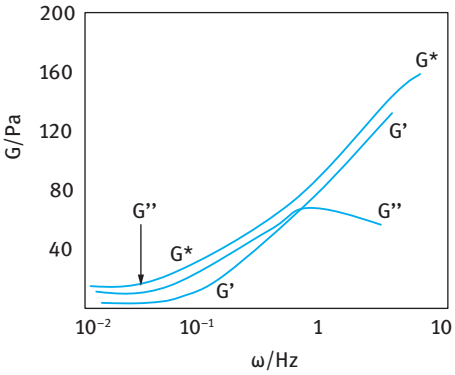

Fig. 3.16: Schematic representation of oscillatory measurements for a viscoelastic liquid.

At sufficiently high frequency, G'' approaches zero and G' becomes nearly equal to G^*; this corresponds to very short timescales whereby the system behaves as a near elastic solid. Very little energy dissipation occurs at such high frequency.

The characteristic frequency ω^* can be used to calculate the relaxation time of the system t^*,

$$t^* = \frac{1}{\omega^*}. \tag{3.46}$$

The relaxation time may be used as a guide for the state of the suspension. For a colloidally stable suspension (at a given particle size distribution), t^* increases with increasing volume fraction of the solid phase, ϕ. In other words, the crossover point shifts to lower frequency with increasing ϕ. For a given suspension, t^* increases with increasing flocculation providing the particle size distribution remains the same (i.e. no Ostwald ripening).

The value of G' also increases with increasing flocculation, since aggregation of particles usually results in liquid entrapment and the effective volume fraction of the suspension shows an apparent increase. With flocculation, the net attraction between the droplets also increases and this results in an increase in G'. G' is determined by the number of contacts between the particles and the strength of each contact (which is determined by the attractive energy).

It should be mentioned that in practice one may not obtain the full curve, due to the frequency limit of the instrument and also measurements at low frequency are time consuming. Usually one obtains part of the frequency dependency of G' and G''. In most cases, one has a more elastic than viscous system. Most suspension systems used in practice are weakly flocculated and they also contain "thickeners" or "structuring" agents to reduce sedimentation and to acquire the right rheological characteristics for application.

The exact values of G' and G'' required depend on the system and its application. In most cases a compromise has to be made between acquiring the right rheological characteristics for the application and the optimum rheological parameters for long-term physical stability.

References

[1] Tadros T. Suspension concentrates. Berlin: De Gruyter; 2017.
[2] Tadros T. Colloids in agrochemicals. Weinheim: Wiley-VCH; 2009.
[3] Tadros TF. Advances Colloid and Interface Science. 1980;12:141.
[4] Tadros TF, editor. Solid/Liquid dispersions. London: Academic Press; 1987.
[5] Parfitt GD. Dispersion of powders in liquids. London: Applied Science Publishers; 1987.
[6] Tadros T. Dispersions of powders in liquids and stabilisation of suspensions. Weinheim: Wiley-VCH; 2012.
[7] Rideal EK. Phil Mag. 1922;44:1152.
[8] Washburn ED. Phys Rev. 1921;17:273.
[9] Rehbinder PA. Colloid J USSR. 1958;20:493.
[10] Rehbinder PA, Likhtman VI. In: Proceedings of International Congress in Surface Active Agents, Vol. 3. London: Butterworth; 1957.
[11] Schukin E, Rhebinder PA. Colloid J USSR. 1958;20:601.
[12] Schick MJ, editor. Nonionic surfactants. New York: Marcel Dekker; 1966.
[13] Schick MJ, editor. Nonionic surfactants: Physical chemistry. New York: Marcel Dekker; 1987.
[14] Schonfeldt N. Surface active ethylene oxide adducts. USA: Pergamon Press; 1970.
[15] Smolders CA. Rec Trav Chim. 1961;80:650.
[16] Asakura A, Oosawa F. J Chem Phys. 1954;22:1235. J Polymer Sci. 1958;93:183.
[17] Tadros T. Surfactants in agrochemicals. New York: Marcel Dekker; 1994.
[18] Thompson W (Lord Kelvin). Phil Mag. 1871;42:448.
[19] Bachelor GK. J Fluid Mech. 1972;52:245.
[20] Bachelor GK. J Fluid Mech. 1976;1:79.
[21] Reed CC, Anderson JL. AICHE J. 1980;26:814.
[22] Buscall R, Goodwin JW, Ottewill RH, Tadros TF. J Colloid Interface Sci. 1982;85:78.
[23] Krieger IM, Advances Colloid and Interface Sci. 1971;3:45.
[24] van Olphen H. Clay colloid chemistry. New York: Wiley; 1963.
[25] Norrish K. Discussion Faraday Soc. 1954;18:120.
[26] von Smoluchowski M. Handbuch der Electricitat und des Magnetismus, Vol. II. Leipzig: Barth; 1914.
[27] Tadros T. Rheology of dispersions. Weinheim: Wiley-VCH; 2010.

4 Suspoemulsions

4.1 Introduction

Suspoemulsions are mixtures of suspensions and emulsions that are applied in many agrochemical formulations. Two active ingredients are formulated, with one as an aqueous suspension and the other as an oil/water emulsion [1]. A schematic representation of suspoemulsions is given in Fig. 4.1. Two main types can be distinguished:

(i) a system in which the solid particles and emulsion droplets remain as separate entities;
(ii) a system in which the solid particles are dispersed in the oil droplets. The first system is the one that is commonly applied in agrochemical formulations.

As mentioned above, with suspoemulsions two active ingredients are formulated together which offers convenience to the farmer and also may result in synergism in biological efficacy. A wider spectrum of disease control may be achieved, particularly with many fungicides and herbicides. With many suspoemulsions an adjuvant that enhances the biological efficacy is added.

The formulation of suspoemulsions is not an easy task; one may produce a stable suspension and emulsion separately but when these are mixed they become unstable due to the following interactions:

(i) Homoflocculation of the suspension particles, which can happen if the dispersing agent used for preparing the suspension is not strongly adsorbed and hence it becomes displaced by the emulsifier which is more strongly adsorbed but not a good stabilizer for the suspension particles.
(ii) Emulsion coalescence, which can happen if the emulsifier is not strongly adsorbed at the O/W or W/O interface, resulting in its partial or complete displacement by the suspension dispersant which is not a good emulsion stabilizer and this results in coalescence of the emulsion droplets with ultimate separation of oil (for O/W) or water (for W/O).

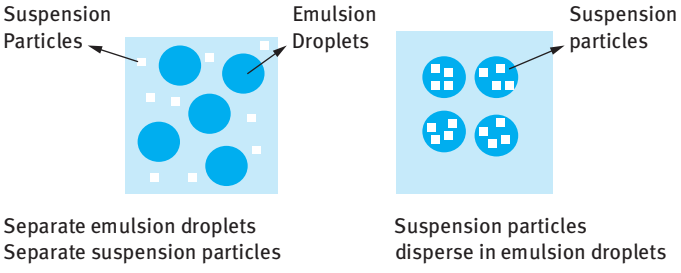

Fig. 4.1: Schematic representation of suspoemulsions.

https://doi.org/10.1515/9783110578997-005

(iii) Heteroflocculation between the oil droplets and suspension particles; the latter may be partially wetted by the oil and they may reside at the O/W interface (this is particularly the case if the oil droplets are much larger than the suspension particles). Heteroflocculation can also occur with suspension particles dispersed in an O/W emulsion.
(iv) Phase transfer and crystallization that can happen when the suspension particles have some solubility in the oil phase. The small suspension particles, which have higher solubility than the larger ones (due to curvature effects), may become dissolved in the oil phase and they become recrystallized onto the larger suspension particles (a form of Ostwald ripening process). Large and sometimes needle-shaped crystals may be produced as a result of crystal habit modification (that sometimes occurs with Ostwald ripening).

One of the most useful methods to study interaction in suspoemulsions is rheology, in particular viscoelastic measurements [1, 2].

4.2 Systems investigated for studying interactions

Agrochemical suspoemulsions consisting of chlorothalonil (density $\rho = 1.85\,\mathrm{g\,cm^{-3}}$) or dichlobutrazol (density $\rho = 1.25\,\mathrm{g\,cm^{-3}}$) suspensions were used. These suspensions were prepared by bead milling using Synperonic NP1800 (nonyl phenol with 13 mol propylene oxide, PPO, and 27 mol ethylene oxide, PEO). Tridemorph (density $\rho = 0.87\,\mathrm{g\,cm^{-3}}$) emulsions were prepared using the same surfactants and the emulsification was carried out using a high speed stirrer, namely Silverson mixer.

For comparison, two model suspoemulsions were used:

(i) The first consisted of polystyrene latex suspensions (mean volume diameter, VMD = 1.84 μm) that was prepared using the surfactant-free method [3] and then stabilized with Synperonic PE P94 (an A–B–A block of PEO–PPO–PEO with 47 PPO units and 42 PEO units). This was mixed with isoparaffinic oil-in-water emulsion (stabilized with Synperonic PE L92 with 47 PPO units and 16 PEO units) that was prepared using a Silverson mixer.
(ii) Suspoemulsions of polystyrene latex containing grafted PEO chains (with molecular weight ≈ 2000), prepared using the "aquersemer method" [4] having a Z-average particle radius of 310 ± 10 nm that was mixed with hexadecane-in-water emulsions (stabilized with Pluronic PE L92) having a Z-average particle radius of 310 ± 10 nm.

The particle size was determined using dynamic light scattering referred to as photon correlation spectroscopy (PCS). (A Malvern PCS instrument was used). The equilibrium sediment and cream volumes were obtained using measuring cylinders at room temperature. Viscoelastic measurements were carried out using a Bohlin VOR.

4.3 Creaming/sedimentation of suspoemulsions

Assuming that a stable suspoemulsion (in the colloid sense) could be prepared, e.g. by the use of a polymeric dispersant and emulsifier, the creaming and/or sedimentation behaviour of the suspoemulsion shows different patterns depending on the density difference between the oil droplets and suspension particles as well as the total volume fraction ϕ of the whole system.

The above behaviour could be illustrated by using the above mentioned agrochemical suspoemulsions consisting of an oil, namely tridemorph (an aliphatic-like oil with a density $\rho = 0.87\ g\ cm^{-3}$) and two different suspensions namely dichlobutrazol (with $\rho = 1.25\ g\ cm^{-3}$) and chlorothalonil (with $\rho = 1.85\ g\ cm^{-3}$).

To ensure colloid stability and absence of heteroflocculation, both the emulsion and suspension were prepared using the above mentioned A–B–C block copolymer (Synperonic NPE 1800) consisting of an anchor chain (B–C) of propylene oxide (13 mol) and nonyl phenol and a stabilizing chain of polyethylene oxide (23 mol).

Synperonic NPE 1800 is an excellent emulsifier for tridemorph and it is also an excellent dispersant for both dichlobutrazol and chlorothalonil. The colloid stability of both emulsion and suspension was confirmed by optical microscopy, which showed no coalescence of the emulsion or flocculation of the suspension. In addition, when mixing the emulsion and suspension there was no heteroflocculation. The suspoemulsions were prepared by simple mixing of the emulsion and suspension, keeping the total volume fraction ϕ constant while varying the ratio of suspension to emulsion. Two ϕ values were investigated, < 0.2 and > 0.2, and a comparison was made between systems with small density difference (dichlobutrazol/tridemorph) and large density difference (chlorothalonil/tridemorph). The results are illustrated in Fig. 4.2–4.4.

When the density difference between the suspension particles and emulsion droplets is not large and $\phi < 0.2$, the emulsion creams and the suspension sediments separate (Fig. 4.2). When the density difference between the suspension particles and emulsion droplets is small but $\phi > 0.2$ the system forms a cream layer when the suspension: emulsion ratio is 2 : 8 and it forms a sediment layer when the ratio is 8 : 2

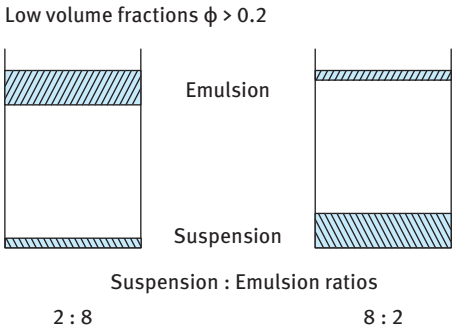

Fig. 4.2: Chlorothalonil/tridemorph ($\phi < 0.2$).

High volume fractions $\phi < 0.2$

When ρ mixure < 1 the emulsion and the suspension both cream
When ρ mixure > 1 the emulsion and the suspension both sediment

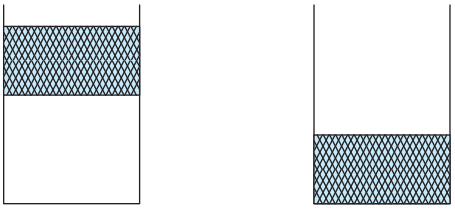

Fig. 4.3: Chlorothalonil/tridemorph ($\phi > 0.2$).

Large density difference – all volume fractions

When the density difference between the suspension and
the emulsion is large (chlorotalonil/ tridemorph $\Delta\rho \approx 1.85–0.87$)
ρ mixure > 1 for all suspension : emulsion ratios

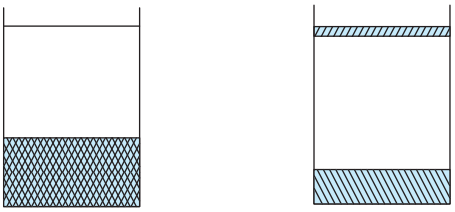

Fig. 4.4: Chlorothalonil/tridemorph (all volume fractions).

(Fig. 4.3). When the density difference between the suspension particles and emulsion droplets is large, then the average density of the suspension particle/emulsion droplet is >1 and in this case sedimentation is observed when the ratio is 2 : 8 but some creaming occurs when the ratio is 8 : 2 (Fig. 4.4).

The above creaming/sedimentation behaviour indicates some interaction between the emulsion droplets and suspension particles. A particularly useful method to illustrate the interactions in suspoemulsions is to compare the total observed sediment plus cream height with that based on simple additivity. This is illustrated in Fig. 4.5 for chlorothalonil/tridemorph suspoemulsions. It can be seen from Fig. 4.5 that the observed sediment + cream heights are smaller than would be expected from simple additivity. It is possible that the small suspension particles become trapped between the larger oil droplets in the cream layer and the small suspension particles become entrapped between the larger suspension particles. Some deformation of the oil droplets may also occur in the sedimented layer.

4.4 Reduction of suspension/emulsion interaction and prevention of instability

Optical microscopic investigation of some other suspoemulsions showed heteroflocculation and this could be reduced or eliminated using Atlox 4913 (an acrylic graft copolymer of polymethylmethacrylate backbone and PEO chains) [5]. The use of strongly "anchored" dispersants and emulsifiers is crucial for reduction of the interaction between the particles and droplets. The interaction can also be significantly reduced by the addition of rheology modifiers such hydroxyethyl cellulose (HEC) or xanthan gum. These thickeners produce a "three-dimensional" gel network by the overlap of the polymer coils of hydroxyethyl cellulose, HEC, or the double helices of xanthan gum. Apart from their effect in reducing creaming and sedimentation by producing a high residual viscosity (at low shear rates) these polymers will also prevent trapping of the oil droplets into the suspension and the suspension particles into the emulsion.

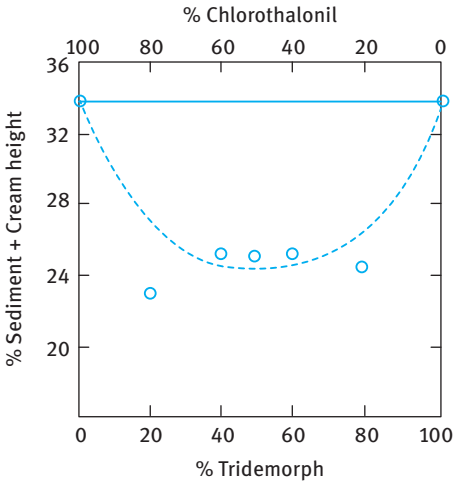

Fig. 4.5: Comparison of experimental, --- and predicted (based on additivity), — sediment + cream heights for chlorothalonil/tridemorph suspoemulsions.

Heteroflocculation results from the competitive adsorption between the dispersant and emulsifier, particularly when these are not strongly anchored to the surfaces. Displacement of some or all of the dispersant by the emulsifier and vice versa may result in attraction between the particles and droplets. The repulsive barrier is weakened in both cases. If the particles are partially wetted by the oil they may reside at the O/W interface if the oil droplets are sufficiently large.

The above processes of attraction may continue for long periods of time and ultimately the suspoemulsion becomes physically unstable. Any flocculation will result in entrapment of the liquid between the particles in floc structure and this causes a significant increase in the viscosity of the system.

Competitive adsorption may be reduced by using the same surfactant for dispersing the solid and emulsifying the oil. This was demonstrated above when using Synperonic NPE 1800. However, since this molecule shows some reversible adsorption, interaction between the particles and droplets is not completely prevented.

A better method for reducing competitive adsorption is to use a polymeric surfactant that is strongly and irreversibly adsorbed on the suspension particles and emulsion droplets, such as the graft copolymer of polymethylmethacrylate backbone with several polyethylene oxide chains grafted onto it [5]. This graft copolymer (Atlox 4913) has a weight average molecular weight of ≈ 20 000 and it adsorbs strongly and irreversibly on hydrophobic particles, e.g. polystyrene latex and most agrochemical suspensions. By using the above graft copolymer as dispersant and an A–B–A block copolymer of PEO (A) and polypropylene oxide (PPO) (B) as emulsifier one can obtain very stable suspoemulsions. A good polymeric stabilizer is INUTEC® SP1 (ORAFTI, Belgium) that consists of an inulin (linear polyfructose with degree of polymerization > 23) chain on which several alkyl chains are grafted [6]. This polymeric surfactant adsorbs on hydrophobic particles and emulsion droplets by multipoint attachment with several alkyl groups leaving strongly hydrated loops and tails of polyfructose that provide an effective steric barrier.

Coalescence of the emulsion droplets on storage accelerates the instability of the suspoemulsion. Large oil droplets can induce heteroflocculation with the suspension particles residing at the O/W interface. Emulsion coalescence can be reduced by one or more of the following methods:

(i) Reduction of droplet size by using a high pressure homogenizer.
(ii) Use of an effective emulsion stabilizer such as INUTEC® SP1.
(iii) Incorporation of an oil-soluble polymeric surfactant such as Atlox 4912 (or Arlacel P135 which can be used in cosmetics). This is an A–B–A block copolymer of polyhydroxy stearic acid (PHS, A) and PEO (B).

4.5 Summary of the criteria for preparing a stable suspoemulsion

(i) Use of a strongly adsorbed (“anchored”) dispersant by multipoint attachment of a block or graft copolymer.
(ii) Use of a polymeric stabilizer for the emulsion (also with multipoint attachment), e.g. INUTEC® SP1.
(iii) Preparation of the suspension and the emulsion separately and allowing enough time for complete adsorption (equilibrium).
(iv) Using low shear when mixing the suspension and the emulsion.
(v) When dissolving an active in an oil (e.g. with many agrochemicals) one should choose an oil in which the suspension particles are insoluble and also the oil should not wet the particles.

(vi) Increasing dispersant and emulsifier concentrations to ensure that the lifetime of any bare patches produced during collision is very short.
(vii) Reducing emulsion droplet size by using a high pressure homogenizer; the smaller droplets are less deformable and coalescence is prevented. In addition, accumulation of the suspension particles at the O/W interface is prevented.
(viii) Use of a rheology modifier such as HEC or xanthan gum that produces a viscoelastic solution that prevents creaming or sedimentation and prevents entrapment of the oil droplets in between the suspension particles or the suspension particles in between the emulsion droplets.
(ix) If possible it is preferable to use a higher volume fraction of the oil when compared with the suspension. In many cases flocculation is more rapid at higher solid volume fractions. The emulsion oil phase volume can be increased by incorporation of an inert oil.

4.6 Preparation of suspoemulsion by emulsification of the oil into the suspension

When the preparation a suspoemulsion with a high volume fraction ϕ of suspension and emulsion (e.g. $\phi > 0.4$) is required, it is preferable to emulsify the oil directly into a prepared suspension. In this case one prepares the suspension first (e.g. by bead milling) using the polymeric dispersant. The suspension is left to equilibrate for sufficient time (preferably overnight) to endure complete adsorption of the polymer. The polymeric emulsifier is then added and the oil is emulsified into the SC using for example a Silverson or Ultra-Turrax. Overmixing which may result in orthokinetic (or shear) flocculation and dilatancy must be avoided and the whole system should be cooled as much as possible during emulsification.

4.7 Prevention of crystallization

This is by far the most serious instability problem with suspoemulsions (particularly with many agrochemicals). It arises from the partial solubility of the suspension particles into the oil droplets. The process is accelerated at higher temperatures and also on temperature cycling. The smaller particles will have higher solubility than the larger one. This is due to the fact that the higher the curvature the higher the solubility as described by the Kelvin equation [7],

$$S(r) = S(\infty) \exp\left(\frac{2\gamma V_m}{rRT}\right), \tag{4.1}$$

where $S(r)$ is the solubility of a particle with radius r and $S(\infty)$ is the solubility of a particle with infinite radius (the bulk solubility), γ is the S/L interfacial tension, R is the gas constant and T is the absolute temperature.

On storage, the smaller particles will dissolve in the oil and they recrystallize on the larger particles which may be at the vicinity of the O/W interface. Some crystal habit modification may be produced and large plates or needles are formed which can reach several μm.

Several procedures may be applied to inhibit recrystallization:

(i) Diluting the oil phase with another inert oil in which the particles are insoluble.
(ii) Use of a strongly adsorbed polymeric surfactant such as, Atlox 4913 or INUTEC® SP1, that prevents entry of the suspension particles into the oil droplets.
(iii) Addition of electrolytes in the continuous phase. This has the effect of enhancing the polymeric surfactant adsorption, thus preventing particle entry into the oil droplets.
(iv) Use of crystal growth Inhibitors: e.g. flat dye molecules which are insoluble in the oil and are strongly adsorbed on the particle surface. This prevents particle entry into the oil droplets.
(v) Use of analogues of the solid active ingredient (having the same basic structure) that are insoluble in the oil and become incorporated on the surface of the solid particles.
(vi) Use of thickeners such as HEC and xanthan gum. This will increase the low shear rate viscosity of the medium and hence slow down the diffusion of the small particles, thus preventing their entry into the oil droplets. These thickeners can produce gels in the continuous phase that are viscoelastic and this can prevent particle diffusion.

4.8 Model suspoemulsion of polystyrene latex and isoparaffinic oil stabilized with Pluronic PE (PEO–PPO–PEO A–B–A block copolymer)

The interaction was investigated using viscoelastic measurements [8, 9]. As an illustration, Fig. 4.6 shows typical plots of G^* (complex modulus), G' (storage or elastic modulus), G'' (loss or viscous modulus) and η' (dynamic viscosity) as a function of frequency (Hz) for 90 % emulsion and 10 % latex, both stabilized with Pluronic PE block copolymer. The results of Fig. 4.6 were obtained at low strain amplitudes (i.e. in the linear viscoelastic region). Both G^* and G' show a rapid increase with increasing frequency above 0.1 Hz. However, G'', which is higher than G' at frequencies below 1 Hz, starts to decrease with increasing frequency above 1 Hz. The dynamic viscosity shows a decrease with increasing frequency, as expected (shear thinning system).

A well-defined crossover point ($G' = G''$) can be identified from which the relaxation time of the system can be calculated:

$$\tau = \frac{1}{\omega^*} \tag{4.2}$$

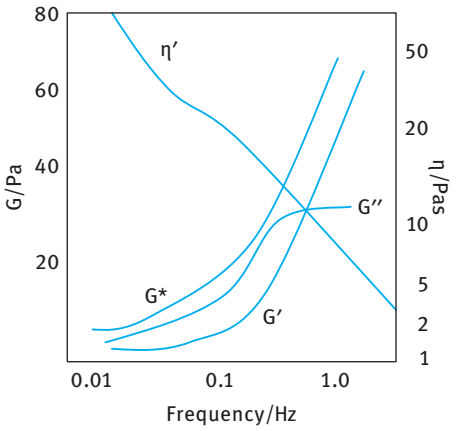

Fig. 4.6: Variation of G^*, G', G'' and η' with frequency for a suspoemulsion of 90 % isoparaffinic oil-in-water emulsion and 10 % polystyrene latex.

where ω^* is the characteristic frequency (rad s^{-1}) at the crossover point. Note that $\omega = 2\pi\upsilon$, where υ is the frequency in Hz.

Similar results were obtained for other suspoemulsions containing various emulsion: latex ratios. The same trend was also obtained for the emulsion and latex dispersions alone. Addition of the latex to the emulsion causes a shift in τ values to higher frequencies, indicating stronger interaction between the latex particles and emulsion droplets.

Fig. 4.7 shows the variation of G^*, G' and G'' at $\phi = 0.57$ and $\upsilon = 1$ Hz with percentage emulsion and latex in the suspoemulsion.

The emulsion has much higher moduli than the latex at the same volume fraction. Although the emulsion has a VMD (0.98 µm) that is close to that of the latex (1.18 µm), the former is much more polydisperse than the latter. The much smaller emulsion droplets present may account for the higher moduli of the emulsion when compared to the latex. As the proportion of latex in the suspoemulsion is increased,

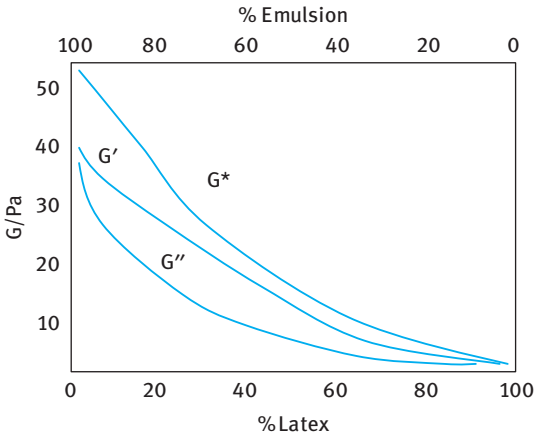

Fig. 4.7: Variation of G^*, G' and G'' with percentage emulsion and latex; $\phi = 0$.

the moduli decrease. Replacement of emulsion with latex would mean replacing a proportion of the smaller emulsion droplets with larger latex particles and this results in reduction of the moduli values. It should be mentioned, however, that the mixture of emulsion and latex becomes relatively more elastic than viscous, indicating stronger interaction between the emulsion droplets and the latex particles.

4.9 Model systems of polystyrene latex with grafted PEO chains and hexadecane emulsions

It is clear from the above discussion that the interaction between suspension particles and emulsion droplets depends on the nature of the stabilizer used for the particles and droplets. For that reason, we investigated model systems in which the latex particles contain grafted PEO chains (with no possible desorption) and the emulsion was based on hexadecane stabilized with Pluronic PE L92 (containing 20 % PEO). The particle and droplet radii were very similar (315 and 280 nm respectively) in order to avoid complications arising from the change in particle size distribution on mixing the suspension and emulsion.

Steady state shear stress-shear rate curves were used to obtain the relative viscosity (η_r)–volume fraction (ϕ) relationship for the latex and emulsion. The results are shown in Fig. 4.8, which also contains the theoretically predicted curve based on the Dougherty–Krieger equation [10],

$$\eta_r = \left[1 - \left(\frac{\phi}{\phi_p}\right)\right]^{-[\eta]\phi_p}, \tag{4.3}$$

where ϕ_p is the maximum packing fraction and $[\eta]$ is the intrinsic viscosity that is equal to 2.5 for hard spheres.

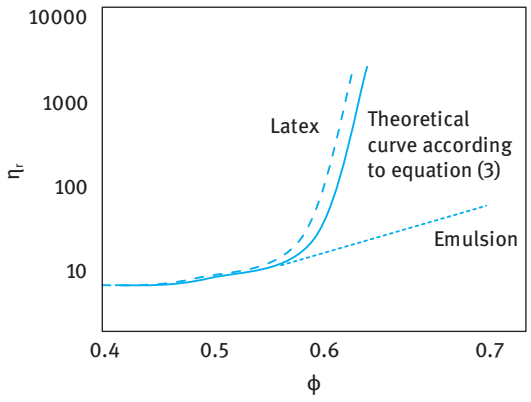

Fig. 4.8: η_r–ϕ curves for latexes and emulsions.

Two values for ϕ_p were used, namely 0.60 and 0.61 for the emulsion and the latex respectively. Reasonable agreement between the experimental $\eta_r - \phi$ curve and the theoretical curve based on equation (4.3) for the latex dispersions was obtained indicating that this system behaves as near hard spheres. However, the results for the emulsion deviate from the theoretical curves since the emulsion droplets are deformable.

Fig. 4.9 shows log-log plots of the elastic modulus G' (measured at low strain amplitudes to ensure the linear viscoelastic region and frequency of 1 Hz) versus volume fraction of the latex, emulsion and various mixtures of emulsion-latex systems. All results are similar for volume fraction below ≈ 0.62, indicating that the interactions between the emulsion droplets and latex particles are of the same nature and both particles and droplets behave as near hard spheres. However at $\phi > 0.62$, the behaviour of the latexes and emulsions differs significantly, as indicated by the much reduced slope of the log G'–log ϕ curve for the emulsions when compared with the latexes. Above this volume fraction, the interaction between the emulsion droplets is quite high and the system can reduce this interaction by deformation of the emulsion droplets. This situation is not possible with the latexes, where the particles are rigid. Similar behaviour is observed for the suspoemulsion when the percentage of the emulsion in the mixture is greater than 60 %. This implies that the behaviour of emulsions and suspoemulsions with more than 60 % emulsion is close in its rheological behaviour to concentrated emulsions and this has implications for the formulation of suspoemulsions.

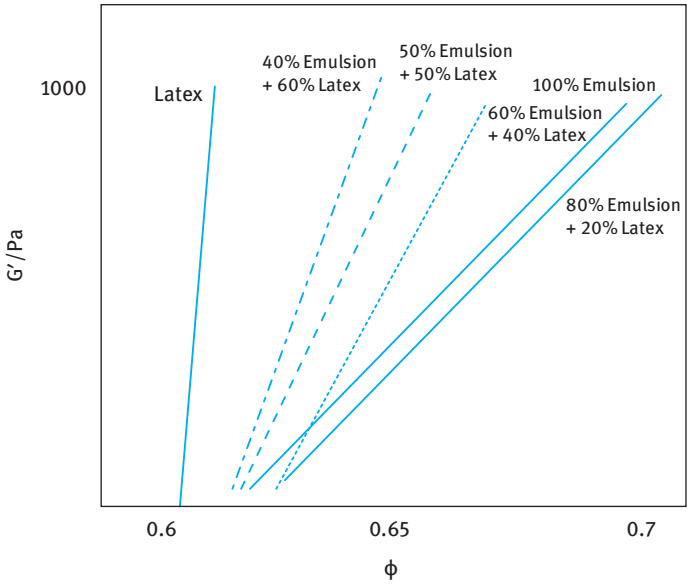

Fig. 4.9: Log-log plots of G' versus ϕ for latexes, emulsions and their mixtures.

Tab. 4.1: Parameters to fit equation (4.4) for emulsion, latex and their mixtures.

% emulsion	$a\gamma/R_{32}$	b
100	9896 ± 690	0.63 ± 0.01
80	9900 ± 1700	0.63 ± 0.01
60	17500 ± 2000	0.63 ± 0.03
50	20700 ± 2200	0.63 ± 0.01
40	23700 ± 2200	0.62 ± 0.02
20	≈ 100000	0.61 ± 0.01
0	≈ 1000000	0.62 ± 0.02

The parameter b corresponds to the volume fraction at the onset of elasticity.

The G'–ϕ curves can be analysed using the model suggested by Princen [11], who assumed a system of cylinders arranged in a hexagonal array. When such an arrangement is strained, the total interface is increased; this creates a restoring force that is proportional to the interfacial tension γ. Using this model Princen [11] derived an expression relating the shear modulus G_0 (which can be replaced by the high frequency modulus G') to the volume fraction ϕ,

$$G' = a\left(\frac{\gamma}{R_{32}}\right)\phi^{1/3}(\phi - b), \tag{4.4}$$

where a and b are constants that are equal to 1.7 and 0.71 respectively. The origin of the constant b is the value of the maximum packing of undistorted cylinders in the array. R_{32} is the average volume to surface ratio of the radius R (the Sauter radius).

For the latex–emulsion systems studied, R_{32} for the emulsion is constant and due to the excess surfactant in the emulsion, γ is expected to depend little on the composition. The values of the parameters to fit the data of Fig. 4.9 are given in Tab. 4.1.
The mixture of latex and emulsion may be regarded as two elastic elements in series with the appropriate volume fractions,

$$\frac{1}{G_m} = \frac{f_e}{G_e} + \frac{(1 - f_e)}{G_L}, \tag{4.5}$$

where G_m, G_e and G_L are the elastic moduli of the mixture, emulsion and latex respectively. f_e is the weight fraction of the emulsion in the mixture.

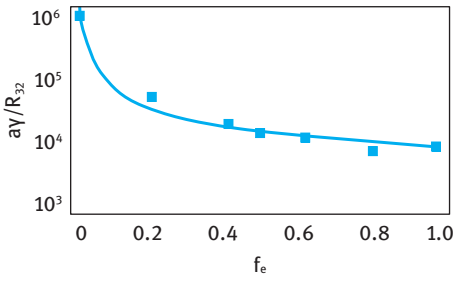

Fig. 4.10: $(a\gamma/R_{32})$ versus f_e; line drawn using equation (4.5).

A plot of the linear lines of Fig. 4.9 (which is equal to ay/R_{32}) is shown in Fig. 4.10 together with the predicted line based on equation (4.5). The agreement between the values of the slopes and those predicted using equation (4.5) is good.

4.10 Conclusions

Mixtures of suspensions and emulsions (suspoemulsions) may undergo interaction (homo- or heteroflocculation) that depends on the nature of the dispersant/emulsifier system, the particle size distribution and the density difference between the particles and droplets. In cases where heteroflocculation occurs, strongly anchored dispersing agent for the suspension (mostly graft copolymers) are necessary to prevent their displacement from the particles. An efficient emulsifier is also required to prevent any coalescence of the droplets. Crystallization of the particles may occur on storage, particularly when the solid particles have some appreciable solubility in the oil droplets. To prevent this, it is necessary to incorporate an oil with much lower solubility for the solid. In addition, polymeric surfactants strongly anchored to the solid particles are necessary. Crystal growth inhibitors such as some dyes may also be incorporated.

To illustrate the interaction between particles and oil droplets in a suspoemulsion, model systems of latex suspensions and oil-in-water emulsions based on paraffinic oils have been investigated using rheological techniques. The results illustrate the possible deformation of the oil droplets at high volume fractions. This was reflected in the viscoelastic properties of the latex–emulsion mixtures. The results could be analysed using a model based on a system of cylinders arranged in a hexagonal array.

References

[1] Tadros T. Colloids in agrochemicals. Weinheim: Wiley-VCH; 2009.
[2] Tadros T. Rheology of dispersions. Weinheim: Wiley-VCH; 2010.
[3] Goodwin JW, Hearn J, Ho CC, Ottewill RH. Colloid and Polymer Science. 1974;252:464.
[4] Bromley C. Colloids and Surfaces. 1986;17:1.
[5] Heath D, Knott RD, Knowles DA, Tadros TF. ACS Symposium Series. 1984;254:2.
[6] Tadros TF, Vandamme A, Levecke B, Booten K, Stevens CV. Advances Colloid Interface Sci. 2004;108–109:207.
[7] Thompson W (Lord Kelvin). Phil Mag. 1871;42:448.
[8] Pons R, Rossi P, Tadros TF. J Phys Chem. 1995;99:12624.
[9] Tadros T, Cutler J, Pons R, Rossi P. Investigations of the interactions between suspensions and emulsions (suspoemulsions). In: Ottewill RH, Rennie AR, editors. Modern aspects of colloidal dispersions. Dordrecht: Kluwer; 1998.
[10] Krieger IM, Advances Colloid and Interface Sci. 1972;3:111.
[11] Princen HM, Kiss AD. J Colloid Interface Sci. 1986;112:427.

5 Oil-based suspension concentrates

5.1 Introduction

Oil-based suspensions are currently used for the formulation of many agrochemicals, in particular those which are chemically unstable in aqueous media [1]. These suspensions allow one to use oils (such as methyl oleate) which may enhance the biological efficacy of the active ingredient. In addition, one may incorporate water-insoluble adjuvants in the formulation. The most important criterion for the oil used is to have minimum solubility of the active ingredient otherwise Ostwald ripening or crystal growth will occur on storage.

The oil-based suspension has to be diluted into water to produce an oil-in-water emulsion. A self-emulsifiable system has to be produced and this requires the presence of the appropriate surfactants for self-emulsification. The surfactants used for self-emulsification should not interfere with the dispersing agent that is used to stabilize the suspension particles in the nonaqueous media. Displacement of the dispersing agent with the emulsifiers can lead to flocculation of the suspension.

To prevent sedimentation of the particles (since the density of the active ingredient is higher than that of the oil in which it is dispersed), an appropriate rheology modifier (antisettling agent) that is effective in the nonaqueous medium must be incorporated in the suspension. This rheology modifier should not interfere with the self-emulsification process of the oil-based suspension.

Two main types of nonaqueous suspensions may be distinguished:

(i) Suspensions in polar media such as alcohol, glycols, glycerol, esters. These media have a relative permittivity $\varepsilon_r > 10$. In this case, double layer repulsion plays an important role, in particular when using ionic dispersing agents.

(ii) Suspensions in nonpolar media, $\varepsilon_r < 10$, such as hydrocarbons (paraffinic or aromatic oils) which can have a relative permittivity as low as 2. In this case, charge separation and double layer repulsion are not effective and hence one has to depend on the use of dispersants that produce steric stabilization.

5.2 Stability of suspensions in polar media

This follows the same principles as aqueous suspensions (described in Chapter 3), but one must take into account the "incomplete" dissociation of the ionic species which is the case when $\varepsilon_r < 40$. This could result in a low surface charge and hence a low zeta potential. However, the latter may be sufficient to produce an effective energy barrier that prevents any flocculation as explained by the Deryaguin–Landau–Verwey–Overbeek (DLVO) theory [2, 3].

https://doi.org/10.1515/9783110578997-006

Due to the lack of complete dissociation one cannot use the electrolyte concentration for calculating the thickness of the double layer. In this case one has to obtain the effective electrolyte concentration that must take into account the incomplete dissociation. The effective ionic concentration C can be determined from conductivity measurements and this allows one to calculate the double layer thickness ($1/\kappa$).

$$\frac{1}{\kappa} = \left(\frac{\varepsilon_r \varepsilon_0 kT}{2e^2 N_A C \times 10^3} \right)^{1/2} \tag{5.1}$$

where ε_0 is the permittivity of free space, k is the Boltzmann constant, T is the absolute temperature, e the electronic charge and N_A is Avogadro's constant.

Since the effective ionic concentration in a polar medium is less than that in water, the double layer will be more extended. For polar substances in polar media, such as TiO_2 in glycol, the double layer charge may be sufficient for effective repulsion to occur and in this case a stable dispersion may be produced. For hydrophobic particles, such as the case with agrochemicals stabilized with ionic surfactants or polyelectrolytes, the double layer charge is also effective for stabilization of the suspension.

In the above case, one may describe stability using the classical theory of colloid stability due to Deryaguin, Landau, Verwey and Overbeek (DLVO theory) [2, 3]. For systems, where $\kappa a > 1$ (where a is the particle radius) and weak interaction, the electrostatic repulsion, G_{elec}, is given by the following expression,

$$G_{elec} = 4\pi\varepsilon_r \varepsilon_0 a \psi_0^2 \ln[1 + \exp(-\kappa h)]. \tag{5.2}$$

h is the surface-to-surface separation and ψ_0 is the surface potential which can be replaced by the measured zeta potential. G_{elec} decreases exponentially with increasing h and the rate of decay increases with increasing electrolyte concentration.

The van der Waals attraction is simply given by the expression [4],

$$G_A = -\frac{Aa}{12h}, \tag{5.3}$$

where A is the effective Hamaker constant,

$$A = (A_{11}^{1/2} - A_{22}^{1/2})^2. \tag{5.4}$$

A_{11} is the Hamaker constant of the particles and A_{22} is the Hamaker constant of the medium. G_A increases with decreasing h and at very short distances it reaches very high values.

The basis of the DLVO theory is to sum G_{elec} and G_A at all distances,

$$G_T = G_{elec} + G_A. \tag{5.5}$$

The general form of the G_T–h curve is schematically shown in Fig. 5.1, which shows the case at low electrolyte concentrations. The manner in which G_T varies with interparticle distance is determined by the way by which G_{elec} and G_A vary with h. G_{elec} decays exponentially with h and approaches 0 at large separation distances. G_A decays with h as an inverse power law and a residual attraction remains at large values of h. The G_T–h curve shows two minima (at long and short distances of separation) and one maximum (at intermediate distance), as illustrated in Fig. 5.1.

At large h, $G_A > G_{elec}$ resulting in a shallow secondary minimum. At small h, $G_A \gg G_{elec}$ resulting in a deep primary minimum. At intermediate h, $G_{elec} > G_A$ resulting in an energy maximum $G_{max.}$ Three cases can be distinguished:

(i) G_{max} large ($> 25kT$), resulting in a colloidally stable suspension.
(ii) G_{max} small or absent, resulting in an unstable suspension (coagulated).
(iii) G_{max} intermediate and G_{sec} deep ($1–10kT$), resulting in weak (reversible) flocculation.

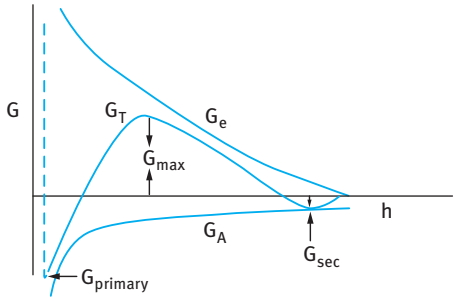

Fig. 5.1: Energy–distance curves according to the DLVO theory.

It should be mentioned that for hydrophobic particles in polar solvents, stabilized by ionic surfactants, the surface charge may be very low and hence electrostatic stabilization cannot be achieved. For this case it is essential to use a dispersant that strongly adsorbs on the particle surface (with an anchor B chain). This dispersant should contain stabilizing chains (A chains) that are strongly solvated by the medium. The use of block and graft copolymers for stabilizing particles in polar media follows the same principles that are applied for stabilization in nonpolar media. This stabilizing mechanism is referred to as steric stabilization and will be discussed below.

The choice of dispersants for stabilizing suspensions in polar media is not an easy task. The "anchor" chain B needs to be insoluble in the polar medium and to have high affinity to the surface. Since most polymer chains have some solubility in nonaqueous polar media, it is very difficult to have strong adsorption to the particle surface. The stabilizing chains A have to be highly soluble in the polar solvent and strongly solvated by its molecules. This is not as difficult as the choice of the B chains. For these reasons it is difficult to find commercially available dispersant for stabilizing hydrophobic particles in polar media.

5.3 Stability of suspensions in nonpolar media

For nonpolar media such as hydrocarbon oils (e.g. paraffinic oils) or some modified vegetable oils such as methyl oleate that are commonly used for the formulation of oil-based suspensions, the relative permittivity is lower than 10 and can reach values as low as 2. In this case the double layer is very extended, since the effective ionic concentration is very small ($\approx 10^{-10}$ mol dm^{-3}) and $(1/\kappa)$ can be as high as 10 μm. In this case, the double layer repulsion plays a very minor role. Effective stabilization requires the presence of an adsorbed layer of an effective dispersant with particular properties (sometimes referred to as "protective colloid").

The most effective dispersants are polymeric surfactants, which may be classified into two main categories [5, 6]: (i) homopolymers and (ii) block and graft copolymers. The homopolymers adsorb as random coils with tail-train-loop configurations. In most cases there is no specific interaction between the homopolymer and the particle surface and it seldom can provide effective stabilization. The block and graft copolymers can provide effective stabilization providing they satisfy the following criteria:

(i) Strong adsorption of the dispersant to the particle surface. This can be provided by a block B that is chosen to be insoluble in the nonaqueous medium and has some affinity to the particle surface. In cases when the affinity to the surface is not strong, one can rely on "rejection anchoring" whereby the insoluble B chain is rejected towards the surface as a result of its insolubility in the nonaqueous medium.
(ii) Strongly solvated A blocks that provide effective steric stabilization as a result of their unfavourable mixing and loss of entropy when the particles approach each other in the suspension.
(iii) A reasonably thick adsorbed layer to prevent any strong flocculation.

Based on the above principles, various dispersants have been designed for suspensions in nonaqueous medium. One of the most effective stabilizing chains in nonaqueous media is poly(12-hydroxystearic acid) (PHS) that has a molar mass in the region of 1000–2000 Daltons. This chain is strongly solvated in most hydrocarbon oils (paraffinic or aromatic oils). It is also strongly solvated in many esters, such as methyl oleate that is commonly used for oil-based suspensions. For the B chain, one can choose a polar chain such as polyethylene imine or polyvinylpyrrolidone, which is insoluble in most oils. The B chain could also be polystyrene or polymethylmethacrylate, which is insoluble in aliphatic hydrocarbons and may have some affinity to the hydrophobic agrochemical particle.

For full characterization of the adsorbed polymer layer one needs to determine the following parameters [5, 6]:

(i) Amount of polymer adsorbed per unit area, Γ. This requires determining the adsorption isotherms at various temperatures. The influence of solvency for the stabilizing chain should be studied.

(ii) Number of segments in direct contact with the surface, p (in trains). This can be obtained using pulse gradient NMR [6].
(iii) The adsorption energy per segment χ^s. For polymer adsorption to occur, a minimum value for χ^s is required to overcome the entropy loss when the polymer adsorbs at the surface. The adsorption energy can be determined using microcalorimetry.
(iv) Extension of the layer from the surface, i.e. segment density distribution $\rho(z)$ or the adsorbed layer thickness δ. The most convenient method for determining δ is to use dynamic light scattering, usually referred to as photon correlation spectroscopy (PCS) [7]. For this purpose, model small spherical particles such as polymethylmethacrylate can be used.

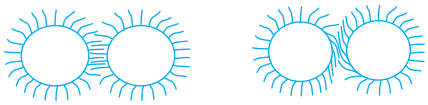

Fig. 5.2: Schematic representation of the interaction between particles containing adsorbed polymer layers.

When two particles with adsorbed polymer layers, each with thickness δ, approach to a distance of separation h that is smaller than twice the adsorbed layer thickness 2δ the layers will either overlap or they become compressed [5, 6]. This is illustrated in Fig. 5.2. In both cases, there will be an increase in the local segment density of the polymer chains in the interaction region. Provided the dangling chains (the A chains in A–B, A–B–A block or BA_n graft copolymers) are in a good solvent, this local increase in segment density in the interaction zone will result in strong repulsion as a result of two main effects:

(i) Increase in the osmotic pressure in the overlap region as a result of the unfavourable mixing of the polymer chains, when these are in good solvent conditions [8]. This is referred to as osmotic repulsion or mixing interaction and it is described by a free energy of interaction G_{mix}.
(ii) Reduction of the configurational entropy of the chains in the interaction zone; this entropy reduction results from the decrease in the volume available for the chains when these are either overlapped or compressed. This is referred to as volume restriction interaction, entropic or elastic interaction and it is described by a free energy of interaction G_{el}.

The combination of G_{mix} and G_{el} is usually referred to as the steric interaction free energy, G_s, i.e.,

$$G_s = G_{mix} + G_{el}. \tag{5.6}$$

The sign of G_{mix} depends on the solvency of the medium for the chains. If in a good solvent, i.e. the Flory–Huggins interaction parameter χ is less than 0.5, then G_{mix} is positive and the mixing interaction leads to repulsion. In contrast, if $\chi > 0.5$ (i.e. the chains are in poor solvent condition), G_{mix} is negative and the mixing interaction becomes attractive. G_{el} is always positive and hence in some cases one can produce stable dispersions in a relatively poor solvent (enhanced steric stabilization).

In the overlap region, the chemical potential of the polymer chains is now higher than in the rest of the layer (with no overlap). This amounts to an increase in the osmotic pressure in the overlap region; as a result solvent will diffuse from the bulk to the overlap region, thus separating the particles and hence a strong repulsive energy arises from this effect. This repulsive energy can be calculated by considering the free energy of mixing of two polymer solutions, as for example treated by Flory and Krigbaum [9]. The free energy of mixing is given by two terms:

(i) an entropy term that depends on the volume fraction of polymer and solvent;
(ii) an energy term that is determined by the Flory–Huggins interaction parameter χ.

Using the above theory one can derive an expression for the free energy of mixing of two polymer layers (assuming a uniform segment density distribution in each layer) surrounding two spherical particles as a function of the separation distance h between the particles.

The expression for G_{mix} is,

$$\frac{G_{mix}}{kT} = \left(\frac{2V_2^2}{V_1}\right)v_2^2\left(\frac{1}{2} - \chi\right)\left(\delta - \frac{h}{2}\right)^2\left(3R + 2\delta + \frac{h}{2}\right), \tag{5.7}$$

where k is the Boltzmann constant, T is the absolute temperature, V_2 is the molar volume of polymer, V_1 is the molar volume of solvent and v_2 is the number of polymer chains per unit area.

The sign of G_{mix} depends on the value of the Flory–Huggins interaction parameter χ:

- $\chi < 0.5$, G_{mix} is positive and the interaction is repulsive.
- $\chi > 0.5$, G_{mix} is negative and the interaction is attractive.
- The condition $\chi = 0.5$, i.e. $G_{mix} = 0$ is referred to as the θ-condition.

The elastic interaction arises from the loss in configurational entropy of the chains on the approach of a second particle [10]. As a result of this approach, the volume available for the chains becomes restricted, resulting in loss of the number of configurations.

For two flat plates, G_{el} is given by the following expression [10],

$$\frac{G_{el}}{kT} = -2v_2 \ln\left[\frac{\Omega(h)}{\Omega(\infty)}\right] = 2v_2 R_{el}(h), \tag{5.8}$$

where $R_{el}(h)$ is a geometric function whose form depends on the segment density distribution.

It should be stressed that G_{el} is always positive and could play a major role in steric stabilization. It becomes very strong when the separation distance between the particles becomes comparable to the adsorbed layer thickness δ.

Combining G_{mix} and G_{el} with G_A gives the total energy of interaction G_T (assuming there is no contribution from any residual electrostatic interaction), i.e.,

$$G_T = G_{mix} + G_{el} + G_A. \tag{5.9}$$

A schematic representation of the variation of G_{mix}, G_{el}, G_A and G_T with surface–surface separation distance h is shown in Fig. 5.3.

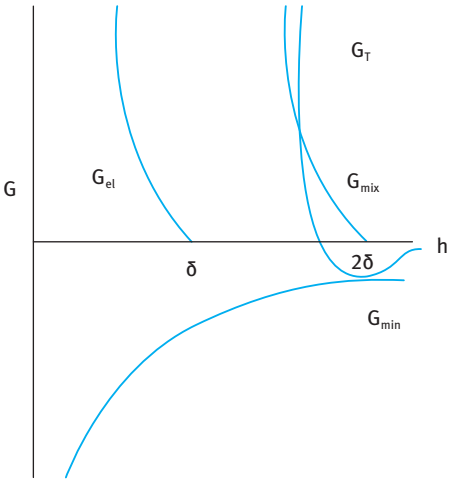

Fig. 5.3: Energy–distance curves for sterically stabilized systems.

G_{mix} increases very sharply with decreasing h when $h < 2\delta$. G_{el} increases very sharply with decreasing h when $h < \delta$. G_T versus h shows a minimum, G_{min}, at separation distances comparable to 2δ. When $h < 2\delta$, G_T shows a rapid increase with decreasing h.

Unlike the G_T–h curve predicted by the DLVO theory (which shows two minima and one energy maximum), the G_T–h curve for systems that are sterically stabilized shows only one minimum, G_{min}, followed by sharp increase in G_T with decreasing h (when $h < 2\delta$). The depth of the minimum depends on the Hamaker constant A, the particle radius R and adsorbed layer thickness δ. G_{min} increases with increasing A and R. At a given A and R, G_{min} increases with decreasing δ (i.e. with decreasing molecular weight, M_w, of the stabilizer). This is illustrated in Fig. 5.4 where G_T versus h is plotted at increasing values of δ/R. The larger the value of δ/R, the smaller the value of G_{min}. In this case the system may approach thermodynamic stability as is the case with nanodispersions.

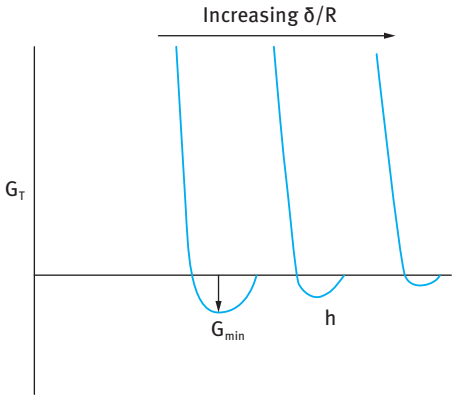

Fig. 5.4: G_T–h curves at increasing values of δ/R.

Several criteria must be satisfied for effective steric stabilization:

(i) Full coverage of the particles by the polymer. The amount of polymer added should correspond to the plateau of the adsorption isotherm. Any bare patches may lead to flocculation as a result of van der Waals attraction and/or bridging.

(ii) Strong adsorption of the polymer to the particle surface, i.e. strong B "anchor" chain. This requires the chain to be insoluble in the medium and to have some affinity to the surface. Lack of a strong "anchor" may lead to chain displacement on approach of the particles in a suspension. This is particularly important for concentrated suspensions.

(iii) The stabilizing chain(s) A should be in good solvent conditions. The Flory–Huggins interaction parameter χ should be less than 0.5 under all storage conditions, e.g. temperature changes.

(iv) An optimum layer thickness δ to ensure that $G_{\min}$ is not deep. This is particularly the case with concentrated suspensions in which weak flocculation may occur at relatively small $G_{\min}$. In most cases, an adsorbed layer thickness in the region 5–10 nm is sufficient. This is particularly the case with graft copolymers where the A chains are stretched ("comb-like" or "brush" structure).

5.4 Settling of suspensions and prevention of formation of dilatant sediments

This follows the same principles as described for aqueous suspension concentrates (see Chapter 3). Settling (or sedimentation) results from gravity forces [11]. When $\rho_{\text{particles}} > \rho_{\text{medium}}$, the gravity force $(4/3)\pi a^3 \Delta\rho g L$ (where g is the acceleration due to gravity and L is the height of the container) will overcome the thermal (Brownian) motion leading to particle sedimentation. Only when $kT > (4/3)\pi a^3 \Delta\rho g L$, does sedimentation become insignificant. This condition is only satisfied with very small particles (< 0.1 μm) and $\Delta\rho < 0.1$. Thus, with most colloidally stable suspensions,

sedimentation is the rule rather than the exception. The particles may sediment individually to the bottom of the container and the repulsive forces necessary to maintain stability allow them to move past each other with the result of the formation of a very compact sediment. The compact sediment, that is technically referred to as "clay" or "cake", is very difficult to redisperse by shaking. Such clays are dilatant (shear thickening) and must be avoided.

For an infinitely dilute suspension of non-interacting particles, the sedimentation velocity v_0 is given by Stokes' law,

$$v_0 = \frac{2}{9}\frac{a^2 \Delta\rho g}{\eta}. \tag{5.10}$$

For 1 µm particles with $\Delta\rho = 0.2$ and $\eta = 10^{-3}$ Pa s (low viscosity oil) $v_0 = 4.4 \times 10^{-7}$ m s^{-1}, whereas for 10 µm particles $v_0 = 4.4 \times 10^{-5}$ m s^{-1}. In a 100 cm container the 1 µm particles will settle in about 3 days and the 10 µm particles will settle in about 40 minutes.

For more concentrated suspensions, the sedimentation velocity v is reduced below the Stokes' velocity v_0 as a result of interparticle interaction. For suspensions with volume fraction $\phi \approx 0.1$, v is related to v_0 by the equation [12],

$$v = v_0(1 - k\phi), \tag{5.11}$$

where $k = 6.55$, a constant that accounts for hydrodynamic interaction.

For suspensions with $\phi > 0.1$, v becomes a complex function of ϕ and only empirical equations are used to describe the sedimentation velocity [11]. When v is plotted against ϕ, an exponential reduction of v with increasing ϕ is found and eventually v approaches zero at some limiting volume fraction [13], the so-called maximum packing fraction ϕ_p. At this maximum packing fraction, the relative viscosity of the suspension approaches infinity.

In most practical suspensions, a volume fraction in the range 0.1–0.5 is used and hence one should use a suspending agent to prevent sedimentation and formation of dilatant clays.

The suspending agent (sometimes referred to as an antisettling agent) should provide a restoring force to overcome gravity.

It is useful to calculate the stress exerted by a particle σ_p in a suspension [14],

$$\sigma_p = \frac{\text{gravity force}}{\text{area}} = \frac{(4/3)\pi a^3 \Delta\rho g}{4\pi a^2} = \frac{a\Delta\rho g}{3}. \tag{5.12}$$

For 10 µm particles with $\Delta\rho = 1$, $\sigma_p = 3.3 \times 10^{-2}$ Pa. This clearly illustrates the need to measure the viscosity at such low stresses (using a constant stress rheometer).

The main criteria for an effective suspending (antisettling) agent are as follows:

(i) It should produce a "three-dimensional" gel network in the continuous phase with optimum rheological characteristics.

(ii) It should have a very high viscosity at low shear rates. A residual (zero shear) viscosity in excess of 100 Pa s is desirable. The residual viscosity can be measured using constant stress (creep) measurements.
(iii) It should have sufficient "bulk" modulus to prevent separation of the suspension and syneresis. The bulk modulus is related to the shear modulus which can be measured using dynamic (oscillatory) techniques.
(iv) The suspending agent should produce a shear thinning system such that on application of the suspension, the high shear viscosity is not too high.

Several suspending systems can be used:

(i) Hydrophobically modified clays (Bentones). Clays such as sodium montmorillonite can be made hydrophobic by addition of long chain alkyl ammonium surfactants (e.g. dodecyl or cetyl trimethyl ammonium chloride). The alkyl ammonium cation exchanges with the Na^+ ions producing a hydrophobic surface and the bentone particles can be dispersed in the nonaqueous medium. The exchange is carried out in an optimum manner such that some hydrophilic sites remain on the bentone particles. On addition of a polar solvent, such as propylene carbonate or alcohol, a gel is produced. The most likely mechanism of gel formation in this case is hydrogen bonding by the polar molecules between the polar sites on the bentone particles.
(ii) Fumed silica. These are commercially available under the trade name "Aerosil" or "Cabosil". They are produced by reaction of silicon tetrachloride with steam. Fine particles (primary particle size < 0.02 μm) are produced with a surface containing silanol groups that are separated by siloxane bonds. When dispersing the fumed silica powder in nonaqueous media a gel is produced by hydrogen bonding between the silanol groups. Chain aggregates are produced and by controlling the dispersion procedure, the adequate rheological characteristics are produced.
(iii) Trihydroxystearin (Thixin). This product is derived from castor oil and it needs both shear and heat for full activation to produce a gel.
(iv) Aluminium magnesium hydroxide stearate. This has been used to gel a number of cosmetic oils and it can provide suspending properties. It could also be applied for oil-based suspensions of agrochemicals. However, one should be careful in applying this system since in many cases the gel strength is too high for adequate dispersion on application.
(v) Use of high molecular weight polymers. Polyethylenes and copolymers of polyethylene can be used to gel mineral oils and several aliphatic solvents. Some of these materials need high incorporation temperatures and one must keep in mind that the cooling procedures affect the final appearance and rheological characteristics of the gel.

The above systems are the most commonly used rheology modifiers in most nonaqueous suspensions. However, two other methods may be applied for reduction of settling of nonaqueous suspensions:

(i) Controlled flocculation (self-structured systems). By reducing the adsorbed layer thickness one can increase the depth of the minimum, G_{min}, to such an extent that weak flocculation may produce a "three-dimensional" gel structure that is sufficient to reduce sedimentation and formation of dilatant clays. The adsorbed layer thickness may be reduced by reducing the molecular weight of the stabilizer by the addition of a small amount of a nonsolvent. This was illustrated in Fig. 5.4 where the energy–distance curve is plotted as a function of the ratio of adsorbed layer thickness to particle radius. This procedure is particularly useful with large and asymmetric particles.

(ii) Depletion flocculation [15]. This is obtained by the addition of "free" (nonadsorbing) polymer to a sterically stabilized suspension. Above a critical volume fraction, ϕ_p^+ of the free polymer, weak flocculation occurs. Above ϕ_p^+, the polymer chains are "squeezed out" from between the particles, leaving a polymer-free zone in the interstices. The higher osmotic pressure outside the particle surfaces causes weak flocculation. This is schematically shown in Fig. 5.5.

The critical polymer volume fraction above which flocculation occurs decreases with increasing molecular weight of the free polymer. Thus, high molecular weight oil-soluble polymers should be used in order to reduce the amount required for flocculation. The amount of free polymer required for flocculation also decreases with increasing the volume fraction of the suspension. Therefore, depletion flocculation is more applicable for concentrated suspensions.

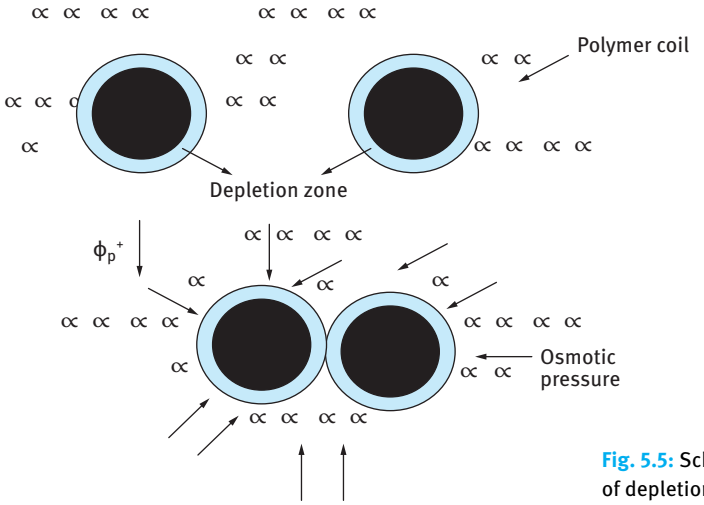

Fig. 5.5: Schematic representation of depletion flocculation.

5.5 Emulsification of oil-based suspensions

The nonaqueous suspension concentrate containing the active ingredient particles and any antisettling system is emulsified into the spray tank before application. Here the same principles that apply for self-emulsification of emulsifiable concentrates (ECs) are applied as discussed below. Alternatively, the nonaqueous suspension concentrate is emulsified into an aqueous solution containing another water-soluble active ingredient (normally an electrolyte such as glyphosate) to produce a combined mixture of two active ingredients. In the first case, spontaneous emulsification is necessary, since only gentle agitation in the spray tank is possible. In the second case, one may apply a normal emulsification procedure if a combined formulation is required. In some cases spontaneous emulsification into an aqueous electrolyte solution may also be required.

The above oil-based suspension concentrates require careful formulation to achieve the required properties:

(i) A stable nonaqueous suspension with adequate weak flocculation (to produce a shear thinning system) and no settling.
(ii) The antisettling agent used in the formulation should be water dispersible (e.g. fumed silica, Aerosil).
(iii) The emulsifying system used should not interfere with the stabilizing polymeric surfactant used for the preparation of the nonaqueous suspension.
(iv) The viscosity of the formulation at intermediate shear rates should be low enough to ensure spontaneity of emulsification.

The first demonstration of spontaneous emulsification was given by Gad [16] who observed that when a solution of lauric acid in oil is carefully placed into an aqueous alkaline solution, an emulsion forms at the interface. It is clear from this experiment that a mixture of lauric acid and sodium laurate is produced and this illustrates the role of the mixed film (which produces an ultra-low interfacial tension). When the right conditions are produced, spontaneous emulsification occurs with minimum agitation. In this experiment, the oil used was Newtonian and it had a relatively low viscosity.

Three mechanisms may be established to explain the process of spontaneous emulsification:

(i) Interfacial turbulence (Fig. 5.6). Interfacial turbulence occurs as a result of mass transfer from one phase to the other. The interface shows unsteady motions; streams of one phase are ejected and penetrate into the second phase, shedding small droplets. Localized reduction in interfacial tension is caused by nonuniform adsorption of the surfactant at the O/W interface or by mass transfer of surfactant molecules across the interface. When the two phases are not in equilibrium, convection currents may be formed, transferring liquid rich in surfactant towards areas of liquid deficient in surfactant. These convection currents lead to local fluctuations in the interfacial tension causing oscillation of the interface (turbu-

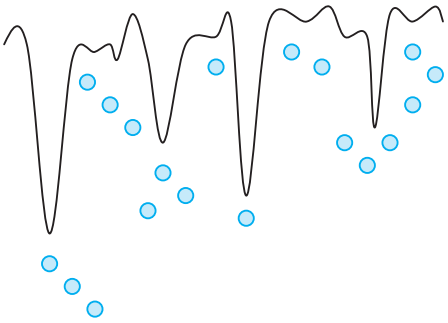

Fig. 5.6: Schematic representation of interfacial turbulence.

lence). Such disturbances may amplify themselves leading to violent interfacial perturbations and eventual disintegration of the interface, when liquid droplets of one phase are "thrown" into the other phase. This mechanism requires the presence of two surfactant molecules or a surfactant plus alcohol. This facilitates the mass transfer and induces interfacial tension gradients. Several "phases" may be produced at the O/W interface as will be discussed later.

(ii) Diffusion and stranding (Fig. 5.7). This is best illustrated by placing an ethanol-toluene mixture (containing say 10 % alcohol) onto water. The aqueous layer eventually becomes turbid as a result of the presence of toluene droplets. In this case interfacial turbulence does not occur, although spontaneous emulsification takes place. The alcohol molecules diffuse into the aqueous phase carrying some toluene molecules in a saturated three-component subphase. At some distance from the interface, the alcohol becomes sufficiently diluted into water and the toluene droplets precipitate as droplets in the aqueous phase.

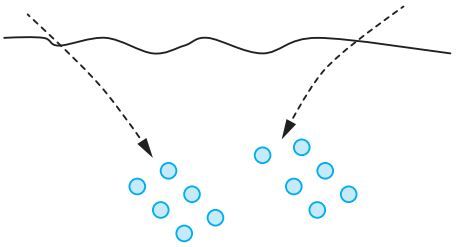

Fig. 5.7: Schematic representation of diffusion and stranding.

The above mechanism requires the presence of a third component (sometimes referred to as the cosurfactant) that increases the miscibility of the two previously immiscible phases (toluene and water). Many emulsifiable concentrates contain a high proportion of a polar solvent such as alcohol or ketone which facilitates spontaneous emulsification. The application of a polar solvent for emulsification of nonaqueous suspension concentrates needs to be tested (its addition may enhance crystal growth). (iii) Production of ultra-low (or transiently negative) interfacial tension (Fig. 5.8). This is the same

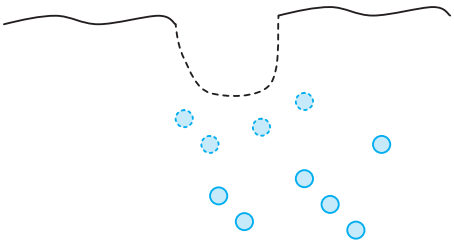

Fig. 5.8: Schematic representation of production of ultra-low interfacial tension.

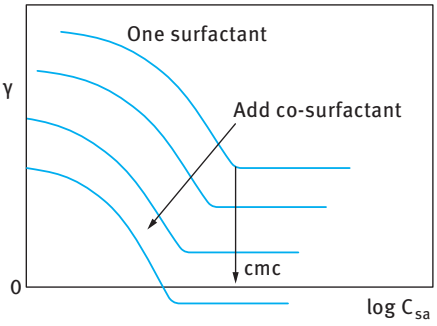

Fig. 5.9: γ–log C curves for surfactant plus cosurfactant.

mechanism for the production of microemulsions. The ultra-low interfacial tension is produced by a combination of a surfactant and cosurfactant. This is illustrated in Fig. 5.9.

Addition of surfactant to the aqueous or oil phase causes a gradual lowering of interfacial tension γ, reaching a limiting value at the critical micelle concentration (cmc). Any further increase in C above the cmc causes little or no further decrease in γ. The limiting value of γ reached with most single surfactants is seldom lower than 0.1 mN m^{-1}, which is not sufficiently low for microemulsion formation. If a surfactant mixture with one predominantly water-soluble surfactant such as sodium dodecyl sulphate, SDS and one predominantly oil-soluble surfactant, usually referred to as the cosurfactant such as pentanol or hexanol, is used the limiting γ value can reach very low values ($< 10^{-2}$ mN m^{-1}) or even becomes transiently negative. When a transient negative interfacial tension is produced, the interface expands spontaneously (producing droplets) adsorbing all surfactant molecules until a small positive γ is reached [17].

The reason for the reduction in interfacial tension when using two molecules can be understood from a consideration of the Gibbs adsorption equation. The reduction in γ is related to the adsorption of the surfactant molecules, which is referred to as the surface excess Γ (mol m^{-2}); For a multicomponent system, the reduction in γ, i.e. dγ is given by the summation of all surface excesses [17],

$$d\gamma = -\sum \Gamma_i RT \, d \ln C_i. \tag{5.13}$$

Thus, for two surfactants γ is reduced twice provided the two molecules are adsorbed simultaneously at the interface. The two surfactant molecules should not interact with each other, otherwise they will lower their respective activities. This explains why the two molecules should vary in nature, one predominantly water-soluble and the other predominantly oil-soluble.

Several other mechanisms have been proposed to explain the dynamics of spontaneous emulsification. Direct observation using phase contrast and polarizing microscopy showed that in some cases vesicles (closed bilayers) are produced in the oil phase near the interface with the water. These vesicles tend to "explode" thereby pulverizing oil droplets into the aqueous phase. The above structures can be produced for example by using a mixture of nonionic surfactant such as $C_{12}E_5$ and a long chain alcohol such as $C_{12}H_{25}OH$ and an oil such as hexadecane. The oil/surfactant mixture is transparent, but on addition of a small amount of water it becomes turbid and vesicles can be observed under the microscope. The interfacial tension of the oil/surfactant mixture/water is also very low.

5.6 Polymeric surfactants for oil-based suspensions and the choice of emulsifiers

When formulating a nonaqueous suspension concentrate that can be spontaneously emulsified into aqueous solutions one should consider the following criteria:

(i) The polymeric emulsifiers should be chosen from the A–B, A–B–A block or BA_n graft copolymer as discussed above. The B chain should be chosen to be insoluble in the oil and should become strongly adsorbed on the particle surface (either by specific interaction or by rejection "anchoring". As discussed before, for nonpolar oils (hydrocarbons) the B chain could be a polar molecule such as polyethylene imine, which adsorbs on the particle by rejection anchoring. The A chain should be soluble in the oil and highly solvated by its molecules – poly(hydroxystearic acid) or polyisobutylene are ideal.

(ii) The emulsifier system should be soluble in the oil phase and it should not cause desorption of the polymeric surfactant. A two-component emulsifier system is normally used, one predominantly water-soluble component (such as an ethoxylated surfactant) and one oil-soluble component, such as a medium or long chain alcohol. In many cases calcium dodecyl benzene sulphonate may be used. The emulsifier system should lower the interfacial tension of O/W to very low values ($< 0.1\,mN\,m^{-1}$).

The ultra-low interfacial tension may be measured using the spinning drop technique. A drop of oil is injected in the aqueous phase that is placed in a capillary tube that can be rotated at high speed to cause deformation of the spherical drop into a cylinder

[17]. From the droplet profile (cylinder radius R) and speed of rotation ω one can calculate γ,

$$\gamma = \frac{\omega^2 \Delta\rho R^4}{4}. \tag{5.14}$$

$\Delta\rho$ is the density difference between water and oil.

5.7 Emulsification into aqueous electrolyte solutions

For preparing a combined formulation with one active ingredient suspended in the oil phase and another active ingredient soluble in water (salt), one can emulsify the nonaqueous suspension into the aqueous electrolyte solution using a polymeric surfactant with high HLB number, e.g. Pluronic PF127 (that contains ≈ 55 units polypropylene oxide, PPO, and two polyethylene oxide (PEO) chains with ≈ 100 units each). The PEO–PPO–PEO block copolymer is insoluble in the oil phase and hence it does not interfere with the polymeric surfactant used for the preparation of the nonaqueous suspension. Depending on the density of the active ingredient in the oil phase and the amount suspended, the density of the oil drops produced could be smaller or larger than that of the aqueous electrolyte. Thus the combined formulation could undergo creaming or settling on storage. It is, therefore, essential to include an antisettling system in the aqueous electrolyte phase, e.g. xanthan gum (Kelzan or Rhodopol) could be applied in this case.

In a formulation in which spontaneous emulsification is required into the aqueous electrolyte solution, one should apply the same principles discussed above, except in this case the emulsifier system should be more hydrophilic (higher HLB number) to prevent "salting-out" of the emulsifier by the electrolyte. The nature and HLB number of the emulsifier system depend on the electrolyte concentration and nature and this could be checked independently using cloud point measurements. The resulting interfacial tension should be low.

5.8 Proper choice of the antisettling system

The antisettling system used for nonaqueous suspensions should be dispersible into water. Fumed silica (Aerosil 200) or microcrystalline cellulose are ideal systems for structuring nonaqueous suspensions. These systems produce a "three-dimensional" gel network in the oil phase by hydrogen bonding between the particles forming chains and cross-chains. These gels produce enough "yield stress" to prevent sedimentation of the coarse active ingredient particles. They also produce a very high viscosity at low shear rates thus preventing sedimentation.

One of the main advantages of these hydrophilic particles is that they can partition into the aqueous phase and this produces two main effects. During partition into the

aqueous phase and crossing the interface, they can enhance the interfacial tension gradients and hence promote the turbulence effect described above. This will facilitate self-emulsification. When these particles leave the oil phase, the yield value and viscosity of the suspension is lowered and this helps the self-emulsification process.

Hydrophilic polymers such as hydroxypropyl cellulose may also be used either alone or in combination with silica or microcrystalline cellulose. The combined particulate-polymer system may be advantageous in reducing sedimentation and enhancing the self-emulsification of the oil. The optimum ratio between particles and polymer depends on the nature of the active ingredient suspended in the oil phase.

5.9 Rheological characteristics of the oil-based suspensions

The rheological characteristics of the nonaqueous suspension (its yield value, zero shear viscosity and elastic modulus) need to be carefully adjusted to achieve the following criteria:

(i) No settling or separation of the nonaqueous suspension on storage under all storage conditions.
(ii) Ease of spontaneous emulsification with minimum agitation.

The above two criteria are not compatible and hence one has to control the rheology very carefully. For preventing settling and separation, one needs a high "yield stress", high zero shear viscosity and high modulus. High rheological parameters reduce the ease of spontaneous emulsification. For these reasons, one need to prepare a highly shear thinning system. The suspension concentrate should have a high viscosity at low shear rates, but once the shear rate exceeds a certain value (say 10–100 s^{-1}) depending on application, the viscosity drops significantly. One can achieve the above effect by proper choice of the antisettling system.

By using an antisettling system that diffuses rapidly into the water phase one can reduce the yield value, zero shear viscosity and modulus during the process of emulsification. Measurement of the rheological parameters is essential when formulating a nonaqueous suspension concentrate and this requires low shear rheometers (constant stress and oscillatory techniques). Details of these techniques are available in several reviews [18, 19].

References

[1] Tadros T. Colloids in agrochemicals. Weinheim: Wiley-VCH; 2009.
[2] Deryaguin BV, Landau L. Acta Physicochem USSR. 1941;14:633.
[3] Verwey EJW, Overbeek JTG. Theory of stability of lyophobic colloids. Amsterdam: Elsevier; 1948.

[4] Hamaker HC. Physica. 1937;4:1058.
[5] Tadros T. Polymeric surfactants. Berlin: De Gruyter; 2017.
[6] Fleer GJ, Cohen-Stuart MA, Scheutjens JMHM, Cosgrove T, Vincent B. Polymers at interfaces. London: Chapman and Hall; 1993.
[7] Pusey PN. In: Green JHS, Dietz R, editors. Industrial polymers: Characterisation by molecular weights. London: Transcripta Books; 1973.
[8] Napper DH. Polymeric stabilisation of colloidal dispersions. London: Academic Press; 1981.
[9] Flory PJ, Krigbaum WR. J Chem Phys. 1950;18:1086.
[10] Mackor EL, van der Waals JH. J Colloid Sci. 1951;7:535.
[11] Tadros T. Settling of Suspensions. In: Tadros T, editor. Solid/liquid dispersions. London; Academic Press; 1987.
[12] Bachelor GK. J Fluid Mech. 1972;52:245.
[13] Krieger IM, Advances Colloid and Interface Sci. 1971;3:45.
[14] Tadros TF. Advances Colloid and Interface Science. 1980;12:141.
[15] Asakura A, Oosawa F. J Chem Phys. 1954;22:1235. J Polymer Sci. 1958;93:183.
[16] Tadros TF. Surfactants in agrochemicals. New York: Marcel Dekker; 1994.
[17] Tadros T. Applied surfactants. Weinheim: Wiley-VCH; 2005.
[18] Tadros TF. Advances Colloid and Interface Science. 1993;1:46.
[19] Tadros TF. Advances Colloid and Interface Science. 1996;68:91.

6 Microemulsions in agrochemicals

6.1 Introduction

Microemulsions are a special class of "dispersions" (transparent or translucent) which are better described as "swollen micelles". The term microemulsion was first introduced by Hoar and Schulman [1, 2] who discovered that by titration of a milky emulsion (stabilized by soap such as potassium oleate) with a medium chain alcohol such as pentanol or hexanol, a transparent or translucent system was produced. A schematic representation of the titration method adopted by Schulman and coworkers [1, 2] is given below,

O/W emulsion	→	Add cosurfactant,	→	Transparent
stabilized by soap		e.g. $C_5H_{11}OH$, $C_6H_{13}OH$		or translucent

The final transparent or translucent system is a W/O microemulsion.

A convenient way to describe microemulsions is to compare them with micelles. The latter, which are thermodynamically stable, may consist of spherical units with a radius that is usually less than 5 nm. Two types of micelles may be considered: normal micelles with the hydrocarbon tails forming the core and the polar head groups in contact with the aqueous medium and reverse micelles (formed in nonpolar media) with a water core containing the polar head groups and the hydrocarbon tails now in contact with the oil. The normal micelles can solubilize oil in the hydrocarbon core forming O/W microemulsions, whereas the reverse micelles can solubilize water forming a W/O microemulsion. A schematic representation of these systems is shown in Fig. 6.1.

A rough guide to the dimensions of micelles, micellar solutions and macroemulsions is as follows: Micelles, $R < 5$ nm (they scatter little light and are transparent); macroemulsions, $R > 50$ nm (opaque and milky); micellar solutions or microemulsions, 5–50 nm (transparent, 5–10 nm, translucent 10–50 nm).

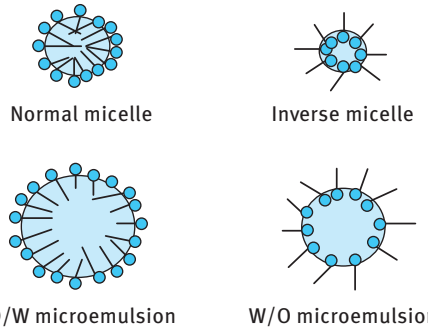

Fig. 6.1: Schematic representation of microemulsions.

https://doi.org/10.1515/9783110578997-007

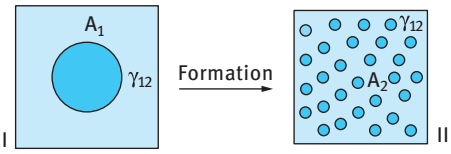

Fig. 6.2: Schematic representation of microemulsion formation.

The classification of microemulsions based on size is not adequate. Whether a system is transparent or translucent depends not only on the size but also on the difference in refractive index between the oil and the water phases. A microemulsion with small size (in the region of 10 nm) may appear translucent if the difference in refractive index between the oil and the water is large (note that the intensity of light scattered depends on the size and an optical constant that is given by the difference in refractive index between oil and water). Relatively large sized microemulsion droplets (in the region of 50 nm) may appear transparent if the refractive index difference is very small. The best definition of microemulsions is based on the application of thermodynamics by consideration of the energy and entropy terms for the formation of microemulsions, schematically represented in Fig. 6.2, which shows the process of formation of a microemulsion from a bulk oil phase (for O/W microemulsion) or bulk water phase (for a W/O microemulsion). A_1 is the surface area of the bulk oil phase and A_2 is the total surface area of all the microemulsion droplets. γ_{12} is the O/W interfacial tension. The increase in surface area when going from state I to state II is ΔA ($= A_2 - A_1$) and the surface energy increase is equal to $\Delta A\gamma_{12}$. The increase in entropy when going from state I to state II is $T\Delta S^{\text{conf}}$ (note that state II has higher entropy since a large number of droplets can arrange themselves in several ways, whereas state I with one oil drop has much lower entropy).

According to the second law of thermodynamics, the free energy of formation of microemulsions ΔG_{m} is given by the following expression,

$$\Delta G_{\text{m}} = \Delta A\gamma_{12} - T\Delta S^{\text{conf}}. \tag{6.1}$$

With macroemulsions, $\Delta A\gamma_{12} \gg T\Delta S^{\text{conf}}$ and $\Delta G_{\text{m}} > 0$. The system is non-spontaneous (it requires energy for formation of the emulsion drops) and it is thermodynamically unstable. With microemulsions, $\Delta A\gamma_{12} \leq T\Delta S^{\text{conf}}$ (this is due to the ultra-low interfacial tension accompanying microemulsion formation) and $\Delta G_{\text{m}} \leq 0$. The system is produced spontaneously and it is thermodynamically stable.

The above analysis shows the contrast between emulsions and microemulsions: With emulsions, an increase of the mechanical energy and an increase in surfactant concentration usually result in the formation of smaller droplets which become kinetically more stable. With microemulsions, neither mechanical energy nor increasing surfactant concentration can result in their formation. The latter is based on a specific combination of surfactants and specific interaction with the oil and the water phases and the system is produced at optimum composition.

Thus, microemulsions have nothing in common with macroemulsions and in many cases it is better to describe the system as "swollen micelles". The best definition of microemulsions is as follows [3]: "system of water + oil + amphiphile that is a single optically isotropic and thermodynamically stable liquid solution". Amphiphiles refer to any molecule that consist of a hydrophobic and a hydrophilic portion, e.g. surfactants, alcohols, etc.

The driving force for microemulsion formation is the low interfacial energy which is overcompensated by the negative entropy of dispersion term. The low (ultra-low) interfacial tension is produced in most cases by the combination of two molecules, referred to as the surfactant and cosurfactant (e.g. medium chain alcohol).

6.2 Application in agrochemicals

As mentioned in Chapter 2, many agrochemicals are formulated as emulsions concentrates (EWs). The agrochemical, which may be an oil, is emulsified into water and a water-based concentrated emulsion (EW) is produced. In cases where the agrochemical is very viscous or semi-solid, a small amount of an oil (which may be aliphatic in nature) may be added before the emulsification process. Unfortunately, EWs suffer from a number of problems such as the difficulty of emulsification and their long-term physical stability. As discussed in Chapter 2, emulsions are thermodynamically unstable systems since their formation involves a high interfacial energy that is not overcome by the relatively small entropy of dispersion. With time, the emulsion tends to reduce its interfacial area by several breakdown processes such as flocculation and coalescence. In addition, most emulsion systems undergo sedimentation or creaming on standing and they require the use of thickeners to modify their rheology. A further complication may arise from Ostwald ripening whereby the smaller droplets dissolve and become deposited on the larger ones. Clearly, to produce a physically stable emulsion of an agrochemical requires a great deal of process control as well prevention of the various breakdown processes.

A very attractive alternative for formulation of agrochemicals is to use microemulsion systems. As mentioned above, these are single optically isotropic and thermodynamically stable dispersions consisting of oil, water and amphiphile (one or more surfactants). As we will see later, the origin of the thermodynamic stability arises from the low interfacial energy of the system which is outweighed by the entropy of dispersion. These systems offer a number of advantages over O/W emulsions for the following reasons. Once the composition of the microemulsion is identified, the system is prepared by simple mixing all the components without the need of any appreciable shear. Due to their thermodynamic stability, these formulations undergo no separation or breakdown on storage (within a certain temperature range depending on the system). The low viscosity of the microemulsion systems ensures their ease of pourability, dispersion on dilution and they leave little residue in the container. Another main attraction

of microemulsions is their possible enhancement of biological efficacy of many agrochemicals. This, as we will see later, is due to the solubilization of the pesticide by the microemulsion droplets.

In this chapter, I will summarize the basic principles involved in the preparation of microemulsions and the origin of their thermodynamic stability. A section will be devoted to emulsifier selection for both O/W and W/O microemulsions. The physical methods that may be applied for the characterization of microemulsions will be briefly described. Finally, a section will be devoted to the possible enhancement of biological efficacy using microemulsions. The role of microemulsions in enhancing wetting, spreading and penetration will be discussed. Solubilization is also another factor that may enhance the penetration and uptake of an insoluble agrochemical.

6.3 Basic principles of microemulsion formation and thermodynamic stability

6.3.1 Mixed film theories [4]

The film (which may consist of surfactant and cosurfactant molecules) is considered as a liquid, "two-dimensional" third phase in equilibrium with both oil and water. Such a monolayer could be a duplex film, i.e. giving different properties on the water side and oil side. The initial "flat" duplex film (see Fig. 6.3) has different tensions at the oil and water sides. This is due to the different packing of the hydrophobic and hydrophilic groups (these groups have different sizes and cross-sectional areas). It is convenient to define a two-dimensional surface pressure π,

$$\pi = \gamma_0 - \gamma. \tag{6.2}$$

γ_0 is the interfacial tension of the clean interface, whereas γ is the interfacial tension with adsorbed surfactant.

One can define two values for π at the oil and water phases, π_o and π_w, which for a flat film are not equal, i.e. $\pi'_o \neq \pi'_w$. As a result of the difference in tensions, the film will bend until $\pi_o = \pi_w$. If $\pi'_o > \pi'_w$, the area at the oil side has to expand (resulting in a reduction of π'_o) until $\pi_o = \pi_w$. In this case a W/O microemulsion is produced. If $\pi'_w > \pi'_o$, the area at the water side expands until $\pi_w = \pi_o$. In this case an O/W micro emulsion is produced.

According to the duplex film theory, the interfacial tension γ_T is given by the following expression [5],

$$\gamma_T = \gamma_{(O/W)} - \pi, \tag{6.3}$$

where $(\gamma_{o/w})_a$ is the interfacial tension that is reduced by the presence of the alcohol.

The value of $(\gamma_{o/w})_a$ is significantly lower than $\gamma_{o/w}$ in the absence of the alcohol (for example, for hydrocarbon/water $\gamma_{o/w}$ is reduced from 50 to 15–20 mN m^{-1} on the addition of a significant amount of a medium chain alcohol like pentanol or hexanol.

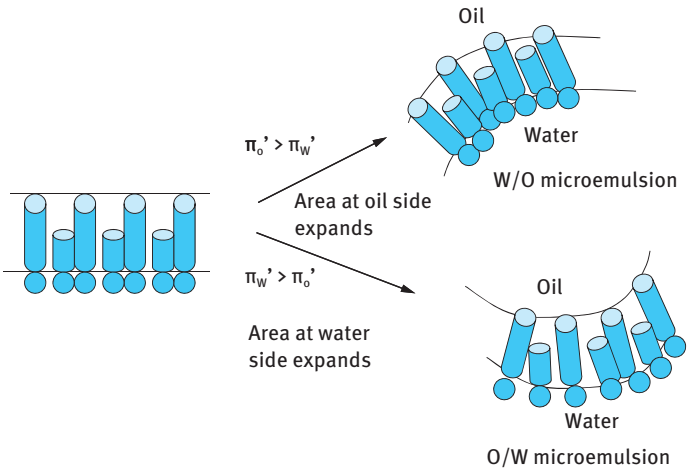

Fig. 6.3: Schematic representation of film bending.

Contributions to π are considered to be due to crowding of the surfactant and cosurfactant molecules and penetration of the oil phase into the hydrocarbon chains of the interface.

According to equation (6.3) if $\pi > (\gamma_{o/w})_a$, γ_T becomes negative and this leads to expansion of the interface until γ_T reaches a small positive value. Since $(\gamma_{o/w})_a$ is of the order of 15–20 mN m^{-1}, surface pressures of this order are required for γ_T to approach a value of zero.

The above duplex film theory can explain the nature of the microemulsion: The surface pressures at the oil and water sides of the interface depend on the interactions of the hydrophobic and hydrophilic potions of the surfactant molecule at both sides respectively. If the hydrophobic groups are bulky in nature relative to the hydrophilic groups, then for a flat film such hydrophobic groups tend to crowd, forming a higher surface pressure at the oil side of the interface; this results in bending and expansion at the oil side forming a W/O microemulsion. An example for a surfactant with bulky hydrophobic groups is Aerosol OT (dioctyl sulphosuccinate). If the hydrophilic groups are bulky, such as is the case with ethoxylated surfactants containing more than 5 ethylene oxide units, crowding occurs at the water side of the interface. This produces an O/W microemulsion.

6.3.2 Solubilization theories

These concepts were introduced by Shinoda and co-workers [6] who considered microemulsions to be swollen micelles that are directly related to the phase diagram of their components. Consider the phase diagram of a three-component system of water, ionic surfactant and medium chain alcohol as described in Fig. 6.4.

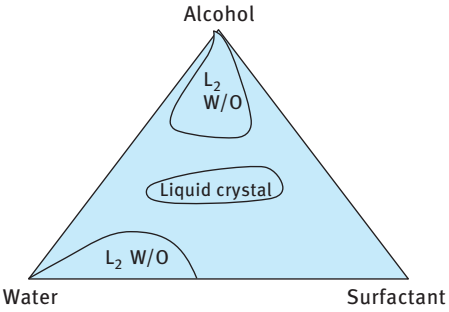

Fig. 6.4: Schematic representation of a three-component phase diagram.

At the water corner and at low alcohol concentration, normal micelles (L_1) are formed since in this case there are more surfactant molecules than alcohol molecules. At the alcohol (cosurfactant) corner, inverse micelles (L_2) are formed, since in this region there are more alcohol molecules than surfactant molecules. These L_1 and L_2 are not in equilibrium but are separated by a liquid crystalline region (lamellar structure with equal number of surfactant and alcohol molecules). The L_1 region may be considered an O/W microemulsion, whereas the L_2 may be considered a W/O microemulsion.

Addition of a small amount of oil, that is miscible with the cosurfactant but not with the surfactant, and water changes the phase diagram only slightly. The oil may be simply solubilized in the hydrocarbon core of the micelles. Addition of more oil leads to fundamental changes of the phase diagram, as illustrated in Fig. 6.5 where 50 : 50 of W : O are used. To simplify the phase diagram, the ^{50}W/^{50}O are presented on one corner of the phase diagram.

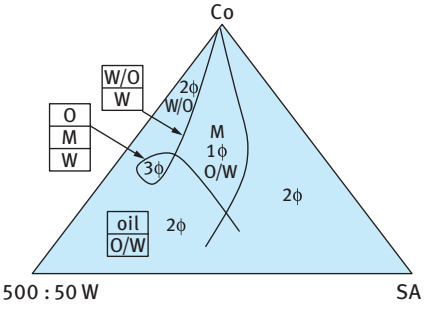

Fig. 6.5: Schematic representation of the pseudoternary phase diagram of oil/water/surfactant/cosurfactant.

Near the cosurfactant (co) corner the changes are small compared to the three-phase diagram (Fig. 6.4). The O/W microemulsion near the water–surfactant (sa) axis is not in equilibrium with the lamellar phase, but with a non-colloidal oil + cosurfactant phase. If co is added to such a two-phase equilibrium at fairly high surfactant concentration all oil is taken up and a one-phase microemulsion appears. Addition of co at low sa concentration may lead to separation of an excess aqueous phase before all oil is taken up in the microemulsion. A three-phase system is formed, containing a

microemulsion that cannot be clearly identified as W/O or O/W and that presumably is similar to the lamellar phase swollen with oil or to a more irregular intertwining of aqueous and oily regions (bicontinuous or middle phase microemulsion). The interfacial tensions between the three phases are very low ($0.1–10^{-4}$ mN m^{-1}). Further addition of co to the three-phase system makes the oil phase disappear and leaves a W/O microemulsion in equilibrium with a dilute aqueous sa solution. In the large one phase region, continuous transitions from O/W to middle phase to W/O microemulsions are found.

Solubilization can also be illustrated by considering the phase diagrams of nonionic surfactants containing poly(ethylene oxide) (PEO) head groups. Such surfactants do not generally need a cosurfactant for microemulsion formation. A schematic representation of oil and water solubilization by nonionic surfactants is given in Fig. 6.6. At low temperatures, the ethoxylated surfactant is soluble in water and at a given concentration is capable of solubilizing a given amount of oil. The oil solubilization increases rapidly with increasing temperature near the cloud point of the surfactant. This is illustrated in Fig. 6.6, which shows the solubilization and cloud point curves of the surfactant. Between these two curves, an isotropic region of O/W solubilized system exists. At any given temperature, any increase in the oil weight fraction above the solubilization limit results in oil separation (oil solubilized + oil). At any given surfactant concentration, any increase in temperature above the cloud point results in separation into oil, water and surfactant. If one starts from the oil phase with dissolved surfactant and adds water, solubilization of the latter takes place and solubilization increases with reduction of temperature near the haze point. Between the solubilization and haze point curves, an isotropic region of W/O solubilized system exists. At any given temperature, any increase in water weight fraction above the solubilization limit results in water separation (W/O solubilized + water). At any given surfactant concentration, any decrease in temperature below the haze point results in separation to water, oil and surfactant.

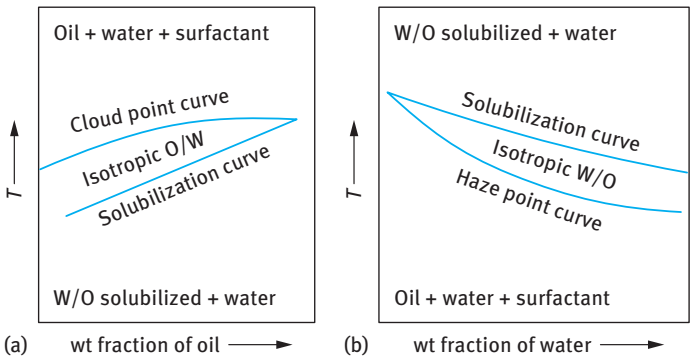

Fig. 6.6: Schematic representation of solubilization: (a) oil solubilized in a nonionic surfactant solution; (b) water solubilized in an oil solution of a nonionic surfactant.

With nonionic surfactants, both types of microemulsions can be formed depending on the conditions. With such systems, temperature is the most crucial factor since the solubility of surfactant in water or oil depends on temperature. Microemulsions prepared using nonionic surfactants have a limited temperature range.

6.3.3 Thermodynamic theory of microemulsion formation and stability

The spontaneous formation of the microemulsion with decreasing free energy can only be expected if the interfacial tension is so low that the remaining free energy of the interface is over-compensated for by the entropy of dispersion of the droplets in the medium [7, 8].

Single surfactants do lower the interfacial tension γ, but in most cases the critical micelle concentration (cmc) is reached before γ is close to zero. Addition of a second surfactant of a completely different nature (i.e. predominantly oil-soluble such as an alcohol) then lowers γ further and very small, even transiently negative values may be reached [9]. This is illustrated in Fig. 6.7, which shows the effect of addition of the cosurfactant on the γ–log c_{sa} curve.

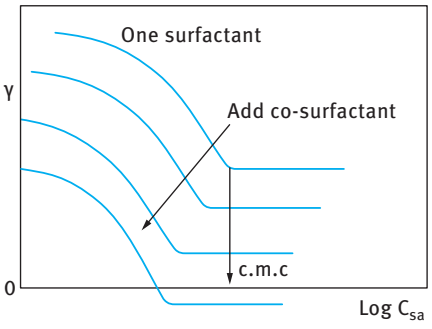

Fig. 6.7: γ–log C_{sa} curves for surfactant + cosurfactant.

It can be seen that addition of cosurfactant shifts the whole curve to low γ values and the cmc is shifted to lower values. The reason for the lowering of γ when using two surfactant molecules can be understood by considering the Gibbs adsorption equation for multicomponent systems [9]. For a multicomponent system i, each with an adsorption Γ_i (mol m^{-2}, referred to as the surface excess), the reduction in γ, i.e. dγ, is given by the following expression,

$$d\gamma = -\sum \Gamma_i \, d\mu_i = -\sum \Gamma_i RT \, d \ln C_i, \tag{6.4}$$

where μ_i is the chemical potential of component i, R is the gas constant, T is the absolute temperature and C_i is the concentration (mol dm^{-3}) of each surfactant component.

For two components, sa (surfactant) and co (cosurfactant), equation (6.4) becomes,

$$d\gamma = -\Gamma_{sa} RT d\ln C_{sa} - \Gamma_{co} RT d\ln C_{co}. \tag{6.5}$$

Integration of equation (6.5) gives,

$$\gamma = \gamma_0 - \int_0^{C_{sa}} \Gamma_{sa} RT \, d\ln C_{sa} - \int_0^{C_{co}} \Gamma_{co} RT \, d\ln C_{co}, \tag{6.6}$$

which clearly shows that γ_0 is lowered by two terms, both from surfactant and cosurfactant.

The two surfactant molecules should adsorb simultaneously and they should not interact with each other, otherwise they lower their respective activities. Thus, the surfactant and cosurfactant molecules should vary in nature, one predominantly water soluble (such as an anionic surfactant) and the other predominantly oil soluble (such as a medium chain alcohol). In some cases a single surfactant may be sufficient for lowering γ far enough for microemulsion formation to become possible, e.g. Aerosol OT (sodium diethyl hexyl sulphosuccinate) and many nonionic surfactants.

6.3.4 Factors determining W/O versus O/W microemulsions

The duplex film theory predicts that the nature of the microemulsion formed depends on the relative packing of the hydrophobic and hydrophilic portions of the surfactant molecule, which determine the bending of the interface. For example, a surfactant molecule such as Aerosol OT favours the formation of W/O microemulsion, without the need of a cosurfactant. As a result of the presence of a stumpy head group and large volume to length (V/l) ratio of the nonpolar group, the interface tends to bend with the head groups facing onwards, thus forming a W/O microemulsion. The molecule has $V/l > 0.7$, which is considered necessary for formation of a W/O microemulsion. For ionic surfactants such as SDS for which $V/l < 0.7$, microemulsion formation needs the presence of a cosurfactant (the latter has the effect of increasing V without changing l).

The importance of geometric packing was considered in detail by Mitchell and Ninham [10] who introduced the concept of the packing ratio P,

$$P = \frac{V}{l_c a_0}, \tag{6.7}$$

where a_0 is the head group area and l_c is the maximum chain length.

P gives a measure of the hydrophilic-lipophilic balance. For values of $P < 1$ (usually $P \approx 1/3$), normal or convex aggregates are produced (normal micelles). For values of $P > 1$, inverse micelles are produced. P is influenced by many factors: hydrophilicity of the head group, ionic strength and pH of the medium and temperature.

P also explains the nature of the microemulsion produced using nonionic surfactants of the ethoxylate type: *P* increases with increasing temperature (as a result of the dehydration of the PEO chain). A critical temperature (PIT) is reached at which *P* reaches 1 and above this temperature inversion occurs to a W/O system.

The influence of the surfactant structure on the nature of the microemulsion can also be predicted from thermodynamic theory. The most stable microemulsion would be that in which the phase with the smaller volume fraction forms the droplets (the osmotic pressure increases with increasing ϕ). For a W/O microemulsion prepared using an ionic surfactant such as Aerosol OT, the effective volume (hard-sphere volume) is only slightly larger than the water core volume, since the hydrocarbon tails may penetrate to a certain extent when two droplets come together. For an O/W microemulsion, the double layers may expand to a considerable extent, depending on the electrolyte concentration (the double layer thickness is of the order of 100 nm in 10^{-5} mol dm^{-3} 1 : 1 electrolyte and 10 nm in 10^{-3} mol dm^{-3} electrolyte). Thus the effective volume of O/W microemulsion droplets can be significantly higher than the core oil droplet volume and this explains the difficulty of preparing O/W microemulsions at high ϕ values when using ionic surfactants.

A schematic representation of the effective volume for W/O and O/W microemulsions is shown in Fig. 6.8.

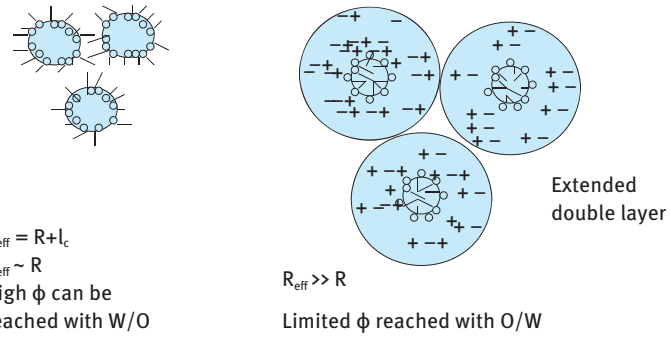

Fig. 6.8: Schematic representation of W/O and O/W microemulsion droplets.

6.4 Characterization of microemulsions using scattering techniques

Scattering techniques provide the most obvious methods for obtaining information on the size, shape and structure of microemulsions. The scattering of radiation, e.g. light, neutrons, X-ray, etc. by particles has been successfully applied for the investigation of many systems such as polymer solutions, micelles and colloidal particles. In all these methods, measurements can be made at sufficiently low concentration to

avoid complications arising from particle–particle interactions. The results obtained are extrapolated to infinite dilution to obtain the desired property, such as the molecular weight and radius of gyration of a polymer coil, the size and shape of micelles, etc. Unfortunately this dilution method cannot be applied for microemulsions, which depend on a specific composition of oil, water and surfactants. The microemulsions cannot be diluted by the continuous phase, since this dilution results in breakdown of the microemulsion. Thus, when applying the scattering techniques to microemulsions measurements have to be made at finite concentrations and the results obtained have to be analysed using theoretical treatments to take into account the droplet–droplet interaction.

Two scattering methods can be applied, namely time-average (static) light scattering and dynamic (quasi-elastic) light scattering (referred to as photon correlation spectroscopy, PCS).

In time-average (static) light scattering, the intensity of scattered light $I(Q)$ is measured as a function of scattering vector Q [11],

$$Q = \left(\frac{4\pi n}{\lambda}\right)\sin\left(\frac{\theta}{2}\right) \tag{6.8}$$

where n is the refractive index of the medium, λ is the wavelength of light and θ is the angle at which the scattered light is measured.

For a fairly dilute system, $I(Q)$ is proportional to the number of particles N, the square of the individual scattering units V_p and some property of the system (material constant) such as its refractive index,

$$I(Q) = [(\text{material constant})(\text{instrument constant})]NV_p^2. \tag{6.9}$$

The instrument constant depends on the geometry of the apparatus (the light path length and the scattering cell constant).

For more concentrated systems, $I(Q)$ also depends on the interference effects arising from particle–particle interaction,

$$I(Q) = [(\text{instrument constant})(\text{material constant})]NV_p^2P(Q)S(Q), \tag{6.10}$$

where $P(Q)$ is the particle form factor which allows the scattering from a single particle of known size and shape to be predicted as a function of Q. For a spherical particle of radius R,

$$P(Q) = \left[\frac{(3\sin QR - QR\cos QR)}{(QR)^3}\right]^2. \tag{6.11}$$

$S(Q)$ is the so-called "structure factor" which takes into account the particle–particle interaction. $S(Q)$ is related to the radial distribution function $g(r)$ (which gives the number of particles in shells surrounding a central particle) [12],

$$S(Q) = 1 - \frac{4\pi N}{Q}\int_0^\infty [g(r) - 1]r\sin QR\,\mathrm{d}r. \tag{6.12}$$

For a hard-sphere dispersion with radius R_{HS} (which is equal to $R + t$, where t is the thickness of the adsorbed layer),

$$S(Q) = \frac{1}{[1 - NC(2QR_{HS})]}, \tag{6.13}$$

where C is a constant.

One usually measures $I(Q)$ at various scattering angles θ and then plots the intensity at some chosen angle (usually 90°), i_{90} as a function of the volume fraction ϕ of the dispersion. Alternatively, the results may be expressed in terms of the Rayleigh ratio R_{90},

$$R_{90} = \left(\frac{i_{90}}{I_0}\right) r_s^2. \tag{6.14}$$

I_0 is the intensity of the incident beam and r_s is the distance from the detector.

$$R_{90} = K_0 MCP(90)S(90). \tag{6.15}$$

K_0 is an optical constant (related to the refractive index difference between the particles and the medium). M is the molecular mass of scattering units with weight fraction C.

For small particles (as is the case with microemulsions) $P(90) \approx 1$ and,

$$M = \frac{4}{3}\pi R_c^3 N_A, \tag{6.16}$$

where N_A is Avogadro's constant.

$$C = \phi_c \rho_c, \tag{6.17}$$

where ϕ_c is the volume fraction of the particle core and ρ_c is their density.

Equation (6.15) can be written in the simple form,

$$R_{90} = K_1 \phi_c R_c^3 S(90), \tag{6.18}$$

where $K_1 = K_0(4/3)N_A\rho_c^2$.

Equation (6.18) shows that to calculate R_c from R_{90} one needs to know $S(90)$. The latter can be calculated using equations (6.12) and (6.13).

The above calculations were obtained using a W/O microemulsion of water/xylene/sodium dodecyl benzene sulphonate (NaDBS)/hexanol [11]. The microemulsion region was established using the quaternary phase diagram. W/O microemulsions were produced at various water volume fractions using increasing amounts of NaDBS: 5, 10.9, 15 and 20 %. The results for the variation of R_{90} with the volume fraction of the water core droplets at various NaDBS concentrations showed that, with the exception of the 5 % NaDBS results, all the others showed an initial increase in R_{90} with increasing ϕ, reaching a maximum at a given ϕ, after which R_{90} decreases with any further increase in ϕ. These results were used to calculate R as a function

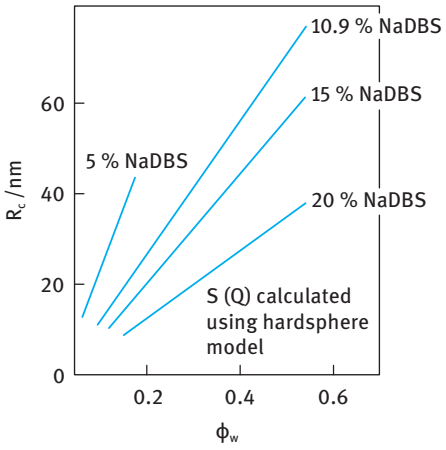

Fig. 6.9: Variation of R_c with ϕ_W for W/O microemulsions.

of ϕ using the hard-sphere model discussed above (equation (6.13)). This is shown in Fig. 6.9.

It can be seen that with an increase in ϕ, at constant surfactant concentration, R increases (the ratio of surfactant to water decreases with increasing ϕ). At any volume fraction of water, an increase in surfactant concentration results in a decrease in the microemulsion droplet size (the ratio of surfactant to water increases).

One can compare the results obtained from light scattering with those obtained from the interfacial area. If one assumes that all surfactant and cosurfactant molecules are adsorbed at the interface, it is possible to calculate the total interfacial area of the microemulsion from a knowledge of the area occupied by surfactant and cosurfactant molecules.

$$\begin{aligned}\text{total interfacial area} = {} & \text{total number of surfactant molecules} \\ & \times \text{area per surfactant molecule } A_s \\ & + \text{total number of cosurfactant molecules} \\ & \times \text{area per cosurfactant molecule } A_{co}.\end{aligned}$$

The total interfacial area A per kg of microemulsion is given by the expression,

$$A = \frac{(n_s N_A A_s + n_{co} N_A A_{co})}{\phi}. \tag{6.19}$$

n_s and n_{co} are the number of moles of surfactant and cosurfactant.

A is related to the droplet radius R (assuming all the droplets are of the same size) by,

$$A = \frac{3}{R\rho}. \tag{6.20}$$

Using reasonable values for A_s and A_{co} (30 A^2 for NaDBS and 20 A^2 for hexanol) R was calculated and the results were compared with those obtained using light scattering results. Two conditions were considered:

(a) all hexanol molecules were adsorbed;
(b) part of the hexanol adsorbed to give a molar ratio of hexanol to NaDBS of 2 : 1.

Good agreement was obtained between the two results.

In dynamic light scattering (PCS) technique one measures the intensity fluctuation of scattered light by the droplets as they undergo Brownian motion [13]. When a light beam passes through a colloidal dispersion, an oscillating dipole movement is induced in the particles, thereby radiating the light. Due to the random position of the particles, the intensity of scattered light, at any instant, appears as random diffraction ("speckle" pattern). As the particles undergo Brownian motion, the random configuration of the pattern will fluctuate, such that the time taken for an intensity maximum to become a minimum (the coherence time), corresponds approximately to the time required for a particle to move one wavelength λ. Using a photomultiplier of active area about the diffraction maximum (i.e. one coherent area) this intensity fluctuation can be measured. The analogue output is digitized (using a digital correlator) that measures the photocount (or intensity) correlation function of scattered light.

The photocount correlation function $G^{(2)}(\tau)$ is given by,

$$g^{(2)} = B[1 + \gamma^2 g^{(1)}(\tau)]^2, \tag{6.21}$$

where τ is the correlation delay time.

The correlator compares $g^{(2)}(\tau)$ for many values of τ. B is the background value to which $g^{(2)}(\tau)$ decays at long delay times. $g^{(1)}(\tau)$ is the normalized correlation function of the scattered electric field and γ is a constant (≈ 1).

For monodispersed noninteracting particles,

$$g^{(1)}(\tau) = \exp(-\Gamma\gamma). \tag{6.22}$$

Γ is the decay rate or inverse coherence time that is related to the translational diffusion coefficient D,

$$\Gamma = DK^2, \tag{6.23}$$

where K is the scattering vector,

$$K = \left(\frac{4\pi n}{\lambda_0}\right)\sin\left(\frac{\theta}{2}\right). \tag{6.24}$$

The particle radius R can be calculated from D using the Stokes–Einstein equation,

$$D = \frac{kT}{6\pi\eta_0 R}, \tag{6.25}$$

where η_0 is the viscosity of the medium.

The above analysis only applies for very dilute dispersions. With microemulsions which are concentrated dispersions, corrections are needed to take into account the interdroplet interaction. This is reflected in plots of $\ln g^{(1)}(\tau)$ versus τ, which become nonlinear, implying that the observed correlation functions are not single exponentials. As with time-average light scattering, one needs to introduce a structure factor in calculating the average diffusion coefficient. For comparative purposes, one calculates the collective diffusion coefficient D, which can be related to its value at infinite dilution D_0 by [14],

$$D = D_0(1 + \alpha\phi), \tag{6.26}$$

where α is a constant that is equal to 1.5 for hard spheres with repulsive interaction.

6.5 Characterization of microemulsions using conductivity

Conductivity measurements may provide valuable information on the structural behaviour of microemulsions. In the early applications of conductivity measurements, the technique was used to determine the nature of the continuous phase. O/W microemulsions should give fairly high conductivity (that is determined by that of the continuous aqueous phase) whereas W/O microemulsions should give fairly low conductivity (that is determined by that of the continuous oil phase).

As an illustration, Fig. 6.10 shows the change in electrical resistance (reciprocal of conductivity) with the ratio of water to oil (V_w/V_o) for a microemulsion system prepared using the inversion method [15]. Fig. 6.10 indicates the change in optical clarity and birefringence with the ratio of water to oil. At low V_w/V_o, a clear W/O microemulsion is produced with a high resistance (oil continuous). As V_w/V_o increases, the resistance decreases, and in the turbid region, hexanol and lamellar micelles are produced. Above a critical ratio, inversion occurs and the resistance decreases producing O/W microemulsion.

Conductivity measurements were also used to study the structure of the microemulsion, which is influenced by the nature of the cosurfactant. This is illustrated in Fig. 6.11 for systems based on various cosurfactants with different alkyl chain length. The cosurfactant chain length was gradually increased from C_2 (ethanol) to C_7 (heptanol). With the short chain alcohols ($C < 5$), the conductivity shows a rapid increase above a critical ϕ value. With longer chain alcohols, namely hexanol and heptanol, the conductivity remains very low up to a high water volume fraction [16, 17]. With the short chain alcohols, the system shows percolation above a critical water volume fraction. Under these conditions the microemulsion is "bicontinuous". With the longer chain alcohols, the system is non-percolating and one can define definite water cores. This is sometimes referred to as a "true" microemulsion.

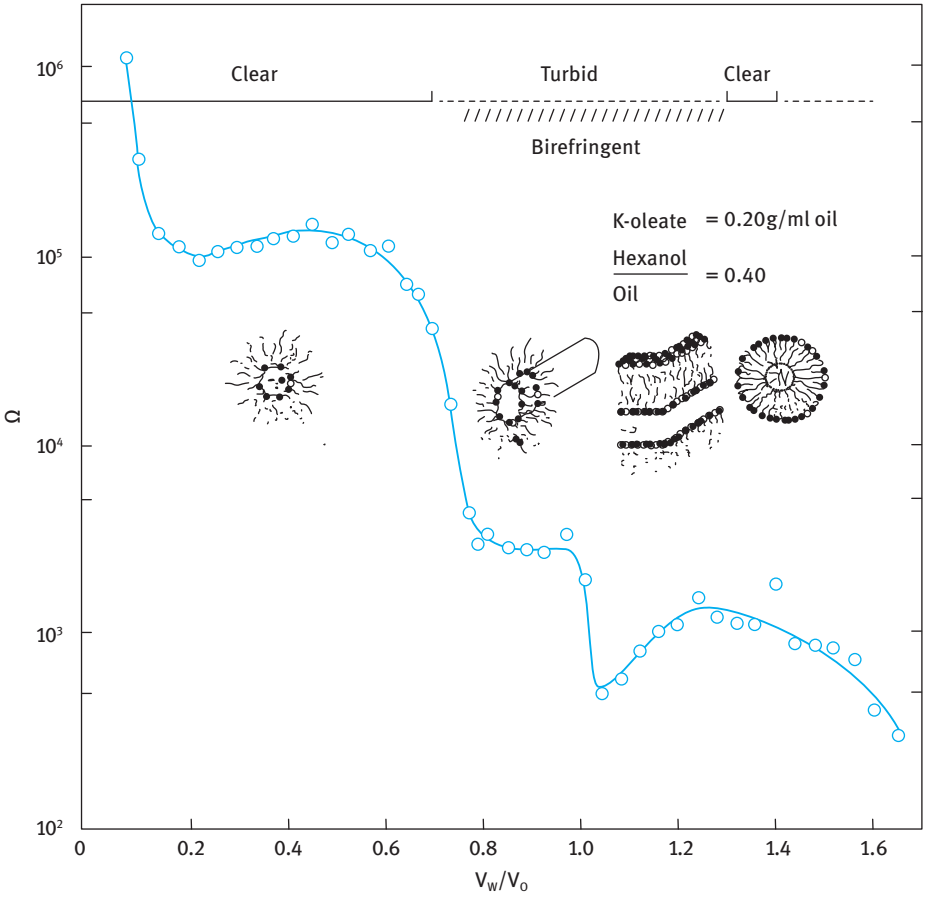

Fig. 6.10: Electrical resistance versus V_w/V_o.

6.6 NMR Measurements

Lindman and co-workers [18–20] demonstrated that the organization and structure of microemulsions can be elucidated from self-diffusion measurements of all the components (using pulse gradient or spin echo NMR techniques). Within a micelle, the molecular motion of the hydrocarbon tails (translational, reorientation and chain flexibility) is almost as rapid as in a liquid hydrocarbon. In a reverse micelle, water molecules and counterions are also highly mobile. For many surfactant-water systems, there is a distinct spatial separation between hydrophobic and hydrophilic domains. The passage of species between different regions is an improbable event and this occurs very slowly.

Thus, self-diffusion, if studied over macroscopic distances, should reveal whether the process is rapid or slow depending on the geometrical properties of the inner struc-

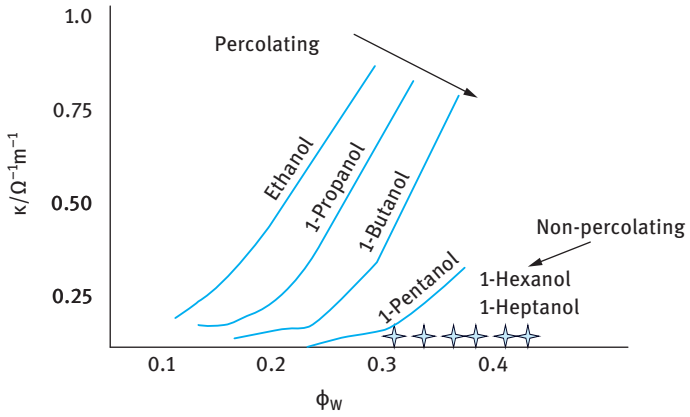

Fig. 6.11: Variation of conductivity with water volume fraction for various cosurfactants.

ture. For example, a phase that is water continuous and oil discontinuous should exhibit rapid diffusion of hydrophilic components, while the hydrophobic components should diffuse slowly. An oil continuous but water discontinuous system should exhibit rapid diffusion of the hydrophobic components. One would expect that a bicontinuous structure should give rapid diffusion of all components.

Using the above principle, Lindman and co-workers [18–20] measured the self-diffusion coefficients of all components consisting of various components, with particular emphasis on the role of the cosurfactant. For microemulsions consisting of water, hydrocarbon, an anionic surfactant and a short chain alcohol (C_4 and C_5), the self-diffusion coefficient of water, hydrocarbon and cosurfactant was quite high, of the order of 10^{-9} m^2 s^{-1}, i.e. two orders of magnitude higher than the value expected for a discontinuous medium (10^{-11} m^2 s^{-1}). This high diffusion coefficient was attributed to three main effects: Bicontinuous solutions, easily deformable and flexible interface and absence of any large aggregates. With microemulsions based on long chain alcohols (e.g. decanol), the self-diffusion coefficient for water was low, indicating the presence of definite (closed) water droplets surrounded by surfactant anions in the hydrocarbon medium. Thus, NMR measurements could clearly distinguish between the two types of microemulsion systems.

6.7 Selection of surfactants for formulation of microemulsions

The formulation of microemulsions is still an art, since understanding the interactions at a molecular level, at the oil and water sides of the interface is far from being achieved. However, some rules may be applied for the selection of emulsifiers for formulating O/W and W/O microemulsions. These rules are based on the same principles that are applied for the selection of emulsifiers for macroemulsions described

in Chapter 2. Three main methods may be applied for such a selection, namely the hydrophilic-lipophilic balance (HLB), the phase inversion temperature (PIT) and the cohesive energy ratio (CER) concepts. As mentioned in Chapter 2, the HLB concept is based on the relative percentage of hydrophilic to lipophilic (hydrophobic) groups in the surfactant molecule. Surfactants with a low HLB number (3–6) normally form W/O emulsions, whereas those with high HLB number (8–18) form O/W emulsions. Given an oil to be microemulsified, the formulator should first determine its required HLB number. Several procedures may be applied for determining the HLB number depending on the type of surfactant that needs to be used. These procedures were described before in Chapter 2. Once the HLB number of the oil is known, one must try to find the chemical type of emulsifier which best matches the oil. Hydrophobic portions of surfactants which are similar to the chemical structure of the oil should be looked at first.

The PIT system provides information on the type of oil, phase volume relationships and concentration of the emulsifier. The PIT system is established on the proposition that the HLB number of a surfactant changes with temperature and that the inversion of the emulsion type occurs when the hydrophile and lipophile tendencies of the emulsifier just balance. At this temperature no emulsion is produced. From a microemulsion viewpoint, the PIT has an outstanding feature since it can throw some light on the chemical type of the emulsifier needed to match a given oil. Indeed, the required HLB values for various oils estimated from the PIT system compare very favourably with those prepared using the HLB system described above. This shows a direct correlation between the HLB number and the PIT of the emulsion.

As discussed in Chapter 2, the CER concept provides a more quantitative method for the selection of emulsifiers. The same procedure can also be applied for microemulsions.

6.8 Role of microemulsions in enhancing biological efficacy

The role of microemulsions in enhancing biological efficiency can be described in terms of the interactions at various interfaces and their effect on transfer and performance of the agrochemical [21]. This will be described in detail in Chapter 8 and only a summary is given here. The application of an agrochemical as a spray involves a number of interfaces, where interaction with the formulation plays a vital role. The first interface during application is that between the spray solution and the atmosphere (air) which governs the droplet spectrum, rate of evaporation, drift, etc. In this respect the rate of adsorption of the surfactant at the air/liquid interface is of vital importance. Since microemulsions contain high concentrations of surfactant and mostly more than one surfactant molecule is used for their formulation, then on diluting a microemulsion on application, the surfactant concentration in the spray solution will be sufficiently high to cause efficient lowering of the surface tension γ. As discussed

above, two surfactant molecules are more efficient in lowering γ than either of the two components. Thus, the net effect will be production of small spray droplets, which as we will see later, adhere better to the leaf surface. In addition, the presence of surfactants in sufficient amounts will ensure that the rate of adsorption (which is the situation under dynamic conditions) is fast enough to ensure coverage of the freshly formed spray by surfactant molecules.

The second interaction is between the spray droplets and the leaf surface, whereby the droplets impinging on the surface undergo a number of processes that determine their adhesion and retention and further spreading on the target surface. The most important parameters that determine these processes are: the volume of the droplets and their velocity, the difference between the surface energy of the droplets in flight, E_0, and their surface energy after impact, E_s. As mentioned above, microemulsions which are effective in lowering the surface tension of the spray solution ensure the formation of small droplets which do not usually undergo reflection if they are able to reach the leaf surface. Clearly, the droplets need not be too small otherwise drift may occur. One usually aims at a droplet spectrum in the region of 100–400 μm. As will be discussed in Chapter 8, the adhesion of droplets is governed by the relative magnitude of the kinetic energy of the droplet in flight and its surface energy as it lands on the leaf surface. Since the kinetic energy is proportional to the third power of the radius (at constant droplet velocity), whereas the surface energy is proportional to the second power, one would expect that sufficiently small droplets will always adhere. For a droplet to adhere, the difference in surface energy between free and attached drop ($E_0 - E_s$) should exceed the kinetic energy of the drop, otherwise bouncing will occur. Since E_s depends on the contact angle, θ, of the drop on the leaf surface, it is clear that low values of θ are required to ensure adhesion, particularly with large drops that have high velocity. Microemulsions when diluted in the spray solution usually give low contact angles of spray drops on leaf surfaces as a result of lowering the surface tension and their interaction with the leaf surface.

Another factor which can affect biological efficacy of foliar spray application of agrochemicals is the extent to which a liquid wets and covers the foliage surface. This, in turn, governs the final distribution of the agrochemical over the areas to be protected. Several indices may be used to describe the wetting of a surface by the spray liquid, of which the spread factor and spreading coefficient are probably the most useful. The spread factor is simply the ratio between the diameter of the area wetted on the leaf, D, and the diameter of the drop, d. This ratio is determined by the contact angle of the drop on the leaf surface. The lower the value of θ, the higher the spread factor. As mentioned above, microemulsions usually give low contact angle for the drops produced from the spray. The spreading coefficient is determined by the surface tension of the spray solution as well as the value of θ. Again, with microemulsions diluted in a spray, both γ and θ are sufficiently reduced and this results in a positive spreading coefficient. This ensures rapid spreading of the spray liquid on the leaf surface.

Another important factor for control of biological efficacy is the formation of "deposits" after evaporation of the spray droplets, which ensure the tenacity of the particles or droplets of the agrochemical. This will prevent removal of the agrochemical from the leaf surface by the falling rain. Many microemulsion systems form liquid crystalline structures after evaporation, which have high viscosity (hexagonal or lamellar liquid crystalline phases). These structures will incorporate the agrochemical particles or droplets and ensure their "stickiness" to the leaf surface.

One of the most important roles of microemulsions in enhancing biological efficacy is their effect on the penetration of the agrochemical through the leaf. Two effects may be considered which are complimentary. The first effect is due to enhanced penetration of the chemical as a result of the low surface tension. For penetration to occur through fine pores, a very low surface tension is required to overcome the capillary (surface) forces. These forces produce a high pressure gradient that is proportional to the surface tension of the liquid. The lower the surface tension, the lower the pressure gradient and the higher the rate of penetration. The second effect is due to solubilization of the agrochemical within the microemulsion droplet. Solubilization results in an increase in the concentration gradient thus enhancing the flux due to diffusion. This can be understood from a consideration of Fick's first law,

$$J_{\mathrm{D}} = D\left(\frac{\partial C}{\partial x}\right), \tag{6.27}$$

where J_{D} is the flux of the solute (amount of solute crossing a unit cross section in unit time), D is the diffusion coefficient and $(\partial C/\partial x)$ is the concentration gradient. The presence of the chemical in a swollen micellar system will lower the diffusion coefficient. However, the presence of the solubilizing agent (the microemulsion droplet) increases the concentration gradient in direct proportionality to the increase in solubility. This is because Fick's law involves the absolute gradient of concentration, which is necessarily small as long as the solubility is small, but not its relative rate. If the saturation is noted by S, Fick's law may be written as,

$$J_{\mathrm{D}} = D \times 100S\left(\frac{\partial \%S}{\partial x}\right), \tag{6.28}$$

where $(\partial \%S/\partial x)$ is the gradient in relative value of S. Equation (6.28) shows that for the same gradient of relative saturation, the flux caused by diffusion is directly proportional to saturation. Hence, solubilization will in general increase transport by diffusion, since it can increase the saturation value by many orders of magnitude (that outweighs any reduction in D). In addition, the solubilization enhances the rate of dissolution of insoluble compounds and this will have the effect of increasing the availability of the molecules for diffusion through membranes.

References

[1] Hoar TP, Schulman JH. Nature. 1943;152:102.
[2] Prince LM. Microemulsion theory and practice. New York: Academic Press; 1977.
[3] Danielsson I, Lindman B. Colloids and Surfaces. 1983;3:391.
[4] Schulman JH, Stoeckenius W, Prince LM. J Phys Chem. 1959;63:1677.
[5] Prince LM. Adv Cosmet Chem. 1970;27:193.
[6] Shinoda K, Friberg S. Adv Colloid Interface Sci. 1975;4:281.
[7] Ruckenstein E, Chi JC. J Chem Soc Faraday Trans II. 1975;71:1690.
[8] Overbeek JTG. Faraday Disc Chem Soc. 1978;65:7.
[9] Overbeek JTG. de Bruyn PL, Verhoeckx F. In: Tadros TF, editor. Surfactants. London: Academic Press; 1984. p. 111–132.
[10] Mitchell DJ, Ninham BW. J Chem Soc Faraday Trans II. 1981;77:601.
[11] Baker RC, Florence AT, Ottewill RH, Tadros TF. J Colloid Interface Sci. 1984;100:332.
[12] Ashcroft NW, Lekner J. Phys Rev. 1966;45:33.
[13] Pusey PN. In: Green JHS, Dietz R, editors. Industrial polymers: Characterisation by molecular weights. London: Transcripta Books; 1973.
[14] Cazabat AN, Langevin D. J Chem Phys. 1981;74:3148.
[15] Prince LM. Microemulsion theory and practice. New York: Academic Press; 1977.
[16] Lagourette B, Peyerlasse J, Boned C, Clausse M. Nature. 1969;281:60.
[17] Clausse M, Peyerlasse J, Boned C, Heil J, Nicolas-Margantine L, Zrabda A. In: Mittal KL, Lindman B, editors. Solution properties of surfactants. Plenum Press; 1984. Vol. 3, p. 1583.
[18] Lindman B, Winnerstrom H. In: Borschke FL, editor. Topics in current chemistry 87. Heidelberg: Springer-Verlag; 1980. p. 1–83.
[19] Winnerstrom H, Lindman B. Phys Rep. 1970;52:1.
[20] Lindman B, Stilbs P, Moseley ME. J Colloid Interface Sci. 1981;83:569.
[21] Tadros T. Colloids in agrochemicals. Weinheim: Wiley-VCH; 2009.

7 Controlled-release formulations

7.1 Introduction

Controlled-release formulations of agrochemicals offer a number of advantages such as improvement of residual activity, reduction of application dosage, stabilization of the core active ingredient (AI) against environmental degradation, reduction of mammalian toxicity by reducing worker exposure, reduction of phytotoxicity, reduction of fish toxicity and reduction of environmental pollution. One of the main advantages of using controlled-release formulations, in particular microcapsules, is the reduction of physical incompatibility when mixtures are used in the spray tank. They also can reduce biological antagonism when mixtures are applied in the field.

7.2 Types of controlled-release systems

Several types of controlled-release systems can be identified:

(i) Microcapsules with particles in the size range 1–100 μm that consist of a distinct capsule wall (mostly a polymer) surrounding the agrochemical core.
(ii) Microparticles (size range 1–100 μm) consisting of a matrix in which the agrochemical is uniformly dissolved or dispersed.
(iii) Granules with matrix particles of 0.2–2.0 mm with the agrochemical uniformly dissolved or dispersed within the matrix [1].

Microencapsulation of agrochemicals is mainly carried out by interfacial condensation, in situ polymerization and coacervation. Interfacial condensation [2] is perhaps the most widely used method for encapsulation in industry. The AI, which may be oil-soluble, oil dispersible or an oil itself is first emulsified in water using a convenient surfactant or polymer. A hydrophobic monomer A is placed in the oil phase (oil droplets of the emulsion) and a hydrophilic monomer B is placed in the aqueous phase. The two monomers interact at the interface between the oil and the aqueous phase forming a capsule wall around the oil droplet. Two main types of systems may be identified. For example, if the material to be encapsulated is oil-soluble, oil-dispersible or an oil itself, an oil-in-water (O/W) emulsion is first prepared. In this case the hydrophobic monomer is dissolved in the oil phase which forms the dispersed phase. The role of the surfactant in this process is crucial since an oil-water emulsifier (with high hydrophilic-lipophilic balance, HLB) is required. Alternatively, a polymeric surfactant such as partially hydrolyzed polyvinyl acetate (referred to as polyvinyl alcohol, PVA) or an ethylene oxide–propylene oxide–ethylene oxide, PEO–PPO–PEO (Pluronic) block copolymer can be used. The emulsifier controls the droplet size distribution and hence the size of capsules formed. On the other hand, if the material to be encapsulated is

https://doi.org/10.1515/9783110578997-008

water-soluble, a water-in-oil (W/O) emulsion is prepared using a surfactant with a low HLB number or an A–B–A block copolymer of polyhydroxystearic acid-polyethylene oxide-polyhydroxystearic acid (PHS–PEO–PHS). In this case the hydrophilic monomer is dissolved in the aqueous internal phase droplets.

In interfacial polymerization, the monomers A and B are polyfunctional monomers capable of causing polycondensation or polyaddition reaction at the interface [2]. Examples of oil-soluble monomers are polybasic acid chloride, bis-haloformate and polyisocyanates, whereas water-soluble monomers can be polyamine or polyols. Thus, a capsule wall of polyamide, polyurethane or polyurea may be formed. Some trifunctional monomers are present to allow crosslinking reactions. If water is the second reactant with polyisocyanates in the organic phase, polyurea walls are formed. The latter modification has been termed in situ interfacial polymerization [3].

One of the most useful microencapsulation processes involves reactions that produce formation of urea-formaldehyde (UF) resins. Urea, along with other ingredients such as amines, maleic anhydride copolymers or phenols, are added to the aqueous phase that contains oily droplets of the active ingredient that is to be encapsulated. Formaldehyde or formaldehyde oligomers are added and the reaction conditions are adjusted to form UF condensates, sometimes referred to as aminoplasts, that should preferentially wet the disperse phase [1]. The reaction is continued to completion over several hours. Fairly high activity products can be obtained. A modification of this technique is the use of etherified UF resins. The UF prepolymers are dissolved in the organic phase, along with the active ingredient, through the use of protective colloids (such as PVA), and the reaction is initiated through temperature and acid catalyst. This promotes the formation of the shell in the organic phase adjacent to the interface between the bulk-oil phase droplets and the aqueous phase solution [1].

It should be mentioned that the role of surfactants in the encapsulation process is very important. Apart from their direct role in the preparation of microcapsule dispersions, surfactants can be used to control the release of the active ingredient (AI) from the microcapsule dispersion. For example, Wade et al. [5] have shown that the efficacy of an edifenphos suspension can be improved by addition of a surfactant either to the aqueous medium or to the core. This was attributed to the possible solubilization of the AI by the surfactant micelles, thus increasing the release rate.

There are generally two mechanisms for release of the active ingredient (AI) from a capsule.

(i) Diffusion of the AI through the microcapsule wall.
(ii) Destruction of the microcapsule wall by either physical means, e.g. mechanical power, or by chemical means, e.g. hydrolysis, biodegradation, thermal degradation, etc.

The release behaviour is controlled by several factors such as particle size, wall thickness, type of wall material, wall structure (porosity, degree of polymerization, crosslink density, additives, etc.), type of core material (chemical structure,

physical state, presence or absence of solvents) and amount or concentration of the core material. The release behaviour is determined by interaction of these factors and optimization is essential for achieving the desirable release rate.

In order to get better performance of the microcapsule for biological efficacy, time dependent or site-specific release is desirable. It is essential in this case to develop various functional microcapsules that are specific to the target organism (e.g. for insecticides). Temperature, pH, light, enzyme responsive microcapsules are desirable.

The simplest release kinetics of microcapsules is diffusion controlled as predicted by Fick's first law. The amount of AI that diffuses through the wall of a microcapsule, $\mathrm{d}m/\mathrm{d}t$ (mol s^{-1}) is proportional to the diffusion coefficient D, the surface area A and the concentration gradient $\mathrm{d}c/\mathrm{d}x$ (where $\mathrm{d}c$ is the difference in concentration between the inside and outside wall and $\mathrm{d}x$ is the thickness of the capsule wall,

$$\frac{\mathrm{d}m}{\mathrm{d}t} = -DA\frac{\mathrm{d}c}{\mathrm{d}x}. \tag{7.1}$$

Equation (7.1) clearly shows that the release rate increases with increasing A (i.e. when using small capsules) and decreasing $\mathrm{d}x$ (thinner capsule wall). To decrease the rate of diffusion one has to use larger capsules and thicker capsule walls.

There are four types of encapsulation utilizing the system of phase separation from aqueous solution [2]:

(i) Complex coacervation or phase separation resulting from two oppositely charged colloids neutralizing one another.
(ii) Simple coacervation, where a non-electrolyte such as alcohol causes formation of a separate polymer-rich phase.
(iii) Salt coacervation, where a polymer separates as a result of a salting-out process.
(iv) Precipitation and insolubilization of a polymer by changing the pH of the aqueous solution system.

An example of complex coacervation is the interaction between gelatin and gum arabic [4]. In this case a dispersion of oil in a dilute solution of gelatin-gum arabic mixture is prepared. Gelatin usually has an isoelectric point (IEP) at about pH = 4.8, whereas gum arabic, which contains only carboxylic groups, is usually negative over a wide range of pH values. Thus, by lowering the pH to a value below the IEP of gelatin, say to pH 4.0, the gelatin acquires a positive charge and becomes coacervated with gum arabic, forming capsules around the oil droplets. Various other anionic polyelectrolytes may be used such as sodium alginate, agar, polyvinyl benzene sulphonic acid, etc. In general, effective materials include polymers, surface active agents and organic compounds which have acid groups in the molecule [2].

Encapsulation by phase separation can also be applied in nonaqueous media. This is particularly suitable for encapsulation of water-soluble materials. A W/O emulsion of the active ingredient is dissolved in the water droplets using an oil-soluble

polymer. Phase separation of the oil-soluble polymer may be induced by addition of another polymer, nonsolvent or by changing the temperature.

Salt coacervation is best exemplified by the formation of calcium alginate capsules. In this process a drop of a solution, an emulsion or suspension containing the AI and sodium alginate is dropped into a solution of calcium chloride. When the drop touches the calcium chloride solution, a membrane of calcium alginate forms instantaneously, maintaining the drop shape in this aqueous/aqueous system. Calcium ions diffuse in, gelling the entire drop. This drop is then placed in a solution of a polycation which displaces the calcium ions from the outer surface, forming a permanent membrane. This capsule is then placed in sodium citrate, which slowly solubilizes the calcium through the formation of a soluble citrate complex, ungelling the internal portion of the drop. By controlling the molecular weight of the reactants and the times of reaction, the thickness and size selectivity of the permanent wall can be controlled over a wide range.

Microencapsulation of solid particles is by far the most challenging process of encapsulation since one has to coat the particles individually without any aggregation. These particles cover the size range 0.1–5 μm with an average of 1–2 μm. Clearly, when encapsulating these particles one has to make sure that the smallest size fraction is retained without any aggregation. This is vital for biological efficacy since the smaller particles are more effective for disease control (due to their higher solubility when compared with the larger particles). Beestan [5] suggested an injection treatment coating method for encapsulation of solid particles. This method utilizes air at sonic velocity to atomize the coating material and accelerate the particles in such a manner that they become coated on all surfaces. The liquid coating material may be melted wax or resins, solutions of polymers or coating materials or suspensions of film-forming solids such as polymer latexes. Coating is accomplished by metering the solid particles in the shear zone concurrently with metering the liquid-coating material into the air stream. The latter is accelerated to the speed of sound through a restriction zone to give a shear zone of sufficient intensity to affect coating. The mixing action within the shear zone coats the solid particles individually with the coating material. On-line particle size measurement of the encapsulated solid particles showed that the particle size range of the solid particles remain virtually unchanged by this injection treatment coating process, indicating that individual particles of all sizes are discretely coated.

Another method that can be applied to encapsulate solid particles is a modification of the coacervation process described above. In this method a technique of solvent evaporation is used to precipitate the polymers as intact coatings. The solid particles are suspended in a solvent solution of the polymer and emulsified into a liquid. The emulsion is then heated to evaporate the solvent causing the polymer to insolubilize as a coating around the suspended particles. Alternatively, a nonsolvent for the polymer is added to the suspension of particles in polymer solution, causing the solvent to phase separate and the polymers to insolubilize to coatings.

Matrix-based microparticles are of three main types [6]:

(i) Matrix powders where the active ingredient (AI) is dispersed throughout the matrix and the mixture is ground (if necessary) to form a powder that can be applied as wettable powder. Surface active agents are incorporated to aid wetting and dispersion of the microparticles. The matrices used include polymers such as lignin, starch, proteins, high molecular weight natural polymers such as waxes, cyclodextrin, synthetic polymers such as urea formaldehyde resins or acrylic acid polymers. Inorganic materials such as glass, silica or diatomaceous earth can also be used. These inorganic materials can also act as carriers.
(ii) Carriers plus matrix whereby the particles are based on a porous powder that is used as a carrier. Two types can be distinguished, namely co-loaded (where the AI/matrix mixture is loaded into the carrier) and postcoated (where the AI is loaded into the carrier and the matrix is then loaded separately).
(iii) Matrix emulsions whereby the microparticles are made by emulsifying a hot solution of the AI plus matrix, typically in water. On cooling, the emulsion droplets solidify producing an aqueous suspension of the microparticles.

Generally speaking, one component of the formulation, the "matrix", will be responsible for the controlled release of the formulation. It is convenient to consider the controlled release as being due to interaction among the AI, the matrix and the environment. Matrix systems where the AI is uniformly dispersed through a matrix material are the basis of commercial formulations [7]. Three models may be used for describing the behaviour of such systems. The first two mechanisms apply where the AI is uniformly dispersed throughout the matrix and is essentially impermeable to water or the external environment. Leaching of the AI occurs at the edge of the particle, setting up a concentration gradient within the particle that provides the driving force for diffusion of the AI to the edge of the particle and into the external environment. In such a system, the rate of release is governed by the solubility of the AI in the matrix, the diffusion coefficient for the transport of the AI through the matrix and the geometry of the particle. Matrix particles usually contain pores and cracks, thus increasing the effective surface area between the particle and the external environment and hence the release rate. The second mechanism is applied to rigid, often glassy matrices where diffusion of the AI within the matrix of the active is negligible. Leaching is controlled by surface exposure of the AI through biological or chemical degradation of the matrix. The third mechanism applies to systems where the matrix material is permeable to the external environment, e.g. water. This corresponds to a system where the AI is dispersed in a latex. In this case water permeates the matrix through a combination of capillary and osmotic effects. The AI dissolves and diffuses to the edge of the particle into the surrounding medium. The process is diffusion controlled and is governed by the solubility and diffusion coefficient of the AI in water.

Many agrochemicals are formulated as water dispersible granules (WG) which disperse quickly and completely when added to water. The main advantage of WGs is that

they avoid the use of solvents, thus reducing the risk during manufacture and to farm workers during application. In addition, they can be applied for slow release as will be discussed below. Several processes can be applied to produce WGs of insoluble AI:

(i) Those in which the starting materials are essentially dry and are subsequently made wet and then redried.
(ii) Those in which the starting materials are wet and are granulated and dried.

A typical composition of a WG is one or two AIs, dispersing agent, suspending agent, wetting agent, binder (such as lignosulphonate or a gum) and a filler (mineral filler or water-soluble salt).

As mentioned above, granulation is carried out using a dry or wet route process. Several dry route processes are possible such as pan granulation, fluid-bed granulation, Schugi granulator, extrusion and peg or pin granulator [8]. The wet route process can be carried out by spray drying or spray granulation [8].

Approaches to achieve controlled release in granules fall into two main categories:

(i) The matrix (monolith) with the AI dispersed throughout the structure.
(ii) The reservoir in which a polymeric coating entraps the AI with or without a support [9].

Particle size and uniformity are very important, especially in applications where the duration of release is critical. Three types of granule dimensions can be distinguished, namely fine granules 0.3–2.5 mm in diameter, microgranules 0.1–0.6 mm and macrogranules 2–6 mm. A formulation containing a range of particle sizes (from dusts to macrogranules) will have an extended period of effectiveness. A controlled-release system based on a monolithic polymer granule made from extruding the AI with a release-rate-modifying inert material ("porisogen") in a thermoplastic matrix can play an important role for pest management for periods (following a single treatment of a non-persistent agrochemical) up to 2–3 years.

Although the above approach based on synthetic polymers is the most successful of the controlled-release granules, natural polymers showed great success in matrix formulations for AI delivery. Examples of natural polymers are crosslinked starch, polysaccharides, crosslinked alginates and cellulose derivatives. To provide effective delay of release, alginate gels crosslinked with calcium require the incorporation of absorbents such as silica, alumina, clays or charcoal. Further control of the release rate could be achieved by combining kaolin clay with linseed oil in the granule. Other gel forming polymers include carboxymethyl cellulose stabilized with gelatin and crosslinked with cupric or aluminium ions. Coating of granules with rate-controlling polymer film can also be applied. Controlled delivery of agrochemicals has also been obtained with superabsorbent acrylamide and acrylate polymers.

The biodegradability of the formulating material is an important aspect of controlled release for environmental applications. Several synthetic and natural poly-

mers used for formulating granules are biodegradable. The delivery of bioactives from controlled-release granules can be enhanced by inclusion of biosurfactants.

Several lignin-based granules have been introduced for controlled-release of several AIs. Lignin is a polyphenolic material that occurs in the cell wall of most terrestrial plants, where it is strongly associated with carbohydrates. It is a polymer produced by random dehydrogenation of a number of phenolic precursors linked to the polysaccharide component of the plant cell. This produces a complex structure without any regular repeating monomer. Lignin is separated from lignocellulosic plants by physical or chemical means.

Several agrochemicals are formulated as granules using lignin, in particular for oil application. The AI is characterized by some physicochemical properties such as moderate sorption on soil components, low volatility, moderate to high melting points, crystallinity and low to moderate water solubility. Such properties make them compatible with alkali lignins for preparing matrices by melting the components together. This produces a glassy matrix upon cooling.

The compatibility of a lignin and an agrochemical can be assessed by observing a film of the melt mixture under the microscope for presence of unsolvated lignin particles. Where solvation occurs, the melting point of the agrochemical is depressed and this can be determined using differential scanning calorimetry (DSC). The density of the glassy adhesive matrix is usually lower than that of the lignin and often less than that of the AI. This can be explained by the presence of voids or pores that cannot be observed by microscopy.

The effect of water on the matrix formulation varies according to the agrochemical compatibility with the lignin and the ratio of AI to lignin. With highly compatible AI such as diuron, the surface of the matrix changes from dark brown to dull light brown on exposure to water. With further exposure some swelling occurs and the outer region is very porous. Diffusion of diuron is enhanced compared to that in the unswollen glassy interior. The swelling and water uptake depends to a large extent on the lignin type used.

7.3 Mechanism of controlled release from microparticles

The release of AI from conventional formulations generally follows an exponential decay, i.e. the release rate is proportional to the concentration of the AI remaining in the formulation. This decay follows first order kinetics, which means that the initial concentration in the environment is initially very high (often resulting in an undesirable toxic effect) and decreases rapidly to a low (ineffective) level. In contrast, a controlled-release formulation generally exhibits lower initial concentrations and a longer time before the concentration decreases to an ineffective level. This is schematically illustrated in Fig. 7.1, which clearly shows that when using a conventional formulation several treatments are required for biological control. During these treatments the

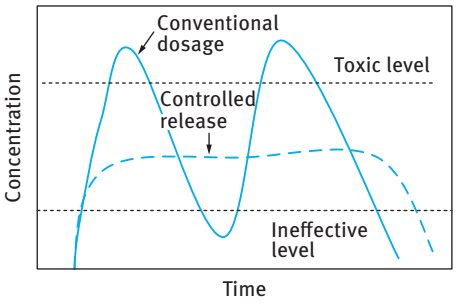

Fig. 7.1: Release of active ingredient from conventional and controlled-release formulations.

AI concentration may reach an undesirable high concentration which is above the toxic limit. In contrast, a controlled-release formulation maintains an effective concentration that is sufficient for bioefficacy without reaching the toxic limit. Thus, with a conventional treatment a higher dose of AI is required to maintain bioefficacy. This dose is significantly reduced when using a controlled-release formulation. The high AI concentrations reached with conventional formulations can also have adverse effects on toxicity of humans, birds, fish, etc.

Most controlled-release systems rely on diffusion of AI through a rate controlling membrane or polymer matrix. Transport through a polymer membrane or matrix occurs by a solution-diffusion process, whereby the AI first dissolves in the polymer and then diffuses across the polymer to the external surface, where the concentration is lower. As discussed before, the process follows Fick's first law of diffusion (equation (7.1)).

The rate of AI release from controlled-release systems can follow a variety of patterns, ranging from first-order (exponential) decay (as with conventional systems) to zero-order kinetics in which the release rate is constant over most of the lifetime of the device. In the latter case the release rate decreases proportionally to the square root of time. A comparison of the release kinetics is shown in Fig. 7.2. As can be clearly seen, the zero-order kinetics (membrane coated reservoir) results in lower peak concentration and more extended release when compared with the case of first order kinetics.

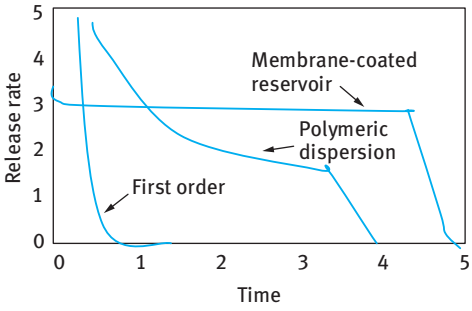

Fig. 7.2: Comparison of release kinetics observed from controlled-release formulations.

As mentioned before, the most common types of controlled-release microparticles are membrane-coated reservoirs and polymeric matrices. A reservoir system consists of a core of pure or saturated AI surrounded by a rate-controlling membrane (polymer shells). The AI is released from the reservoir system by diffusion through the rate-controlling membrane at a constant rate (zero-order kinetics) and this follows Fick's law. For a spherical capsule with outer and inner radii r_2 and r_1 and hence a membrane thickness of $(r_2 - r_1)$, the release rate at time t, $\mathrm{d}M_t/\mathrm{d}t$, is given by the following equation,

$$\frac{\mathrm{d}M_t}{\mathrm{d}t} = 4\pi D \frac{\mathrm{d}c}{\mathrm{d}x} \frac{r_2 r_1}{(r_2 - r_1)}, \tag{7.2}$$

where D is the diffusion coefficient of the AI and $\mathrm{d}c/\mathrm{d}x$ is the concentration gradient within the membrane.

The release rate remains constant as long as D and $\mathrm{d}c/\mathrm{d}x$ remain constant. However, the latter values are temperature dependent and hence the release rate will increase with increasing temperature. In many cases the release rate is doubled for every 10 °C increase in temperature. In addition, $\mathrm{d}c/\mathrm{d}x$ remains constant as long as the activity of the AI remains constant within the reservoir. If the activity of the AI decreases as a result of the release of the chemical, the release rate will decrease.

Another important factor that affects the release rate of membrane-coated reservoir type microparticles is the polydispersity of the system. The release rate from each microparticle may be constant and hence initially the release rate may also be constant. However, with time the release rate may change as a result of polydispersity. The quantity of AI in the microparticle is a function of its volume, i.e. the cube of the radius, but the release rate is a function of the radius. Thus, the duration, which is approximately equal to the mass of the AI divided by the release rate, is a function of the square of the radius. Thus, the smaller microparticles become depleted before the larger ones and this results in a decrease of the overall release rate from a collection of microparticles with different sizes.

It should also be mentioned that to maintain a constant release rate, the membrane must remain intact. In general, large microparticles and those with high loading of AI are more susceptible to rupture, resulting in rapid release.

With matrix type microparticles in which the AI is dispersed or dissolved in a polymeric matrix, the release of the AI occurs by diffusion through the matrix to the surface and hence the process follows Fick's law (equation (7.1)). However, the release kinetics can depend on the quantity of the AI and whether this is dispersed or dissolved in the matrix.

The mechanism of release from lignin matrix granules intended for use in soil and aqueous media is studied by immersing the granule in water under static, stirred or flowing conditions. Granules prepared from various lignin types always show release rates that decrease with time. This is illustrated in Fig. 7.3, which also shows the dependency on lignin type.

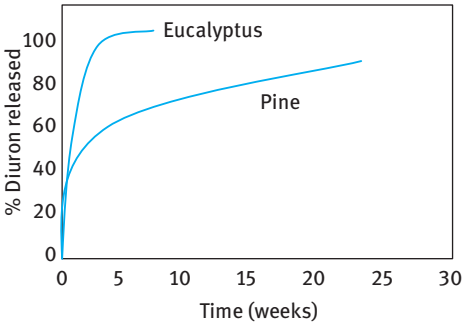

Fig. 7.3: Percentage release of diuron (50 %) from granules based on two different lignin types.

The release kinetics fitted the generalized model [9],

$$\frac{M_t}{M_z} = kt^n + c \tag{7.3}$$

where M_t/M_z is the proportion of AI released at time t, the constant k incorporates the polymer properties, the exponent n characterizes the transport mechanism and c is a constant.

The results of Fig. 7.3 could be fitted to equation (7.3) giving an exponent n ranging from 0.35 to 0.53 indicating that the release is mainly diffusion controlled.

References

[1] Scher HB. Controlled-Release Delivery Systems for Pesticides. New York: Marcel Dekker; 1999.
[2] Kondo A. Microcapsule Processing and Technology. New York: Marcel Dekker; 1979.
[3] Morgan PW, Kvolek SL. J Polym Sci. 1947;2:90.
[4] Bunderberg de Jong HC. Complex Colloid System. In: Ktuyt HR, editor. Colloid Science, Vol. II. Amsterdam: Elsevier; 1949.
[5] Beetsman GB. In: Scher HB, editor. Controlled-Release Delivery Systems for Pesticides. New York: Marcel Dekker; 1999.
[6] Park DJ, Jackson WR, McKinnon IR, Marshall M. In: Scher HB, editor. Controlled-Release Delivery Systems for Pesticides. New York: Marcel Dekker; 1999.
[7] Bahadir M, Pfister G. Controlled Release Formulations of Pesticides. In: Bowers WS, Ebing W, Martin D, editors. Controlled Release, Biochemical Effects of Pesticides and Inhibition of Plant Pathogenic Fungi. Berlin: Springer-Verlag; 1990. p. 1–64.
[8] Woodford AR. Dispersible Granules. In: Van Valkenberg W, Sugavanan B, Khetan SK, editors. Pesticide Formulation. Vienna: UNIDO, New Delhi, India: New Age International (P) Ltd.; 1998. Chapter 9.
[9] Wilkins RM, editor. Controlled Delivery of Crop Protection Agents. London: Taylor and Francis; 1990.

8 Interfacial aspects of agrochemical spray formulations

8.1 Introduction

The discovery and development of effective agrochemicals that can be used with maximum efficiency and minimum risk to the user requires the optimization of their transfer to the target during application. In this way the agrochemical can be used in an effective manner, thus minimizing any waste during application. Optimization of the transfer of the agrochemical to the target requires careful analysis of the steps involved during application. Most agrochemicals are applied as liquid sprays, particularly for foliar application. The spray volume applied ranges from high values of the order of 1000 litres per hectare (whereby the agrochemical concentrate is diluted with water) to ultra-low volumes of the order of 1 litre per hectare (when the agrochemical formulation is applied without dilution). Various spray application techniques are used, of which spraying using hydraulic nozzles is probably the most common. In this case, the agrochemical is applied as spray droplets with a wide spectrum of droplet sizes (usually in the range 100–400 μm in diameter). On application, parameters such as droplet size spectrum, their impaction and adhesion, sliding and retention, wetting and spreading are of prime importance in ensuring maximum capture by the target surface as well as adequate coverage of the target surface. In addition to these "surface chemical" factors, i.e. the interaction with various interfaces, other parameters that affect biological efficacy are deposit formation, penetration and interaction with the site of action. Deposit formation, i.e. the residue left after evaporation of the spray droplets, has a direct effect on the efficacy of the pesticide, since such residues act as "reservoirs" of the agrochemical and hence they control the efficacy of the chemical after application. The penetration of the agrochemical and its interaction with the site of action is very important for systemic compounds. Enhancement of penetration is sometimes crucial to avoid removal of the agrochemical by environmental conditions such as rain and or/wind. All these factors are influenced by surfactants and polymers. In addition, some adjuvants that are used in combination with the formulation consist of oils and/or surfactant mixtures. The role of these adjuvants in enhancing biological efficacy is far from being understood and in most cases they are arrived at by a trial and error procedure.

There are generally two main approaches for the selection of adjuvants:

(i) An interfacial (surface) physicochemical approach that is designed to increase the dose of the agrochemical received by the target plant or insect, i.e. enhancement of spray deposition, wetting, spreading, adhesion and retention.

(ii) Uptake activation enhanced by addition of a surfactant which is the result of specific interactions between the surfactant, the agrochemical and the target species.

https://doi.org/10.1515/9783110578997-009

These interactions may not be related to the intrinsic surface active properties of the surfactant/adjuvant.

The above two approaches must be considered when selecting an adjuvant for a given agrochemical and the type of formulation that is being used. The most important adjuvants are:

(i) Surface active agents.
(ii) Polymers.

In some cases these are used in combination with crop oils (e.g. methyl oleate). Several complex recipes may be used and in many cases the exact composition of an adjuvant is not exactly known.

Adjuvants are applied in two different ways:

(i) Being incorporated in the formulation, mostly the case with flowables (SCs and EWs).
(ii) Used in tank mixtures during application. Such adjuvants can be complex mixtures of several surfactants, oils, polymers, etc.

The choice of an adjuvant depends on:

(i) The nature of the agrochemical, water soluble or insoluble (lipophilic) whereby its solubility and log P values are important.
(ii) The mode of action of the agrochemical, i.e. systemic or nonsystemic, selective or nonselective.
(iii) The type of formulation that is used, i.e. flowable, EC, grain, granule, capsule, etc.

As mentioned above, most important adjuvants are surface active agents of the anionic, nonionic or zwitterionic type. In some cases polymers are added as stickers or anti-drift agents. As mentioned in Chapter 1, the surfactant molecules accumulate at various interfaces as a result of their dual nature. Basically, a surfactant molecule consists of a hydrophobic chain (usually a hydrogenated or fluorinated alkyl or alkyl aryl chain with 8 to 18 carbon atoms) and a hydrophilic group or chain (ionic or polar nonionic such as polyethylene oxide). At the air/water interface (as for spray droplets) and the solid/liquid interface (such as the leaf surface), the hydrophobic group points towards the hydrophobic surface (air or leaf) leaving the hydrophilic group in bulk solution. This results in lowering of the air/liquid surface tension, γ_{LV}, and the solid/liquid interfacial tension, γ_{SL}. As the surfactant concentration is gradually increased both γ_{LV} and γ_{SL} decrease until the critical micelle concentration (cmc) is reached, after which both values remain virtually constant. This situation represents the conditions under equilibrium whereby the rate of adsorption and desorption are the same. The situation under dynamic conditions, such as during spraying, may be more complicated since the rate of adsorption is not equal to the rate of formation of droplets. Above the cmc, micelles are produced, which at low C values are essentially spherical (with an aggregation number in the region of 50–100 monomers). Depending on

the conditions (e.g. temperature, salt concentration, structure of the surfactant molecules) other shapes may be produced, e.g. rod-shaped and lamellar micelles. Since micelles play a vital role when considering adjuvants, it is essential to understand their properties in some detail. As mentioned in Chapter 3, micelle formation is a dynamic process, i.e. a dynamic equilibrium is set up whereby surface active agent molecules are constantly leaving the micelles while others enter the micelles (the same applies to the counterions). The dynamic process of micellization is described by two relaxation processes:

(i) A short relaxation time τ_1 (of the order of 10^{-8}–10^{-3} s) which is the lifetime for a surfactant molecule in a micelle.
(ii) A longer relaxation time τ_2 (of the order of 10^{-3}–1 s) which is a measure of the micellization–dissolution process.

τ_1 and τ_2 depend on the surfactant structure, its chain length and these relaxation times determine some of the important factors in selecting adjuvants, such as the dynamic surface tension (discussed below).

The cmc of nonionic surfactants is usually two orders of magnitude lower than the corresponding anionic of the same alkyl chain length. This explains why nonionics are generally preferred when selecting adjuvants. For a given series of nonionics, with the same alkyl chain length, the cmc decreases with decreasing number of ethylene oxide (EO) units in the chain. Under equilibrium, the γ–log C curves shift to lower values as the EO chain length decreases. However, under dynamic conditions, the situation may be reversed, i.e. the dynamic surface tensions could become lower for the surfactant with the longer EO chain. This trend is understandable if one considers the dynamics of micelle formation. The surfactant with the longer EO chain has a higher cmc and it forms smaller micelles when compared with the surfactant containing shorter EO chain. This means that the lifetime of a micelle with a longer EO chain is shorter than that with a shorter EO chain. This explains why the dynamic surface tension of a solution of a surfactant containing longer EO chain can be lower than that of a solution of an analogous surfactant (at the same concentration) with a shorter EO chain.

For a series of anionic surfactants with the same ionic head group, the lifetime of a micelle decreases with decreasing the alkyl chain length of the hydrophobic component. Branching of the alkyl chain could also play an important role in the lifetime of a micelle. It is, therefore, important to carry out dynamic surface tension measurements when selecting a surfactant as an adjuvant as this may play an important role in spray retention.

However, the above measurements should not be taken in isolation as other factors may also play an important role, e.g. solubilization which may require larger micelles. The selection of a surfactant as an adjuvant requires knowledge of the factors involved, which will be discussed in some detail below.

At high surfactant concentrations (usually above 10 %) several liquid crystalline phases are produced as discussed in Chapter 1. Three main types of liquid crystals may be distinguished:

(i) Hexagonal (middle) phase that consists of cylindrical anisotropic units with high viscosity.
(ii) Cubic, body-cantered isotropic phase with a viscosity that is higher than the hexagonal phase.
(iii) Lamellar (neat) phase consisting of sheet-like units that are anisotropic, but with a viscosity that is lower than the hexagonal phase.

The above phases may form during evaporation of a spray drop. In some cases a middle phase is first produced that on further evaporation may produce a cubic phase, which in view of its very high viscosity may entrap the agrochemical. This could be advantageous for some of the systemic fungicides which require "deposits" that act as reservoirs for the chemical. The viscous cubic phases may also enhance the tenacity of the agrochemical particles (particularly with SCs) and hence enhance rain fastness. In some other applications, a lamellar phase is preferred as this provides some mobility (due to its lower viscosity).

The various phases produced by a surfactant can be related to its structure. An important parameter that can be used to predict the phase behaviour of surfactants is the critical packing parameter (CPP), that was described above (CPP = v/la, where v is the volume of the hydrocarbon chain with a length l and a is the cross-sectional area of the hydrophilic head group). For spherical micelles CPP $\leq 1/3$, for cylindrical micelles $1 >$ CPP $> 1/2$ and for lamellar micelles CPP ≈ 1.

Study of the phase behaviour of surfactants (which can be obtained using polarizing microscopy) is crucial in the selection of adjuvants. The interaction of the above units with the agrochemical is crucial in determining performance (e.g. solubilization). Similar interactions may also occur between the above structural units and the leaf surface (wax solubilization).

The application of an agrochemical as a spray involves a number of interfaces, where the interaction with the formulation plays a vital role. The first interface during application is that between the spray solution and the atmosphere (air), which governs the droplet spectrum, rate of evaporation, drift, etc. In this respect, the rate of adsorption of the surfactant and/or polymer at the air/liquid interface is of vital importance. This requires dynamic measurements of parameters such as surface tension which will give information on the rate of adsorption. This subject will be dealt with in the first part of this section. The second interface is that between the impinging droplets and the leaf surface (with insecticides the interaction with the insect surface may be important). The droplets impinging on the surface undergo a number of processes that determine their adhesion and retention and further spreading on the target surface. The rate of evaporation of the droplet and the concentration gradient of the surfactant across the droplet governs the nature of the deposit formed. These

processes of impaction, adhesion, retention, wetting and spreading will be discussed in subsequent parts in this chapter. The interaction with the leaf surface will be described in terms of the various surface forces involved.

8.2 Interactions at the air/solution interface and their effect on droplet formation

In a spraying process, a liquid is forced through an orifice (the spray nozzle) by application of a hydrostatic pressure to form droplets. Before describing what happens in a spraying process, it is beneficial to consider the processes that occur when a drop is formed at various time intervals. If the time of formation of a drop is large (greater say than 1 minute), the volume of the drop depends on the properties of the liquid such as its surface tension and the dimensions of the orifice, but is independent of the time of its formation. However, at shorter times of formation of the drop (less than 1 minute), the drop volume depends on the time of its formation. The loosening of the drop, which occurs when its weight W exceeds the surface force $2\pi r\gamma$ (i.e. $W > 2\pi r\gamma$), progresses at a speed that is determined by the viscosity and surface tension of the liquid. However, during this loosening process the hydrostatic pressure pumps more liquid into the drop and this is represented by a "hump" in the W–t curve. The height of the "hump" increases with increasing viscosity, perhaps because the rate of contraction diminishes as the viscosity rises.

At short t values, W becomes smaller since the liquid in the drop has considerable kinetic energy even before the drop breaks loose. The liquid coming into the drop imparts downward acceleration and this may cause separation before the drop has reached the value given by the equation,

$$W = 2\pi r\gamma f\left(\frac{g\rho r^2}{2\gamma}\right), \tag{8.1}$$

where ρ is the density and r is the radius of the orifice. Equation (8.1) is the familiar equation for calculating the surface or interfacial tension from the drop weight or volume.

When the hydrostatic pressure is raised further, i.e. at even shorter t values than those described above, no separate drops are formed at all and a continuous jet issues from the orifice. Then at even higher hydrostatic pressure, the jet breaks into droplets, the phenomenon usually referred to as spraying. The process of break-up of jets (or liquid sheets) into droplets is the result of surface forces. The surface area and consequently the surface free energy (area × surface tension) of a sphere is smaller than that of a less symmetrical body. Hence small liquid volumes of other shapes tend to give rise to smaller spheres. For example, a liquid cylinder becomes unstable and divides into two smaller droplets as soon as the length of the liquid cylinder is greater than its circumference. This occurs on accidental contraction of the long liquid cylinder.

A prolate spheroid tends to give two spherical drops when the length of the spheroid is greater than 3–9 times its width. A very long cylinder with radius r (for example a jet) tends to divide into drops with a volume equal to $(9/2)\pi r^3$. Since the surface area of two unequal drops is smaller than that of two equal drops with the same total volume, the formation of a polydisperse spray is more probable.

The effect of surfactants and/or polymers on the droplet size spectrum of a spray can be, at a first instant, described in terms of their effect on the surface tension. Since surfactants lower the surface tension of water, one would expect that their presence in the spray solution would result in the formation of smaller droplets. This is similar to the process of emulsification described in Chapter 2. As a result of the low surface tension in the presence of surfactants, the total surface energy of the droplets produced on atomization is lower than that in the absence of surfactants. This implies that less mechanical energy is required to form the droplets when a surfactant is present. This leads to smaller droplets at the same energy input. However, the actual situation is not simple, since one is dealing with a dynamic situation. In a spraying process a fresh liquid surface is continuously being formed. The surface tension of that liquid depends on the relative ratio between the time taken to form the interface and the rate of adsorption of the surfactant from bulk solution to the air/liquid interface. The rate of adsorption of a surfactant molecule depends on its diffusion coefficient and its concentration (see below). Clearly, if the rate of formation of a fresh interface is much faster than the rate of adsorption of the surfactant, the surface tension of the spray liquid will not be far from that of pure water. Alternatively, if the rate of formation of the fresh surface is much slower than that of the rate of adsorption, the surface tension of the spray liquid will be close to that of the equilibrium value of the surface tension. The actual situation is somewhere in between and the rate of formation of a fresh surface is comparable to that of the rate of surfactant adsorption. In this case, the surface tension of the spray liquid will be in between that of a clean surface (pure water) and the equilibrium value of the surface tension which is reached at times larger than that required to produce the jet and the droplets. This shows the importance of the measurement of dynamic surface tension and rate of surfactant adsorption.

The rate of surfactant adsorption may be described by application of Fick's first law. When concentration gradients are set up in the system, or when the system is stirred, then the diffusion to the interface may be expressed in terms of Fick's first law, i.e.,

$$\frac{\mathrm{d}\Gamma}{\mathrm{d}t} = \frac{D}{\delta}\frac{N_\mathrm{A}}{100}C(1-\theta), \tag{8.2}$$

where Γ is the surface excess (number of moles of surfactant adsorbed per unit area), t is the time, D is the diffusion coefficient of the surfactant molecule, δ is the thickness of the diffusion layer, N_A is Avogadro's constant and θ is the fraction of the surface already covered by adsorbed molecules. Equation (8.2) shows that the rate of surfactant diffusion increases with increasing D and C. The diffusion coefficient of a surfactant molecule is inversely proportional to its molecular weight. This implies that shorter

chain surfactant molecules are more effective in reducing the dynamic surface tension. However, the limiting surface tension reached by a surfactant molecule decreases as its chain length increases and hence a compromise is usually made when selecting a surfactant molecule. Usually one chooses a surfactant with a chain length of the order of 12 carbon atoms. In addition, the higher the surfactant chain length, the lower its cmc (see Chapter 1) and hence lower concentrations are required when using a longer chain surfactant molecule. Again, a problem with longer chain surfactants is their high Krafft temperatures (becoming only soluble at temperatures higher than ambient). Thus, an optimum chain length is usually necessary for optimizing the spray droplet spectrum.

As mentioned above, the faster the rate of adsorption of surfactant molecules, the greater the effect on reducing the droplet size. However, with liquid jets there is an important factor that may enhance surfactant adsorption. Addition of surfactants reduces the surface velocity (which is in general lower than the mean velocity of flow of the jet) below that obtained with pure water. This results from surface tension gradients which can be explained as follows. Where the velocity profile is relaxing, the surface is expanding, i.e. it is newly formed, and might even approach the composition and surface tension of pure water. A little further downstream, appreciable adsorption of the surfactant will have occurred, giving rise to a back spreading tendency from this part of the surface in the direction back towards the cleaner surface immediately adjacent to the nozzle. This phenomenon is thus a form of the Marangoni effect (see Chapter 2), which reduces the surface velocity near the nozzle and induces some liquid circulation which accelerates the adsorption of the surfactant molecules by as much as ten times. This effect casts doubt on the use of liquid jets to obtain the rate of adsorption. Indeed, under conditions of jet formation, it is likely that the surface tension approaches its equilibrium value very closely. Thus, one should be careful in using dynamic surface tension values, as for example measured using the maximum bubble pressure method.

The influence of polymeric surfactants on the droplet size spectrum of spray liquids is relatively more complicated since adsorbed polymers at the air/liquid interface produce other effects than simply reducing the surface tension. In addition, polymeric surfactants diffuse very slowly to the interface and it is doubtful if they have an appreciable effect on the dynamic surface tension. In most agrochemical formulations, polymers are used in combination with surfactants and this makes the situation more complicated. Depending on the ratio of polymer to surfactant in the formulation, various effects may be envisaged. If the concentration of the polymer is appreciably greater than the surfactant and interaction between the two components is strong, the resulting "complex" will behave more like a polymer. On the other hand, if the surfactant concentration is appreciably higher than that of the polymer and interaction between the two molecules is still strong, one may end up with polymer–surfactant "complexes" as well as free surfactant molecules. The latter will behave as free molecules and a reduction in the surface tension may be sufficient even under dynamic

conditions. However, the role of the polymer–surfactant "complex" could be similar to that of the free polymer molecules. The latter produce a viscoelastic film at the air-water interface that may modify the droplet spectrum and the adhesion of the droplets to the leaf surface. The situation is far from being understood and fundamental studies are required to evaluate the role of polymer in spray formation and droplet adhesion.

The above discussion is related to the case where a polymeric surfactant is used for the formulation of agrochemicals as discussed in Chapters 1 and 2 on emulsions and suspension concentrates. However, in many agrochemical applications high molecular weight materials such as polyacrylamide, polyethylene oxide or guar gum are sometimes added to the spray solution to reduce drift. It is well known that incorporation of high molecular weight polymers favours the formation of larger drops. The effect can be reached at very low polymer concentrations when the molecular weight of the polymer is fairly high ($> 10^6$). The most likely explanation of how polymers affect the droplet size spectrum is in terms of their viscoelastic behaviour in solution. High molecular weight polymers adopt spatial conformations in bulk solution, depending on their structure and molecular weight. Many flexible polymer molecules adopt a random coil configuration which is characterized by a root mean square radius of gyration, R_G. The latter depends on the molecular weight and the interaction with the solvent. If the polymer is in good solvent conditions, e.g. polyethylene oxide in water, the polymer coil becomes expanded and R_G can reach high values, of the order of several tens of nms. At relatively low polymer concentrations, the polymer coils are separated and the viscosity of the polymer solution increases gradually with increasing its concentration. However, at a critical polymer concentration, to be denoted by C^*, the polymer coils begin to overlap and the solutions show a rapid increase in viscosity with any further increase in the concentration above C^*. This concentration C^* is defined as the onset of the semi-dilute region. C^* decreases with increasing molecular weight of the polymer and at very high molecular weights it can be as low as 0.01 %. Under this condition of polymer coil overlap, the spray jet opposes deformation and this results in the production of larger drops. This phenomenon is applied successfully to reduce drift. Some polymers also produce conformations that approach a rod-like or double helix structure. An example of this is xanthan gum, which is used with many emulsions and suspension concentrates to reduce sedimentation. If the concentration of such polymer is appreciable in the formulation, then even after extensive dilution on spraying (usually by 100 to 200 fold) the concentration of the polymer in the spray solution may be sufficient to cause production of larger drops. This effect may be beneficial if drift is a problem. However, it may be undesirable if relatively small droplets are required for adequate adhesion and coverage. Again, the ultimate effect required depends on the application methods and the mode of action of the agrochemical. Fundamental studies of the various effects are required to arrive at the optimum conditions. The effect of the various surfactants and polymers should be studied in spray application during the formulation of the agrochemical. In most cases, the formulation chemist concentrates on producing the best system that pro-

duces long-term physical stability (shelf life). It is crucial to investigate the effect of the various formulation variables on the droplet spectrum, their adhesion, retention and spreading. In addition, simultaneous investigations should be made on the effect of the various surfactants on the penetration and uptake of the agrochemical.

One of the problems with many anti-drift agents is their shear degradation. At the high shear rates involved in spray nozzles (which may reach several thousand s^{-1}), the polymer chain may degrade into smaller units and this results in considerable reduction of the viscosity. This will have the effect of reducing the anti-drift effect. It is, therefore, essential to choose polymers that are stable to the high shear rates involved in a spraying process.

8.3 Spray impaction and adhesion

When a drop of a liquid impinges on a solid surface, e.g. a leaf, one of several states may arise depending on the conditions. The drop may bounce or undergo fragmentation into two or more droplets which in turn may bounce back and return to the surface with a lower kinetic energy. Alternatively, the drop may adhere to the leaf surface after passing through several stages, where it flattens, retracts, spreads and finally rests to form a hemispherical cap. In some cases, the droplet may not adhere initially but floats as an individual drop for a fraction of a second or even several seconds and can either adhere to the surface or leave it again.

The most important parameters that determine which one of the above mentioned stages is reached are: the mass (volume) of the droplet, its velocity in flight and the distance between the spray nozzle and the target surface, the difference between the surface energy of the droplet in flight, E_0 and its surface energy after impact, E_s, and displacement of air between the droplet and the leaf.

Droplets in the region of 20–50 µm in diameter do not usually undergo reflection if they are able to reach the leaf surface. Such droplets have a low momentum and can only reach the surface if they travel in the direction of the air stream. On the other hand, large droplets of the order of few thousand micrometres in diameter undergo fragmentation. Droplets within the range 100–400 µm, which covers the range produced by most spray nozzles, may be reflected or retained depending on a number of parameters such as the surface tension of the spray solution, surface roughness and elasticity of the drop surface. A study by Brunskill [1] showed that with drops of 250 µm, 100 % adhesion is obtained when the surface tension of the liquid was lowered (using methanol) to 39 N m^{-1}, whereas only 4 % adhesion occurred when the surface tension, γ, was 57 N m^{-1}. For any given spray solution (with a given surface tension), a critical droplet diameter exists below which adhesion is high and above which adhesion is low. The critical droplet diameter increases as the surface tension of the spray solution decreases. The viscosity of the spray solution has only a small effect on the adhesion of large drops, but with small droplets adhesion increases with

increasing viscosity. As expected, the percentage of adhering droplets decreases as the angle of incidence of the target surface increases.

A simple theory for bouncing and droplet adhesion has been formulated by Hartley and Brunskill [2], who considered an ideal case where there are no adhesion (short-range) forces between the liquid and solid substrate and the liquid has zero viscosity. During impaction, the initially spherical droplet will flatten into an oblately spheroidal shape until the increased area has stored the kinetic energy as increased surface energy. This is often followed by an elastic recoil towards the spherical form and later beyond it with the long axis normal to the surface. During this process, energy will be transformed into upward kinetic energy and the drop may leave the surface in a state of oscillation between the spheroidal forms. This sequence was confirmed using high speed flash illumination.

When the reflected droplet leaves in an elastically deformed condition, the coefficient of restitution must be less than unity since part of the translational energy is transformed to vibrational energy. Moreover, the distortion of droplets involves loss of energy as heat by operation of viscous forces. The effect of increasing the viscosity of the liquid is rather complex, but at a very high viscosity liquids usually have a form of elasticity operating during deformations of very short duration. Reduction of deformation as a result of increasing viscosity will affect adhesion.

As mentioned above, the adhesion of droplets is governed by the relative magnitude of the kinetic energy of the droplet in flight and its surface energy as it lands on the leaf surface. Since the kinetic energy is proportional to the third power of the radius (at constant droplet velocity) whereas the surface energy is proportional to the second power of the radius, one would expect that sufficiently small droplets will always adhere. However, this is not always the case since smaller droplets fall with smaller velocities. Indeed, the kinetic energy of sufficiently small drops, in the Stokesian range, falling at their terminal velocity, is proportional to the seventh power of the radius. In the 100–400 μm range, it is nearly proportional to the fourth power of the radius.

Consider a droplet of radius r (sufficiently small for gravity to be neglected) falling onto a solid surface and spreading with an advancing contact angle, θ_A, and having a spherical upper surface of radius R. The surface energy of the droplet in flight, E_0, is given by,

$$E_0 = 4\pi r^2 \gamma_{LA}, \tag{8.3}$$

where γ_{LA} is the liquid/air surface tension.

The surface energy of the spread drop is given by the following equation,

$$E_s = A_1\gamma_{LA} + A_2\gamma_{SL}, -A_2\gamma_{SA} \tag{8.4}$$

where A_1 is the area of the spherical air/liquid interface, A_2 is that of the plane circle of contact with the solid surface, γ_{SL} is the solid/liquid interfacial tension and γ_{SA} that of the solid/air interface.

From Young's equation,

$$\gamma_{SA} = \gamma_{SL} + \gamma_{LA}\cos\theta. \tag{8.5}$$

Therefore, the surface energy of the droplet spreading on the leaf surface is given by the equation,

$$E_s = \gamma_{LA}(A_1 - A_2\cos\theta). \tag{8.6}$$

The volume of a free drop is $(4/3)\pi r^3$, whereas that of the spread drop is $\pi R^3[(1 - \cos\theta) + (1/3)(\cos^3\theta)]$ so that,

$$\frac{4}{3}\pi r^3 = \pi R^3\left[(1-\cos\theta) + \frac{1}{3}(\cos^3\theta - 1)\right], \tag{8.7}$$

and,

$$A_1 = 2\pi R^2(1-\cos\theta), \tag{8.8}$$

$$A_2 = \pi R^2\sin^2\theta. \tag{8.9}$$

Combining equations (8.6)–(8.9) one can obtain the minimum energy barrier between attached and free drop,

$$\frac{E_0 - E_s}{E_0} = 1 - 0.39[2(1-\cos\theta) - \sin^2\theta\cos\theta][1 - \cos\theta + (1/3)(\cos^3\theta - 1]^{-2/3}. \tag{8.10}$$

A plot of $(E_0 - E_s)/E_0$ shows that this ratio decreases rapidly from its value of unity when $\theta = 0$ to a near zero value when $\theta > 160°$. This plot can be used to calculate the critical contact angle required for adhesion of water droplets, with a surface tension $\gamma = 72\,\text{mN m}^{-1}$ at 20 °C, of various sizes and velocities. As an illustration, consider a water droplet of 100 µm diameter falling with its terminal velocity v of $\approx 0.25\,\text{m s}^{-1}$. The kinetic energy of the drop is 1.636×10^{-9} J, whereas its surface energy in flight is 2.26×10^{-9} J. The surface energy of the attached drop at which the kinetic energy is just balanced is 2.244×10^{-9} J. The contact angle at which this occurs can be obtained by calculating the fraction $(E_0 - E_s)/E_0$ and interpolation using the above mentioned plot. This gives $(E_0 - E_s)/E_0 = 0.00723$ and $\theta \approx 160°$. Thus, providing that droplets of this size form an angle that is less than 160°, they will stick to the leaf surface. It is thus not surprising that droplets of this size do not need any surfactant for adhesion. For a 200 µm droplet, with a velocity of $1\,\text{m s}^{-1}$, the critical contact angle is 87° and this shows that in this case surfactants are required for adhesion. The higher the velocity of the drop, the lower the critical contact angle required for adhesion. With larger drops, this critical contact angle becomes smaller and smaller and this clearly shows the importance of surfactants for ensuring drop adhesion.

It should be mentioned, however, that the above calculations are based on "idealized" conditions, i.e. droplets falling on a smooth surface. Deviation is expected when dealing with practical surfaces such as leaf surfaces. The latter are rough, containing leaf hairs and wax crystals that are distributed in different ways depending

on the nature of the leaf and climatic conditions. Under such conditions, the adhesion of droplets may occur at critical contact angle values that are either smaller or larger than those predicted from the above calculations. The critical θ values will certainly be determined by the topography of the leaf surface. As we will see later, the definition and measurement of the contact angle on a rough surface are not straightforward. In spite of these complications, experimental results on droplet adhesion seem to support the predictions from the above simple theory. These experimental results showed little dependence of adhesion of spray droplets on surfactant concentration. Since with most spray systems the contact angles obtained were lower than the critical value for adhesion (except for droplets that are larger the 400 µm), then in most circumstances surfactant addition had only a marginal effect on droplet adhesion. However, one should not forget that the surfactant in the spray solution determines the droplet size spectrum. Also addition of surfactants will certainly affect the adhesion of droplets moving at high velocities and on various plant species. The situation is further complicated by the dynamics of the process, which depends on the nature and concentration of the surfactant added. For fundamental investigations, measurements of the dynamic surface tension and contact angle are required both on model and practical surfaces. These measurements are now easy to perform due to advances in instrumentation such as the maximum bubble pressure method for measuring dynamic surface tension and high speed video equipment for measuring the dynamic contact angle. Such techniques will enable the formulation chemist and the biologist to understand the role and the function of the surfactant in spray solutions.

8.4 Droplet sliding and spray retention

Many agrochemical applications involve high volume sprays, whereby with continuous spraying the volume of the drops continues to grow in size by impaction of more spray droplets upon them and by coalescence with neighbouring drops on the surface. During this process, the amount of spray retained increases steadily, provided the liquid drops which are impacted are also retained. However, on further spraying, the drops continue to grow in size until they reach a critical value above which they begin to slide down the surface and "drop off", the so called "run-off" condition. At the point of "incipient run-off" the volume of the spray retained is a maximum. The retention at this point is governed by the movement of the liquid drops on the solid surface. Bikerman [3] stated that the percentage of droplets sticking to a plant after having touched it should depend upon the tilt of the leaf, the size of the droplets and the contact angle at the plant leaf/droplet/air interface. However, such a process is complicated and governed by many other factors [4] such as droplet spectrum, velocity of impacting droplets, volatility and viscosity of the spray liquid and ambient conditions.

Several authors [4] have tried to relate the resistance to movement of liquid drops on a tilted surface to the surface tension and the contact angles (advancing and receding) of liquid droplets with the solid surface. A detailed analysis was given by Furmidge [4] which is summarized below.

Consider a droplet of mass m on a plane surface that is inclined at an angle α from the horizontal (Fig. 8.1). Due to gravity the droplet will start to slide down with a slow constant velocity. Assuming the droplet has a rectangular plan view (Fig. 8.1), with width ω and it has moved a distance dl, then the work done by the droplet in moving such a distance, W_g, is given by,

$$W_g = mg \sin \alpha. \tag{8.11}$$

The above force is opposed by the surface force resulting from wetting and dewetting of the leaf surface as the droplet slides downwards. In moving down, an area $\omega\, \mathrm{d}l$ of the leaf is wetted by the droplet and a similar area is dewetted by the trailing edge. The work of wetting per unit area of the surface is equal to $\gamma_{LA}(\cos \theta_A + 1)$, whereas that of dewetting is given by $\gamma_{LA}(\cos \theta_R + 1)$, where θ_A and θ_R are the advancing and receding contact angles respectively. Thus the surface force, W_s, is given by,

$$W_s = \gamma_{LA} \omega\, \mathrm{d}l(\cos \theta_R - \cos \theta_A). \tag{8.12}$$

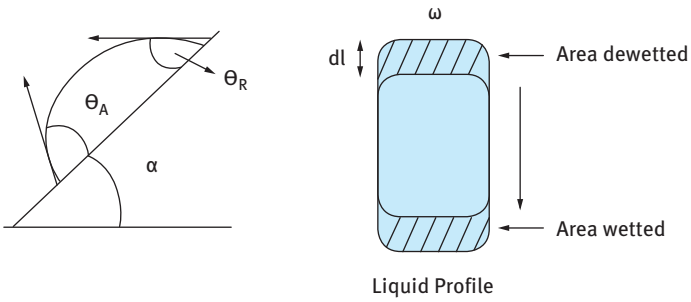

Fig. 8.1: Representation of drop profile on a tilted surface.

At equilibrium, $W_g = W_s$ and,

$$\frac{mg \sin \alpha}{\omega} = \gamma_{LA}(\cos \theta_R - \cos \theta_A). \tag{8.13}$$

If the impaction of the spray is uniform and the spray droplets are reasonably homogeneous in size, the total volume of spray retained in an area L^2 of surface is proportional to the time of spraying until the time when the first droplet runs off the surface. Also, the volume v of spray retained per unit area, R, at the moment of "incipient run-off" is given by,

$$R = \frac{kv}{\omega^2}, \tag{8.14}$$

where k is a constant. Equation (8.14) gives the critical relationship of m/ω for the movement of liquid droplets on a solid surface. As the surface is sprayed, the adhering drops grow in size until the critical value of m/ω is reached and during this period they remain more or less circular in plan form. Since the droplets are small, the deforming effect of gravity may be ignored and they may be regarded as spherical caps whose volume v is given by the expression,

$$v = \frac{\pi(1 - \cos\theta)^2(2 + \cos\theta)\omega^3}{24\sin^3\theta} = \frac{m}{\rho}. \tag{8.15}$$

Combining equations (8.14) and (8.15), it is possible to obtain an expression for ω, the diameter of the adhering droplet in terms of the surface forces given above, i.e. γ_{LA} and θ,

$$\omega = \left[\frac{24\sin^3\theta_A\gamma_{LA}(\cos\theta_R - \cos\theta_A)}{\pi\rho(1 - \cos\theta_A)^2(2 + \cos\theta)g\sin\alpha}\right]^{1/2}. \tag{8.16}$$

Combining equations (8.14)–(8.16), one obtains an expression of spray retention, R, in terms of γ_{LA} and θ, i.e.,

$$R = k\left[\frac{\pi\gamma_{LA}(\cos\theta_R - \cos\theta_A)}{24\rho g\sin\alpha}\right]^{1/2}\left[\frac{(1 - \cos\theta_A)^2(2 + \cos\theta_A)}{\sin^3\theta_A}\right]^{1/2}. \tag{8.17}$$

The value of k depends on the droplet spectrum, since it relates to the rate of build-up of critical droplets and their distribution. However, equation (8.17) does not take into account the flattening effect of the droplet on impact, which results in reduction of θ and increase of ω above the values predicted by equation (8.16). Thus, equation (8.17) is only likely to be valid under conditions of small impaction velocity. In this case, retention is governed by the surface tension of the spray liquid, the difference between θ_A and θ_R (i.e. the contact angle hysteresis) and the value of θ_A.

Equation (8.17) can be further simplified by removing the constant terms and standardizing sin α as equal to 1. A further simplification is to replace the second term between square brackets on the right-hand side of equation (8.17) by θ_M, the arithmetic mean of θ_A and θ_R. In this way a retention factor, F, may be defined by the following simple expression,

$$F = \theta_M\left[\frac{\gamma_{LA}(\cos\theta_R - \cos\theta_A)}{\rho}\right]^{1/2}. \tag{8.18}$$

Equation (8.18) shows that F depends on γ_{LA}, the difference between θ_R and θ_A and θ_M. At any given value of θ_A and γ_{LA}, F increases rapidly with increasing $(\theta_A - \theta_R)$, it reaches a maximum and then decreases. At any given $(\theta_A - \theta_R)$ and γ_{LA}, F increases rapidly with increasing θ_A (and also θ_M). With systems having the same contact angles, F increases with increasing γ_{LA}, but the effect is not very large since $F \propto \gamma_{LA}^{1/2}$. Obviously, any variation in γ_{LA} is accompanied by a change in contact angles and hence one cannot investigate these parameters in isolation. In general, by increasing the surfactant concentration, γ_{LA}, θ_A and θ_R are reduced. The relative extent to which

these three values are affected depends on surfactant nature, its concentration and the surface properties of the leaf. This is a very complex problem and predictions are almost impossible.

It should also be mentioned that the above treatment does not take into account the effect of surface roughness and presence of hairs which play a significant role. A difference in the amount of liquid retained of up to an order of magnitude may be encountered, at constant F value, between say a hairy and a smooth leaf. Besides these large variations in surface properties between leaves of various species, there are also variations within the same species depending on age, environmental conditions and position. However, contact angle measurements on leaf surfaces are not easy and one has to make several measurements and subject the results to statistical analysis. Thus, at best the measured F values can be used as a guideline to compare various surface active agents on leaf surfaces of a particular species that are grown under standard conditions.

Several other factors affect retention, of which droplet size spectrum, droplet velocities and wind speed are probably the most important. Usually, retention increases with a reduction of droplet size, but is significantly reduced at high droplet velocities and wind speeds. The impact velocity effect becomes more marked as the receding contact angle decreases. Wind reduces the volume of spray that can be retained, particularly when θ_A and θ_R are fairly large because little force is required to move the drop along the surface. As θ_A and θ_R become small, the wind effect becomes less significant and it becomes negligible when θ_A and θ_R are close to zero. The leaf structure is also important, since less spray is lost due to wind movements from leaves with a very rough surface when compared with smooth leaves. Thus, care should be taken when results are obtained on plants grown under standard conditions, such as glass houses. These results should not be extrapolated to the field conditions, since plants grown under normal environmental conditions may have surfaces that are vastly different from those grown in glass houses. In order to obtain a realistic picture on spray retention, measurements should be made on field-grown plants and the results obtained may be correlated to those obtained on glass house plants. In this case, it is possible to use glass house plants for the selection of surfactants, if an allowance is made for the difference between the two sets of results.

8.5 Wetting and spreading

Another factor that can affect the biological efficacy of foliar spray application of agrochemicals is the extent to which the liquid wets, spreads and covers the foliage surface. This, in turn, governs the final distribution of the agrochemical over the area to be protected. The optimum degree of coverage in any spray application depends on the mode of action of the agrochemical and the nature of the pest to be controlled. With nonsystemic agrochemicals, the cover required depends on the mobility or loca-

tion of the pest. The more static the pest, the greater is the need for complete coverage on those areas of the plant liable to attack. Under those conditions, good spreading of the liquid spray with maximum coverage is required. On the other hand, satisfactory cover is ensured with systemic agrochemicals provided the spray liquid is brought into contact with those areas of the plant through which the agrochemical is absorbed. Since, as we will see later, high penetration requires high concentration gradients, an optimum situation may be required here, whereby one achieves adequate coverage of those areas where penetration occurs, without too much spreading over the total leaf surface since these usually results in "thin" deposits. These "thin" deposits do not give adequate "reservoirs", which are sometimes essential to maintain a high concentration gradient, thus enhancing penetration. In addition, thick deposits produced from droplets with limited spreading can increase the tenacity of the agrochemical and ensure the longer term protection by the agrochemical. This situation may be required with many systemic fungicides.

Many leaf surfaces represent the most unwettable of most known surfaces. This is due to the predominantly hydrophobic nature of the leaf surface which is usually covered with crystalline wax of straight chain paraffinic alcohols in the range 24–35 carbon atoms. The crystals may be less than 1 μm thick and only few μms apart, giving the surface "micro-roughness" and the "real" area of the surface can be several times the "gross" (apparent) area. When a water drop is placed on a leaf surface, it takes the form of a spherical cap that is characterized by the contact angle θ. From the balance of tensions, one obtains the following expression,

$$\gamma_{SA} = \gamma_{SL} + \gamma_{LA} \cos\theta. \tag{8.19}$$

Equation (8.19) is the familiar Young's equation which applies to a liquid drop on a smooth surface.

Wetting is sometimes simply assessed by the value of the contact angle; the smaller the angle the better the liquid is said to wet the solid. Complete wetting implies a contact angle of zero, whereas complete non-wetting dictates an angle of contact of 180°. However, contact angle measurements are not easy on real surfaces since a great variation in the value is obtained at various locations of the surface. In addition, it is very difficult to obtain an equilibrium value. This is due to the heterogeneity of the surface and its roughness. Thus, in most practical systems such as spray drops on leaf surfaces, the contact angle exhibits hysteresis, i.e. its value depends on the history of the system and varies according to whether the given liquid is tending to advance across or recede from the leaf surface. The limiting angles achieved just prior to movement of the wetting line (or just after movement ceases) are known as the advancing and receding contact angles, θ_A and θ_R, respectively.

For a given system, $\theta_A > \theta_R$ and θ can usually take any value between these two limits without discernible movement of the wetting line. Since smaller angles imply better wetting, it is clear that the contact angle always changes in such a direction as to oppose wetting line movement.

The use of contact angle measurements to assess wetting depends upon equilibrium thermodynamic arguments, which unfortunately is not the real situation. In the practical situation of spraying, the liquid has to displace the air or another fluid attached to the leaf surface and hence measurement of dynamic contact angles, i.e. those associated with moving wetting lines is more appropriate. Such measurements require special equipment such as video cameras and image analysis and they should enable one to obtain a more accurate assessment of wetting by the spray liquid.

As mentioned above, the contact angle often undergoes hysteresis so that θ cannot be defined unambiguously by experiment. This hysteresis is accounted for by surface roughness, surface heterogeneity and metastable configurations. Surface roughness can be taken into account by introducing a term r in Young's equation, where r is the ratio of real to apparent surface area, i.e.,

$$r\gamma_{SA} = r\gamma_{SL} + \gamma_{LA}\cos\theta. \tag{8.20}$$

Thus, the contact angle on a rough surface is given by the expression,

$$\cos\theta = \frac{r(\gamma_{SA} - \gamma_{SL})}{\gamma_{LA}}. \tag{8.21}$$

In other words, the contact angle on a rough surface, θ, is related to that on a smooth surface, θ^0, by the equation,

$$\cos\theta = r\cos\theta^0 \tag{8.22}$$

Equation (8.22) shows that surface roughness increases the magnitude of $\cos\theta^0$, whether its value is positive or negative. If $\theta^0 < 90°$, $\cos\theta^0$ is positive and it becomes more positive as a result of roughness, i.e. $\theta < \theta^0$ or roughness in this case enhances wetting. In contrast, if $\theta^0 > 90°$, $\cos\theta^0$ is negative and roughness increases the negative value of $\cos\theta^0$, i.e. roughness results in $\theta > \theta^0$. This means that if $\theta^0 > 90°$ roughness makes the surface even more difficult to wet.

The influence of surface heterogeneity was analysed by Cassie and Baxter [5]. The possibility of adoption of metastable configurations as a result of surface roughness was suggested by Deryaguin [6]. He considered the wetting line to move in a series of thermodynamically irreversible jumps from one metastable configuration to the next.

Assuming an idealized rough surface consisting of concentric patterns of sinusoidal corrugations, one may relate the apparent contact angle θ to that on a smooth surface θ^0 by the following simple equation,

$$\theta = \theta^0 + \alpha \tag{8.23}$$

where α is the slope of the solid surface at the wetting line. The value of θ is, therefore, dependent on the location of the wetting line and, hence, upon factors such as drop volume and gravitational forces. A model heterogeneous surface may be represented by a series of concentric bands having alternate characteristic contact angles θ' and

θ'', such that $\theta' > \theta''$. A drop of a liquid placed on this type of surface will spread or retract until the wetting line assumes some configuration such that $\theta' > \theta > \theta''$.

In spite of the above complications, measurements of contact angles of spray liquids on leaf surfaces are still most useful in defining the wetting and spreading of the spray. A very useful index for measuring the spreading of a liquid on a solid surface is Harkin's spreading coefficient, S, which is defined by the change in tension when solid/liquid and liquid/air interfaces are replaced by a solid/air interface. In other words, S is the work required to destroy a unit area each of the solid/liquid and liquid/air interfaces while forming a unit area of the solid/air interface, i.e.,

$$S = \gamma_{SA} - (\gamma_{SL} + \gamma_{LA}). \tag{8.24}$$

If S is positive, the liquid will usually spread until it completely wets the solid. If S is negative, the liquid will form a non-zero contact angle. This can be clearly shown if equation (8.24) is combined with Young's equation, i.e.,

$$S = \gamma_{LV}(\cos\theta - 1). \tag{8.25}$$

Clearly if $\theta > 0$, S is negative and this implies only partial wetting. In the limit $\theta = 0$, S is equal to zero and this represents the onset of complete wetting. A positive S implies rapid spreading of the liquid on the solid surface. Indeed by measuring the contact angle only, one can define a spread factor, SF, which is the ratio between the diameter of the area wetted on the leaf, D, and the diameter of the drop d, i.e.,

$$\mathrm{SF} = \frac{D}{d}. \tag{8.26}$$

Provided θ is not too small (> 5°), the spread factor can be calculated from θ, i.e.,

$$\mathrm{SF} = \left[\frac{4\sin^3\theta}{(1-\cos\theta)^2(2+\cos\theta)}\right]^{1/3}. \tag{8.27}$$

A plot of SF versus θ shows a rapid increase in SF when $\theta < 35°$. The most practical method of measuring the spread factor is to apply drops of known volume on the leaf surface using a micro-applicator. By using a tracer material, such as a fluorescent dye, one may be able to measure the spread area directly, using for example image analysis. This area can be converted to an equivalent sphere allowing D to be obtained.

An alternative method of defining wetting and spreading is through measuring the work of adhesion, W_a, which is the work required to separate a unit area of the solid/liquid interface to leave a unit area each of the liquid/air and solid/air respectively, i.e.,

$$W_a = (\gamma_{LA} + \gamma_{SA}) - \gamma_{SL}. \tag{8.28}$$

Again using Young's equation, one obtains the following expression for W_a,

$$W_a = \gamma_{LA}(\cos\theta + 1). \tag{8.29}$$

Another useful concept for assessing the wettability of surfaces is that introduced by Zisman and collaborators [7], namely the critical surface tension of wetting, γ_c. These authors found that for a given surface and a series of related liquids such as n-alkanes, siloxanes or dialkyl ethers, $\cos\theta$ is a reasonably linear function of γ_{LA}. The surface tension at the point where the line cuts the $\cos\theta = 1$ axis is known as the critical surface tension of wetting, γ_c. It is the surface tension of a liquid that would just spread to give complete wetting.

Several authors tried to relate the critical surface tension to the solid/liquid interfacial tension, or at least its dispersion component, γ_S^d. From the above discussion, it is clear that for enhancement of wetting and spreading of liquids on leaf surfaces, one needs to lower the contact angle of the droplets. This is usually achieved by the addition of surfactants, which adsorb at various interfaces and modify the local interfacial tension. Since most leaf surfaces are nonpolar low energy surfaces, increasing surfactant concentration enhances wetting. This explains why most agrochemical formulations contain high concentrations of surfactants to enhance wetting and spreading. However, as we will see later, surfactants play other roles in deposit formation, distribution of the agrochemical on the target surface and enhancement of penetration of the chemical.

Although the role played by a surfactant is complex, these materials sometimes referred to as wetting agents or simply adjuvants need to be carefully selected for the optimization of biological efficacy. To date, surfactants are still selected by the formulation chemist on the basis of a trial and error procedure. However, some guidelines may be applied in such a selection. As discussed in Chapter 2, the HLB system may be initially applied for choosing the most common wetting agents. The latter have HLB numbers between 7 and 9. As discussed in Chapter 1, nonionic surfactants usually have two orders of magnitude lower critical micelle concentrations (cmc) when compared with their ionic counterparts at the same alkyl chain length. Since the limiting value of the surface tension is reached at concentrations above the cmc, it is clear that many nonionic surfactants are more effective as wetting agents since after dilution of the formulation, the concentration of the nonionic surfactant in the spray solution may be higher than its cmc. However, many nonionic surfactants with HLB numbers in the range 7–9 undergo phase separation at high concentrations and/or temperatures. This may limit their incorporation in the formulation at high concentrations. In some cases, addition of a small amount of an ionic surfactant may be beneficial in reducing this phase separation and raising the cloud point of the nonionic surfactant. Thus, many agrochemical formulations contain complex mixtures of surfactants which are carefully arrived at by the formulation chemist. The composition of such mixtures is usually kept confidential.

Another important property of the surfactant that is selected for a given agrochemical is its effect on the leaf structure and the cuticle. Surfactants that cause significant damage to the leaf are described as phytotoxic and in many crops such damage must be avoided. This can sometimes limit the choice, since in some cases the best wetter

may not be the best from the phytotoxicity point of view and a compromise has to be made. This shows that selecting the surfactant can be difficult and requires careful investigation of many surface chemical properties as well as its interaction with the leaf surface and the cuticle. In addition, its effect on deposit formation and penetration of the agrochemical need to be separately investigated.

8.6 Evaporation of spray drops and deposit formation

The object of spraying is often to leave a long-lasting deposit of particulate fungicide or insecticide or a residue able to penetrate the cuticle in the case of systemic pesticides and herbicides or to be transferred locally within the crop by its own slower evaporation. The form of residue left by evaporation of the carrier liquid depends to a large extent on the rate of evaporation and most importantly on the nature and concentration of surfactant and other ingredients in the formulations. Evaporation from a spray drop tends to occur most rapidly near the edges since these receive the necessary heat most rapidly from the air by conduction through the dry surround of the leaf. This results in a higher concentration of surfactant at the edge, causing surface tension gradients and convection (arising from the associated density difference). Surface tension gradients cause a Marangoni effect (see Chapter 5) with liquid circulation within the drop that causes the particles to be preferentially deposited at the edge. Convection within the drop leads to preferential precipitation near the edge because the particles can first become "wedged" between the solid/liquid and liquid/air interface.

The type and composition of the spray deposit depend to a large extent on the type of formulation as well as the concentration and type of dispersing agent (for suspensions) or emulsifier (for emulsifiable concentrates and emulsions). Additives such as wetters, humectants, stickers also affect the nature of the deposit. It should be also mentioned that during evaporation of a spray droplet containing dispersed particles or droplets, these may undergo some physical changes on drying. For example, the solid particles of a suspension may undergo recrystallization forming different shape particles which will affect the final form of the deposit. Both suspension particles and emulsion droplets may also undergo flocculation, coalescence and Ostwald ripening, all of which affect the nature of the deposit. Following such changes during evaporation is not easy and requires special techniques such as microscopy and differential scanning calorimetry.

Another important factor in deposits is the tenacity of the resulting particles or droplets. Strong adhesion between the particles or droplets and the leaf surface is required to prevent removal of these particles or droplets by the rain. The adhesion forces between a particle or droplet are determined by the van der Waals attraction and the area of contact between the particles and the surface. Several other factors may affect adhesion, namely electrostatic attraction, chemical and hydrogen bonding. The area of contact between the particle and the surface is determined by its size

and shape. It is obvious that by reducing the particle size of a suspension, one increases the total area of contact between them and the leaf surface, when compared with coarser particles of the same total mass. The shape of the particle also affects the area of contact. For example, flat or cubic-like particles will have larger areas of contact when compared with needle shaped crystals of the same equivalent volume. Several other factors may affect adhesion such as the water solubility of the agrochemical. In general, the lower the solubility, the greater the rain fastness.

One of the most important factors that affect deposit formation is the phase separation that occurs during evaporation. As discussed in Chapter 1, surfactants form liquid crystalline phases when their concentration exceeds a certain value that depends on the nature of the surfactant, it hydrocarbon chain length and the nature and length of the hydrophilic portion of the molecules. During evaporation, liquid crystals of very high viscosity such as hexagonal or cubic phases may be produced at first. Such highly viscous (and elastic structures) will incorporate any particles or droplets and they act as reservoirs for the chemical. As a result of solubilization of the chemical, penetration and uptake may be enhanced (see below). With further evaporation, the hexagonal and cubic phases may produce lamellar structures with lower viscosity than former phases. Such structures will affect the distribution of particles or droplets in the deposit. Thus, the choice of a particular surfactant for an agrochemical formulation necessitates a study of its phase diagram in order to identify the nature of the liquid crystalline phases that are produced on increasing its concentration. The effect of temperature on the liquid crystalline structures is also important. Liquid crystalline structures "melt" above a critical temperature producing liquid phases that contain micelles. These liquid phases have much lower viscosity and hence the particles or droplets of the agrochemical within these liquid phases become mobile. The temperature at which such melting occurs depends on the structure of the surfactant molecule and hence the choice depends on the mode of action of the agrochemical and the environmental conditions encountered such as temperature and humidity. It should also be mentioned that the liquid crystalline structures will be affected by other additives in the formulation such the antifreeze and electrolytes. In addition, the particles or droplets of the agrochemical may affect the liquid crystalline structures produced and this requires a detailed study of the phase diagram in the presence of the various additives as well as in the presence of the agrochemical. Various methods may be applied for such investigations, such as polarizing microscopy, differential scanning calorimetry and rheology.

8.7 Solubilization and its effect on transport

Solubilization is the incorporation of an insoluble substance (usually referred to as the substrate) into surfactant micelles (the solubilizer). Solubilization may also be referred to the formation of a thermodynamically stable, isotropic solution of a sub-

stance, normally insoluble or slightly soluble in water by the introduction of an additional amphiphilic component or components. Solubilization can be determined by measuring the concentration of the chemical that can be incorporated in a surfactant solution while remaining isotropic, as a function of its concentration. At concentrations below the cmc, the amount of chemical that can be incorporated in the solution increases slightly above its solubility in water. However, just above the cmc, the concentration of the chemical that can be incorporated in the micellar solution increases rapidly with a further increase in surfactant concentration. This rapid increase just above the cmc is usually described as the onset of solubilization. One may differentiate three different locations of the substrate in the micelles. The most common location is in the hydrocarbon core of the micelle. This is particularly the case for a lipophilic nonpolar molecule as is the case with most agrochemicals. Alternatively, the substrate may be incorporated in between the surfactant chains of the micelle, i.e. by co-micellization. This is sometimes referred to as penetration in the palisade layer, in which one may distinguish between deep and short penetration. The third way of incorporation is by simple adsorption on the surface of the micelle. This is particularly the case with polar compounds.

Several factors affect solubilization of which the structure of the surfactant and solubilizate, temperature and addition of electrolyte are probably the most important. Generalizations about the manner in which the structural characteristics of the surfactant affect its solubilizing capacity are complicated by the existence of different solubilization sites within the micelles. For deep penetration within the hydrocarbon core of the micelle, solubilization increases with increasing alkyl chain length of the surfactant. On the other hand, if solubilization occurs in the hydrophilic portion of the surfactant molecules, e.g. its polyethylene oxide chain, then the capacity increases with increasing hydrophilic chain length. The solubilizate structure can also play a major role. For example, polarity and polarizability, chain branching, molecular size and shape and structure have been shown to have various effects. The temperature also has an effect on the extent of micellar solubilization, which is dependent on the structure of the solubilizate and of the surfactant. In most cases, solubilization increases with increasing temperature. This is usually due to the increase of the solubility of the solubilizate and an increase of micellar size with nonionic ethoxylated surfactants. Addition of electrolytes to ionic surfactants usually causes an increase in the micelle size and a reduction in the cmc, and hence an increase in the solubilization capacity. Non-electrolytes that are capable of being incorporated in the micelle, e.g. alcohols, lead to an increase in the micelle size and hence to an increase in solubilization.

As discussed in Chapter 6, microemulsions, which may be considered as swollen micelles, are more effective in solubilization of many agrochemicals. Oil-in-water microemulsions contain a larger hydrocarbon core than surfactant micelles and hence they have larger capacity for solubilizing lipophilic molecules such as agrochemicals. However, with polar compounds O/W microemulsions may not be as

effective as micelles of ethoxylated surfactants in solubilizing the chemical. Thus, one has to be careful in applying microemulsions without knowledge of the interaction between the agrochemical and the various components of the microemulsion system.

The presence of micelles or microemulsions will have significant effects on the biological efficacy of an insoluble pesticide. In the first instance, surfactants will affect the rate of solution of the chemical. Below the cmc, surfactant adsorption can aid wetting of the particles and consequently increases the rate of dissolution of the particles or agglomerates. Above the cmc, the rate of dissolution is affected as a result of solubilization. According to the Noyes–Whitney relation [8], the rate of dissolution is directly related to the surface area of the particles A and the saturation solubility, C_s, i.e.,

$$\frac{dC}{dt} = kA(C_s - C), \tag{8.30}$$

where C is the concentration of the solute.

Higuchi [9] assumed that an equilibrium exists between the solute and solution at the solid/solution interface and that the rate of movement of the solute into the bulk is governed by the diffusion of the free and solubilized solute across a stagnant layer. Thus, the effect of surfactant on the dissolution rate will be related to the dependency of that rate on the diffusion coefficient of the diffusing species and not on their solubilities as suggested by equation (8.30). However, experimental results have not confirmed this hypothesis and it was concluded that the effect of solute solubilization involves more steps than a simple effect on the diffusion coefficient. For example, it has been argued that the presence of surfactants may facilitate the transfer of solute molecules from the crystal surface into solution, since the activation energy of this process was found to be lower in the presence of surfactant than its absence in water. On the other hand, Chan, Evans and Cussler [10] considered a multistage process in which surfactant micelles diffuse to the surface of the crystal, become adsorbed (as hemimicelles) and form mixed micelles with the solubilizate. The latter is dissolved and it diffuses away into bulk solution, removing the solute from the crystal surface. This multistage process, which directly involves surfactant micelles, will probably enhance the dissolution rate.

Apart from the above effect on dissolution rate, surfactant micelles also affect membrane permeability of the solute. Solubilization can, under certain circumstances, help the transport of an insoluble chemical across a membrane. The driving force for transporting the substance through an aqueous system is always the difference in its chemical potential (or to a first approximation to the difference of its relative saturation) between the starting point and its destination. The principal steps involved are dissolution, diffusion or convection in bulk liquid and crossing of a membrane. As mentioned above, solubilization will enhance the diffusion rate by affecting transport away from the boundary layer adjacent to the crystal. It should be mentioned, however, that to enhance transport the solution should remain saturated,

i.e. excess solid particles must be present since an unsaturated solution has a lower activity.

Diffusion in bulk liquid obeys Fick's first law, i.e.,

$$J_D = D\left(\frac{\partial C}{\partial x}\right), \tag{8.31}$$

where J_D is the flux of solute (amount of solute crossing a unit cross section in unit time), D is the diffusion coefficient and $(\partial C/\partial x)$ is the concentration gradient. The presence of the chemical in a micelle will lower D, since the radius of a micelle is obviously greater than that of a single molecule. Since the diffusion coefficient is inversely proportional to the radius of the diffusing particle, D is generally reduced when the molecule is transported by a micelle. Assuming that the volume of the micelle is about 100 times greater than a single molecule, the radius of the micelle will only be about 10 times larger than that of a single molecule. Thus, D will be reduced by about a factor of 10 when the molecule diffuses within a micelle when compared with that of a free molecule. However, the presence of micelles increases the concentration gradient in direct proportionality to the increase in incorporation of the chemical by the micelle. This is because Fick's law involves the absolute concentration gradient which is necessarily small as long as the solubility is small, and not its relative rate. If the saturation is represented by S, Fick's law may be written as,

$$J_D = D \times 100S\left(\frac{\partial \%S}{\partial x}\right), \tag{8.32}$$

where $(\partial \%S/\partial x)$ is the gradient in relative value of S. Equation (8.32) shows that for the same gradient of relative saturation, the flux caused by diffusion is directly proportional to saturation. Hence, solubilization will in general increase transport by diffusion, since it can increase the saturation value by many orders of magnitude (that outweighs the reduction in D).

Solubilization also increases transport by convection since the flux of this process, J_C, is directly proportional to the velocity of the moving liquid and the concentration of the solute C. Moreover, one would expect that solubilization enhances transport through a membrane by an indirect mechanism. Since solubilization reduces the steps involving diffusion and convection in bulk liquid, it permits application of a greater fraction of the total driving force to transport through the membrane. In this way, solubilization accelerates the transport through the membrane, even if the resistance to this step remains unchanged. It should also be mentioned that enhancement of transport as a result of solubilization does not necessarily involve transport of any micelles. The latter are generally too large to pass through membranes.

The above discussion clearly demonstrates the role of surfactant micelles in the transport of agrochemicals. Since the droplets applied to foliage undergo rapid evaporation, the concentration of the surfactant in the spray deposits can reach very high values which allow considerable solubilization of the agrochemical. This will certainly

enhance transport as discussed above. Since the lifetime of a micelle is relatively short, usually less than 1 ms (see Chapter 1), such units break up quickly, releasing their contents near the site of action and produce a large flux by increasing the concentration gradient. However, there have been few systematic investigations to study this effect in more detail and this should certainly be a topic of research in the future.

8.8 Interaction between surfactant, agrochemical and target species

For the selection of adjuvants that can be used for enhancing biological efficacy, one has to consider the specific interactions that may take place between the surfactant, agrochemical and target species. This is usually described in terms of an activation process for uptake of the chemical into the plant. This mechanism is particularly important for systemic agrochemicals.

Several key factors may be identified in the uptake activation process:

(i) In the spray droplet.
(ii) In the deposit formed on the leaf surface.
(iii) In the cuticle before or during penetration.
(iv) In tissues underlying the site of application.

Four main sites were considered by Stock and Holloway [11] for increase of uptake of the agrochemical into a leaf:

(i) On the surface of the cuticle.
(ii) Within the cuticle itself.
(iii) In the outer epidermal wall underneath the cuticle.
(iv) At the cell membrane of internal tissues.

The activator surfactant is initially deposited together with the agrochemical and it can penetrate the cuticle reaching other sites of action and hence the role of the surfactant in the activation process can be very complex. The net effect of surfactant interactions at any of the sites of action is to enhance the mass transfer of an agrochemical from a solid or liquid phase on the outside of the cuticle to the aqueous phase of the internal tissues of the treated leaf. As discussed above, solubilization can play a major role in activating the transport of the agrochemical molecules. With many nonpolar systemic fungicides, which are mostly applied as suspension concentrates, the presence of micelles can enhance the rate of dissolution of the chemical and this results in increased availability of the molecules. It also leads to an increase in the flux as discussed above.

It has been suggested that cuticular wax can be solubilized by surfactant micelles (by the same mechanism of solubilization of the agrochemical). However, no evidence could be presented (for example using SEM) to show wax disruption by the micelles.

Schonherr [12] suggested that the surfactants interact with the waxes of the cuticle and thus increase the fluidity of this barrier. This hypothesis is sometimes referred to as wax "plasticization" (similar to the phenomenon of glass transition temperature reduction of polymers by addition of plasticizers). Some measurements of uptake using surfactants with various molecular weights and HLB numbers offered some support for this hypothesis.

Several other mechanisms have been suggested by Stock and Holloway [11] for uptake activation:

(i) Prevention of crystal formation in deposits. It is often assumed that the foliar uptake of an agrochemical from a crystalline deposit will be less than that from an amorphous one.
(ii) Retention of moisture in deposits by humectant action. The humectant theory has arisen mainly from the observation that the uptake of highly soluble chemicals was promoted by high EO surfactants such as Tween 20.
(iii) Promotion of uptake of solutions via stomatal infiltration. This hypothesis stemmed from the observation of rapid uptake of agrochemicals (within the first 10 minutes) when using superwetters such as Silwett L-77, which is capable of reducing the surface tension of water to values as low as 20 mN m^{-1}.

References

[1] Brunskill RT. Proceeding of the Third Weed Conference. Association of British Manufacturers; 1956. p. 593.
[2] Hartley GS, Brunskill RG. Surface phenomena in chemistry and biology. New York: Pergamon Press; 1958. p. 214–223.
[3] Bikerman JJ. Ind Eng Chem. 1940;13:443.
[4] Furmidge CGL. J Colloid Interface Sci. 1962;17:309.
[5] Cassie ABD, Dexter S. Trans Faraday Soc. 1944;40:546.
[6] Deryaguin BV. CR Acad Sci USSR. 1946;51:361.
[7] Zisman WA. Adv Chem Ser. 1964:43.
[8] Attwood D, Florence AT. Surfactant systems. London: Chapman and Hall; 1983.
[9] Higuchi WI. J Pharm Sci. 1964;53:532 and 1967;56:315.
[10] Chan AF, Evans DF, Cussler EL. A J Chem. 1976;22:1006.
[11] Stock D, Hollaway PJ. Pesticide Sci. 1993;37:233.
[12] Schonherr J. Pesticide Sci. 1993;39:213.

Part II: **Colloid and interface science in paints and coatings**

9 General introduction

Paints or surface coatings are complex multiphase colloidal systems that are applied as a continuous layer to a surface [1, 2]. A paint usually contains pigmented materials to distinguish it from clear films that are described as lacquers or varnishes. The main purpose of a paint or surface coating is to provide aesthetic appeal as well as to protect the surface. For example, a motor car paint can enhance the appearance of the car body by providing colour and gloss and it also protects the car body from corrosion.

When considering a paint formulation one must know the specific interaction between the paint components and substrates. This subject is of particular importance when one considers the deposition and adhesion of the components to the substrate. The latter can be wood, plastic, metal, glass, etc. The interaction forces between the paint components and the substrate must be considered when formulating any paint. In addition, the method of application can vary from one substrate and another.

For many applications it has been recognized that to achieve the required property, such as durability, strong adhesion to the substrate, opacity, colour, gloss, mechanical properties, chemical resistance, corrosion protection, etc., requires the application of more than one coat. The first two or three coats coat (referred to as the primer and undercoat) are applied to seal the substrate and provide strong adhesion to the substrate. The topcoat provides the aesthetic appeal such as gloss, colour, smoothness, etc. This clearly explains the complexity of paint systems which require fundamental understanding of the processes involved, such as particle-surface adhesion, colloidal interaction between the various components, mechanical strength of each coating, etc.

Most paint formulations consist of disperse systems (solid-in-liquid dispersions). The disperse phase consists of primary pigment particles (organic or inorganic) which provide the opacity, colour and other optical effects. These are usually in the submicron range. Other coarse particles (mostly inorganic) are used in the primer and undercoat to seal the substrate and enhance adhesion of the top coat. The continuous phase consists of a solution of polymer or resin which provides the basis for a continuous film that seals the surface and protects it from the outside environment. Most modern paints contain latexes which are used as film formers. The latexes are prepared by emulsion and dispersion polymerization, as will be described in Chapter 10. These latexes (with a glass transition temperature mostly below ambient temperature) coalesce on the surface and form a strong and durable film. Other components may be present in the paint formulation such as corrosion inhibitors, driers, fungicides, etc.

In this introductory chapter I will give a brief account of the properties of the main components in a paint formulation, namely the disperse particles and the medium in which they are dispersed (the film formers and the solvent).

The primary pigment particles (normally in the submicron range) are responsible for the opacity, colour and anti-corrosive properties. The principal pigment in use

https://doi.org/10.1515/9783110578997-010

is titanium dioxide, due to its high refractive index, and it is the one that is used to produce white paint. To produce maximum scattering, the particle size distribution of titanium dioxide has to be controlled within a narrow limit. Rutile, with a refractive index of 2.76, is preferred over anatase that has a lower refractive index of 2.55. Thus, the primary pigment particles (normally in the submicron range) are responsible for the opacity, colour and anti-corrosive properties. To produce maximum scattering, the particle size distribution of titanium dioxide has to be controlled: rutile gives the possibility of higher opacity than anatase and it is more resistant to chalking on exterior exposure. To obtain maximum opacity the particle size of rutile should be within 220–140 nm. The surface of rutile is photoactive and it is surface coated with silica and alumina in various proportions to reduce its photoactivity.

Coloured pigments may consist of inorganic or organic particles. For a black pigment one can use carbon black, copper carbonate, manganese dioxide (inorganic) or aniline black (organic). For yellow one can use lead, zinc, chromates, cadmium sulphide, iron oxides (inorganic) or nickel azo yellow (organic). For blue/violet one can use ultramarine, Prussian blue, cobalt blue (inorganic) or phthalocyanin, indanthrone blue, carbazol violet (organic). For red one can use red iron oxide, cadmium selenide, red lead, chrome red (inorganic) or toluidine red, quinacridones (organic).

The colour of a pigment is determined by the selective absorption and reflection of the various wavelengths of visible light (400–700 nm) that impinges on it. For example, a blue pigment appears so because it reflects the blue wavelengths in the incident white light and absorbs the other wavelengths. Black pigments absorb all the wavelengths of incident light almost totally, whereas a white pigment reflects all the visible wavelengths.

The primary shape of pigmented particles is determined by their chemical nature, their crystalline structure (or lack of it) and the way the pigment is created in nature or made synthetically. Pigments as primary particles may be spherical, nodular, needle or rod-like, or plate-like (lamellar). This is illustrated in Fig. 9.1.

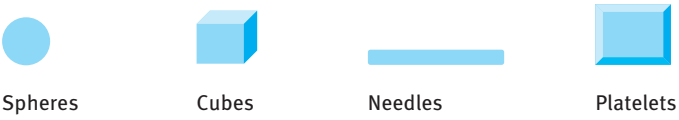

Fig. 9.1: Schematic representation of particle shape.

The pigments are usually supplied in the form of aggregates (where the particles are attached at their faces) or agglomerates (where the particles are attached at their corners). When dispersed in the continuous phase, these aggregates and agglomerates must be dispersed into single units. This requires the use of an effective wetter/dispersant as well as application of mechanical energy. This process of dispersion will be discussed in detail in Chapter 11.

In paint formulations, secondary pigments are also used. These are referred to as extenders, fillers and supplementary pigments. They are relatively cheaper than the primary pigments and they are incorporated in conjunction with the primary pigments for a variety of reasons such as cost effectiveness, enhancement of adhesion, reduction of water permeability, enhancement of corrosion resistance, etc. For example, in primer or undercoat (matt latex paint), coarse particle extenders such as calcium carbonate are added in conjunction with TiO_2 to achieve whiteness and opacity in a matt or semi-matt product. The particle size of extenders ranges from submicron to few tens of microns. Their refractive index is very close to that of the binder and hence they do not contribute to the opacity from light scattering. Most extenders used by the paint industry are naturally occurring materials such as barytes (barium sulphate), chalk (calcium carbonate), gypsum (calcium sulphate) and silicates (silica, clay, talc or mica). However, more recently synthetic polymeric extenders have been designed to replace some of the TiO_2. A good example is spindrift, which consists of polymer beads that consist of spherical particles (up to 30 µm in diameter) that contain submicron air bubbles and a small proportion of TiO_2. The small air bubbles (< 0.1 µm) reduce the effective refractive index of the polymer matrix, thus enhancing the light scattering of TiO_2.

The refractive index (RI) of any material (primary or secondary pigment) is a key to its performance. As is well known, the larger the difference in refractive index between the pigment and the medium in which it is dispersed, the greater the opacity effect. A summary of the refractive indices of various extender and opacifying pigments is given in Tab. 9.1.

Tab. 9.1: Refractive indices (RI) of extenders and opacifying pigments.

Extender pigments	RI	Opacifying white pigments	RI
Calcium carbonate	1.58	Zinc sulphide	1.84
China clay	1.56	Zinc oxide	2.01
Talc	1.55	Zinc sulphide	2.37
Barytes	1.64	TiO_2 anatase	2.55
		TiO_2 rutile	2.76

The refractive index of the medium in which the pigment is dispersed ranges from 1.33 (for water) to 1.4–1.6 (for most film formers). Thus rutile will give the highest opacity, whereas talc and calcium carbonate will be transparent in fully bound surface coatings. Another important fact that affects light scattering is the particle size and hence to obtain the maximum opacity from rutile an optimum particle size of 250 nm is required. This explains the importance of good dispersion of the powder in the liquid that can be achieved by a good wetting/dispersing agent as well as application of sufficient milling efficiency.

For coloured pigments, the refractive index of the pigment in the non-absorbing, or highly reflecting, part of the spectrum affects the performance as an opacifying material. For example, Pigment Yellow 1 and Arylamide Yellow G give lower opacity than Pigment Yellow 34 Lead Chromate. Most suppliers of coloured pigments attempt to increase the opacifying effect by controlling the particle size.

The nature of the pigment's surface plays a very important role in its dispersion in the medium as well as its affinity to the binder. For example, the polarity of the pigment determines its affinity for alkyds, polyesters, acrylic polymers and latexes that are commonly used as film formers. In addition, the nature of the pigment's surface determines its wetting characteristics in the medium in which it is dispersed (which can be aqueous or nonaqueous) as well as the dispersion of the aggregates and agglomerates into single particles. It also affects the overall stability of the liquid paint. Most pigments are surface treated by the manufacturer to achieve optimum performance. As mentioned above, the surface of rutile particles is treated with silica and alumina in various proportions to reduce its photoactivity. If the pigment has to be used in a nonaqueous paint, its surface is also treated with fatty acids and amines to make it hydrophobic for incorporation in an organic medium. This surface treatment enhances the dispersibility of the paint, its opacity and tinting strength, its durability (glass retention, resistance to chalking and colour retention). It can also protect the binder in the paint formulation.

The dispersion of the pigment powder in the continuous medium requires several processes, namely wetting of the external and internal surface of the aggregates and agglomerates, separation of the particles from these aggregates and agglomerates by application of mechanical energy, displacement of occluded air and coating of the particles with the dispersion resin. It is also necessary to stabilize the particles against flocculation, either by electrostatic double layer repulsion and/or steric repulsion. The process of wetting and dispersion of pigments will be described in detail in Chapter 11.

The dispersion medium can be aqueous or nonaqueous depending on application. It consists of a dispersion of the binder in the liquid (which is sometimes referred to as the diluent). The term solvent is frequently used to include liquids that do not dissolve the polymeric binder. Solvents are used in paints to enable the paint to be made and they enable application of the paint to the surface. In most cases the solvent is removed after application by simple evaporation and if the solvent is completely removed from the paint film it should not affect the performance of the paint film. However, in the early life of the film, solvent retention can affect hardness, flexibility and other film properties. In water-based paints, the water may act as a true solvent for some of the components but it should be a nonsolvent for the film former. This is particularly the case with emulsion paints.

With the exception of water, all solvents, diluents and thinners used in surface coatings are organic liquids with low molecular weight. Two types can be distinguished, hydrocarbons (both aliphatic and aromatic) and oxygenated compounds such as ethers, ketones, esters, ether alcohols, etc. Solvents, thinners and diluents

control the flow of the wet paint on the substrate to achieve a satisfactory smooth, even, thin film, which dries in a predetermined time. In most cases mixtures of solvents are used to obtain the optimum condition for paint application. The main factors that must be considered when choosing solvent mixtures are their solvency, viscosity, boiling point, evaporation rate, flash point, chemical nature, odour and toxicity.

The solvent power or solvency of a given liquid or mixture of liquids determines the miscibility of the polymer binder or resin. It also has a big effect on the attraction between particles in a paint formulation. A very useful parameter that describes solvency is the Hildebrand solubility parameter δ [3] which is related to the energy of association of molecules in the liquid phase, in terms of "cohesive energy density". The latter is simply the ratio of the energy required to vaporize 1 cm^3 of liquid ΔE_v to its molar volume V_m. The solubility parameter δ is simply the square root of that ratio,

$$\delta = \left(\frac{\Delta E_v}{V_m} \right). \tag{9.1}$$

Liquids having similar values of δ are miscible, whereas those with significant difference are immiscible. The solubility parameters of liquids can be determined experimentally by measuring the energy of vaporization. For polymers, one can determine the solubility parameter using an empirical approach by contacting the polymer with liquids with various δ values and observing whether or not dissolution occurs. The solubility parameter of the polymer is taken as the average of two δ values for two solvents that appear to dissolve the polymer. A better method is to calculate the solubility parameter from the "molar attraction constant" G of the constituent parts of the molecule [4],

$$\delta = \left(\frac{\rho \sum G}{M} \right), \tag{9.2}$$

where ρ is the density of the polymer and M is its molecular weight.

Hansen [5] extended Hildebrand's concept by considering three components for the solubility parameter: a dispersion component δ_d, a polar component δ_p and a hydrogen bonding component δ_h,

$$\delta^2 = \delta_d^2 + \delta_p^2 + \delta_h^2. \tag{9.3}$$

Values of δ and its components are tabulated in the book by Barton [6].

As mentioned above, the dispersion medium consists of a solvent or diluent and the film former. The latter is also sometimes referred to as a "binder", since it functions by binding the particulate components together and this provides the continuous film- forming portion of the coating. The film former can be a low molecular weight polymer (oleoresinous binder, alkyd, polyurethane, amino resins, epoxide resin, unsaturated polyester), a high molecular weight polymer (nitrocellulose, solution vinyls, solution acrylics), an aqueous latex dispersion (polyvinyl acetate, acrylic or styrene/butadiene) or a nonaqueous polymer dispersion (NAD). In this introductory chapter I will only briefly describe film formers based on polymer solutions. The subject of

polymer latexes and nonaqueous dispersions will be dealt with in Chapter 10. The polymer solution may exist in the form of a fine particle dispersion in a nonsolvent. In some cases the system may be a mixed solution/dispersion, implying that the solution contains both single polymer chains and aggregates of these chains (sometimes referred to as micelles). A striking difference between a polymer that is completely soluble in the medium and that which contains aggregates of that polymer is the viscosity reached in both cases. A polymer that is completely soluble in the medium will show a higher viscosity at a given concentration compared to another polymer (at the same concentration) that produces aggregates. Another important difference is the rapid increase in the solution viscosity with increasing molecular weight for a completely soluble polymer. If the polymer makes aggregates in solution, an increase in molecular weight of the polymer does not show a dramatic increase in viscosity.

The earliest film-forming polymers used in paints were based on natural oils, gums and resins. Modified natural products are based on cellulose derivatives such as nitrocellulose, which is obtained by nitration of cellulose under carefully specified conditions. Organic esters of cellulose such as acetate and butyrate can also be produced. Another class of naturally occurring film formers are those based on vegetable oils and their derived fatty acids (renewable resource materials). Oils used in coatings include linseed oil, soya bean oil, coconut oil and tall oil. When chemically combined into resins, the oil contributes flexibility and with many oils oxidative crosslinking potential. The oil can also be chemically modified, for example hydrogenated castor oil can be combined with alkyd resins to produce some specific properties of the coating.

Another early binder used in paints are the oleoresinous vehicles that are produced by heating together oils and either natural or certain preformed resins, so that the resin dissolves or disperses in the oil portion of the vehicle. However, these oleoresinous vehicles have been replaced later by alkyd resins, which are probably one of the first applications of synthetic polymers in the coating industry. These alkyd resins are polyesters obtained by reaction of vegetable oil triglycerides, polyols (e.g. glycerol) and dibasic acids or their anhydrides. These alkyd resins enhance the mechanical strength, drying speed and durability over and above those obtained using the oleoresinous vehicles. The alkyds have also been modified by replacing part of the dibasic acid with a diisocyanate (such toluene diisocyanate, TDI) to produce greater toughness and quicker drying characteristics.

Another type of binder is based on polyester resins (both saturated and unsaturated). These are typically composed mainly of co-reacted di- or polyhydric alcohols and di- or tri-basic acid or acid anhydride. They have also been modified using silicone to enhance their durability.

More recently, acrylic polymers have been used in paints due to their excellent properties of clarity, strength and chemical and weather resistance. Acrylic polymers refer to systems containing acrylate and methylacrylate esters in their structure along with other vinyl unsaturated compounds. Both thermoplastic and thermosetting sys-

tems can be made, the latter are formulated to include monomers possessing additional functional groups that can further react to give crosslinks following the formation of the initial polymer structure. These acrylic polymers are synthesized by radical polymerization. The main polymer-forming reaction is a chain propagation step which follows an initial initiation process. A variety of chain transfer reactions are possible before chain growth ceases by a termination process.

Radicals produced by transfer, if sufficiently active, can initiate new polymer chains where a monomer is present which is readily polymerized. Radicals produced by chain transfer agents (low molecular weight mercaptans, e.g. primary octyl mercaptan) are designed to initiate new polymer chains. These agents are introduced to control the molecular weight of the polymer.

The monomers used for the preparation of acrylic polymers vary in nature and can generally be classified as "hard" (such as methylmethacrylate, styrene and vinyl acetate) or "soft" (such as ethyl acrylate, butyl acrylate, 2-ethyl hexyl acrylate). Reactive monomers may also have hydroxyl groups (such as hydroxy ethyl acrylate). Acidic monomers such as methacrylic acid are also reactive and may be included in small amounts so that the acid groups may enhance pigment dispersion. Practical coating systems are usually copolymers of "hard" and "soft". The polymer hardness is characterized by its glass transition temperature, T_g. The T_g (K) of the copolymer can be estimated from the T_g of the individual T_g (K) of the homopolymers with weight fractions W_1 and W_2,

$$\frac{1}{T_g} = \frac{W_1}{T_{g1}} + \frac{W_2}{T_{g2}}. \tag{9.4}$$

The vast majority of acrylic polymers consist of random copolymers. By controlling the proportion of "hard" and "soft" monomers and the molecular weight of the final copolymer one arrives at the right property that is required for a given coating. As mentioned above, two types of acrylic resins can be produced, namely thermoplastic and thermosetting. The former find application in automotive topcoats although they suffer from some disadvantages like cracking in cold conditions and this may require a process of plasticization. These problems are overcome by using thermosetting acrylics which improve the chemical and alkali resistance. Also it allows one to use higher solid contents in cheaper solvents. Thermosetting resins can be self-crosslinking or may require a co-reacting polymer or hardener.

In a paint film the pigment particles need to undergo a process of deposition to the surfaces (that is governed by long range forces such as van der Waals attraction and electrical double layer repulsion or attraction). This process of deposition is also affected by polymers (nonionic, anionic or cationic) which can enhance or prevent adhesion. Once the particles reach the surface they have to adhere strongly to the substrate. This process of adhesion is governed by short-range forces (chemical or nonchemical). The same applies to latex particles which also undergo a process of deposition, adhesion and coalescence.

Control of the flow characteristics of paints is essential for their successful application. All paints are complex systems consisting of various components such as pigments, film formers, latexes and rheology modifiers. These components interact with each other and the final formulation becomes non-Newtonian showing complex rheological behaviour. The paint is usually applied in three stages, namely transfer of the paint from the bulk container, transfer of the paint from the applicator (brush or roller) to the surface to form a thin even film and flow-out of film surface, coalescence of polymer particles (latexes) and loss of the medium by evaporation. During each of these processes the flow characteristics of the paint and its time relaxation produce interesting rheological responses. This will be described in Chapter 13.

References

[1] Tadros T. Colloids in paints. Weinheim: Wiley-VCH; 2010.
[2] Lambourne R, editor. Paint and surface coatings: Theory and practice. Chichester: Ellis Horwood; 1987.
[3] Hildebrand JH, Scott R. The solubility of non-electrolytes. 3rd edition. New York: Reindold, 1950.
[4] Hildebrand JH, Scott R. Regular solutions. New Jersey: Prentice Hall, 1962.
[5] Hansen CM. J Paint Technol. 1967;39:505. 1967;39:511. 1967:104.
[6] Barton AFM. Handbook of solubility parameters and other cohesive parameters. New York: CRC Press; 1983.

10 Emulsion, dispersion and suspension polymerization preparation of polymer colloids and their stabilization

10.1 Introduction

As mentioned in Chapter 9, emulsion polymers (latexes) are the most commonly used film formers in the coating industry. This is particularly the case with aqueous emulsion paints that are used for home decoration. These aqueous emulsion paints are applied at room temperature and the latexes coalesce on the substrate forming a thermoplastic film. Sometimes functional polymers are used for crosslinking in the coating system. The polymer particles are typically submicron (0.1–0.5 μm).

Generally speaking, there are three methods for the preparation of polymer dispersions, namely emulsion, dispersion and suspension polymerization. In emulsion polymerization, monomer is emulsified in a nonsolvent, commonly water, usually in the presence of a surfactant. A water-soluble initiator is added, and particles of polymer form and grow in the aqueous medium as the reservoir of the monomer in the emulsified droplets is gradually used up [1]. In dispersion polymerization (which is usually applied for preparation of nonaqueous polymer dispersion, commonly referred to as nonaqueous dispersion polymerization, NAD) monomer, initiator, stabilizer (referred as protective agent) and solvent initially form a homogeneous solution [2]. The polymer particles precipitate when the solubility limit of the polymer is exceeded. The particles continue to grow until the monomer is consumed. In suspension polymerization, the monomer is emulsified in the continuous phase using a surfactant or polymeric suspending agent. The initiator (which is oil soluble) is dissolved in the monomer droplets and the droplets are converted into insoluble particles, but no new particles are formed.

10.2 Emulsion polymerization

As mentioned above, in emulsion polymerization, the monomer, e.g. styrene or methyl methacrylate that is insoluble in the continuous phase, is emulsified using a surfactant that adsorbs at the monomer/water interface [1]. The surfactant micelles in bulk solution solubilize some of the monomer. A water-soluble initiator such as potassium persulphate $K_2S_2O_8$ is added and this decomposes in the aqueous phase forming free radicals that interact with the monomers, forming oligomeric chains. It has long been assumed that nucleation occurs in the "monomer swollen micelles". The reasoning behind this mechanism was the sharp increase in the rate of reaction above the critical micelle concentration and that the number of particles formed and their size depend to

https://doi.org/10.1515/9783110578997-011

a large extent on the nature of the surfactant and its concentration (which determines the number of micelles formed) [3]. However, this mechanism has later been disputed and it was suggested that the presence of micelles means that excess surfactant is available and molecules will readily diffuse to any interface.

The most accepted theory of emulsion polymerization is referred to as the coagulative nucleation theory [4, 5]. A two-step coagulative nucleation model was proposed by Napper and co-workers [4, 5]. In this process the oligomers grow by propagation and this is followed by a termination process in the continuous phase. A random coil is produced which is insoluble in the medium and this produces a precursor oligomer at the θ-point. The precursor particles subsequently grow primarily by coagulation to form true latex particles. Some growth may also occur by further polymerization. The colloidal instability of the precursor particles may arise from their small size, and the slow rate of polymerization can be due to reduced swelling of the particles by the hydrophilic monomer [4, 5]. The role of surfactants in these processes is crucial, since they determine the stabilizing efficiency and the effectiveness of the surface active agent ultimately determines the number of particles formed. This was confirmed by using surface active agents of different nature. The effectiveness of any surface active agent in stabilizing the particles was the dominant factor and the number of micelles formed was relatively unimportant.

A typical emulsion polymerization formulation contains water, 50 % monomer blended for the required T_g, surfactant (and often colloid), initiator, pH buffer and fungicide. Hard monomers with a high T_g used in emulsion polymerization may be vinyl acetate, methyl methacrylate and styrene. Soft monomers with a low T_g include butyl acrylate, 2-ethylhexyl acrylate, vinyl versatate and maleate esters. Most suitable monomers are those with low, but not too low, water solubility. Other monomers such as acrylic acid, methacrylic acid, and adhesion promoting monomers may be included in the formulation. It is important that the latex particles coalesce as the diluent evaporates. The minimum film-forming temperature (MFFT) of the paint is a characteristic of the paint system. It is closely related to the T_g of the polymer, but the latter can be affected by materials present such as surfactant and the inhomogeneity of the polymer composition at the surface. High T_g polymers will not coalesce at room temperature and in this case a plasticizer ("coalescing agent") such as benzyl alcohol is incorporated in the formulation to reduce the T_g of the polymer, thus reducing the MFFT of the paint. Clearly, for any paint system one must determine the MFFT since, as mentioned above, the T_g of the polymer is greatly affected by the ingredients in the paint formulation.

Several types of surfactants can be used in emulsion polymerization and a summary of the various classes is given in Tab. 10.1.

The role of surfactants is two-fold, firstly to provide a locus for the monomer to polymerize and secondly to stabilize the polymer particles as they form. In addition, surfactants aggregate to form micelles (above the critical micelle concentration) and these can solubilize the monomers. In most cases a mixture of anionic and nonionic

Tab. 10.1: Surfactants used in emulsion polymerization.

Anionic – Carboxylates: $C_nH_{2n+1}COO^-X$ – Sulphates: $C_nH_{2n+1}OSO_3^-X$ – Sulphonates: $C_nH_{2n+1}SO_3^-X$ – Phosphates: $C_nH_{2n+1}OPO(OH)O^-X$ with n being the range 8–16 atoms and the counter ion X is usually Na^+. Several other anionic surfactants are commercially available such as sulphosuccinates, isethionates and taurates and these are sometimes used for special applications.
Cationic Alkyl trimethyl ammonium chloride, where R contains 8–18 C atoms, e.g. dodecyl trimethyl ammonium chloride, $C_{12}H_{25}(CH_3)_3NCl$.
Zwitterions N-alkyl betaines which are derivatives of trimethyl glycine $(CH_3)_3NCH_2COOH$ (that is described as betaine). An example of betaine surfactant is lauryl amido propyl dimethyl betaine $C_{12}H_{25}CON(CH_3)_2CH_2COOH$. These alkyl betaines are sometimes described as alkyl dimethyl glycinates.
Nonionic Alcohol ethoxylates, alkyl phenol ethoxylates, fatty acid ethoxylates, monoalkaolamide ethoxylates, sorbitan ester ethoxylates, fatty amine ethoxylates and ethylene oxide–propylene oxide copolymers (sometimes referred to as polymeric surfactants). Multihydroxy products such as glycol esters, glycerol (and polyglycerol) esters, glucosides (and polyglucosides), sucrose esters. Amine oxides and sulphinyl surfactants (nonionics with a small head group).

surfactant is used for optimum preparation of polymer latexes. Cationic surfactants are seldom used, except for some specific applications where a positive charge is required on the surface of the polymer particles.

In addition to surfactants, most latex preparations require the addition of a polymer (sometimes referred to as "protective colloid") such as partially hydrolysed polyvinyl acetate (commercially referred to as polyvinyl alcohol, PVA), hydroxyethyl cellulose or a block copolymer of polyethylene oxide (PEO) and polypropylene oxide (PPO). These polymers can be supplied with various molecular weights or proportions of PEO and PPO. When used in emulsion polymerization they can be grafted by the growing chain of the polymer being formed. They assist in controlling the particle size of the latex, enhancing the stability of the polymer dispersion and controlling the rheology of the final paint.

A typical emulsion polymerization process involves two stages known as the seed stage and the feed stage. In the seed stage, an aqueous charge of water, surfactant, and colloid is raised to the reaction temperature (85–90 °C) and 5–10 % of the monomer mixture is added along with a proportion of the initiator (a water-soluble persulphate). In this seed stage, the formulation contains monomer droplets stabilized by surfactant, a small amount of monomer in solution as well as surfactant monomers and

micelles. Radicals are formed in solution from the breakdown of the initiator and these radicals polymerize the small amount of monomer in solution. These oligomeric chains will grow to some critical size, the length of which depends on the solubility of the monomer in water. The oligomers build up to a limiting concentration and this is followed by a precipitous formation of aggregates (seeds), a process similar to micelle formation, except in this case the aggregation process is irreversible (unlike surfactant micelles which are in dynamic equilibrium with monomers).

In the feed stage, the remaining monomer and initiator are fed together and the monomer droplets become emulsified by the surfactant remaining in solution (or by extra addition of surfactant). Polymerization proceeds as the monomer diffuses from the droplets, through the water phase, into the already forming growing particles. At the same time, radicals enter the monomer-swollen particles causing both termination and re-initiation of polymerization. As the particles grow the remaining surfactant from the water phase is adsorbed onto the surface of particles to stabilize the polymer particles. The stabilization mechanism involves both electrostatic and steric repulsion. The final stage of polymerization may include a further shot of initiator to complete the conversion.

According to the theory of Smith and Ewart [3] of the kinetics of emulsion polymerization, the rate of propagation R_p is related to the number of particles N formed in a reaction by the equation,

$$-\frac{d[M]}{dt} = R_p k_p N n_{av}[M], \tag{10.1}$$

where $[M]$ is the monomer concentration in the particles, k_p is the propagation rate constant and n_{av} is the average number of radicals per particle.

According to equation (10.1), the rate of polymerization and the number of particles are directly related to each other, i.e. an increase in the number of particles will increase the rate. This has been found for many polymerizations, although there are some exceptions. The number of particles is related to the surfactant concentration $[S]$ by the equation [3],

$$N \approx [S]^{3/5}. \tag{10.2}$$

Using the coagulative nucleation model, Napper et al. [4, 5] found that the final particle number increases with increasing surfactant concentration with a monotonically diminishing exponent. The slope of $d(\log N_c)/d(\log t)$ varies from 0.4 to 1.2. At high surfactant concentration, the nucleation time will be long in duration since the new precursor particles will be readily stabilized. As a result, more latex particles are formed and eventually will outnumber the very small precursor particles at long times. The precursor/particle collisions will become more frequent and fewer latex particles are produced. The dN_c/dt will approach zero and at long times the number of latex particles remains constant. This shows the inadequacy of the Smith–Ewart theory which predicts a constant exponent (3/5) at all surfactant concentrations. For this reason, the coagulative nucleation mechanism has now been accepted as the most probable

theory for emulsion polymerization. In all cases, the nature and concentration of surfactant used is very crucial and this is very important in the industrial preparation of latex systems.

Most reports on emulsion polymerization have been limited to commercially available surfactants, which in many cases are relatively simple molecules such as sodium dodecyl sulphate and simple nonionic surfactants. However, studies on the effect of surfactant structure on latex formation have revealed the importance of the structure of the molecule. Block and graft copolymers (polymeric surfactants) are expected to be better stabilizers when compared to simple surfactants. The use of these polymeric surfactants in emulsion polymerization and the stabilization of the resulting polymer particles are discussed below.

Several block copolymers are used as stabilizers in emulsion polymerization. Most aqueous emulsion and dispersion polymerization reported in the literature are based on a few commercial products with a broad molecular weight distribution and varying block composition. The results obtained from these studies could not establish what effect the structural features of the block copolymer has on their stabilizing ability and effectiveness in polymerization. Fortunately, model block copolymers with well-defined structures could be synthesized and their role in emulsion polymerization has been investigated using model polymers and model latexes.

A series of well-defined A–B block copolymers of polystyrene-block–polyethylene oxide (PS–PEO) were synthesized [6] and used for emulsion polymerization of styrene. These molecules are "ideal" since the polystyrene block is compatible with the polystyrene formed and thus it forms the best anchor chain. The PEO chain (the stabilizing chain) is strongly hydrated with water molecules and it extends into the aqueous phase forming the steric layer necessary for stabilization (see Chapter 12). However, the PEO chain can become dehydrated at high temperature (due to the breaking of hydrogen bonds), thus reducing the effective steric stabilization. Thus emulsion polymerization should be carried out at temperatures well below the theta (θ)-temperature of PEO (see Chapter 12).

Five block copolymers were synthesized [6] with various molecular weights of the PS and PEO blocks. The molecular weight of the polystyrene block and the resulting PS–PEO polymer was determined using gel permeation chromatography. The mole percent of ethylene oxide and the percent of PEO in the block were determined using H^1 NMR spectroscopy. The molecular weight of the blocks varied from M_n = 1000–7000 for PS and M_w = 3000–9000 for PEO. These five block copolymers were used for emulsion polymerization of styrene at 50 °C (well below the θ-temperature of PEO). The results indicated that for efficient anchoring the PS block needs not be more than 10 monomer units. The PEO block should have a $M_w \geq 3000$. However, the ratio of the two blocks is very important; for example if the wt% of PEO is ≤ 3000, the molecule becomes insoluble in water (not sufficiently hydrophilic) and no polymerization could occur when using this block copolymer. In addition, the 50 % PEO block could produce a latex, but it was unstable and coagulated at 35 % conversion.

It became clear from these studies that the % PEO in the block copolymer plays an important role and this should exceed 75 %. However, the overall molecular weight of the block copolymer is also very important. For example, if one uses a PS block with M_n = 7000, the PEO molecular weight have to be 21 000, which is too high and may result in bridging flocculation, unless one prepares a very dilute latex.

Another systematic study of the effect of block copolymer on emulsion polymerization was carried out using block of poly(methylmethacrylate)-block–polyethylene oxide (PMMA–PEO) for the preparation of PMMA latexes. The ratio and molecular weight of PMMA to PEO in the block copolymer was varied. Ten different PMMA–PEO blocks were synthesized [6] with M_n for PMMA varying between 400 and 2500. The M_w of PEO was varied between 750 and 5000. The recipe for MMA polymerization consisted of 100 monomer, 800 g water, 20 g PMMA–PEO block copolymer and 0.5 g potassium persulphate. The polymerization was carried out at 45 °C which is well below the θ-temperature of PEO. The rate of polymerization R_p was calculating by using latex samples drawn from the reaction mixture at various time intervals (the amount of latex was determined gravimetrically). The particle size of each latex was determined by dynamic light scattering (photon correlation spectroscopy, PCS). The number of particles N in each case was calculated from the weight of the latex and the z-average diameter. The results obtained were used to study the effect of the anchoring group PMMA, molecular weight, the effect of PEO molecular weight and the effect of the total molecular weight of the block copolymer. The results are summarized in Tab. 10.2 and 10.3.

The results of the systematic study (Tab. 10.2 and 10.3) of varying the PMMA and PEO block molecular weight, the % PEO in the chain as well as the overall molecular weight clearly show the effect of these factors on the resulting latex. For example, when using a block copolymer with 400 molecular weight of PMMA and 750 molecular weight of PEO (i.e. containing 65 wt% PEO) the resulting latex has fewer particles when compared with the other surfactants. The most dramatic effect was obtained when the PMMA molecular weight was increased to 900 while keeping the PEO molecular

Tab. 10.2: Effect of PMMA and PEO molecular weight in the diblock.

M_n PMMA	M_w PEO	wt% PEO	$R_p \times 10^4$ (mol l^{-1} s)	D (nm)	$N \times 10^{-13}$ (cm^{-3})
400	750	65	1.3	213	1.7
400	2000	83	1.5	103	14.7
400	5000	93	2.4	116	10.3
900	750	46	Unstable latex	—	—
800	2000	71	3.4	92	20.6
800	5000	86	3.2	106	13.5
1300	2000	61	2.4	116	10.3
1200	5000	81	4.6	99	16.6
1900	5000	72	3.4	110	11.4
2500	5000	67	2.2	322	0.4

Tab. 10.3: Effect of total molecular weight of the PMMA–PEO diblock.

M_w	wt% PEO	$R_p \times 10^4$ (mol l^{-1} s)	D (nm)	$N \times 10^{-13}$ (cm^{-3})
1150	65	1.3	213	1.7
2400	83	1.5	103	14.7
2800	71	3.4	92	20.6
3300	61	2.4	99	16.6
6200	81	4.6	99	16.6
6900	72	3.4	110	11.4
7500	67	2.2	322	0.4

weight (750) the same. This block copolymer contains only 46 wt% PEO and it became insoluble in water due to the lack of hydrophilicity. The latex produced was unstable and it collapsed at the early stage of polymerization. The PEO molecular weight of 750 is insufficient to provide effective steric stabilization. By increasing the molecular weight of PEO to 2000 or 5000 while keeping the PMMA molecular weight at 400 or 800 a stable latex was produced with a small particle diameter and large number of particles. The best results were obtained by keeping the molecular weight of PMMA at 800 and that of PEO at 2000. This block copolymer gave the highest conversion rate, the smallest particle diameter and the largest number of particles (see Tab. 10.3). It is interesting to note that by increasing the PEO molecular weight to 5000 while keeping the PMMA molecular weight at 800, the rate of conversion decreased, the average diameter increased and the number of particles decreased when compared with the results obtained using 2000 molecular weight for PEO. It seems that when the PEO molecular weight is increased the hydrophilicity of the molecule increased (86 wt% PEO) and this reduced the efficiency of the copolymer. It seems that by increasing hydrophilicity of the block copolymer and its overall molecular weight, the rate of adsorption of the polymer to the latex particles and its overall adsorption strength may have decreased. The overall molecular weight of the block copolymer and its overall hydrophilicity have a big effect on the latex production (see Tab. 10.3). Increasing the overall molecular weight of the block copolymer above 6200 resulted in a reduction in the rate of conversion, an increase in the particle diameter and a reduction in the number of latex particles. The worst results were obtained with an overall molecular weight of 7500 while reducing the PEO wt%, in which case particles with 322 nm diameter were obtained and the number of latex particles is significantly reduced.

The importance of the affinity of the anchor chain (PMMA) to the latex particles was investigated by using different monomers [6]. For example, when using styrene as the monomer the resulting latex was unstable and it showed the presence of coagulum. This can be attributed to the lack of chemical compatibility of the anchor chain (PMMA) and the polymer to be stabilized, namely polystyrene. This clearly indicates that block copolymers of PMMA–PEO are not suitable for emulsion polymerization of styrene. However, when using vinyl acetate monomer, whereby the resulting

poly(vinyl acetate) latex should have strong affinity to the PMMA anchor, no latex was produced when the reaction was carried out at 45 °C. It was speculated that the water solubility of the vinyl acetate monomer resulted in the formation of oligomeric chain radicals which could exist in solution without nucleation. Polymerization at 60 °C, which did nucleate particles, was found to be controlled by chain transfer of the vinyl acetate radical with the surfactant, resulting in broad molecular weight distributions.

Emulsion polymerization of MMA using triblock copolymers was carried out with PMMA-block–PEO–PMMA using blocks with the same PMMA molecular weight (800 or 900) while varying the PEO molecular weight from 3400 to 14 000 in order to vary the loop size. Although the rate of polymerization was not affected by the loop size, the particles with the smallest diameter were obtained with the 10 000 molecular weight PEO. Comparing the results obtained using the triblock copolymer with those obtained using diblock copolymer (while keeping the PMMA block molecular weight the same) showed the same rate of polymerization. However, the average particle diameter was smaller and the total number of particles larger when using the diblock copolymer. This clearly shows the higher efficacy of the diblock copolymer when compared with the triblock copolymer.

Graft copolymers were also used as stabilizers in emulsion polymerization. The first systematic study of the effect of graft copolymers was carried out by Piirma and Lenzotti [7] who synthesized well characterized graft copolymers with different backbone and side chain lengths. Several grafts of poly(p-methylstyrene)-graft–polyethylene oxide, (PMSt)–$(PEO)_n$, were synthesized and used in styrene emulsion polymerization. Three different PMSt chain lengths (with molecular weight of 750, 2000 and 5000) and three different PEO chain lengths were prepared. In this way the structure of the amphipathic graft copolymer could be changed in three different ways:

(i) three different PEO graft chain lengths;
(ii) three different backbone chain lengths with the same wt% PEO;
(iii) four different wt% PEO grafts.

Piirma and Lenzotti [7] first investigated the graft copolymer concentration required to produce the highest conversion rate, the smallest particle size and the largest number of latex particles. The monomer-to-water ratio was kept at 0.15 to avoid overcrowding of the resulting particles. They found that a concentration of 18 g/100 g monomer (2.7 % aqueous phase) was necessary to obtain the above results, after which a further increase in graft copolymer concentration did not significantly increase the rate of polymerization or increase the number of particles used. Using the graft copolymer concentration of 2.7 % aqueous phase, the results showed an increase in the number of particles with increasing conversion reaching a steady value at about 35 % conversion. Obviously, before that conversion, new particles are still being stabilized from the oligomeric precursor particles, after which all precursor particles are assimilated by the existing particles. The small size of the latex produced, namely 30–40 nm, clearly indicates the efficiency with which this graft copolymer stabilizes the dispersion.

Three different backbone chain lengths of M_n 1140, 4270 and 24 000 were used while the weight percent of PEO (82 %) was kept the same, which is equivalent to 3, 10 and 55 PEO chains per backbone respectively. The results showed that the rate of polymerization, particle diameter and number of particles was similar for the three cases. Since the graft copolymer concentration was the same in each case, it can be concluded that one molecule of the highest molecular graft is just as effective as 18 molecules of the lowest molecular weight graft in stabilizing the particles.

Four graft copolymers were synthesized with a PMSt backbone with M_w = 4540 while increasing the wt% of PEO: 68, 73, 82 and 92 wt% (corresponding to 4.8, 6, 10 and 36 grafts per chain). The results showed a sharp decrease (by more than one order of magnitude) in the number of particles as the wt% of PEO is increased from 82 to 94 %. The reason for this reduction in the number of particles is the increased hydrophilicity of the graft copolymer, which could result in desorption of the molecule from the surface of the particle. In addition, a graft with 36 side chains does not leave enough space for anchoring by the backbone.

The effect of PEO side chain length on emulsion polymerization using graft copolymers was systematically studied by keeping the backbone molecular weight the same (1380) while gradually increasing the PEO molecular weight of the side chains from 750 to 5000. For example, by increasing M_w of PEO from 750 to 2000 while keeping the wt% of PEO roughly the same (84 and 82 wt% respectively) the number of side chains in the graft decreases from 10 to 3. The results showed a decrease in the rate of polymerization as the number of side chains in the graft increases. This is followed by a sharp reduction in the number of particles produced. This clearly shows the importance of spacing of the side chains to ensure anchoring of the graft copolymer to the particle surface, which is stronger with the graft containing a smaller number of side chains. If the number of side chains for the PEO with M_w of 2000 is increased from 3 to 9 (93 wt% of PEO) the rate of polymerization and number of particles decreases. Using a PEO chain with M_w of 5000 (92 wt% PEO) and 3 chains per graft gives the same result as the PEO 2000 with 3 side chains. Any increase in the number of side chains in the graft results in a reduction in the rate of polymerization and the number of latex particles produced. This clearly shows the importance of spacing of the side chains of the graft copolymer.

Similar results were obtained using a graft copolymer of poly(methyl methacrylate-co-2-hydroxypropyl methacrylate)-graft-polyethylene oxide, PMMA(PEO)$_n$, for emulsion polymerization of methyl methacrylate. As with PMSt(PEO)$_n$ graft, the backbone molecular weight had little effect on the rate of polymerization or the number of particles used. The molecular weight of the PEO side chains was varied at constant M_w of the backbone (10 000). Three PEO grafts with M_w of 750, 2000 and 5000 were used. Although the rate of polymerization was similar for the three graft copolymers, the number of particles was significantly lower with the graft containing PEO 750. This shows that this short PEO chain is not sufficient for stabilizing the particles. The overall content of PEO in the graft also has a large effect. Using the

same backbone chain length while changing the wt% of PEO 200, it was found that the molecule containing 67 wt% PEO is not sufficient to stabilize the particles when compared with a graft containing 82 wt% PEO. This shows that a high concentration of PEO in the adsorbed layer is required for effective steric stabilization. The chemical nature of the monomer also plays an important role. For example, stable latexes could be produced using PMSt$(PEO)_n$ graft, but not with PMMA$(PEO)_n$ graft.

More recently, a novel graft copolymer of hydrophobically modified inulin (INUTEC® SP1) has been used in emulsion polymerization of styrene, methyl methacrylate, butyl acrylate and several other monomers [8]. All lattices were prepared by emulsion polymerization using potassium persulphate as initiator. The z-average particle size was determined by photon correlation spectroscopy (PCS) and electron micrographs were also taken.

Emulsion polymerization of styrene or methylmethacrylate showed an optimum weight ratio of (INUTEC)/monomer of 0.0033 for PS and 0.001 for PMMA particles. The (initiator)/(monomer) ratio was kept constant at 0.001 25. The monomer conversion was higher than 85 % in all cases. Latex dispersions of PS reaching 50 % and of PMMA reaching 40 % could be obtained using such low concentration of INUTEC® SP1. Fig. 10.1 shows the variation of particle diameter with monomer concentration.

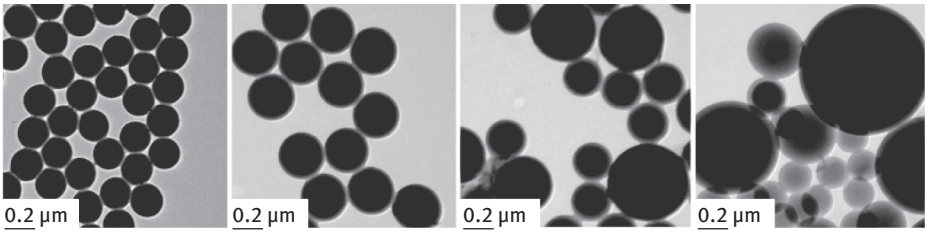

(5 wt%) (10 wt%) (30 wt%) (40 wt%)

(a) PS latexes

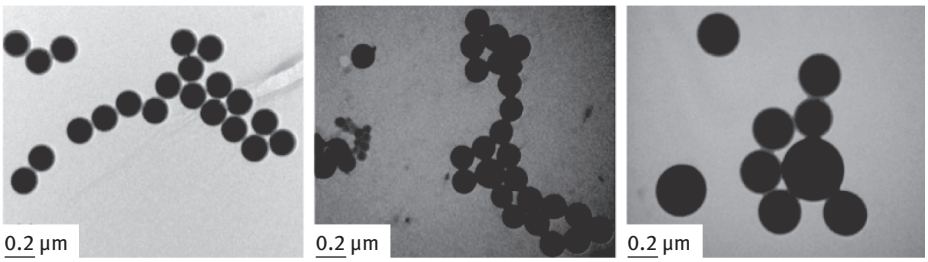

(10 wt%) (20 wt%) (30 wt%)

(b) PMMA Latexes

Fig. 10.1: Electron micrographs of the latexes.

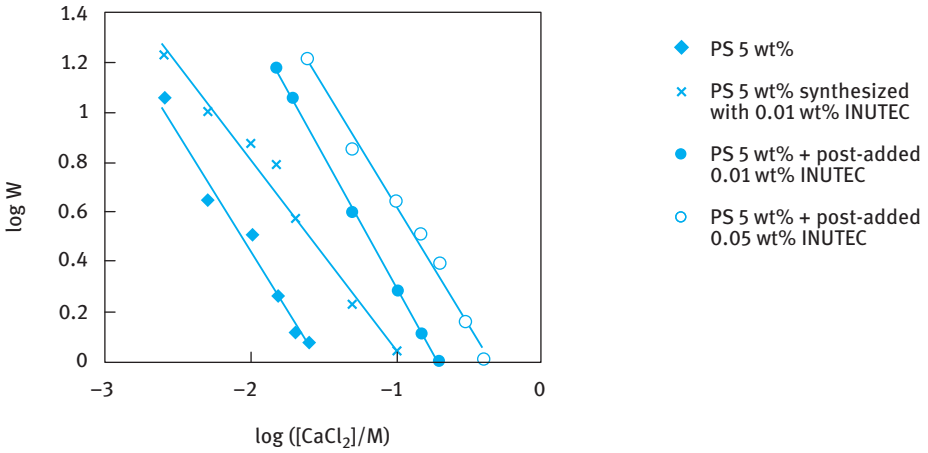

Fig. 10.2: Influence of post addition of INUTEC® SP1 on latex stability.

The stability of the latexes was determined by determining the critical coagulation concentration (CCC) using $CaCl_2$. The CCC was low (0.0175–0.05 mol dm^{-3}) but this was higher than that for the latex prepared without surfactant. Post addition of INUTEC® SP1 resulted in a large increase in the CCC, as illustrated in Fig. 10.2 which shows log W–log C curves (where W is the ratio between the fast flocculation rate constant to the slow flocculation rate constant, referred to as the stability ratio) at various additions of INUTEC® SP1.

As with the emulsions, the high stability of the latex when using INUTEC® SP1 is due to the strong adsorption of the polymeric surfactant on the latex particles and formation of strongly hydrated loops and tails of polyfructose that provide effective steric stabilization. Evidence for the strong repulsion produced when using INUTEC® SP1 was obtained from atomic force microscopy investigations [9] in which the force between hydrophobic glass spheres and a hydrophobic glass plate, both containing an adsorbed layer of INUTEC® SP1, was measured as a function of distance of separation both in water and in the presence of various Na_2SO_4 concentrations. The results are shown in Fig. 10.3 and 10.4.

10.3 Polymeric surfactants for stabilizing preformed latex dispersions

For this purpose, polystyrene (PS) latexes were prepared using the surfactant-free emulsion polymerization. Two latexes with z-average diameter of 427 and 867 (as measured using photon correlation spectroscopy, PCS) that are reasonably monodisperse were prepared [10]. Two polymeric surfactants, namely Hypermer CG-6 and Atlox 4913 (UNIQEMA, UK) were used. Both are graft ("comb") type, consist-

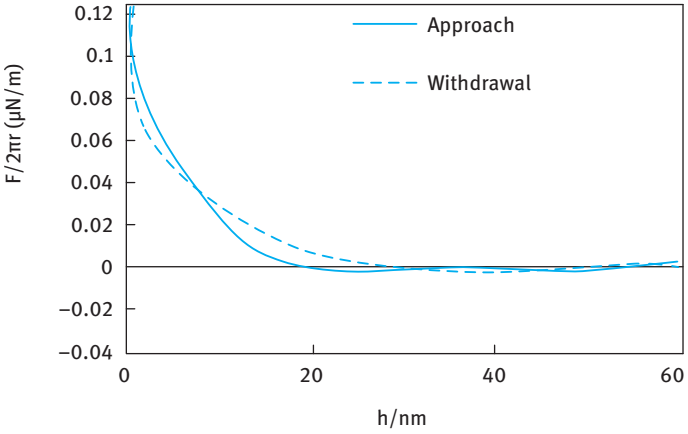

Fig. 10.3: Force–distance curves between hydrophobized glass surfaces containing adsorbed INUTEC® SP1 in water.

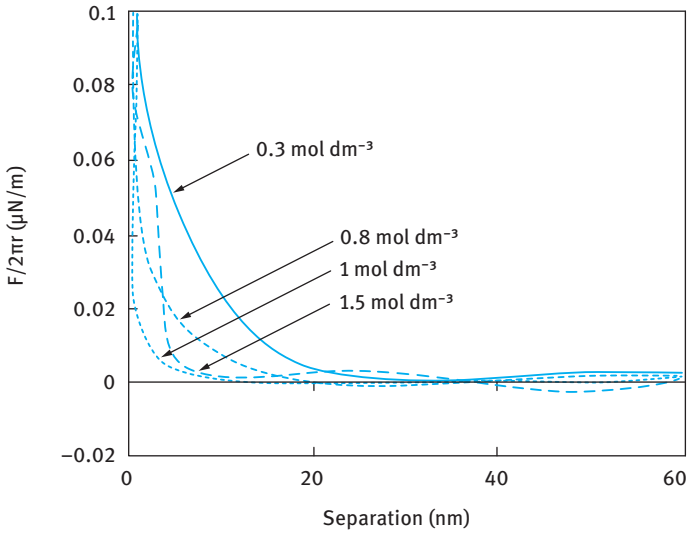

Fig. 10.4: Force–distance curves for hydrophobized glass surfaces containing adsorbed INUTEC® SP1 at various Na_2SO_4 concentrations.

ing of polymethylmethacrylate/polymethacrylic acid (PMMA/PMA) backbone with methoxy-capped polyethylene oxide (PEO) side chains (M = 750 Daltons). Hypermer CG-6 is the same graft copolymer as Atlox 4913 but it contains higher proportion of methacrylic acid in the backbone. The average molecular weight of the polymer is ≈ 5000 Daltons. Fig. 10.5 shows a typical adsorption isotherm of Atlox 4913 on the two latexes. Similar results were obtained for Hypermer CG-6, but the plateau adsorption

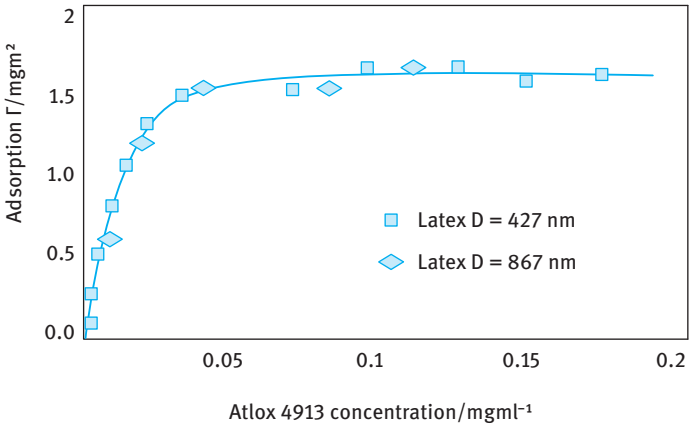

Fig. 10.5: Adsorption isotherms of Atlox 4913 on the two latexes at 25 °C.

was lower (1.2 mg m^{-2} compared with 1.5 mg m^{-2} for Atlox 4913). It is likely that the backbone of Hypermer CG-6 that contains more PMA is more polar and hence less strongly adsorbed. The amount of adsorption was independent of particle size.

The influence of temperature on adsorption is shown in Fig. 10.6. The amount of adsorption increases with increasing temperature. This is due to the poorer solvency of the medium for the PEO chains. The PEO chains become less hydrated at higher temperature and the reduction of solubility of the polymer enhances adsorption.

The adsorbed layer thickness of the graft copolymer on the latexes was determined using rheological measurements. Steady state (shear stress σ–shear rate γ) measurements were carried out and the results were fitted to the Bingham equation to

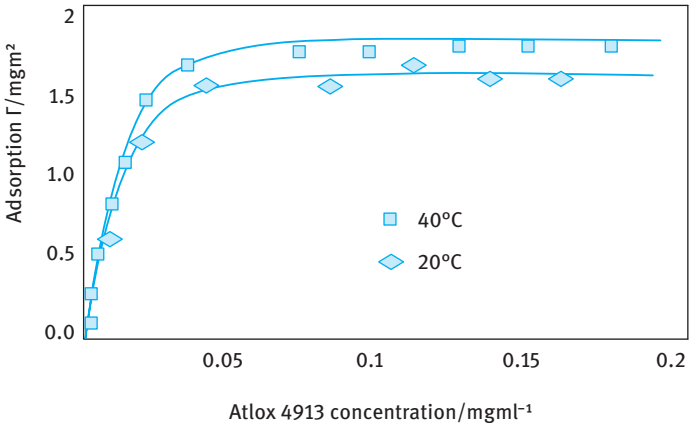

Fig. 10.6: Effect of temperature on adsorption of Atlox 4913 on PS.

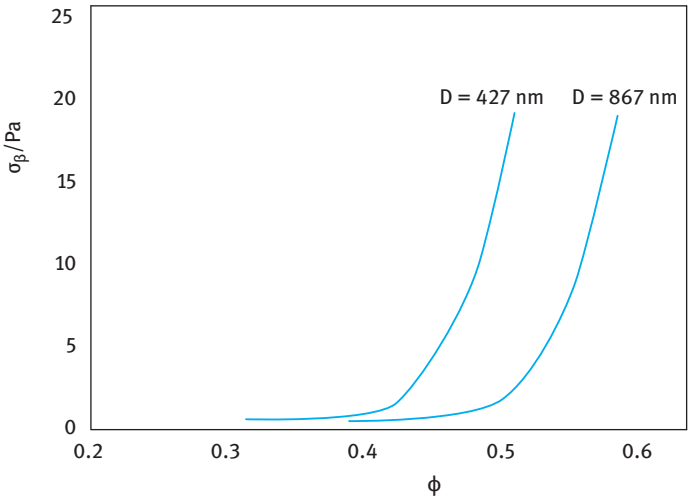

Fig. 10.7: Variation of yield stress with latex volume fraction for Atlox 4913.

obtain the yield value σ_β and the high shear viscosity η of the suspension,

$$\sigma = \sigma_\beta + \eta\dot{\gamma}. \tag{10.3}$$

As an illustration, Fig. 10.7 shows a plot of σ_β versus volume fraction ϕ of the latex for Atlox 4913. Similar results were obtained for latexes stabilized using Hypermer CG-6.

At any given volume fraction, the smaller latex has higher σ_β when compared to the larger latex. This is due to the higher ratio of adsorbed layer thickness to particle radius, Δ/R, for the smaller latex. The effective volume fraction of the latex ϕ_{eff} is related to the core volume fraction ϕ by the equation,

$$\phi_{\text{eff}} = \phi\left[1 + \frac{\Delta}{R}\right]^3. \tag{10.4}$$

ϕ_{eff} can be calculated from the relative viscosity η_{r} using the Dougherty–Krieger equation,

$$\eta_{\text{r}} = \left[1 - \left(\frac{\phi_{\text{eff}}}{\phi_{\text{p}}}\right)\right]^{-[\eta]\phi_{\text{p}}}, \tag{10.5}$$

where ϕ_{p} is the maximum packing fraction.

The maximum packing fraction ϕ_{p} can be calculated using the following empirical equation [10],

$$\frac{(\eta_{\text{r}}^{1/2} - 1)}{\phi} = \left(\frac{1}{\phi_{\text{p}}}\right)(\eta^{1/2} - 1) + 1.25. \tag{10.6}$$

The results showed a gradual decrease of adsorbed layer thickness Δ with increasing the volume fraction ϕ. For the latex with diameter D of 867 nm and Atlox 4913, Δ decreased from 17.5 nm at $\phi = 0.36$ to 6.5 at $\phi = 0.57$. For Hypermer CG-6 with the same

latex, Δ decreased from 11.8 nm at $\phi = 0.49$ to 6.5 at $\phi = 0.57$. The reduction of Δ with increasing ϕ may be due to overlap and/or compression of the adsorbed layers as the particles come close to each other at higher volume fraction of the latex.

The stability of the latexes was determined using viscoelastic measurements. For this purpose, dynamic (oscillatory) measurements were used to obtain the storage modulus G^*, the elastic modulus G' and the viscous modulus G'' as a function of strain amplitude γ_0 and frequency ω (rad s^{-1}). The method relies on the application of a sinusoidal strain or stress and the resulting stress or strain is measured simultaneously. For a viscoelastic system, the strain and stress sine waves oscillate with the same frequency but out of phase. From the time shift Δt and ω, one can obtain the phase angle shift δ.

The ratio of the maximum stress σ_0 to the maximum strain γ_0 gives the complex modulus $|G^*|$

$$|G^*| = \frac{\sigma_0}{\gamma_0}. \tag{10.7}$$

$|G^*|$ can be resolved into two components: Storage (elastic) modulus G', the real component of the complex modulus; loss (viscous) modulus G'', the imaginary component of the complex modulus. The complex modulus can be resolved into G' and G'' using vector analysis and the phase angle shift δ,

$$G' = |G^*| \cos \delta \tag{10.8}$$

$$G'' = |G^*| \sin \delta \tag{10.9}$$

G' is measured as a function of electrolyte concentration and/or temperature to assess the latex stability. As an illustration, Fig. 10.8 shows the variation of G' with temperature for latex stabilized with Atlox 4913 in the absence of any added electrolyte and in the presence of 0.1, 0.2 and 0.3 mol dm^{-3} Na_2SO_4. In the absence of electrolyte, G' showed no change with temperature up to 65 °C.

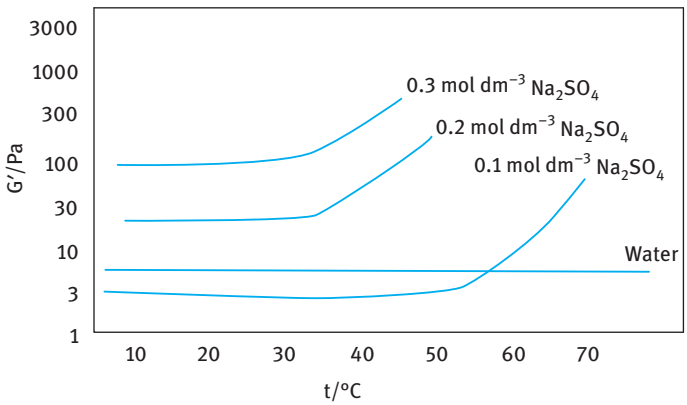

Fig. 10.8: Variation of G' with temperature in water and at various Na_2SO_4 concentrations.

In the presence of 0.1 mol dm^{-3} Na_2SO_4, G' remained constant up to 40 °C above which G' increased with a further increase in temperature. This temperature is denoted as the critical flocculation temperature (CFT). The CFT decreases with increasing electrolyte concentration reaching ≈ 30 °C in 0.2 and 0.3 mol dm^{-3} Na_2SO_4. This reduction in CFT with increasing electrolyte concentration is due to the reduction in solvency of the PEO chains with increasing electrolyte concentrations. The latex stabilized with Hypermer CG-6 gave relatively higher CFT values when compared to that stabilized using Atlox 4913.

10.4 Dispersion polymerization

This method is usually applied for the preparation of nonaqueous latex dispersions and hence it is referred to as NAD. The method has also been adapted to prepare aqueous latex dispersions by using an alcohol-water mixture. In the NAD process the monomer, normally an acrylic, is dissolved in a nonaqueous solvent, normally an aliphatic hydrocarbon, and an oil soluble initiator and a stabilizer (to protect the resulting particles from flocculation, sometimes referred to as "protective colloid") are added to the reaction mixture. The most successful stabilizers used in NAD are block and graft copolymers. These block and graft copolymers are assembled in a variety of ways to provide the molecule with an "anchor chain" and a stabilizing chain. The anchor chain should be sufficiently insoluble in the medium and have a strong affinity to the polymer particles produced. In contrast, the stabilizing chain should be soluble in the medium and strongly solvated by its molecules to provide effective steric stabilization. The length of the anchor and stabilizing chains has to be carefully adjusted to ensure strong adsorption (by multipoint attachment of the anchor chain to the particle surface) and a sufficiently "thick" layer of the stabilizing chain that prevents close approach of the particles to a distance where the van der Waals attraction becomes strong.

Several configurations of block and graft copolymers are possible, as illustrated in Fig. 10.9. Typical preformed graft stabilizers based on poly(12-hydroxy stearic acid) (PHS) are simple to prepare and effective in NAD polymerization. Commercial 12-hydroxystearic acid contains 8–15 % palmitic and stearic acids, which limit the molecular weight during polymerization to an average of 1500–2000. This oligomer may be converted to a "macromonomer" by reacting the carboxylic group with glycidyl methacrylate. The macromonomer is then copolymerized with an equal weight of methyl methacrylate (MMA) or similar monomer to give a "comb" graft copolymer with an average molecular weight of 10 000–20 000. The graft copolymer contains on average 5–10 PHS chains pendent from a polymeric anchor backbone of PMMA. This graft copolymer can stabilize latex particles of various monomers.

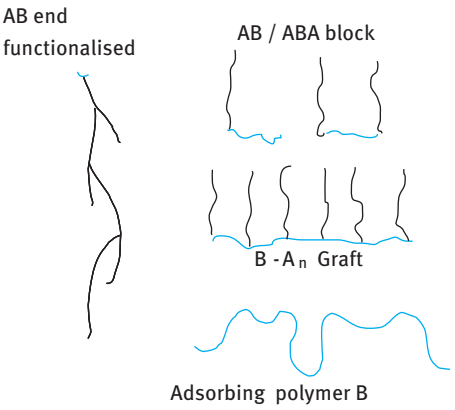

Fig. 10.9: Configurations of block and graft copolymers.

Tab. 10.4: Block and graft copolymers used in dispersion polymerization.

Polymeric surfactant	Continuous phase	Disperse polymer
Polystyrene-block–poly(dimethyl siloxane)	Hexane	Polystyrene
Polystyrene-block–poly(methacrylic acid)	Ethanol	Polystyrene
Polybutadiene-graft–poly(methacrylic acid)	Ethanol	Polystyrene
Poly(2-ethylhexyl acrylate)-graft–poly(vinyl acetate)	Aliphatic hydrocarbon	Poly(methyl methacrylate)
Polystyrene-block–poly(t-butylstyrene)	Aliphatic hydrocarbon	Polystyrene

Several other examples of block and graft copolymers that are used in dispersion polymerization are given in Tab. 10.4 which also shows the continuous phase and disperse polymer that can be used with these polymers.

Two main criteria must be considered in the process of dispersion polymerization:

(i) the insolubility of the formed polymer in the continuous phase;
(ii) the solubility of the monomer and initiator in the continuous phase.

Initially, dispersion polymerization starts as a homogeneous system but after sufficient polymerization, the insolubility of the resulting polymer in the medium forces it to precipitate. Initially, polymer nuclei are produced which then grow to polymer particles. The latter are stabilized against aggregation by the block or graft copolymer that is added to the continuous phase before the process of polymerization starts. It is essential to choose the right block or graft copolymer, which should have a strong anchor chain A and good stabilizing chain B as schematically represented in Fig. 10.8.

Dispersion polymerization may be considered a heterogeneous process which may include emulsion, suspension, precipitation and dispersion polymerization. In dispersion and precipitation polymerization, the initiator must be soluble in the continuous phase, whereas in emulsion and suspension polymerization the initiator is chosen to be soluble in the disperse phase of the monomer. A comparison of the

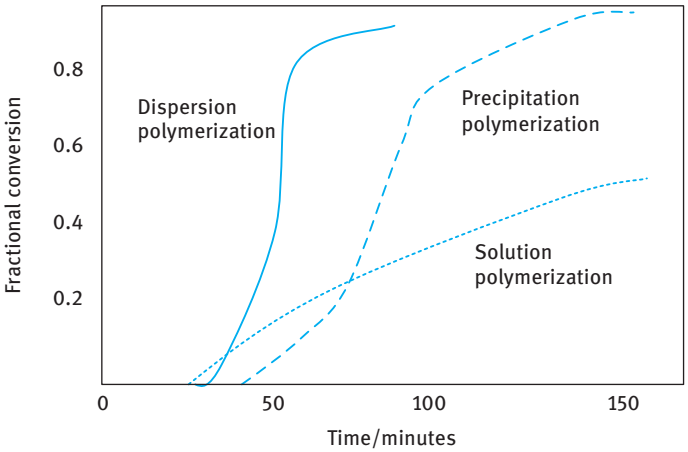

Fig. 10.10: Comparison of rates of polymerization.

rate of polymerization of methylmethacrylate at 80 °C for the three systems was given by Barrett and Thomas [11], as illustrated in Fig. 10.10. The rate of dispersion polymerization is much faster than that of precipitation or solution polymerization. The enhancement of the rate in precipitation polymerization over solution polymerization has been attributed to the hindered termination of the growing polymer radicals.

Several mechanisms have been proposed to explain the mechanism of emulsion polymerization; however, no single mechanism can explain all happenings in emulsion polymerization. Barrett and Thomas [11] suggested that particles are formed in emulsion polymerization by two main steps:

(i) Initiation of monomer in the continuous phase and subsequent growth of the polymer chains until the latter become insoluble. This process clearly depends on the nature of the polymer and medium.
(ii) The growing oligomeric chains associate with each other, forming aggregates which below a certain size are unstable and they become stabilized by the block or graft copolymer added.

As mentioned before, this aggregative nucleation theory cannot explain all happenings in dispersion polymerization. An alternative mechanism based on Napper's theory [2, 3] for aqueous emulsion polymerization can be adapted to the process of dispersion polymerization. This theory includes coagulation of the nuclei formed and not just association of the oligomeric species. The precursor particles (nuclei), being unstable, can undergo one of the following events to become colloidally stable:

(i) homocoagulation, i.e. collision with other precursor particles;
(ii) growth by propagation, adsorption of stabilizer;
(iii) swelling with monomer.

The nucleation terminating events are diffusional capture of oligomers and heterocoagulation.

The number of particles formed in the final latex does not depend on particle nucleation alone, since other steps are involved which determine how many precursor particles created are involved in the formation of a colloidally stable particle. This clearly depends on the effectiveness of the block or graft copolymer used in stabilizing the particles.

In most cases, an increase in polymeric surfactant concentration (at any given monomer amount) results in the production of larger number of particles with smaller size. This is to be expected since the larger number of particles with smaller size (i.e. larger total surface area of the disperse particles) require more polymeric surfactant for their formation. The molecular weight of the polymeric surfactant can also influence the number of particles formed. For example, Dawkins and Taylor [12] found that in dispersion polymerization of styrene in hexane, increasing the molecular weight of the block copolymer of polydimethyl siloxane-block–polystyrene resulted in the formation of smaller particles, which was attributed to the more effective steric stabilization by the higher molecular weight block.

A systematic study of the effect of monomer solubility and concentration in the continuous phase was carried out by Antl and co-workers [13]. Dispersion polymerization of methyl methacrylate in hexane mixed with a high boiling point aliphatic hydrocarbon was investigated using poly(12-hydoxystyearic acid)–glycidyl methacrylate block copolymer. They found that the methyl methacrylate concentration had a drastic effect on the size of the particles produced. When the monomer concentration was kept below 8.5 %, very small particles (80 nm) were produced and these remained very stable. However, between 8.5 and 35 % monomer the latex produced was initially stable but flocculated during polymerization. An increase in monomer concentration from 35 to 50 % results in the formation of a stable latex, but the particle size increased sharply from 180 nm to 2.6 μm as the monomer concentration increased. The authors suggested that the final particle size and stability of the latex are strongly affected by increased monomer concentration in the continuous phase. The presence of monomer in the continuous phase increases the solvency of the medium for the polymer formed. In a good solvent for the polymer, the growing chain is capable of reaching higher molecular weight before it is forced to phase separate and precipitate.

NAD polymerization is carried in two steps:

(i) Seed stage: the diluent, portion of the monomer, portion of dispersant and initiator (azo or peroxy type) are heated to form an initial low-concentration fine dispersion.
(ii) Growth stage: the remaining monomer together with more dispersant and initiator are then fed over the course of several hours to complete the growth of the particles.

A small amount of transfer agent is usually added to control the molecular weight. Excellent control of particle size is achieved by proper choice of the designed dispersant and correct distribution of dispersant between the seed and growth stages. NAD acrylic polymers are applied in automotive thermosetting polymers and hydroxy monomers may be included in the monomer blend used.

Two main factors must be considered when considering the long-term stability of a nonaqueous polymer dispersion. The first and very important factor is the nature of the "anchor chain" A. As mentioned above, this should have a strong affinity to the produced latex and in most cases it can be designed to be "chemically" attached to the polymer surface. Once this criterion is satisfied, the second and important factor in determining the stability is the solvency of the medium for the stabilizing chain B. As will be discussed in detail, the solvency of the medium is characterized by the Flory–Huggins interaction parameter χ. Three main conditions can be identified: $\chi < 0.5$ (good solvent for the stabilizing chain); $\chi > 0.5$ (poor solvent for the stabilizing chain); and $\chi = 0.5$ (referred to as the θ-solvent). Clearly, to maintain stability of the latex dispersion, the solvent must be better than a θ-solvent. The solvency of the medium for the B chain is affected by addition of a nonsolvent and/or temperature changes. It is, therefore, essential to determine the critical volume fraction (CFV) of a nonsolvent above which flocculation (sometimes referred to as incipient flocculation) occurs. One should also determine the critical flocculation temperature at any given solvent composition, below which flocculation occurs. The correlation between CFV or CFT and the flocculation of the nonaqueous polymer dispersion has been demonstrated by Napper [14], who investigated the flocculation of poly(methyl methacrylate) dispersions stabilized by poly(12-hydroxy stearic acid) or poly(n-lauryl methacrylate-co-glycidyl methacrylate) in hexane by adding a nonsolvent such as ethanol or propanol and cooling the dispersion. The dispersions remained stable until the addition of ethanol transformed the medium to a θ-solvent for the stabilizing chains in solution. However, flocculation did occur under conditions of slightly better than θ-solvent for the chains. The same was found for the CFT, which was 5–15 K above the θ-temperature. This difference was accounted for by the polydispersity of the polymer chains. The θ-condition is usually determined by cloud point measurements and the least soluble component will precipitate first giving values that are lower than the CFV or higher than the CFT.

The process of dispersion polymerization has been applied in many cases using completely polar solvents such as alcohol or alcohol-water mixtures [15, 16]. The results obtained showed completely different behaviour when compared with dispersion polymerization in nonpolar media. For example, results obtained by Lok and Ober [15] using styrene as monomer and hydroxypropyl cellulose as stabilizer, showed a linear increase of particle diameter with increasing weight percent of the monomer. There was no region in monomer concentration where instability occurred (as has been observed for the dispersion polymerization of methyl methacrylate in aliphatic hydrocarbons). Replacing water in the continuous phase with 2-methoxyethanol, Lok

and Ober were able to grow large, monodisperse particles up to 15 μm in diameter. They concluded from these results that the polarity of the medium is the controlling factor in the formation of particles and their final size. The authors suggested a mechanism in which the polymeric surfactant molecule grafts to the polystyrene chain, forming a physically anchored stabilizer (nuclei). These nuclei grow to form the polymer particles. Paine [16] carried out dispersion polymerization of styrene by systematically increasing the alcohol chain length from methanol to octadecanol and using hydroxypropyl cellulose as stabilizer. The results showed an increase in particle diameter with increasing number of carbon atoms in the alcohol, reaching a maximum when hexanol was used as the medium, after which there was a sharp decrease in the particle diameter with a further increase in the number of carbon atoms in the alcohol. Paine explained his results in terms of the solubility parameter of the dispersion medium. The largest particles are produced when the solubility parameter of the medium is closest to those of styrene and hydroxypropyl cellulose.

References

[1] Blakely DC. Emulsion polymerization. London; Elsevier Applied Science; 1975.
[2] Barrett KEJ (Editor). Dispersion polymerization in organic media. Chichester: John Wiley & Sons, Ltd; 1975.
[3] Smith WV, Ewart RH. J Chem Phys. 1948;16:592.
[4] Litchi G, Gilbert RG, Napper DH. J Polym Sci. 1983;21:269.
[5] Feeney PJ, Napper DH, Gilbert RG. Macromolecules. 1984;17:2520. 1987;20:2922.
[6] Piirma I. Polymeric surfactants. Surfactant Science Series, No. 42. New York: Marcel Dekker; 1992.
[7] Piirma I, Lenzotti JR. Br Polymer J. 1959;21:45.
[8] Nestor J, Esquena J, Solans C, Levecke B, Booten K, Tadros TF. Langmuir. 2005;21:4837.
[9] Nestor J, Esquena J, Solans C, Luckham PF, Levecke B, Tadros TF. J Colloid Interface Sci. 2007;311:430.
[10] Liang W, Bognolo G, Tadros TF. Langmuir. 1995;11:2899.
[11] Barrett KEJ and Thomas HR. J Polym Sci Part A1. 1969;7:2627.
[12] Dawkins JV, Taylor G. Polymer. 1987;20:171.
[13] Antl I, Goodwin JW, Hill RD, Ottewill RH, Owen SM, Papworth S, Waters JA. Colloids Surf. 1986;1:67.
[14] Napper DH. Polymeric stabilisation of colloidal dispersions. London: Academic Press; 1983.
[15] Lok KP, Ober CK. Can J Chem. 1985;63:209.
[16] Paine AJ. J Polymer Sci Part A. 1990;28:2485.

11 Pigment dispersion and the role of surfactants in wetting

11.1 Introduction

As mentioned Chapter 9 a paint may be considered as a colloidal dispersion of a pigment (the disperse phase) in a medium that may be aqueous or nonaqueous that contains a polymer (film former) and/or latex particles. The state of dispersion of a pigment in a paint is vital, as it determines its optical properties (e.g. colour), flow properties (rheology), durability, opacity, gloss and storage stability. This chapter will deal with the dispersion of a powder in a liquid.

Dispersion methods are used for preparing suspensions of preformed particles; the term dispersion is used to refer to the complete process of incorporating the solid into a liquid such that the final product consists of fine particles distributed throughout the dispersion medium [1]. This is illustrated in Fig. 11.1.

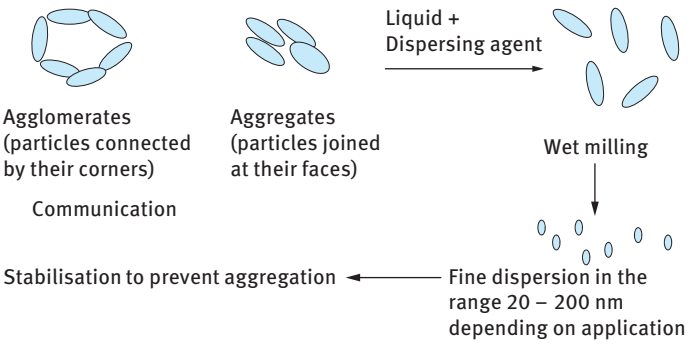

Fig. 11.1: Schematic representation of the dispersion process.

The role of surfactants (or polymers) in the dispersion can be understood by considering the stages involved [1, 2]. Three stages have been considered [3]: Wetting of the powder by the liquid, breaking of the aggregates and agglomerates and comminution (milling) of the resulting particles into smaller units. In this chapter, I will consider the process of powder wetting and the role of surfactants. The process of dispersion of aggregates and agglomerates into single units, as well as reduction of particle size by milling will be considered in Chapter 12.

https://doi.org/10.1515/9783110578997-012

11.2 Powder wetting

Before describing the wetting of powders (that consist of aggregates, where the particles are attached by their "faces", or agglomerates, where the particles are attached by their "corners") it is essential to describe the fundamental process of wetting in general as well as other factors such as adhesion of liquids to surfaces, spreading of liquids on substrates and the importance of the surface energy of the solid [3].

Wetting is a fundamental process in which one fluid phase is displaced completely or partially by another fluid phase from the surface of a solid. A useful parameter to describe wetting is the contact angle θ of a liquid drop on a solid substrate. If the liquid makes no contact with the solid, i.e. $\theta = 180°$, the solid is referred to as non-wettable by the liquid in question. This may be the case for a perfectly hydrophobic surface with a polar liquid such as water. However, when $180° > \theta > 90°$, one may refer to a case of poor wetting. When $0° < \theta < 90°$, partial (incomplete) wetting is the case, whereas when $\theta = 0°$ complete wetting occurs and the liquid spreads on the solid substrate forming a uniform liquid film. The cases of partial and complete wetting are schematically shown in Fig. 11.2, for a liquid on a perfectly smooth solid substrate.

The utility of contact angle measurements depends on equilibrium thermodynamic arguments (static measurements) using the well-known Young's equation [4]. The value depends on:

(i) The history of the system;
(ii) (ii) whether the liquid is tending to advance across or recede from the solid surface (advancing angle θ_A, receding angle θ_R; usually $\theta_A > \theta_R$).

Under equilibrium, the liquid drop takes the shape that minimizes the free energy of the system. Three interfacial tensions can be identified:

- γ_{SV}, solid/vapour area A_{SV};
- γ_{SL}, solid/liquid area A_{SL};
- γ_{LV}, liquid/vapour area A_{LV}.

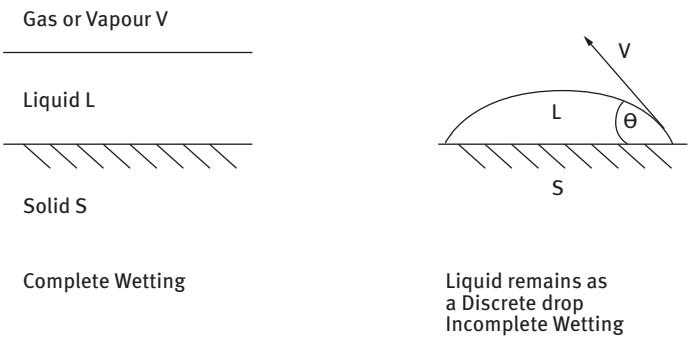

Fig. 11.2: Illustration of complete and partial wetting.

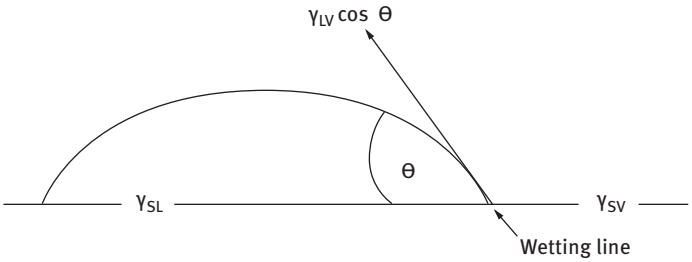

Fig. 11.3: Schematic representation of contact angle and wetting line.

A schematic representation of the balance of tensions at the solid/liquid/vapour interface is shown in Fig. 11.3. The contact angle is that formed between the planes tangent to the surfaces of the solid and liquid at the wetting perimeter. Here, solid and liquid are simultaneously in contact with each other and the surrounding phase (air or vapour of the liquid). The wetting perimeter is referred to as the three-phase line or wetting line. In this region there is an equilibrium between vapour, liquid and solid. $\gamma_{SV}A_{SV} + \gamma_{SL}A_{SL} + \gamma_{LV}A_{LV}$ should be a minimum at equilibrium and this leads to the well-known Young's equation [4],

$$\gamma_{SV} = \gamma_{SL} + \gamma_{LV}\cos\theta, \tag{11.1}$$

$$\cos\theta = \frac{\gamma_{SV} - \gamma_{SL}}{\gamma_{LV}}. \tag{11.2}$$

The contact angle θ depends on the balance between the solid/vapour (γ_{SV}) and solid/liquid (γ_{SL}) interfacial tensions. The angle which a drop assumes on a solid surface is the result of the balance between the adhesion force between solid and liquid and the cohesive force in the liquid,

$$\gamma_{LV}\cos\theta = \gamma_{SV} - \gamma_{SL}. \tag{11.3}$$

If there is no interaction between solid and liquid,

$$\gamma_{SL} = \gamma_{SV} + \gamma_{LV}, \tag{11.4}$$

i.e., $\cos\theta = -1$ or $\theta = 180°$.

If there is strong interaction between solid and liquid (maximum wetting), the latter spreads until Young's equation is satisfied,

$$\gamma_{LV} = \gamma_{SV} - \gamma_{SL}, \tag{11.5}$$

i.e., $\cos\theta = 1$ or $\theta = 0°$; the liquid is described as spreading spontaneously on the solid surface.

When the surface of the solid is in equilibrium with the liquid vapour, we can consider the spreading pressure π, as is illustrated in Fig. 11.4.

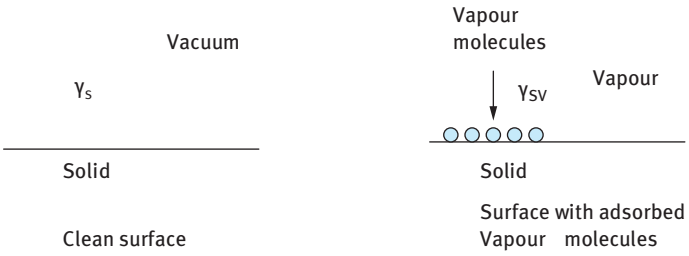

Fig. 11.4: Schematic representation of the spreading pressure.

The solid surface tension is lowered as a result of adsorption of vapour molecules,

$$\pi = \gamma_s - \gamma_{SV}. \tag{11.6}$$

Young's equation can be written as:

$$\gamma_{LV} \cos\theta = \gamma_S - \gamma_{SL} - \pi. \tag{11.7}$$

There is no direct way by which γ_{SV} or γ_{SL} can be measured. The difference between γ_{SV} and γ_{SL} can be obtained from contact angle measurements ($= \gamma_{LV} \cos\theta$). This difference is referred to as wetting tension or adhesion tension,

$$\text{adhesion tension} = \gamma_{SV} - \gamma_{SL} = \gamma_{LV} \cos\theta. \tag{11.8}$$

Gibbs [5] defined the adhesion tension τ as the difference between the surface pressure of the solid/liquid and that between the solid/vapour interface,

$$\tau = \pi_{SL} - \pi_{SV}, \tag{11.9}$$

$$\pi_{SV} = \gamma_s - \gamma_{SV}, \tag{11.10}$$

$$\pi_{SL} = \gamma_s - \gamma_{SL}, \tag{11.11}$$

$$\tau = \gamma_{SV} - \gamma_{SL} = \gamma_{LV} \cos\theta. \tag{11.12}$$

The work of adhesion is a direct measure of the free energy of interaction between solid and liquid; this is illustrated in Fig. 11.5.

$$W_a = (\gamma_{LV} + \gamma_{SV}) - \gamma_{SL}. \tag{11.13}$$

Using Young's equation,

$$W_a = \gamma_{LV} + \gamma_{SV} - \gamma_{LV} \cos\theta = \gamma_{LV}(\cos\theta + 1). \tag{11.14}$$

The work of adhesion depends on: γ_{LV}, the liquid/vapour surface tension and θ, the contact angle between liquid and solid.

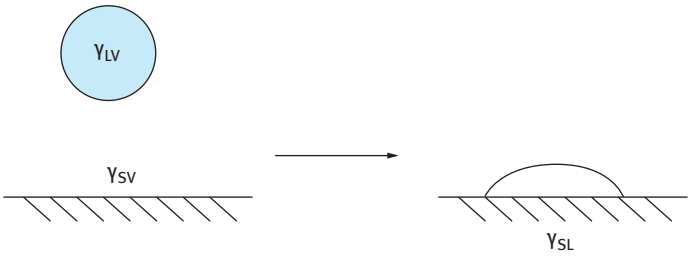

Fig. 11.5: Representation of adhesion of a drop on a solid substrate.

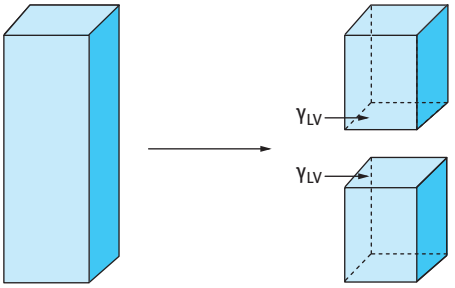

Fig. 11.6: Schematic representation of subdivision of a liquid cylinder.

The work of cohesion W_c is the work of adhesion when the two surfaces are the same. Consider a liquid cylinder with unit cross-sectional area as schematically represented in Fig. 11.6.

$$W_c = 2\gamma_{LV}. \tag{11.15}$$

For adhesion of a liquid on a solid, $W_a \approx W_c$ or $\theta = 0°$ ($\cos\theta = 1$).

Harkins [6, 7] defined the spreading coefficient as the work required to destroy unit area of SL and LV and leave unit area of bare solid SV, as illustrated in Fig. 11.7.

The spreading coefficient S is the difference between the surface energy of the final state and the initial state,

$$S = \gamma_{SV} - (\gamma_{SL} + \gamma_{LV}). \tag{11.16}$$

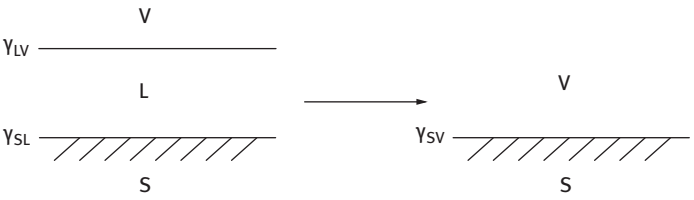

Fig. 11.7: Schematic representation of the spreading coefficient S.

Using Young's equation,

$$\gamma_{SV} = \gamma_{SL} + \gamma_{LV} \cos\theta, \tag{11.17}$$

$$S = \gamma_{LV}(\cos\theta - 1). \tag{11.18}$$

If S is zero (or positive), i.e. $\theta = 0$, the liquid will spread until it completely wets the solid. If S is negative, i.e. $\theta > 0$, only partial wetting occurs. Alternatively, one can use the equilibrium (final) spreading coefficient.

For dispersion of powders into liquids, one usually requires complete spreading, i.e. θ should be zero.

For a liquid spreading on a uniform, non-deformable solid (idealized case), there is only one contact angle; equilibrium value. With real systems (practical solids) a number of stable contact angles can be measured. Two relatively reproducible angles can be measured: largest, advancing angle θ_A; smallest, receding angle θ_R; this is illustrated in Fig. 11.8. θ_A is measured by advancing the periphery of a drop over a surface (e.g. by adding more liquid to the drop). θ_R is measured by pulling the liquid back. $\theta_A - \theta_R$ is referred to as contact angle hysteresis.

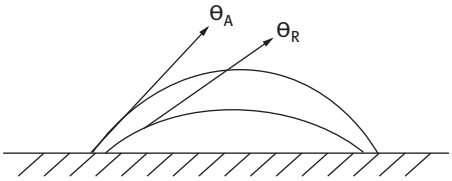

Fig. 11.8: Schematic representation of advancing and receding angles.

Three factors are responsible for contact angle hysteresis:

(i) penetration of wetting liquid into pores during advancing contact angle measurements;
(ii) surface roughness;
(iii) surface heterogeneity.

The first and rear edges both meet the liquid with some intrinsic angle θ_0 (microscopic contact angle). The macroscopic angles θ_A and θ_R vary significantly. This is best illustrated for a surface inclined at an angle α from the horizontal (Fig. 11.9).

θ_0 values are determined by contact of liquid with the "rough" valleys (microscopic contact angle) [8]. θ_A and θ_R are determined by contact of liquid with arbitrary parts on the surface (peak or valley). Surface roughness can be accounted for by comparing the "real" area of the surface A with that of the projected (apparent) area A',

$$r = \frac{A}{A'}, \tag{11.19}$$

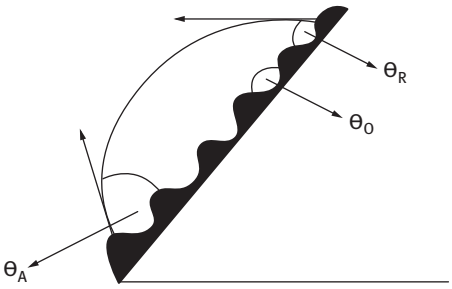

Fig. 11.9: Representation of a drop profile on a rough surface.

where A is the area of surface taking into account all peaks and valleys and A' is the apparent area (same macroscopic dimension); $r > 1$.

$$\cos\theta = r\cos\theta_0, \tag{11.20}$$

where θ is the macroscopic contact angle and θ_0 is the microscopic contact angle.

$$\cos\theta = r\left[\frac{(\gamma_{SV} - \gamma_{SL})}{\gamma_{LV}}\right]. \tag{11.21}$$

If $\cos\theta$ is negative on a smooth surface ($\theta > 90°$), it becomes more negative on a rough surface (θ is larger) and surface roughness reduces wetting. If $\cos\theta$ is positive on a smooth surface ($\theta < 90°$) it becomes more positive on a rough surface (θ is smaller) and roughness enhances wetting.

Most practical surfaces are heterogeneous consisting of "islands" or "patches" with different surface energies. As the drop advances on such a surface, the edge of the drop tends to stop at the boundary of the "island". The advancing angle will be associated with the intrinsic angle of the high contact angle region. The receding angle will be associated with the low contact angle region. If the heterogeneities are very small compared with the dimensions of the liquid drop, one can define a composite contact angle using Cassie's equation [9, 10],

$$\cos\theta = Q_1\cos\theta_1 + Q_2\cos\theta_2, \tag{11.22}$$

where Q_1 is the fraction of surface having contact angle θ_1 and Q_2 is the fraction of surface having contact angle θ_2. θ_1 and θ_2 are the maximum and minimum possible angles.

11.3 Critical surface tension of wetting

A systematic way of characterizing "wettability" of a surface was introduced by Fox and Zisman [11]. For a given substrate and for a series of related liquids (e.g. n-alkanes, siloxanes and dialkyl ethers) a plot of $\cos\theta$ versus γ_{LV} gives a straight line. This is schematically shown in Fig. 11.10.

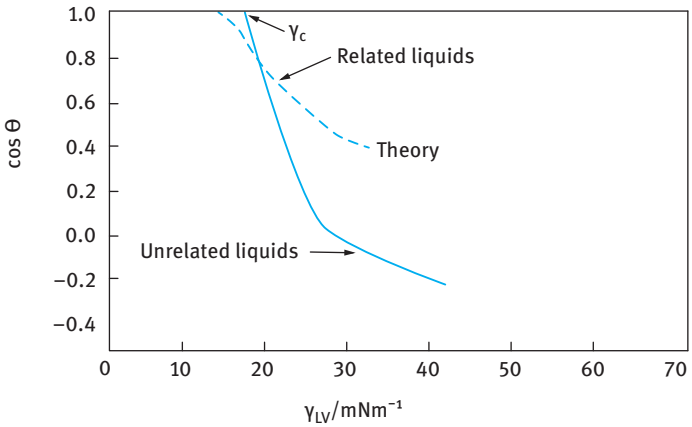

Fig. 11.10: Critical surface tension of wetting.

Extrapolation of the straight line to $\cos\theta = 1$ ($\theta = 0$) gives the critical surface tension of wetting γ_c. Any liquid with $\gamma_{LV} < \gamma_c$ will give $\theta = 0$, i.e. it wets the surface completely; γ_c is the surface tension of a liquid that just spreads on the substrate to give complete wetting.

The above linear relationship can be represented by the following empirical equation,

$$\cos\theta = 1 + b(\gamma_{LV} - \gamma_c). \tag{11.23}$$

High energy solids, e.g. glass, give high γ_c ($> 40\,\text{mN m}^{-1}$). Low energy solids, e.g. hydrophobic surfaces, give lower γ_c ($\approx 30\,\text{mN m}^{-1}$). Very low energy solids such as Teflon (polytetrafluoroethylene, PTFE) give lower γ_c ($< 25\,\text{mN m}^{-1}$).

The above concept explains the degree of wettability of the above surfaces with water; glass being the easiest to wet and Teflon being the most difficult to wet.

11.4 Effect of surfactant adsorption

Surfactants lower the surface tension of water, γ, and they adsorb at the solid/liquid interface. A plot of γ_{LV} versus log C (where C is the surfactant concentration) results in a gradual reduction in γ_{LV} followed by a linear decrease in γ_{LV} with log C (just below the critical micelle concentration, cmc) and when the cmc is reached, γ_{LV} remains virtually constant. This is schematically shown in Fig. 11.11.

From the slope of the linear portion of the γ–log C curve (just below the cmc), one can obtain the surface excess (number of moles of surfactant per unit area at the L/A interface). Using the Gibbs adsorption isotherm,

$$\frac{d\gamma}{d\log C} = -2.303RT\Gamma, \tag{11.24}$$

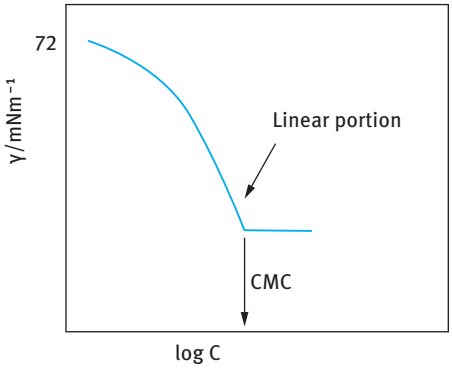

Fig. 11.11: Surface tension–log C curves.

where Γ is the surface excess (mol m^{-2}), R is the gas constant and T is the absolute temperature.

From Γ one can obtain the area per molecule,

$$\text{area per molecule} = \frac{1}{\Gamma N_{\text{av}}}\,(\text{m}^2) = \frac{10^{18}}{\Gamma N_{\text{av}}}\,(\text{nm}^2). \tag{11.25}$$

Most surfactants produce a vertically oriented monolayer just below the cmc. The area/molecule is usually determined by the cross-sectional area of the head group. For ionic surfactants containing say $-OSO_3^-$ or $-SO_3^-$ head groups, the area per molecule is in the region of 0.4 nm^2. For nonionic surfactants containing several moles of ethylene oxide (8–10), the area per molecule can be much larger (1–2 nm^2). Surfactants will also adsorb at the solid/liquid interface. For hydrophobic surfaces, the main driving force for adsorption is by hydrophobic bonding. This results in a lowering of the contact angle of water on the solid surface. For hydrophilic surfaces, adsorption occurs via the hydrophilic group, e.g. cationic surfactants on silica. Initially, the surface becomes more hydrophobic and the contact angle θ increases with increasing surfactant concentration. However, at higher cationic surfactant concentration, a bilayer is formed by hydrophobic interaction between the alkyl groups and the surface becomes more and more hydrophilic and eventually the contact angle reaches zero at high surfactant concentrations.

Smolders [12] suggested the following relationship for change of θ with C,

$$\frac{\text{d}\gamma_{\text{LV}}\cos\theta}{\text{d}\ln C} = \frac{\text{d}\gamma_{\text{SV}}}{\text{d}\ln C} - \frac{\text{d}\gamma_{\text{SL}}}{\text{d}\ln C}. \tag{11.26}$$

Using the Gibbs equation,

$$\sin\theta\left(\frac{\text{d}\gamma}{\text{d}\ln C}\right) = RT(\Gamma_{\text{SV}} - \Gamma_{\text{SL}} - \gamma_{\text{LV}}\cos\theta), \tag{11.27}$$

since $\gamma_{\text{LV}}\sin\theta$ is always positive, then $(\text{d}\theta/\text{d}\ln C)$ will always have the same sign as the RHS of equation (11.27).

Three cases may be distinguished:

- $(d\theta/d \ln C) < 0$; $\Gamma_{SV} < \Gamma_{SL} + \Gamma_{LV} \cos\theta$; addition of surfactant improves wetting.
- $(d\theta/d \ln C) = 0$; $\Gamma_{SV} = \Gamma_{SL} + \Gamma_{LV} \cos\theta$; surfactant has no effect on wetting.
- $(d\theta/d \ln C) > 0$; $\Gamma_{SV} > \Gamma_{SL} + \Gamma_{LV} \cos\theta$; surfactant causes dewetting.

11.5 Wetting of powders by liquids

Wetting of powders by liquids is very important for their dispersion, e.g. in the preparation of concentrated suspensions [1]. The particles in a dry powder form either aggregates or agglomerates. This was illustrated in Fig. 11.1.

It is essential in the dispersion process to wet both external and internal surfaces and displace the air entrapped between the particles. Wetting is achieved by the use of surface active agents (wetting agents) of the ionic or nonionic type that are capable of diffusing quickly (i.e. lower the dynamic surface tension) to the solid/liquid interface and displacing the air entrapped by rapid penetration through the channels between the particles and inside any "capillaries". For wetting of hydrophobic powders into water, anionic surfactants, e.g. alkyl sulphates or sulphonates or nonionic surfactants of the alcohol or alkyl phenol ethoxylates are usually used.

A useful concept for choosing wetting agents from the ethoxylated surfactants is the hydrophilic-lipophilic balance (HLB) concept,

$$\text{HLB} = \frac{\%\ \text{of hydrophilic groups}}{5}. \tag{11.28}$$

Most wetting agents of this class have an HLB number in the range 7–9.

The process of wetting a solid by a liquid involves three types of wetting: adhesion wetting, W_a; immersion wetting W_i; spreading wetting W_s. However, one can consider the work of dispersion wetting W_d as simply resulting from replacement of the solid/vapour interface with the solid/liquid interface.

Dispersion wetting W_d is given by the product of the external area of the powder A and the difference between γ_{SL} and γ_{SV}:

$$W_d = A(\gamma_{SL} - \gamma_{SV}). \tag{11.29}$$

Using Young's equation:

$$W_d = -A\gamma_{LV} \cos\theta. \tag{11.30}$$

Thus wetting of the external surface of the powder depends on the liquid surface tension and contact angle. If $\theta < 90°$ $\cos\theta$ is positive and the work of dispersion is negative, i.e. wetting is spontaneous. The most important parameter that determines wetting of the powder in the dynamic surface tension is $\gamma_{dynamic}$ (i.e. the value at short times). As will be discussed later, $\gamma_{dynamic}$ depends both on the diffusion coefficient of the surfactant molecule as well as its concentration. Since wetting agents are added in

sufficient amounts (γ_{dynamic} is lowered sufficiently), spontaneous wetting is the rule rather than the exception.

Wetting of the internal surface requires penetration of the liquid into channels between and inside the agglomerates. The process is similar to forcing a liquid through fine capillaries. To force a liquid through a capillary with radius r, a pressure p is required that is given by,

$$p = -\frac{2\gamma_{LV}\cos\theta}{r} = \left[\frac{-2(\gamma_{SV} - \gamma_{SL})}{r\gamma_{LV}}\right]. \tag{11.31}$$

γ_{SL} has to be made as small as possible; rapid surfactant adsorption to the solid surface, i.e. low θ. When $\theta = 0$, $p \propto \gamma_{LV}$. Thus for penetration into pores one requires a high γ_{LV}. Thus, wetting of the external surface requires low contact angle θ and low surface tension γ_{LV}. Wetting of the internal surface (i.e. penetration through pores) requires low θ but high γ_{LV}. These two conditions are incompatible and a compromise has to be made: $\gamma_{SV} - \gamma_{SL}$ must be kept at a maximum. γ_{LV} should be kept as low as possible but not too low.

The above conclusions illustrate the problem of choosing the best wetting agent for a particular powder. This requires measurement of the above parameters as well as testing the efficiency of the dispersion process.

For horizontal capillaries (gravity neglected), the depth of penetration l in time t is given by the Rideal–Washburn equation [13],

$$l = \left[\frac{rt\gamma_{LV}\cos\theta}{2\eta}\right]^{1/2}. \tag{11.32}$$

To enhance the rate of penetration, γ_{LV} has to be made as high as possible, θ as low as possible and η as low as possible.

For dispersion of powders into liquids, one should use surfactants that lower θ while not reducing γ_{LV} too much. The viscosity of the liquid should also be kept at a minimum. Thickening agents (such as polymers) should not be added during the dispersion process. It is also necessary to avoid foam formation during the dispersion process.

For a packed bed of particles, r may be replaced by r/k^2, where r is the effective radius of the bed and k is the tortuosity factor, which takes into account the complex path formed by the channels between the particles, i.e.,

$$l^2 = \left(\frac{r\gamma_{LV}\cos\theta}{2\eta k^2}\right)t. \tag{11.33}$$

Thus a plot of l^2 versus t gives a straight line and from the slope of the line one can obtain θ. The Rideal–Washburn equation can be applied to obtain the contact angle of liquids (and surfactant solutions) in powder beds. k should first be obtained using a liquid that produces zero contact angle.

Two methods can be applied for measuring the wettability of powders: (i) Submersion test, sinking time or immersion time. This is by far the most simple (but qualitative) method for assessing the wettability of a powder by a surfactant solution. The time for which a powder floats on the surface of a liquid before sinking into the liquid is measured. 100 ml of the surfactant solution is placed in a 250 ml beaker (of internal diameter of 6.5 cm) and after 30 min standing, 0.30 g of loose powder (previously screened through a 200-mesh sieve) is distributed with a spoon onto the surface of the solution. The time *t* for the 1 to 2 mm thin powder layer to completely disappear from the surface is measured using a stopwatch. Surfactant solutions with different concentrations are used and *t* is plotted versus surfactant concentration, as illustrated in Fig. 11.12.

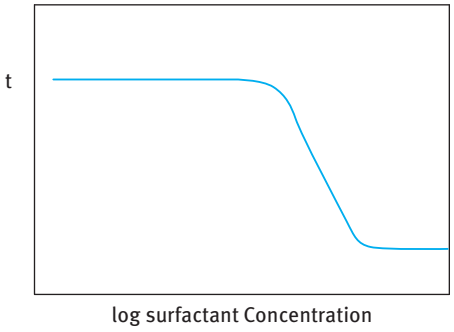

Fig. 11.12: Sinking time as a function of surfactant concentration.

It can be seen from Fig. 11.12 that the sinking time starts to decrease sharply above a critical surfactant concentration, reaching a minimum above this concentration. This procedure can be used to select the most effective wetting agent. The lower the surfactant concentration above which a rapid decrease in sinking time occurs and the lower the minimum wetting time obtained above this concentration, the more effective the wetter is.

(ii) Measurement of contact angles of liquids and surfactant solutions on powders. The simplest procedure is to measure the contact angle on a flat surface of the powder. This requires preparation of a flat surface, for example by using a large crystal of the chemical or by compressing the powder to a thin plate (using high pressure such as is commonly used for IR measurements, for example). However, this procedure is inaccurate since by compressing the powder its surface will change and the measured contact angle will not be representative of the powder in question. However, this procedure may be used to compare various wetting agents and the assumption is made that the lower the surfactant concentration required to reach a zero contact angle, the more effective the wetter is.

The contact angle on powders can be more accurately measured by determining the rate of liquid penetration through a carefully packed bed of powder placed in a

tube fitted with a sintered glass at the end (to retain the powder particles). It is essential to pack the powder uniformly in the tube (a plunger may be used in this case). By plotting l^2 (where l is the distance covered by the liquid flowing under capillary pressure) versus time t a straight line is obtained (equation (11.33)) and its slope is equal to $r\gamma_{LV} \cos\theta/2\eta k^2$ (where r is the equivalent capillary radius and k is tortuosity factor), γ_{LV} is the liquid surface tension and η is the liquid viscosity). This is illustrated in Fig. 11.13. From the slope, $\cos\theta$ is obtained provided r/k^2 is known.

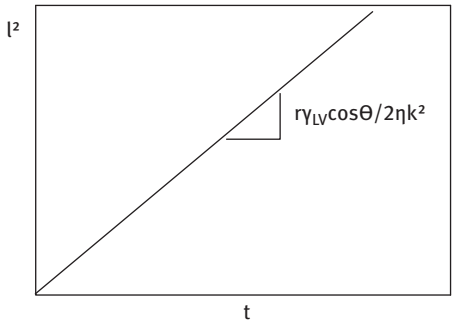

Fig. 11.13: Variation of l^2 with t.

The tortuosity factor k and the ratio of r/k^2 can be obtained by using a liquid that completely wets the powder giving a zero contact angle and $\cos\theta = 1$. The powder is carefully packed in a tube with a sintered glass at the end using a specially designed cell fitted with a plunger for packing the powder (as supplied by Kruss). The cell is placed on the top of liquid hexane, which gives a zero contact angle with most powders. The rate of penetration of hexane through the powder plug is measured by following the increase in weight ΔW of the cell with time. From the plot of ΔW^2 versus t, one can obtain r/k^2 from the slope of the linear line. The cell is then removed and the hexane is allowed to evaporate completely.

The same cell with its powder pack is then placed in surfactant solutions with various concentrations and this allows one to obtain the contact angle as a function of concentration. The most effective wetter will be the one that gives $\theta = 0°$ at the lowest concentration.

11.6 Wetting agents for hydrophobic pigments

The most effective wetting agent is the one that gives a zero contact angle at the lowest concentration. For $\theta = 0°$ or $\cos\theta = 1$, γ_{SL} and γ_{LV} have to be as low as possible [1]. This requires quick reduction of γ_{SL} and γ_{LV} under dynamic conditions during powder dispersion (This reduction should normally be achieved in less than 20 seconds). This requires fast adsorption of the surfactant molecules both at the L/V and S/L interfaces.

It should be mentioned that a reduction of γ_{LV} is not always accompanied by a simultaneous reduction of γ_{SL} and hence it is necessary to have information on both interfacial tensions, which means that measurement of the contact angle is essential in the selection of wetting agents. Measurements of γ_{SL} and γ_{LV} should be carried out under dynamic conditions (i.e. at very short times). In the absence of such measurements, the sinking time described above could be applied as a guide for wetting agent selection.

The most commonly used wetting agents for hydrophobic solids are anionic or nonionic surfactants. To achieve rapid adsorption the wetting agent should be either a branched chain with central hydrophilic group or a short hydrophobic chain with hydrophilic end group. The most commonly used wetting agent is Aerosol OT (diethylhexyl sulphosuccinate):

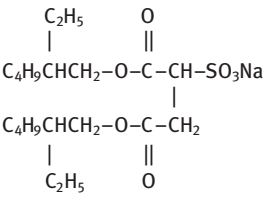

The above molecule has a low critical micelle concentration (cmc) of 0.7 g dm^{-1} and at and above the cmc the water surface tension is reduced to ≈ 25 mN m^{-1} in less than 15 s.

An alternative anionic wetting agent is sodium dodecylbenzene sulphonate with a branched alkyl chain

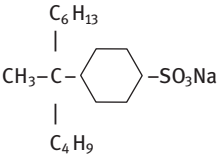

The above molecule has a higher cmc (1 g dm^{-1}) than Aerosol OT. It is also not as effective in lowering the surface tension of water, reaching a value of 30 mN m^{-1} at and above the cmc. It is, therefore, not as effective as Aerosol OT for powder wetting.

Several nonionic surfactants, such as the alcohol ethoxylates, can also be used as wetting agents. These molecules consist of a short hydrophobic chain (mostly C_{10}) which is also branched. A medium chain polyethylene oxide (PEO) mostly consisting of 6 EO units or lower is used. The above molecules also reduce the dynamic surface tension within a short time (< 20 s) and they have reasonably low cmc. In all cases one should use the minimum amount of wetting agent to avoid interference with the dispersant that needs to be added to maintain the colloid stability during dispersion and on storage.

11.7 Dynamics of processing of adsorption and wetting

Most processes of powder wetting work under dynamic conditions and improving their efficiency requires the use of surfactants that lower the liquid surface tension γ_{LV} under these dynamic conditions [14]. The interfaces involved (particles separated from aggregates or agglomerates) are freshly formed and have only a small effective age of some seconds or even less than a millisecond.

The most frequently used parameter to characterize the dynamic properties of liquid adsorption layers is the dynamic surface tension (that is a time dependent quantity). Techniques should be available to measure γ_{LV} as a function of time (ranging from a fraction of a millisecond to minutes and hours or days).

To optimize the use of surfactants, specific knowledge of their dynamic adsorption behaviour rather than equilibrium properties is of great interest [14]. It is, therefore, necessary to describe the dynamics of surfactant adsorption at a fundamental level.

The first physically sound model for adsorption kinetics was derived by Ward and Tordai [15]. It is based on the assumption that the time dependence of surface or interfacial tension, which is directly proportional to the surface excess Γ (mol m^{-2}), is caused by diffusion and transport of surfactant molecules to the interface. This is referred to as "the diffusion controlled adsorption kinetics model". The interfacial surfactant concentration at any time t, $\Gamma(t)$, is given by the following expression,

$$\Gamma(t) = 2\left(\frac{D}{\pi}\right)^{1/2} c_0 t^{1/2} - \int_0^{t^{1/2}} c(0, t-\tau)\, \mathrm{d}(\tau)^{1/2}, \tag{11.34}$$

where D is the diffusion coefficient, c_0 is the bulk concentration and τ is the thickness of the diffusion layer.

The above diffusion controlled model assumes transport by diffusion of the surface active molecules to be the rate controlled step. The so-called "kinetic controlled model" is based on the transfer mechanism of molecules from solution to the adsorbed state and vice versa [14]. A schematic picture of the interfacial region is given in Fig. 11.14, which shows three main states:

(i) adsorption when the surface concentration Γ is lower than the equilibrium value Γ_0;
(ii) equilibrium state when $\Gamma = \Gamma_0$;
(iii) desorption when $\Gamma > \Gamma_0$.

The transport of surfactant molecules from the liquid layer adjacent to the interface (subsurface) is simply determined by molecular movements (in the absence of forced liquid flow). At equilibrium, i.e. when $\Gamma = \Gamma_0$, the flux of adsorption is equal to the flux of desorption. Clearly when $\Gamma < \Gamma_0$, the flux of adsorption predominates, whereas when $\Gamma > \Gamma_0$, the flux of desorption predominates [14].

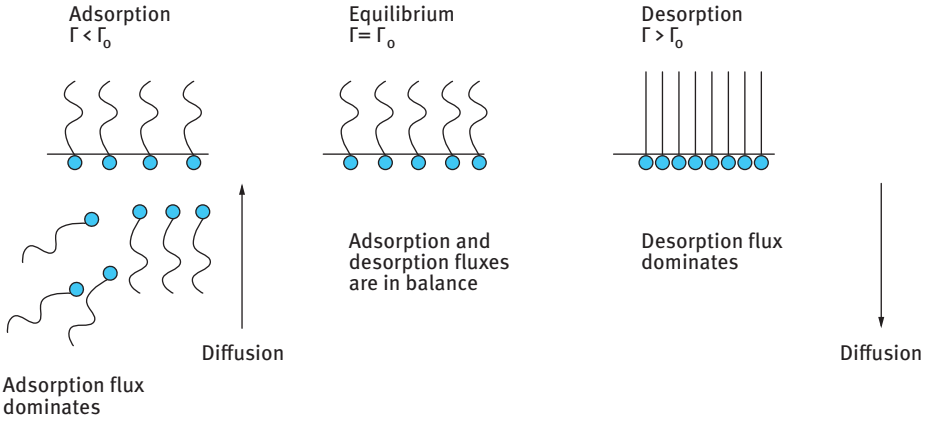

Fig. 11.14: Representation of the fluxes of adsorbed surfactant molecules in the absence of liquid flow.

In the presence of liquid flow, the situation becomes more complicated due to the creation of surface tension gradients [14]. These gradients, described by the Gibbs dilational elasticity, ε, initiate a flow of mass along the interface in the direction of the higher surface or interfacial tension (Marangoni effect). ε is given by the following expression,

$$\varepsilon = A\frac{\mathrm{d}\gamma}{\mathrm{d}A} = \frac{\mathrm{d}\gamma}{\mathrm{d}\ln A}, \tag{11.35}$$

where $\mathrm{d}\gamma$ is the surface tension gradient and $\mathrm{d}A$ is the change in area of the interface.

The above situation can happen, for example, if an adsorption layer is compressed or stretched, as is illustrated in Fig. 11.15.

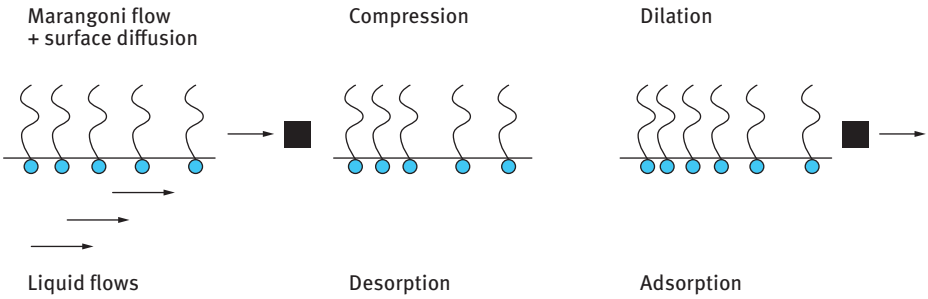

Fig. 11.15: Representation of surfactant transport at the surface and in the bulk of a liquid.

A qualitative model that can describe adsorption kinetics is described by the following equation,

$$\Gamma(t) = c_0\left(\frac{Dt}{\pi}\right)^{1/2}. \tag{11.36}$$

Equation (11.36) gives a rough estimate and results from equation (11.34) when the second term on the right-hand side is neglected.

An equivalent equation to (11.36) has been derived by Paniotov and Petrov [16],

$$c(0,t) = c_0 - \frac{2}{(D\pi)^{1/2}}\int_0^{t^{1/2}} \frac{\mathrm{d}\Gamma(t-\tau)}{\mathrm{d}t}\,\mathrm{d}\tau^{1/2}. \tag{11.37}$$

Hansen [17], Miller and Lukenheimer [18] gave numerical solutions to the integrals of equations (11.36) and (11.37) and obtained a simple expression using a Langmuir isotherm,

$$\Gamma(t) = \Gamma_\infty \frac{c(0,t)}{a_\mathrm{L} + c(0,t)}, \tag{11.38}$$

where a_L is the constant in the Langmuir isotherm (mol m^{-3})

The corresponding equation for the variation of surface tension γ with time is as follows (Langmuir–Szyszkowski equation),

$$\gamma = \gamma_0 + RT\Gamma_\infty \ln\left(1 - \frac{\Gamma(t)}{\Gamma_\infty}\right). \tag{11.39}$$

Calculations based on equations (11.35)–(11.39) are given in Fig. 11.16, with different values of c_0/a_L [20].

Surfactants form micelles above the critical micelle concentration (cmc) of different sizes and shapes, depending on the nature of the molecule, temperature, electrolyte concentration, etc. The dynamic nature of micellization can be described by

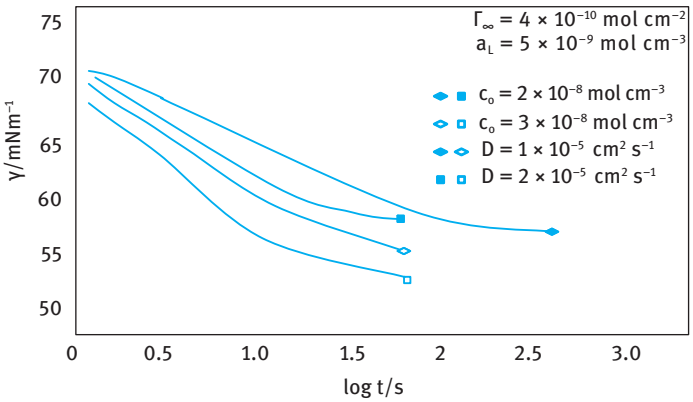

Fig. 11.16: Surface tension γ–log t curves calculated on the basis of equations (11.35)–(11.39).

two main relaxation processes, τ_1 (the lifetime of a monomer in a micelle) and τ_2 (the lifetime of the micelle, i.e. complete dissolution into monomers). The presence of micelles in equilibrium with monomers influences the adsorption kinetics remarkably. After a fresh surface has been formed, surfactant monomers are adsorbed resulting in a concentration gradient of these monomers. This gradient will be equalized by diffusion to re-establish a homogeneous distribution. Simultaneously, the micelles are no longer in equilibrium with monomers within the range of concentration gradient. This leads to a net process of micelle dissolution or rearrangement to re-establish the local equilibrium. As a consequence, a concentration gradient of micelles results, which is equalized by diffusion of micelles [14].

Based on the above concepts, one would expect that the ratio of monomers c_1 to micelles c_m, the aggregation number n, rate of micelle formation k_f and micelle dissolution k_d will influence the rate of the adsorption process. A schematic picture of the kinetic process in the presence of micelles is given in Fig. 11.17.

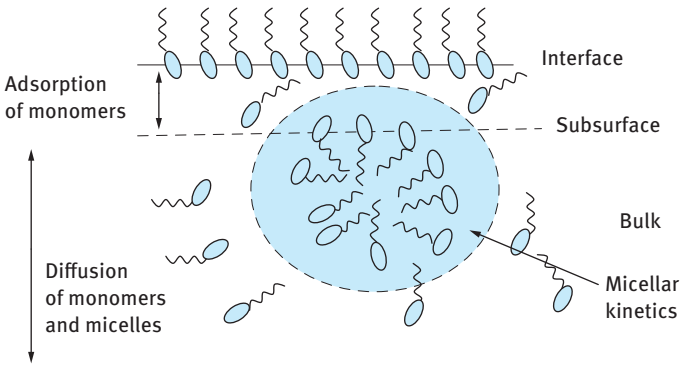

Fig. 11.17: Representation of the adsorption process from a micellar solution.

Fig. 11.17 shows that to describe the kinetics of adsorption, one must take into account the diffusion of monomers and micelles as well as the kinetics of micelle formation and dissolution. Several processes may take place and these are represented schematically in Fig. 11.18. Three main mechanisms may be considered, namely formation-dissolution (Fig. 11.18 (a)), rearrangement (Fig. 11.18 (b)) and stepwise aggregation-dissolution (Fig. 11.18 (c)). To describe the effect of micelles on adsorption kinetics, one should know several parameters such as micelle aggregation number and rate constants of micelle kinetics [14].

The two most suitable techniques for studying adsorption kinetics are the drop volume method and the maximum bubble pressure method. The first method can obtain information on adsorption kinetics in the range of seconds to some minutes. However, it has the advantage of measuring at both the air/liquid and the liquid/liquid

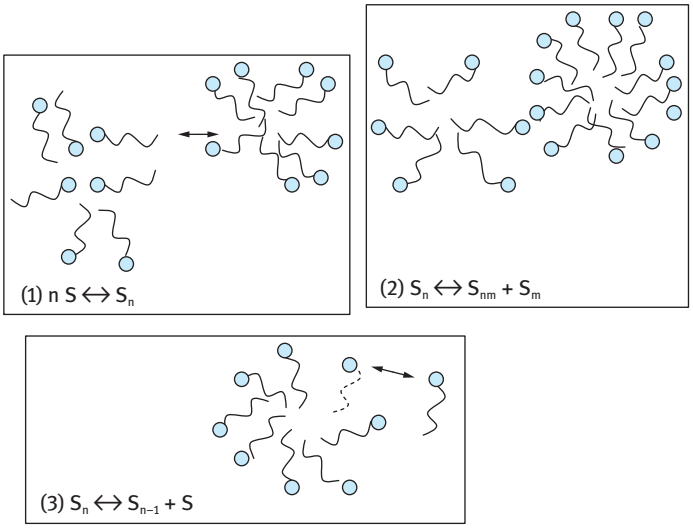

Fig. 11.18: Scheme of micelle kinetics.

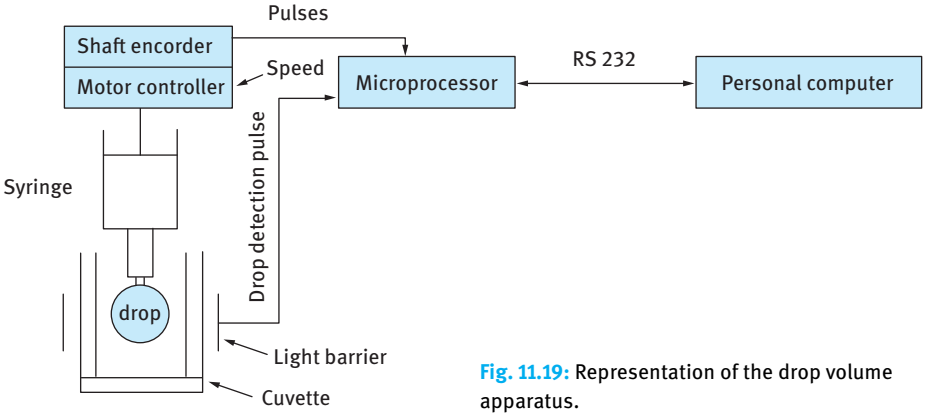

Fig. 11.19: Representation of the drop volume apparatus.

interface. The maximum bubble pressure method allows one to obtain measurements in the millisecond range, but it is restricted to the air/liquid interface.

A schematic representation of the drop volume apparatus [14] is given in Fig. 11.19.

A metering system in the form of a motor-driven syringe allows the formation of the liquid drop at the tip of a capillary, which is positioned in a sealed cuvette. The cuvette is either filled with a small amount of the measuring liquid, to saturate the atmosphere, or with a second liquid in the case of interfacial studies. A light barrier arranged below the forming drop enables the detection of drop-detachment from the capillary. Both the syringe and the light barriers are computer controlled and allow a fully automatic operation of the set-up. The syringe and the cuvette are temperature

controlled by a water jacket which makes it possible to measure interfacial tension in the temperature range 10–90 °C.

As mentioned above, the drop volume method is of dynamic character and it can be used for adsorption processes in the time interval of seconds up to some minutes. At small drop time, the so-called hydrodynamic effect has to be considered [14]. This gives rise to apparently higher surface tension. Kloubek et al. [19] used an empirical equation to account for this effect,

$$V_e = V(t) - \frac{K_v}{t}. \tag{11.40}$$

V_e is the unaffected drop volume and $V(t)$ is the measured drop volume. K_v is a proportionality factor that depends on surface tension γ, density difference $\Delta\rho$ and tip radius r_{cap}.

Miller et al. [20] obtained the following equation for the variation of drop volume $V(t)$ with time,

$$V(t) = V_e + t_0 F = V_e\left(1 + \frac{t_0}{t - t_0}\right), \tag{11.41}$$

where F is the liquid flow per unit time that is given by,

$$F = \frac{V(t)}{t} = \frac{V_e}{t - t_0}. \tag{11.42}$$

The drop volume technique is limited in its application. Under conditions of fast drop formation and larger tip radii, the drop formation shows irregular behaviour.

The maximum bubble pressure technique is the most useful technique for measuring adsorption kinetics at short times, particularly if correction for the so-called "dead time", τ_d, is made. The dead time is simply the time required to detach the bubble after it has reached its hemispherical shape. A schematic representation of the principle of maximum bubble pressure is shown in Fig. 11.20, which shows the evolution of a

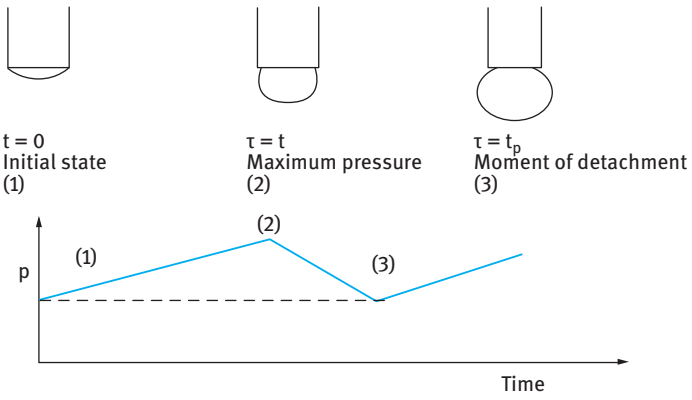

Fig. 11.20: Scheme of bubble evolution and pressure change with time.

bubble at the tip of a capillary. The figure also shows the variation of pressure p in the bubble with time.

At $t = 0$ (initial state), the pressure is low (note that the pressure is equal to $2\gamma/r$; since r of the bubble is large, p is small). At $t = \tau$ (smallest bubble radius that is equal to the tube radius), p reaches a maximum. At $t = \tau_b$ (detachment time), p decreases since the bubble radius increases. The design of a maximum bubble pressure method for high bubble formation frequencies (short surface age) requires the following:

(i) measurement of bubble pressure;
(ii) measurement of bubble formation frequency;
(iii) estimation of surface lifetime and effective surface age.

The first problem can be easily solved if the system volume (which is connected to the bubble) is large enough in comparison with the bubble separating from the capillary. In this case, the system pressure is equal to the maximum bubble pressure. The use of an electric pressure transducer for measuring bubble formation frequency presumes that pressure oscillations in the measuring system are distinct enough and this satisfies (ii). Estimation of the surface lifetime and effective surface age, i.e. (iii), requires estimation of the dead time τ_d. A schematic representation of the set-up for measuring the maximum bubble pressure and surface age is shown in Fig. 11.21. The air coming from a micro-compressor flows first through the flow capillary. The air flow rate is determined by measuring the pressure difference at both ends of the flow capillary with the electric transducer PS1. Thereafter, the air enters the measuring cell and the excess air pressure in the system is measured by a second electric sensor PS2. In the tube which leads the air to the measuring cell, a sensitive microphone is placed.

The measuring cell is equipped with a water jacket for temperature control, which simultaneously holds the measuring capillary and two platinum electrodes, one of which is immersed in the liquid under study and the second is situated exactly oppo-

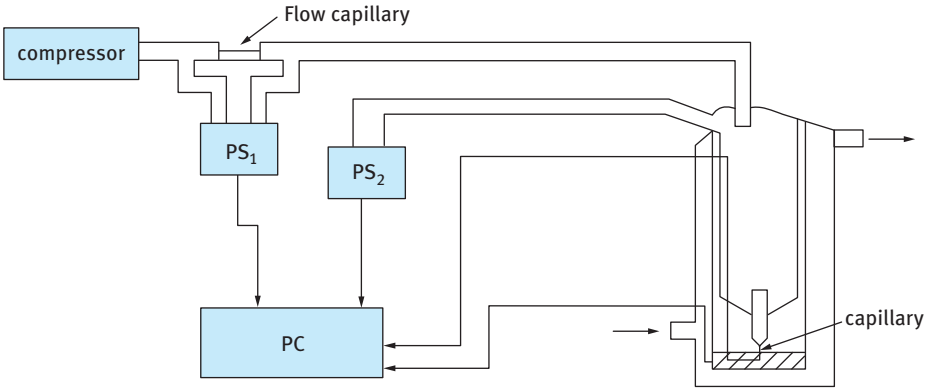

Fig. 11.21: Apparatus for measuring maximum bubble pressure.

site to the capillary and controls the size of the bubble. The electric signals from the gas flow sensor PS1 and pressure transducer PS2, the microphone and the electrodes, as well as the compressor are connected to a personal computer which operates the apparatus and acquires the data.

The value of τ_d, equivalent to the time interval necessary to form a bubble of radius R, can be calculated using Poiseulle's law,

$$\tau_d = \frac{\tau_b L}{Kp}\left(1 + \frac{3r_{ca}}{2R}\right). \tag{11.43}$$

K is given by Poiseulle's law,

$$K = \frac{\pi r^4}{8\eta l}. \tag{11.44}$$

η is the gas viscosity, l is the length, L is the gas flow rate and r_{ca} is the radius of the capillary.

The calculation of dead time τ_d can be simplified when taking into account the existence of two gas flow regimes for the gas flow leaving the capillary: bubble flow regime when $\tau > 0$ and jet regime when $\tau = 0$ and hence $\tau_b = \tau_d$. A typical dependency of p on L is shown in Fig. 11.22.

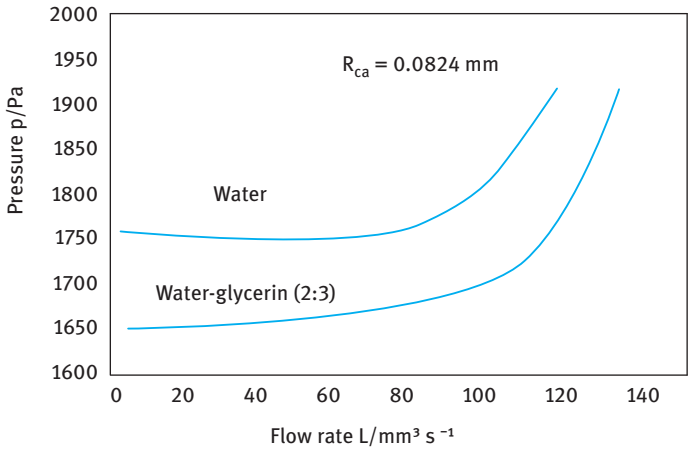

Fig. 11.22: Dependency of p on gas flow rate L at 30 °C.

On the right-hand side of the critical point the dependency of p on L is linear in accordance with Poiseulle's law. Under these conditions,

$$\tau_d = \tau_b \frac{Lp_c}{L_c p}, \tag{11.45}$$

where L_c and p_c are related to the critical point, and L and p are the actual values of the dependency left from the critical point.

The surface lifetime can be calculated from,

$$\tau = \tau_b - \tau_d = \tau_b\left(1 - \frac{Lp_c}{L_c p}\right). \tag{11.46}$$

The critical point in the dependency of p and L can be easily located and is included in the software of the computer program.

The surface tension value in the maximum bubble pressure method is calculated using the Laplace equation,

$$p = \frac{2\gamma}{r} + \rho hg + \Delta p, \tag{11.47}$$

where ρ is the density of the liquid, g is the acceleration due to gravity, h is the depth the capillary is immersed in the liquid and Δp is a correction factor to allow for hydrodynamic effects.

References

[1] Tadros T. Dispersions of powders in liquids and stabilisation of suspensions. Weinheim: Wiley-VCH; 2012.
[2] Tadros T. Interfacial phenomena and colloid stability, Vol. 1. Berlin: De Gruyter; 2015.
[3] Blake TB. Wetting. In: Tadros TF, editor. Surfactants. London: Academic Press; 1984.
[4] Young T. Phil Trans Royal Soc (London). 1805;95:65.
[5] Gibbs JW. Collected works. Vol. 1. New York: Longman; 1928.
[6] Harkins WD. J Phys Chem. 1937;5:135.
[7] Harkins WD. The physical chemistry of surface films. New York: Reinhold; 1952.
[8] Wenzel RN. Ind Eng Chem. 1936;28:988.
[9] Cassie ABD, Dexter S. Trans Faraday Soc. 1944;40:546.
[10] Cassie ABD. Disc Faraday Soc. 1948;3:361.
[11] Zisman WA. Adv Chem Ser. 1964;43:1.
[12] Smolders CA. Rec Trav Chim. 1960;80:650.
[13] Davies JT, Rideal EK. Interfacial phenomena. New York: Academic Press; 1969.
[14] Dukhin SS, Kretzscmar G, Miller R. Dynamics of adsorption at liquid interfaces. Amsterdam: Elsevier Publishers; 1995.
[15] Ward AFH, Tordai L. J Phys Chem. 1946;14:453.
[16] Panaitov I, Petrov JG. Ann Univ Sofia Fac Chem. 1968/69;64:385.
[17] Hansen RS. J Phys Chem. 1960;64:637.
[18] Miller R, Lunkenheimer K. Z Phys Chem. 1978;259:863.
[19] Kloubek J, Friml K, Krejci K. Check Chem Commun. 1976;41:1845.
[20] Miller R, Hoffmann A, Hartmann R, Schano KH, Halbig A. Advanced Materials. 1992;4:370.

12 Breaking of aggregates and agglomerates (deagglomeration) and size reduction

12.1 Dispersion of aggregates and agglomerates into single particles

All pigments are supplied as powders consisting of aggregates (where the particles are connected by their surfaces) or agglomerates (where the particles are connected by their corners) [1–3]. For example, pigmentary titanium dioxide mostly exists in powder form as loose agglomerates of several tens of μm in diameter [4]. These pigments are surface coated by the manufacturer for two main reasons. Firstly, the surface coating reduces the cohesive forces of the powder, thus assisting the deagglomeration process. Secondly, the coating (SiO_2 and Al_2O_3) deactivates the surface rutile pigment (by reducing the photochemical activity), which would otherwise accelerate the degradation of the resin on weathering.

The "grinding stage" in mill base manufacture is not a comminution stage but a dispersion process of the pigment agglomerates, whereby the latter are separated into "single" primary particles. However, some of the primary particles may consist of sinters of TiO_2 crystals produced during the surface coating stage. To separate the particles in an aggregate or agglomerate, one requires the use of a wetting/dispersing system. The wetting agent, which is usually a short chain surfactant molecule, can seldom prevent the reaggregation of the primary particles after the dispersion process. Thus, to prevent the reaggregation of particles, a dispersing agent is required. The dispersing agent may replace the wetting agent at the S/L interface or become co-adsorbed with the wetting agent. The dispersant produces an effective repulsive barrier on close approach of the particles. This repulsive barrier is particularly important for concentrated pigment dispersions (that may contain more than 50 % by volume of solids).

The main criteria for an effective dispersant are:

(i) Strong adsorption or "anchoring" to the particle surface.

(ii) High repulsive barrier. The stabilizing chain A of the dispersant must provide an effective repulsive barrier to prevent flocculation by van der Waals attraction. Three main mechanisms of stabilization can be considered: Electrostatic, as for example produced by ionic surfactants [5, 6]; steric, as produced by nonionic polymeric surfactants of the A–B, B–A–B, A–B–A or AB_n graft copolymer type (where A is the "anchor" chain and B is the "stabilizing" chain) [7]; electrosteric, as produced by polyelectrolytes.

(iii) Strong solvation of the stabilizing B chain, i.e. it should be in a good solvent condition, i.e. very soluble in the medium and strongly solvated by its molecules. Solvation of the chain by the medium is determined by the chain/solvent (Flory–Huggins) interaction parameter χ. In good solvent conditions, $\chi < 0.5$ and hence

https://doi.org/10.1515/9783110578997-013

the mixing or osmotic interaction is positive (repulsive). χ should be maintained at < 0.5 under all conditions, e.g. low and high temperature, in the presence of electrolytes and other components of the formulation such as addition of anti-freeze (mostly propylene glycol).

(iv) Reasonably thick adsorbed layer. The adsorbed layer thickness of the B chains, usually described by a hydrodynamic value δ_h (i.e. the thickness δ plus any contribution from the solvation shell), should be sufficiently large to prevent the formation of a deep minimum that may result in flocculation (although reversible) and an increase in the viscosity of the suspension. A value of $\delta_h > 5$ nm is usually sufficient to prevent the formation of a deep minimum.

12.2 Classification of dispersants

12.2.1 Surfactants

- Anionic, e.g. sodium dodecyl sulphate (SDS) $C_{12}H_{25}OSO_3Na$. Sodium dodecylbenzene sulphonate (NaDBS). $C_{12}H_{25}$–⬡–SO_3Na.
- Cationic, e.g. Dodecyl trimethyl ammonium chloride $C_{12}H_{25}N(CH_3)_3Cl$.
- Amphoteric, e.g. Betaines; lauryl amido propyl dimethyl betaine $C_{12}H_{25}CON(CH_3)_2CH_2COOH$.
- Nonionic Surfactants: The most common nonionic surfactants are the alcohol ethoxylates R–O–$(CH_2–CH2–O)_n$–H, e.g. $C_{13/15}(EO)_n$ with n being 7, 9, 11 or 20.

These surfactants are not the most effective dispersants since the adsorption by the $C_{13/15}$ chain is not very strong. To enhance the adsorption on hydrophobic surfaces a polypropylene oxide (PPO) chain is introduced in the molecule giving R–O–$(PPO)_m$–$(PEO)_n$–H. A more effective nonionic surfactant with a strong adsorption is obtained by using a tristyrylphenol with PEO, e.g.

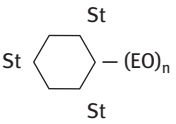

The tristyrylphenol hydrophobic chain adsorbs strongly on a hydrophobic surface.

12.2.2 Polymeric surfactants

Homopolymers consisting of the same repeating units such as poly(ethylene oxide) (PEO) or poly(vinylpyrrolidone) are not good dispersants for hydrophobic solids in aqueous media. This is due to the poor "anchor" of the chain to the surface and the

high solubility of the polymer in water. In most cases these homopolymers do no adsorb at all on the particles since the loss in configurational entropy on adsorption is not compensated by an adsorption energy (the adsorption energy per segment χ_s is very low).

The most effective polymeric surfactants as dispersants are those of the A–B, B–A–B block and AB_n or BA_n graft types [8]. The "anchor chain", A, is chosen to be highly insoluble in the medium and to have a strong affinity to the surface. Examples of A chains for hydrophobic solids are polystyrene (PS), polymethylmethacrylate (PMMA), poly(propylene oxide) (PPO) or alkyl chains provided these have several attachments to the surface. The stabilizing B chain has to be soluble in the medium and strongly solvated by its molecules. The B chain/solvent interaction should be strong giving a Flory–Huggins χ-parameter < 0.5 under all conditions. Examples of B chains are polyethylene oxide (PEO), polyvinyl alcohol (PVA) and polysaccharides (e.g. polyfructose). Several examples of commercially available B–A–B block copolymers are: B–A–B block copolymers of PEO and PPO: Pluronics. Several molecules of PEO–PPO–PEO are available with various proportions of PEO and PPO. The commercial name is followed by a letter L (liquid), P (paste) and F (flake). This is followed by two numbers that represent the composition. The first digit represents the PPO molar mass and the second digit represents the % PEO. Pluronic F68 (PPO molecular mass 1508–1800 + 80 % or 140 mol EO). Pluronic L62 (PPO molecular mass 1508–1800 + 20 % or 15 mol EO). In many cases two Pluronics with high and low EO content are used together to enhance the dispersing power.

Graft copolymers of the AB_n type are also available, for example AB_n graft copolymer based on polymethylmethacrylate (PMMA) backbone (with some polymethacrylic acid) on which several PEO chains (with average molecular weight of 750) are grafted:

```
~~~~~~~PMMA~~~~~~~~
   |     |     |     |
  PEO   PEO   PEO   PEO
```

It is a very effective dispersant, particularly for high solids content suspensions. The graft copolymer is strongly adsorbed on hydrophobic surfaces with several attachment points by the small PMMA loops of the backbone and a strong steric barrier is obtained by the highly hydrated PEO chains in aqueous solutions.

A novel BA_n graft has been synthesized, namely INUTEC® SP1 [9] consisting of an inulin linear polyfructose chain A (with degree of polymerization > 23) on which several alkyl chains have been grafted:

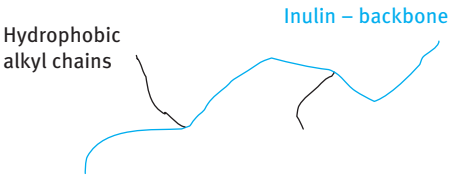

The polymeric surfactant adsorbs with multipoint attachment with several alkyl chains.

Another commercially available "blocky" copolymer is partially hydrolysed polyvinyl acetate, commercially referred to as polyvinyl alcohol (PVA). The molecule contains short blocks of polyvinyl acetate (PVAc) which form the anchor chains to the hydrophobic surface, leaving several loops and tails of PVA chains that are strongly hydrated to give an effective steric barrier:

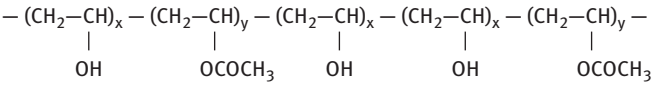

Several commercial PVA grades are available with molecular weights in the range 20 000–100 000 and acetate content in the range 4–12 %. The molecule is designated by two numbers representing the degree of hydrolysis and viscosity of 4 % solution (which gives a rough estimate of molecular weight. For example, Moviol 88/10 refers to a degree of hydrolysis of 88 % (12 % acetate groups) and a viscosity of 10 mPas of 4 % solution.

12.2.3 Polyelectrolytes

Naphthalene formaldehyde sulphonated condensate:

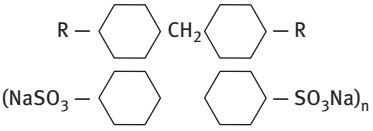

n varies between 2 and 9 units, i.e. the molecule has a wide distribution of molecular weights.

Further commercially available dispersants are the lignosulphonates, which are isolated from the waste liquor from wood pulping by the sulphite process, during which lignin is sulphonated. They are also produced by sulphonating lignin by alkaline pulping of wood by the Krafft process. Lignosulphonates as dispersants are mixtures of polyelectrolytes with a molecular weight ranging from 2000 to 10 000. The exact structure of lignosulphonates is not completely known but guaiacylpropyl groups with the sulphate groups attached to the aliphatic chains of lignin have been identified. The degree of sulphonation varies from 0.3 to 1.0 per phenyl unit. The commercial products, namely Polyfon (Wesvaco) and Ufoxane (Borregard) are described by degree of sulphonation per 840 units of lignin. For example, Polyfon H has a degree of sulphonation of 0.5, whereas Polyfon T has a degree of 2.0. The most effective lignosulphonates for hydrophobic solids in aqueous solution are those with lower degree of sulphonation that give higher adsorption.

12.3 Assessment and selection of dispersants

12.3.1 Adsorption isotherms

These are by far the most quantitative methods for assessing the dispersing power [1–3]. Known amounts of solids (mg) with a surface area A ($m^2\,g^{-1}$) are equilibrated at constant temperature with dispersant solutions with various concentrations C_1. The bottles containing the various dispersions are rotated for several hours until equilibrium is reached. The particles are removed from the dispersant solution by centrifugation and/or filtration through millipore filters. The dispersant concentration in the supernatant liquid C_2 is analytically determined by a suitable technique that can measure low concentrations.

The amount of adsorption Γ (mg m^{-2} or mol m^{-2}) is calculated:

$$\Gamma = \frac{(C_1 - C_2)}{mA}. \tag{12.1}$$

A plot of Γ versus C_2 gives the adsorption isotherm. Two types of isotherms can be distinguished: a Langmuir type for reversible adsorption of surfactants (Fig. 12.1) and a high affinity isotherm (Fig. 12.2) for irreversible adsorption of polymeric surfactants.

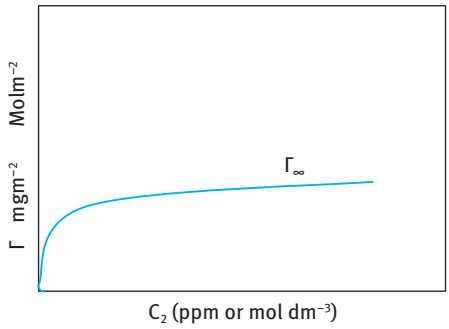

Fig. 12.1: Langmuir type adsorption isotherm.

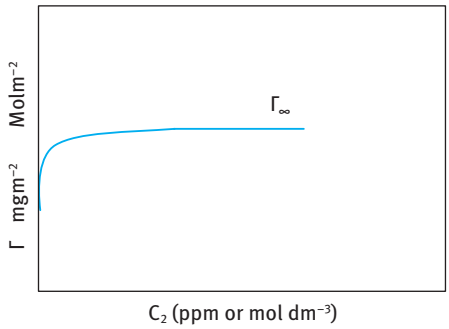

Fig. 12.2: High affinity isotherm.

In both cases a plateau adsorption value Γ_∞ is reached at a given value of C_2. In general, the value of Γ_∞ is reached at lower C_2 for polymeric surfactant adsorption when compared with small molecules. The high affinity isotherm obtained with polymeric surfactants implies that the first added molecules are virtually completely adsorbed and such a process is irreversible. The irreversibility of adsorption is checked by carrying out a desorption experiment. The suspension at the plateau value is centrifuged and the supernatant liquid is replaced by water. After redispersion, the suspension is centrifuged again and the concentration of the polymeric surfactant in the supernatant liquid is analytically determined. Owing to a lack of desorption, the above concentration will be very small indicating that the polymer remains on the particle surface.

12.3.2 Measurement of dispersion and particle size distribution

An effective dispersant should result in complete dispersion of the powder into single particles [1–3]. In addition, on wet milling (comminution) a smaller particle size distribution should be obtained. The efficiency of dispersion and reduction of particle size can be understood from the behaviour of the dispersant. Strong adsorption and an effective repulsive barrier prevent any aggregation during the dispersion process. It is necessary in this case to include the wetter (which should be kept at the optimum concentration). Adsorption of the dispersant at the solid/liquid interface results in lowering of γ_{SL} and this reduces the energy required for breaking the particles into smaller units. In addition, by adsorption in crystal defects, crack propagation occurs (the Rehbinder effect) and this results in the production of smaller particles.

Several methods may be applied for measuring the particle size distribution. Optical microscopy is by far the most valuable tool for a qualitative or quantitative examination of the dispersion. Information on the size, shape, morphology and aggregation of particles can be conveniently obtained with minimum time required for sample preparation. However, optical microscopy has some limitations:

(i) The minimum size that can be detected. The practical lower limit for accurate measurements of particle size is 1.0 μm, although some detection may be obtained down to 0.3 μm.
(ii) Image contrast may not be good enough for observation, particularly when using a video camera which is mostly used for convenience. The contrast can be improved by decreasing the aperture of the iris diaphragm, but this reduces the resolution.

Three main attachments to the optical microscope are possible.

(i) Phase contrast: This utilizes the difference between the diffracted waves from the main image and the direct light from the light source. The specimen is illuminated with a light cone and this illumination is within the objective aperture. The light illuminates the specimen and generates zero order and higher orders of diffracted

light. The zero order light beam passes through the objective and a phase plate which is located at the objective back focal plane. The difference between the optical path of the direct light beam and that of the beam diffracted by a particle causes a phase difference. The constructive and destructive interferences result in brightness changes which enhance the contrast. This produces sharp images, allowing one to obtain particle size measurements more accurately.

(ii) Differential interference contrast (DIC): This gives a better contrast than the phase contrast method. It utilizes a phase difference to improve contrast, but the separation and recombination of a light beam into two beams is accomplished by prisms. DIC generates interference colours and the contrast effects indicate the refractive index difference between the particle and medium.

(iii) Polarized light microscopy: This illuminates the sample with linearly or circularly polarized light, either in a reflection or transmission mode. One polarizing element, located below the stage of the microscope, converts the illumination to polarized light. The second polarizer is located between the objective and the ocular and is used to detect polarized light.

The optical microscope can be used to observe dispersed particles and flocs. Particle sizing can be carried out using manual, semiautomatic or automatic image analysis techniques. In the manual method (which is tedious), the microscope is fitted with a minimum of 10× and 43× achromatic or apochromatic objectives equipped with high numerical apertures (10×, 15× and 20×), a mechanical XY stage, a stage micrometre and a light source. One of the difficulties with the evaluation of dispersions by optical microscopy is the quantification of data. The number of particles in at least six different size ranges must be counted to obtain a distribution. This problem can be alleviated by the use of automatic image analysis, which can also give an indication of the floc size and its morphology.

Electron microscopy utilizes an electron beam to illuminate the sample. The electrons behave as charged particles which can be focused by annular electrostatic or electromagnetic fields surrounding the electron beam. Due to the very short wavelength of electrons, the resolving power of an electron microscope exceeds that of an optical microscope by ≈ 200 times. The resolution depends on the accelerating voltage which determines the wavelength of the electron beam and magnifications as high as 200 000 can be reached with intense beams but this could damage the sample. Mostly the accelerating voltage is kept below 100–200 kV and the maximum magnification obtained is below 100 000. Two main types of electron microscopes are used: transmission (TEM) and scanning (SEM). TEM displays an image of the specimen on a fluorescent screen and the image can be recorded on a photographic plate or film. The sample is deposited on a Formvar (polyvinyl formal) film resting on a grid to prevent charging of the sample. The sample is usually observed as a replica by coating with an electron transparent material (such as gold or graphite). The preparation of the sample for the TEM may alter the state of dispersion and cause aggregation. Freeze fracturing

techniques have been developed to avoid some of the alterations of the sample during sample preparation. Freeze fracturing allows the dispersions to be examined without dilution and replicas can be made of dispersions containing water. It is necessary to have a high cooling rate to avoid the formation of ice crystals. SEM can show particle topography by scanning a very narrowly focused beam across the particle surface. The electron beam is directed normally or obliquely at the surface. The back-scattered or secondary electrons are detected in a raster pattern and displayed on a monitor screen. The image provided by secondary electrons exhibits good three-dimensional detail. The back-scattered electrons, reflected from the incoming electron beam, indicate regions of high electron density. Most SEMs are equipped with both types of detectors. The resolution of the SEM depends on the energy of the electron beam which does not exceed 30 kV and hence the resolution is lower than that obtained by the TEM.

Confocal scanning laser microscopy (CLSM) is a very useful technique for identification of dispersions. It uses a variable pinhole aperture or variable width slit to illuminate only the focal plane by the apex of a cone of laser light. Out-of-focus items are dark and do not distract from the contrast of the image. As a result of extreme depth discrimination (optical sectioning) the resolution is considerably improved (up to 40 % when compared with optical microscopy). The CLSM technique acquires images by laser scanning or uses computer software to subtract out-of-focus details from the in-focus image. Images are stored as the sample is advanced through the focal plane and this allows one to construct three-dimensional images.

Scattering techniques are by far the most useful methods for characterizing dispersions and in principle they can give quantitative information on the particle or droplet size distribution, floc size and shape. The only limitation of the methods is the need to use sufficiently dilute samples to avoid interference such as multiple scattering which makes interpretation of the results difficult. Recently, however, back-scattering methods have been designed to allow one to measure the sample without dilution. In principle, one can use any electromagnetic radiation such as light, X-ray or neutrons, but in most industrial labs only light scattering is applied (using lasers).

Scattering techniques can be conveniently divided into the following classes:

(i) Time-average light scattering, static or elastic scattering.
(ii) Turbidity measurements, which can be carried out using a simple spectrophotometer.
(iii) Light diffraction technique.
(iv) Dynamic (quasi-elastic) light scattering that is usually referred as photon correlation spectroscopy (PCS). This is a rapid technique that is very suitable for measuring submicron particles or droplets (nano-size range).
(v) Back-scattering techniques that are suitable for measuring concentrated samples.

Application of any of these methods depends on the information required and availability of the instrument.

With time-average light scattering, the dispersion is sufficiently diluted to avoid multiple scattering and the sample is illuminated by a collimated light (usually laser) beam. The time-average intensity of scattered light is measured as a function of scattering angle. Three regimes can be identified:

(i) Rayleigh regime, where the particle radius R is smaller than $\lambda/20$ (where λ is the wavelength of incident light). The scattering intensity is given by the equation,

$$I(Q) = [\text{instrument constant}][\text{material constant}]NV_p^2. \tag{12.2}$$

Q is the scattering vector that depends on the wavelength of light used. The material constant depends on the difference between the refractive index of the particle or droplet and that of the medium. N is the number of particles or droplets and V_p is the volume of each particle or droplet. Assuming that the particles are spherical, one can obtain the average size using equation (12.2).

(ii) Rayleigh–Gans–Debye regime (RGD), $\lambda/20 < R < \lambda$. The RGD regime is more complicated than the Rayleigh regime and the scattering pattern is no longer symmetrical about the line corresponding to the 90° angle but favours forward scattering ($\theta < 90°$) or back scattering ($180° > \theta > 90°$).

(iii) Mie regime: $R > \lambda$. The scattering behaviour is more complex than the RGD regime and the intensity exhibits maxima and minima at various scattering angles depending on particle size and refractive index. The Mie theory for light scattering can be used to obtain the particle size distribution using numerical solutions. One can also obtain information on particle shape.

Turbidity measurements (total light scattering technique) can be used to measure particle size, flocculation and particle sedimentation. This technique is simple and easy to use (a single or double beam spectrophotometer or a nephelometer). For nonabsorbing particles, the turbidity τ is given by,

$$\tau = \frac{1}{L}\ln\left(\frac{I_0}{I}\right), \tag{12.3}$$

where L is the path length, I_0 is the intensity of incident beam and I is the intensity of transmitted beam. The particle size measurement assumes that the light scattering by a particle is singular and independent of other particles. Any multiple scattering complicates the analysis. According to Mie theory, the turbidity is related to the particle number N and their cross section πr^2 (where r is the particle radius) by

$$\tau = Q\,\pi r^2 N, \tag{12.4}$$

where Q is the total Mie scattering coefficient. Q depends on the particle size parameter α (which depends on particle diameter and wavelength of incident light λ) and the ratio of refractive index of the particles and medium m. Q depends on α in an oscillatory mode that exhibits a series of maxima and minima whose position depends

on m. For particles with $R < (1/20)\lambda$, $\alpha < 1$ and it can be calculated using Rayleigh theory. For $R > \lambda$, Q approaches 2 and between these two extremes, the Mie theory is used. If the particles are not monodisperse (as is the case with most practical systems), the particle size distribution must be taken into account. Using this analysis one can establish the particle size distribution using numerical solutions.

The light diffraction technique is a rapid and nonintrusive method for determining particle size distributions in the range 2–300 μm with good accuracy for most practical purposes. By combining light diffraction with forward light scattering, it is possible to increase the particle size range to the submicron region. In this way, one can measure the particle size distribution in the range 0.1 to 300 μm. Light diffraction gives an average diameter over all particle orientations since randomly oriented particles pass the light beam. A collimated and vertically polarized laser beam illuminates a particle dispersion and generates a diffraction pattern with the undiffracted beam in the centre. The energy distribution of diffracted light is measured by a detector consisting of light-sensitive circles separated by isolating circles of equal width. The angle formed by the diffracted light increases with decreasing particle size. The angle-dependent intensity distribution is converted by Fourier optics into a spatial intensity distribution. The spatial intensity distribution is converted into a set of photocurrents and the particle size distribution is calculated using a computer. Several commercial instruments are available, e.g. Malvern Mastersizer (Malvern, UK), Horiba (Japan) and Coulter LS Sizer (USA).

Photon correlation spectroscopy (PCS) or dynamic light scattering is a technique that utilizes Brownian motion to measure the particle size. As a result of Brownian motion of dispersed particles, the intensity of scattered light undergoes fluctuations that are related to the velocity of the particles. Since larger particles move less rapidly than the smaller ones, the intensity fluctuation (intensity versus time) pattern depends on particle size and this allows one to obtain the size distribution. In a system where Brownian motion is not interrupted by sedimentation or particle-particle interaction, the movement of particles is random. Thus to apply the PCS technique one must make sure that sedimentation does not occur during the measurement and the system is dilute enough to avoid particle-particle interaction.

The intensity fluctuation of the scattered light is measured using a photomultiplier and information on particle motion is obtained using a digital correlator. PCS allows one to measure the diffusion coefficient D of the particles that is related to the particle radius R by the Stokes–Einstein equation,

$$D = \frac{kT}{6\pi\eta R}, \tag{12.5}$$

where k is the Boltzmann constant, T is the absolute temperature and η is the viscosity of the medium.

The effect of particle interaction at relatively low particle concentration c can be taken into account by expanding the diffusion coefficient into a power series of concentration,

$$D = D_0(1 + k_D c), \tag{12.6}$$

where D_0 is the diffusion coefficient at infinite dilution, k_D is the virial coefficient that is related to particle interaction and c is the particle concentration.

PCS is a rapid, absolute and non-destructive method for particle size measurements. It has some limitations; the main disadvantage is the poor resolution of the particle size distribution. Also it suffers from the limited size range (absence of any sedimentation) that can be accurately measured. Several instruments are commercially available, e.g. by Malvern, Brookhaven, Coulter, etc.

The back-scattering technique is based on the use of fibre optics, sometimes referred to as fibre optic dynamic light scattering (FODLS), and it allows one to measure at high particle number concentrations. FODLS employs either one or two optical fibres. Alternatively, fibre bundles may be used. The exit port of the optical fibre (optode) is immersed in the sample and the scattered light in the same fibre is detected at a scattering angle of 180° (i.e. back-scattering). This technique is suitable for on-line measurements during manufacture of a suspension. Several commercial instruments are available, e.g. Lesentech (USA).

12.4 Wet milling (comminution)

The primary dispersion (sometimes referred to as the mill base) may then be subjected to a bead milling process to produce nanoparticles that are essential for some coating applications. Subdivision of the primary particles into much smaller units in the nano-size range (10–100 nm) requires application of intense energy. In some cases, high pressure homogenizers (such as the Microfluidizer, USA) may be sufficient to produce nanoparticles. This is particularly the case with many organic pigments. In some cases, the high pressure homogenizer is combined with application of ultrasound to produce the nanoparticles.

Milling or comminution (the generic term for size reduction) is a complex process and there is little fundamental information on its mechanism. For the breakdown of single crystals or particles into smaller units, mechanical energy is required. This energy in a bead mill is supplied by impaction of the glass or ceramic beads with the particles. As a result, permanent deformation of the particles and crack initiation result. This will eventually lead to the fracture of particles into smaller units. Since the milling conditions are random, some particles receive impacts far in excess of those required for fracture whereas others receive impacts that are insufficient for the fracture process. This makes the milling operation grossly inefficient and only a small fraction of the applied energy is used in comminution. The rest of the energy is dissipated as heat, vibration, sound, interparticulate friction, etc.

The role of surfactants and dispersants on grinding efficiency is far from being understood. In most cases, the choice of surfactants and dispersants is made by trial and error until a system is found that gives the maximum grinding efficiency. Rehbinder and his collaborators [10] investigated the role of surfactants in the grinding process. As a result of surfactant adsorption at the solid/liquid interface, the surface energy at the boundary is reduced and this facilitates the process of deformation or destruction. The adsorption of surfactants at the solid/liquid interface in cracks facilitates their propagation. This mechanism is referred to as the Rehbinder effect.

Several factors affect the efficiency of dispersion and milling:

(i) The volume concentration of dispersed particles (i.e. the volume fraction).
(ii) The nature of the wetting/dispersing agent.
(iii) The concentration of wetter/dispersant (which determines the adsorption characteristics).

For optimization of the dispersion/milling process the above parameters need to be systematically investigated [4]. From the wetting performance of a surfactant that can be evaluated using sinking time or contact angle measurements one can establish the nature and concentration of the wetting agent. The nature and concentration of dispersing agent required is determined by adsorption isotherm and rheological measurements.

Once the concentration of wetting/dispersing agent is established, dispersions are prepared at various volume fractions keeping the ratio of wetting/dispersing agent to the solid content constant. Each system is then subjected to dispersion/milling process keeping all parameters constant:

(i) Speed of the stirrer (normally one starts at lower speed and gradually increases the speed in increments at fixed time).
(ii) Volume and size of beads relative to the volume of the dispersion (an optimum value is required).
(iii) Speed of the mill. The change of average particle size with time of grinding is established using for example the Mastersizer.

Fig. 12.3 shows a schematic representation of the reduction of particle size with grinding time in minutes using a typical bead mill at various volume fractions.

The presentation in Fig. 12.3 is only schematic and is not based on experimental data. It shows the expected trend. When the volume fraction ϕ is below the optimum (in this case the relative viscosity of the dispersion is low) one requires a long time to achieve size reduction. In addition, the final particle size may be large and outside the nano-range. When ϕ is above the optimum value, the dispersion time is prolonged (due to the relatively high relative viscosity of the system) and the grinding time is also longer. In addition, the final particle size is larger than that obtained at the optimum ϕ. At the optimum volume fraction, both dispersion and grinding time are shorter and also the final particle size is smaller.

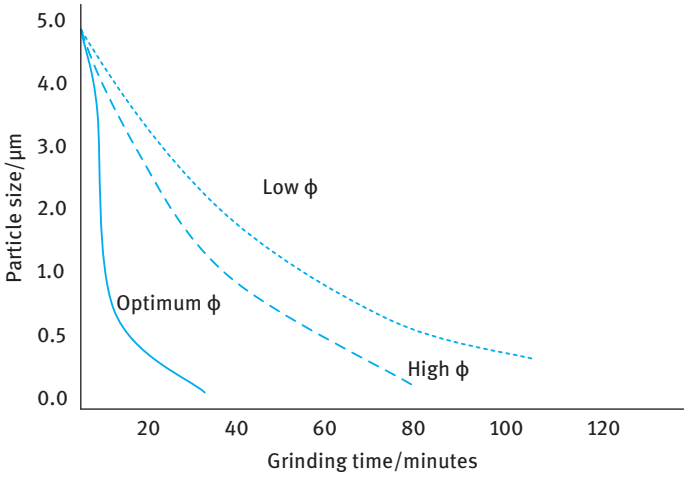

Fig. 12.3: Variation of particle size with grinding time in a typical bead mill.

Bead mills are commonly used for the preparation of nanodispersions. The beads are mostly made of glass or ceramics (which are preferred due to minimum contamination). The operating principle is to pump the premixed, preferably predispersed (using a high speed mixer), mill base through a cylinder containing a specified volume of say ceramic beads (normally 0.5–1 mm diameter to achieve nano-size particles). The dispersion is agitated by a single or multi-disc rotor. The disc may be flat or perforated. The mill base passing through the shear zone is then separated from the beads by a suitable screen located at the opposite end of the feed port [4].

Generally speaking, bead mills may be classified to two types:

(i) Vertical mills with open or closed top.
(ii) Horizontal mills with closed chambers.

The horizontal mills are more efficient and the most commonly used one are: Netzsch (Germany) and Dyno Mill (Switzerland). These bead mills are available in various sizes from 0.5 to 500 litres. The factors affecting the general dispersion efficiency are known reasonably well (from the manufacturer). The selection of the right diameter of the beads is important for maximum utilization. In general, the smaller the size of the beads and the higher their density, the more efficient the milling process.

The centrifugal force transmitted to the grinding beads at the tip of the rotating disc increases considerably by its weight. This applies greater shear to the mill base. This explains why the more dense beads are more efficient in grinding. The speed transmitted to the individual chambers of the beads at the tip of the disc assumes that speed and the force can be calculated.

The centrifugal force F is simply given by

$$F = \frac{v^2}{rg}, \tag{12.7}$$

where v is the velocity, r is the radius of the disc and g is the acceleration due to gravity.

References

[1] Tadros T. Suspension concentrates. Berlin: De Gruyter; 2017.
[2] Tadros T. Dispersions of powders in liquids and stabilisation of suspensions. Weinheim: Wiley-VCH; 2012.
[3] Tadros T. Applied surfactants. Weinheim: Wiley-VCH; 2005.
[4] Tadros T. Colloids in paints. Weinheim: Wiley-VCH; 2010.
[5] Deryaguin BV, Landau L. Acta Physicochem USSR. 1941;14:633.
[6] Verwey EJW, Overbeek JTG. Theory of stability of lyophobic colloids. Amsterdam: Elsevier; 1948.
[7] Napper DH. Polymeric stabilisation of colloidal dispersions. London: Academic Press; 1983.
[8] Tadros T. Polymeric surfactants. Berlin: De Gruyter; 2017.
[9] Tadros TF, Vandamme A, Levecke B, Booten K, Stevens CV. Advances Colloid Interface Sci. 2004;108–109:207.
[10] Rehbinder PA. Colloid J USSR. 1958;20:493.

13 Rheology of paint formulations

13.1 Introduction

As mentioned in Chapter 9, paints are complex colloidal dispersions of solid and "liquid" (latex) particles that are dispersed in a liquid medium (continuous phase) which could be aqueous or nonaqueous depending on the application. The continuous phase also contains various rheological modifiers, which could be polymers or inert fine solid particles. The interaction between the various components in a paint formulation results in a non-Newtonian system with complex rheological behaviour. Control of paint rheology is essential for successful utilization of the paint. Whatever application technique is used, e.g. in a spray gun, brush, roller, etc., three stages must be considered when considering the rheology of a paint [1]:

(i) Transfer of the paint from the bulk container to the applicator.
(ii) Transfer of the paint to the surface to form a thin and even film, i.e. film formation.
(iii) Flow-out of the film surface, coalescence of the polymer latex particles and loss of the medium by evaporation.

Each of these processes requires accurate control of the rheological characteristics.

In the bulk container, the paint should be of sufficiently low viscosity so that it can be readily utilized in the applicator. For application by a brush or a hand roller, the paint should readily penetrate the spaces between the bristles of a brush or the porous surface of the roller. The paint is then held by capillary/surface tension forces during the transfer to the surface to be painted. Control of the brush loading is crucial in any paint application. If the brush loading is too high, the total weight of the paint becomes sufficient to overcome the capillary forces, leading the paint to drip or run off the brush, clearly an undesirable result. In contrast, if the brush load is too low, this results in a thin paint film, or a nonuniform film with thicker film over a smaller surface area [1]. To achieve the optimum film thickness one should control the flow-out properties or rheology of the paint.

Increasing brush loading may be achieved by increasing the bulk paint viscosity or by introducing rheology modifiers. The latter are the most preferred option, since these rheology modifiers produce a shear thinning system, whereby the viscosity of the paint is rapidly reduced during application thus reducing the mechanical effort required to spread it into a film. The recovery of the viscosity after application prevents dripping or running of the paint. In addition, these rheology modifiers produce high residual viscosity thus preventing sedimentation of particles in the paint.

In industrial applications such as spraying or roller coating, control of the paint rheology is crucial. In spraying, the viscosity of the bulk paint must be low enough to allow the paint to be pumped through the fine jet of the spray gun with minimal application of pressure. In most cases, the paint is thinned from the higher solids

https://doi.org/10.1515/9783110578997-014

bulk immediately before application and during such a short period, settling of the particles is less of a problem. The rheology of the diluted paint has a big influence on the droplet spectrum of the sprayed paint [1]. One should avoid the formation of small spray droplets which may undergo drift on application. The use of rheological modifiers is essential to produce the optimum droplet size distribution in the spray.

In the roller coating process, the paint must be considerably thicker than that used in spray processes. The paint should be able to flow under gravity or low pumping energy to the surface of the application roller, where it may be spread to an even layer by the action of a doctor blade or another roller. In this case, the mechanical work required to cause the paint to flow is much less important. However, the paint must be viscous enough to prevent it running off or being thrown off the roller by centrifugal force.

In both spraying and roller coating applications the fluid flow rate and operating speed are very high and in this case both high stresses and high shear rates operate in the process. One should also note that the paint remains in the spray gun or the "nip" between the rollers for a very short time and hence a steady state is never reached. In this case only transient or high frequency rheological measurements are likely to produce relevant rheological parameters. Shear rates as high as $10^5\ s^{-1}$ can be reached in high speed rollers. At such high shear rates and in the presence of high molecular weight polymers in the paint formulation, a high extensional viscosity (which can be several orders of magnitude higher than the shear viscosity) can develop. The extensional viscosity of "thickened" water-based emulsion paints influences the application properties such as tracking, spattering, etc. One would expect that such a high extensional viscosity can interfere with the process of filament or jet rupture to form spray droplets [2].

The next process that must be considered in paint application is film formation. The loading and transfer of the paint by a brush or a roller from the bulk container to the surface to be painted is followed by regular movement of the brush or roller over the surface to transfer the load of the paint from the brush to the surface and spread it out in an even layer. During this process, hand pressure on the brush causes shearing and compression of the brush bristles or fibres of the rubber foam or fibrous mat typically covering the surface of a hand roller. The flow processes involved are very complex and very difficult to analyse. However, some attempts have been made to calculate the range of shear rates involved in paint brush applications. Ranges of $15–30\ s^{-1}$ were estimated for brush dipping and $2500–10\,000\ s^{-1}$ for brush spreading [3, 4].

The third and most important step in paint application is that of flow-out or levelling of the paint film, which involves latex coalescence and loss of medium by evaporation. This has a major influence on colour uniformity, hiding power as well as major flow faults such as sagging and slumping [5–7]. Unfortunately, there is still lack of understanding of the relevant theological parameters that affect these processes. There may be some correlation between elastic recovery and surface irregularity flow-out (levelling). Both pigment dispersions (mill bases) as well as the final paint formula-

tion show viscoelastic behaviour [8, 9]. This clearly demonstrates the importance of dynamic (oscillatory) measurements in the assessment of levelling properties.

Solvent evaporation during application will have a major effect on the rheological properties as well as the surface tension at the wet film/air interface. Evaporation results in an increase in the disperse volume fraction as well as a cooling effect at the film surface. Both effects lead to a tangential surface shearing force. It has been argued that the hydrostatic pressure gradient in a paint film is insufficient to explain the levelling effect. Whilst surface tension tends to produce a flat surface, irrespective of the substrate surface profile underneath, the surface tension gradient developing over the wet film tends to produce a uniform film thickness, i.e. the surface profile of the paint film mirrors exactly the surface profile of the substrate.

Solvent evaporation also leads to gradients in the solvent concentration through the film as well as across the surface. This leads to density gradients which with the surface tension gradients could contribute to circularly patterns being set up in the wet paint film. This may lead to the formation of Bernard cell patterns commonly observed at the surface of boiling or rapidly evaporating bulk liquid samples.

The complexity of the rheology of the applied paint film is shown by its viscoelastic behaviour as well as the nonlinear and time-dependent effects arising from the high shear during application. In addition, due to the concentration gradients through the film thickness, the rheology will also vary through the depth of the film. Rough calculations showed that the operative forces in levelling are in the range 3–5 Pa and in sagging are about 0.8 Pa at the surface of a typical paint film. The shear rates for levelling processes in paint films are in the range 10^{-3}–5×10^{-1}. Since the shear stress resulting from gravitational and surface tension forces control the flow in levelling and sagging, it is important to carry out constant stress (creep) measurements when considering the relation between paint rheology and its flow characteristics. Measurements of shear rates seem to be irrelevant in this case.

From the above discussion, one can summarize the desirable rheological characteristics of a paint formulation. It should have a sufficiently low viscosity to facilitate its transfer to the applicator. However, it should also have a sufficiently high residual (zero shear) viscosity to prevent particle sedimentation and sufficiently high modulus to prevent separation (syneresis). This requires the use of an appropriate rheology modifier which produces a "gel" structure that is easily "broken" during transfer from the bulk container. Because of the high shear rates and short timescales involved in the transfer process, both elasticity and extensional flow processes may modify the pattern of surface irregularities on the paint film. The paint must remain low in viscosity for a sufficient time for the surface irregularities to flow out to an acceptable extent. However, while the viscosity is low, the paint may flow on vertical surfaces under the influence of gravity. If the film thickness (film depth) builds up too much, sagging may become noticeable to the observer and lumps of thickened paint may result in an irregular film which is undesirable. To prevent this from occurring, the initial low viscosity

must be followed by a sharp rise in viscosity either by solvent evaporation and/or elastic recovery. The drying film becomes immobilized and sagging is prevented.

13.2 Experimental techniques for studying paint rheology

Several techniques can be applied for studying paint rheology. During the early stages of paint formulation, i.e. during research and development, one must carry out carefully controlled rheological methods, namely steady state shear stress–shear, constant stress (creep) and dynamic (oscillatory) measurements. The results from these controlled experiments can be applied to arrive at the optimum composition of a given paint formulation. Once this is established, much simpler methods must be used for quality control of the paint during manufacture. In this section I will start with the simple methods for quality control. This is then followed by a comprehensive list of the rheological methods that can be applied during the research and development stage.

13.2.1 Experimental methods for quality control

These methods must be fast, reliable and convenient to apply during paint manufacture. Three methods can be applied, namely by measuring the flow through constrictions, measuring the speed of an object moving through the paint or by measuring the relative speed of motion in a finite sample, the moving object can be shaped in the form of a spindle which is made to rotate in a fixed volume of the paint.

Flow through constrictions is best illustrated by the Ford cup, which has been extensively used in the paint industry [1]. A known volume of the paint is held within a vertical cylindrical cup, whose bottom has a short capillary of controlled length and diameter. The paint is released to flow through the hole in the bottom of the cup (usually by the operator releasing his finger) and the time for the paint to flow out of the cup is measured with a stopwatch. The flow endpoint is normally taken as the point at which the continuous liquid jet breaks up into drops. However, this simple technique suffers from several disadvantages. Firstly, because the liquid height varies during the test, the gravity force driving the liquid through the capillary also varies. Since the paint is non-Newtonian, the viscosity results can be misleading. Secondly, since the capillary is short, stable flow conditions within the capillary are not obtained. This effect together with the entry and exit errors may affect the result, particularly if the paint is elastic in nature. Thirdly, the presence of abrasive particles in the paint may lead to wear of the metal capillary. It is, therefore, necessary to frequently check the Ford cup using Newtonian liquids (e.g. silicone oils) of known viscosity.

Measuring the speed of an object moving through the paint is best illustrated by the Hoeppler-type viscometer whereby a solid ball of varying density serves as the

object. The fall of the ball can be electrically timed between two contacts and the time is a measure of the consistency of the material.

Perhaps the most useful (and commonly used) method for studying paint rheology is based on measuring the relative speed of motion of a spindle rotating in a fixed volume of the paint, as is illustrated by the Brookfield viscometer. Several spindles and rotation speeds are used to cover a wide range of viscosity. However, a limited range of shear rates are possible when using the Brookfield viscometer. An alternative instrument that is widely used in the paint industry is the Stormer viscometer, having a paddle as a rotational member.

Measurement of film flow-out (levelling and sagging) is perhaps the most difficult method for direct measurement of paint film rheology during flow-out (levelling). This is due to the fact that the rheology of paint film material is extremely complex, being not only viscoelastic but extremely nonlinear. In addition, the rheology of a paint film can change rapidly with time, due to solvent evaporation, an increase in solids volume fraction and rheological structure recovery. The paint film may also become inhomogeneous in composition through the film depth. For these reasons it is essential to have rapid methods for following the paint film rheology during flow-out. Several methods can be applied. In the impact method (bouncing ball) a 0.5 cm diameter steel ball (weight 0.5 g) is dropped on to a 1.25 cm thick glass slab coated with the paint under test [10]. The rebound height is measured as a function of time as the film dries. Initially, the rebound height decreases with time, since the viscosity of the film increases owing to solvent loss. Consequently, the energy dissipated by the film during the impact of the ball with the glass also increases and this results in a sharp decrease in the rebound height in this early stage of drying. However, as the film cures (either by autoxidation or "lacquer-type" drying), the film develops some elasticity and the rebound height increases. A schematic representation of the rebound height with drying time is given in Fig. 13.1. Using for example the ball momentum and energy losses, it is not easy to derive a relationship between rebound height and film viscosity. This is due to the additional factors such as the hydrodynamic force (which prevents the ball from actually touching the substrate surface) as well as the paint elasticity effects at the short times of impact (in the region of few tenths of a millisecond). In spite of these drawbacks, the method is simple and one can use paint films on different substrates (glass, metal, wood, etc.) and balls of different size.

The impedance method at high frequency depends on the fact that the mechanical impedance of an elastic shear wave propagating through a medium is changed by the presence of a viscoelastic layer at the surface of the medium. If the elastic wave is completely damped in this layer, the change in the characteristic impedance can be related to the rheological parameters of the layer material. This method can be applied to follow the changes in the paint film rheology during drying and curing. Pulses of high frequency oscillations (in the region of 2–100 MHz) are generated by means of a suitably-excited piezoelectric crystal attached to the support medium [11]. After propagation through the support, the attenuated pulses are again transformed into

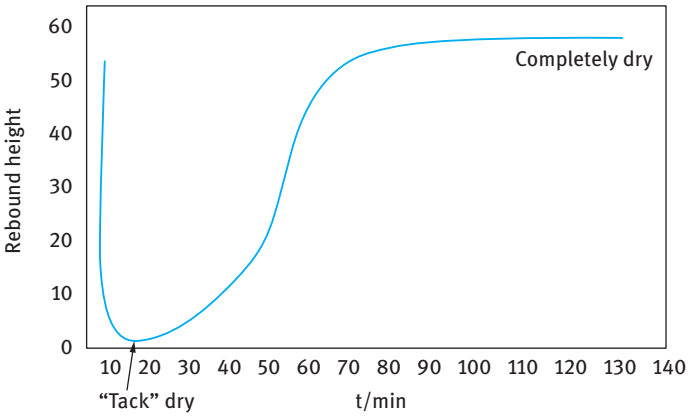

Fig. 13.1: Variation of rebound height with time for a 200 µm refinish paint film on glass.

electrical signals by a piezoelectric crystal attached to the support. This is schematically shown in Fig. 13.2. The phase angle and attenuation of the received pulses are measured and changes in their values are used to compare the rate changes in drying and curing of different paint films. Unfortunately, this technique is limited to measurements of the film properties during only a limited part of the total drying/curing process. In addition, the adhesion of the drying paint film to the substrate can have a big influence on the results.

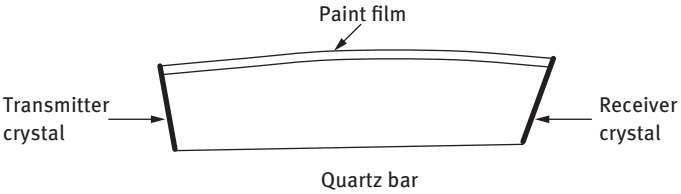

Fig. 13.2: Schematic representation of the impedance technique.

13.2.2 Rheological techniques for research and development of a paint system

Three main rheological methods can be applied:

(i) Steady state shear stress–shear rate measurements with particular attention to time effects (thixotropy).
(ii) Transient methods: Application of constant strain and following the relaxation of the stress with time (stress relaxation measurements) or application of constant stress and following the change of strain with time (creep measurements).
(iii) Dynamic (oscillatory) measurements.

Apart from these methods, two main investigations that are relevant to paint systems must be considered:
(iv) Normal force measurements.
(v) Elongational viscosity measurements.

13.2.2.1 Steady state shear stress–shear rate measurements

In these measurements, one applies different, constant rates of shear to the material and measures the resulting stress [12–15]. To calculate the shear stress–shear rate relationship one should have a well-defined geometry, the most common being the concentric cylinder, the cone and plate and the parallel plate configurations. Most paint systems show a pseudoplastic behaviour, as illustrated in Fig. 13.3 where the stress σ and viscosity η are plotted as a function of shear rate $\dot{\gamma}$.

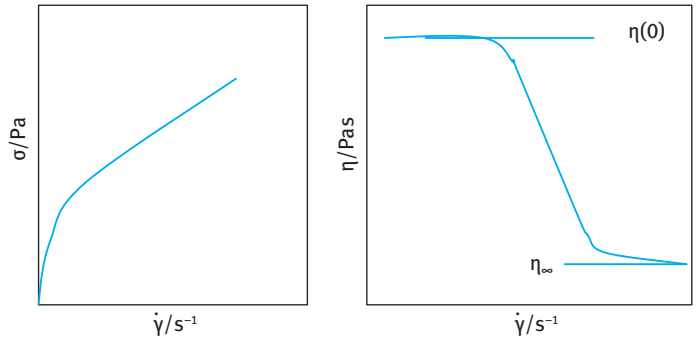

Fig. 13.3: Stress–shear rate and viscosity–shear rate relationship for a pseudoplastic system.

The curve in Fig. 13.3 shows the shear thinning behaviour of the system. It shows two plateaus (Newtonian) regions at low and high shear rate ranges. The low shear rate plateau region gives the residual (sometimes referred to as "zero shear rate") viscosity $\eta(0)$ whereas the high shear rate plateau region gives the lowest viscosity that is reached with a shear thinning system, sometimes referred to as η_∞. These two regions are separated by the shear thinning regime where the viscosity decreases with increasing shear rate. The residual viscosity $\eta(0)$ is an important parameter that determines particle sedimentation. A minimum value is needed to prevent sedimentation. The critical shear rate above which a paint shows the shear thinning behaviour is an important parameter that controls the transfer of the paint to the applicator. This critical shear rate should not be too high, otherwise the transfer of the paint from the container (which requires a low viscosity) becomes very difficult. The high shear rate viscosity η_∞ determines the flow of the paint on the substrate.

Several models have been suggested to analyse the flow curves of pseudoplastic systems:

(i) Power law fluid model,

$$\sigma = k\dot{\gamma}^n, \tag{13.1}$$

where k is the consistency index and n is the shear thinning index; $n < 1$.
By fitting the experimental data to equation (13.1) one can obtain k and n. The viscosity at a given shear rate can be calculated,

$$\eta = \frac{\sigma}{\dot{\gamma}} = \frac{k\dot{\gamma}^n}{\dot{\gamma}} = k\dot{\gamma}^{n-1}. \tag{13.2}$$

(ii) Herschel–Bulkley general model: many systems show a dynamic yield value followed by a shear thinning behaviour. The flow curve can be analysed using the Herschel–Bulkley equation [16]:

$$\sigma = \sigma_\beta + k\dot{\gamma}^n. \tag{13.3}$$

When $\sigma_\beta = 0$, equation (13.3) reduces to the power fluid model. The Herschel–Bulkley equation fits most flow curves with a good correlation coefficient and hence it is the most widely used model.

(iii) The Casson model [17]: This is a semi-empirical linear parameter model that has been applied to fit the flow curves of many paints and printing ink formulations [17],

$$\sigma^{1/2} = \sigma_C^{1/2} + \eta_C^{1/2}\gamma^{1/2}. \tag{13.4}$$

Thus a plot of $\sigma^{1/2}$ versus $\dot{\gamma}^{1/2}$ should give a straight line from which σ_C and η_C can be calculated from the intercept and slope of the line.
One should be careful in using the Casson equation since straight lines are only obtained from the results above a certain shear rate.

(iv) The Cross equation [18]. This can be used to analyse the flow curve of shear thinning systems that show a limiting viscosity $\eta(0)$ in the low shear rate regime and another limiting viscosity $\eta(\infty)$ in the high shear rate regime [18]. These two regimes are separated by a shear thinning behaviour as schematically shown in Fig. 13.4,

$$\frac{\eta - \eta(\infty)}{\eta(0) - \eta(\infty)} = \frac{1}{1 + k\gamma^n}, \tag{13.5}$$

where k is the consistency index and n is the shear thinning index.

13.2.2.2 Thixotropy

Most paints show thixotropic behaviour in addition to being pseudoplastic. Thixotropy was first defined as an isothermal, reversible sol–gel–sol transition [12]. This implies that the paint decreases in viscosity on shear (which is essential for ease of spreading and coating on the substrate), but builds up when the shearing process is

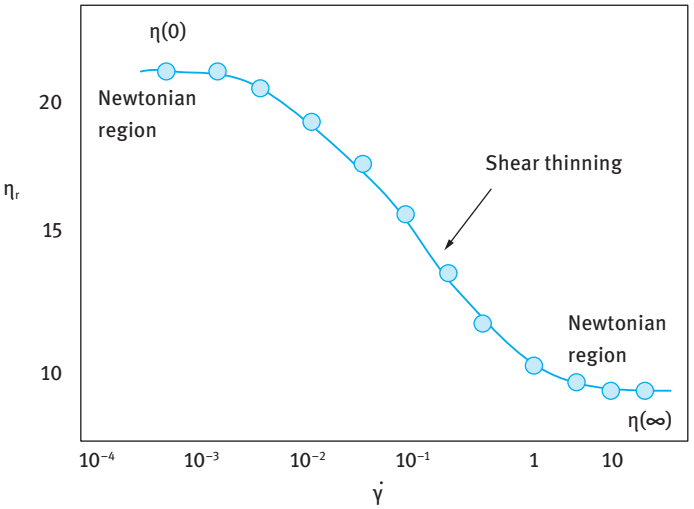

Fig. 13.4: Viscosity versus shear rate for shear thinning system.

stopped. Control of the time required for build-up of viscosity is essential for producing a paint film with the desirable properties. If the viscosity build-up is too fast, one may produce a film with brush marks from the applicator. If the viscosity build-up is too slow, dripping and sagging may occur.

A schematic representation of the thixotropic behaviour of a paint is shown schematically in Fig. 13.5. If the flow could be measured without stirring (i.e. without breaking the structure) the curve AB could be produced [19]. However, when increasing the rate of shear from 0 to $2W$, breakdown of the structure occurs, resulting in curve AC. While a continuous shear rate of $2W$ is applied over a period of time, the consistency of the paint decreases continuously from C to D, where it reaches a constant value, the lowest it can experience at the given shear rate of $2W$. Only a higher shear rate will be able to decrease the consistency further. If the shear is discontinued at point D, the build-up in the consistency of the paint to regain its original structure will follow along curve E, F or G, depending on the time which the particular paint requires for the building-up process.

Generally speaking, two methods can be applied to study thixotropy in a paint formulation. The first and the most commonly used procedure is the loop test in which the shear rate is increased continuously and linearly in time from zero to some maximum value and then decreased to zero in the same way [12]. This is illustrated in Fig. 13.6.

The main problem with the above procedure is the difficulty of interpreting the results. The nonlinear approach used is not ideal for developing loops because by decoupling the relaxation process from the strain one does not allow the recovery of the material. However, the loop test gives a qualitative behaviour of the paint thixotropy.

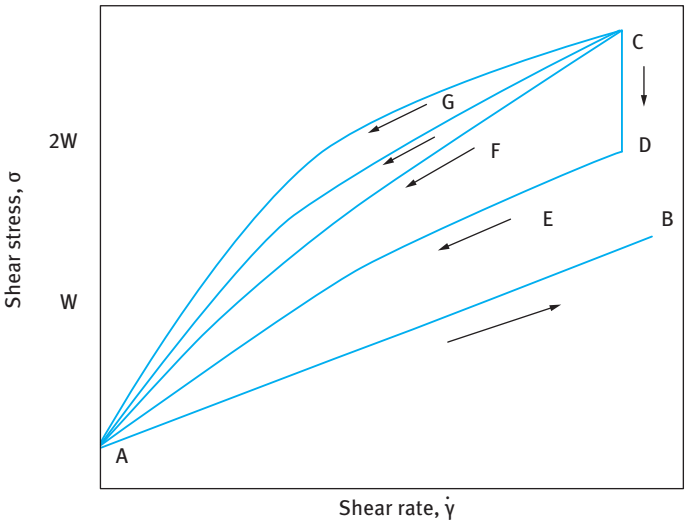

Fig. 13.5: Schematic representation of thixotropic paint.

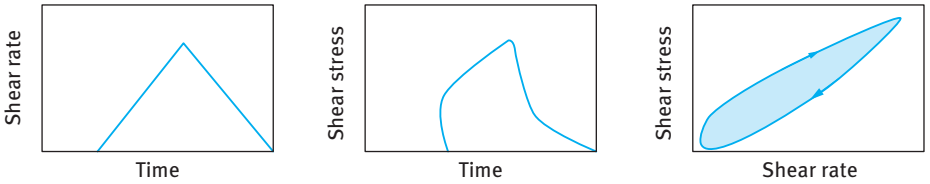

Fig. 13.6: Loop test for studying thixotropy.

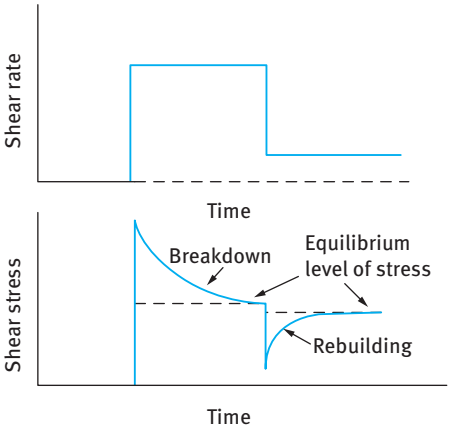

Fig. 13.7: Step change test for studying thixotropy.

An alternative method for studying thixotropy is to apply a step change test, whereby the paint is suddenly subjected to a constant high shear rate and the stress is followed as a function of time as the structure breaks down and an equilibrium value is reached [12]. The stress is further followed as a function of time to evaluate the rebuilding of the structure. A schematic representation of this procedure is shown in Fig. 13.7.

Application of the above tests for a highly elastic paint is not straightforward since there are contributions to the stress growth and decay from viscoelasticity. The occurrence of thixotropy implies that the flow must be taken into account when making predictions of flow behaviour.

13.2.2.3 Transient methods for studying paint rheology

Two transient methods can be applied to study paint rheology:

(i) Stress relaxation after sudden application of strain.
(ii) Strain relaxation after sudden application of stress (creep measurements) [12–15, 20].

In the stress relaxation method, a constant strain γ is applied within a very short period (that must be much smaller than the relaxation time of the sample) and the stress σ is followed immediately as a function of time. For a viscoelastic liquid (which is the case with many paint systems), the stress decreases exponentially with time t and reaches zero at infinite time. This is illustrated in Fig. 13.8.

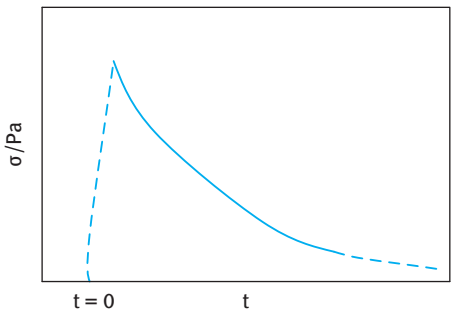

Fig. 13.8: Stress relaxation after sudden application of strain.

If the stress is divided by the applied constant strain one obtains the stress relaxation modulus $G(t)$, which is related to the instantaneous modulus by the following expression,

$$G(t) = \frac{\sigma(t)}{\gamma} = \frac{\sigma(0)}{\gamma} \exp\left(-\frac{t}{\tau_m}\right) = G(0) \exp\left(-\frac{t}{\tau_m}\right). \tag{13.6}$$

For a viscoelastic solid, the modulus reaches a limiting value G_e at long time (sometimes referred to as the equilibrium modulus). This is illustrated in Fig. 13.9.

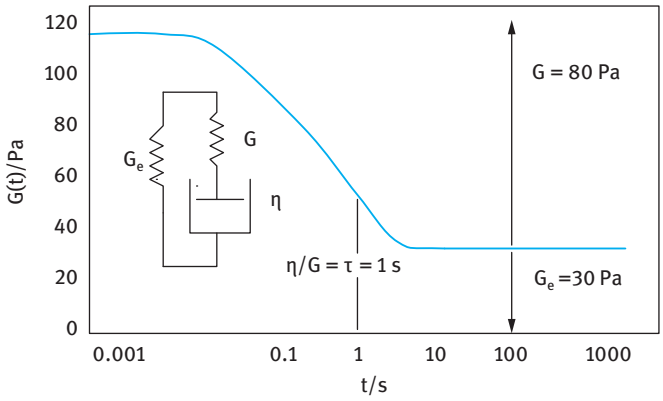

Fig. 13.9: Variation of $G(t)$ with t for a viscoelastic solid.

In this case, equation (13.6) has to be modified to account for G_e

$$G(t) = G(0)\exp\left(-\frac{t}{\tau_m}\right) + G_e. \tag{13.7}$$

Note that according to equation (13.6) that $t = \tau_m$ when $\sigma(t) = \sigma(0)/e$ or when $G(t) = G(0)/e$. This shows that stress relaxation can be used to obtain the relaxation time for a viscoelastic liquid.

In the constant stress (creep) method, a constant stress σ is applied on the system (that may be placed in the gap between two concentric cylinders or a cone and plate geometry) and the strain (relative deformation) γ or compliance J ($= \gamma/\sigma$, Pa^{-1}) is followed as a function of time for a period of t. At $t = t$, the stress is removed and the strain γ or compliance J is followed for another period t.

The above procedure is referred to as "creep measurement". From the variation of J with t when the stress is applied and the change of J with t when the stress is removed (in this case J changes sign) one can distinguish between viscous, elastic and viscoelastic response. This is illustrated in Fig. 13.10.

For viscoelastic response (as is the case with most paint systems) the following trend is observed: at $t = 0$, J shows a sudden increase and this is followed by a slower increase for the time applied. When the stress is removed, J changes sign and J shows an exponential decrease with increasing time (creep recovery), but it does not reach 0 as is the case with an elastic response. This is illustrated in Fig. 13.11.

For a viscoelastic liquid, the compliance $J(t)$ is given by two components: an elastic component J_e that is given by the reciprocal of the instantaneous modulus and a viscous component J_v that is given by $t/\eta(0)$

$$J(t) = \frac{1}{G(0)} + \frac{t}{\eta(0)}. \tag{13.8}$$

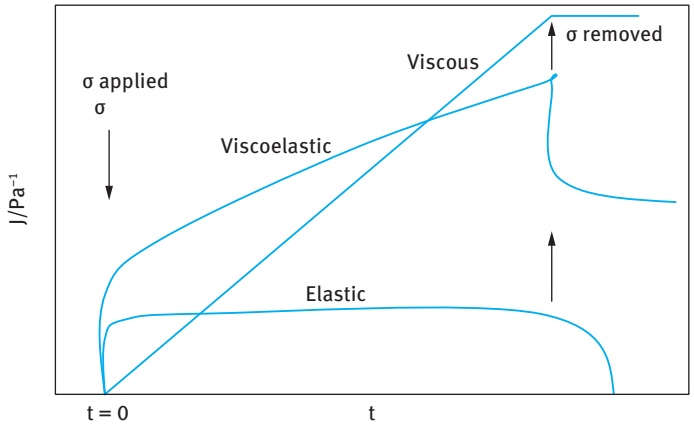

Fig. 13.10: Creep curves for viscous, elastic and viscoelastic responses.

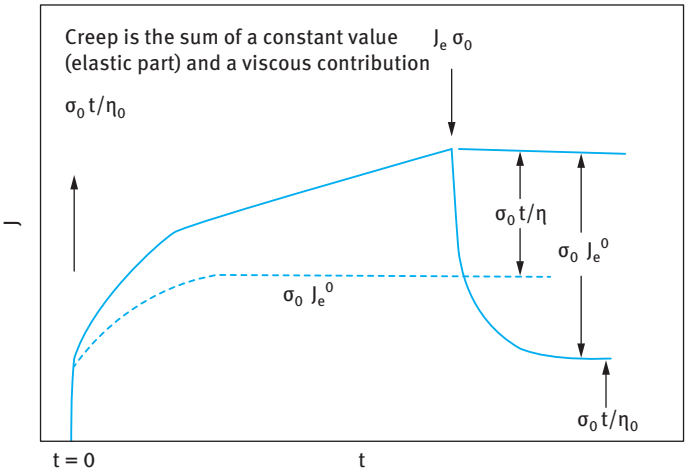

Fig. 13.11: Creep curve for a viscoelastic liquid.

The Maxwell relaxation time τ_M is given by,

$$\tau_M = \frac{\eta(0)}{G(0)}. \tag{13.9}$$

For a viscoelastic solid, complete recovery occurs and the system is characterized by a Kelvin retardation time τ_k that is also given by the ratio of $\eta(0)/G(0)$.

The Berger model (Maxwell + Kelvin) represents most practical paints consisting of a Maxwell element and a Kelvin element. The modulus of the spring in the Maxwell element is G_1 and the viscosity in the dash-pot is η_1. The Maxwell relaxation time is η_1/G_1. The modulus of the spring in the Kelvin element is G_2 and the viscosity in

the dash-pot is η_2. The Kelvin retardation time is η_2/G_2. The Berger model gives an instantaneous elastic response from G_1 and a continuous viscous response from η_1.

More complex models can be introduced: The generalized Maxwell model in which several elements with different relaxation times are introduced. The generalized Kelvin model also consists of several Kelvin elements with different retardation times [12].

In creep experiments one starts with a low applied stress (below the critical stress σ_{cr}) at which the system behaves as a viscoelastic solid with complete recovery [12]. The stress is gradually increased and several creep curves are obtained. Above σ_{cr} the system behaves as a viscoelastic liquid showing only partial recovery. Fig. 13.12 shows a schematic representation of the variation of compliance J with time t at increasing σ (above σ_{cr}).

From the slopes of the lines one can obtain the viscosity η_σ at each applied stress. A plot of η_σ versus σ is shown in Fig. 13.13. This shows a limiting viscosity $\eta(0)$ below σ_{cr} and above σ_{cr} the viscosity shows a sharp decrease with a further increase in σ.

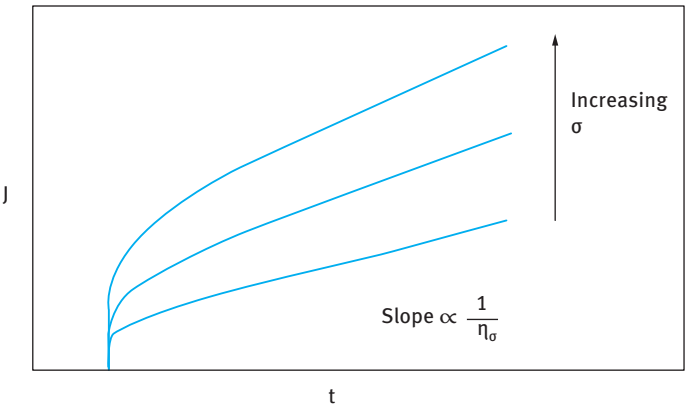

Fig. 13.12: Creep curves at increasing applied stress.

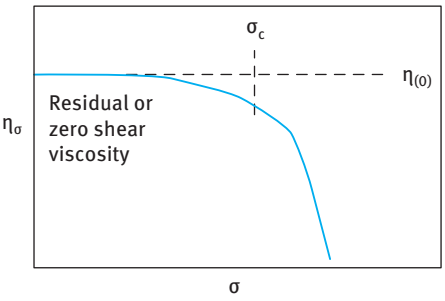

Fig. 13.13: Variation of viscosity with applied stress.

$\eta(0)$ is referred to as the residual or zero shear viscosity, which is an important parameter for predicting sedimentation. σ_{cr} is the critical stress above which the structure "breaks down". It is sometimes referred to as the "true" yield stress.

13.2.2.4 Dynamic (oscillatory) techniques

This is the response of the material to an oscillating stress or strain. When a sample is constrained in, say, a cone and plate or concentric cylinder assembly, an oscillating strain at a given frequency ω (rad s^{-1}) ($\omega = 2\nu\pi$, where ν is the frequency in cycles s^{-1} or Hz) can be applied to the sample. After an initial start-up period, a stress develops in response to the applied strain, i.e. it oscillates with the same frequency. The change of the sine waves of the stress and strain with time can be analysed to distinguish between elastic, viscous and viscoelastic response. Analysis of the resulting sine waves can be used to obtain the various viscoelastic parameters as discussed below

Three cases can be considered: Elastic response, whereby the maximum of the stress amplitude is at the same position as the maximum of the strain amplitude (no energy dissipation). In this case there is no time shift between stress and strain sine waves. Viscous response, whereby the maximum of the stress is at the point of maximum shear rate (i.e. the inflection point) where there is maximum energy dissipation. In this case the strain and stress sine waves are shifted by $\omega t = \pi/2$ (referred to as the phase angle shift δ which in this case is 90°). Viscoelastic response, in this case the phase angle shift δ is greater than 0 but less than 90°.

Let us consider the case of a viscoelastic system as illustrated in Fig. 13.14.

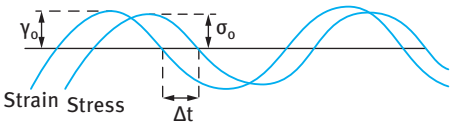

Δt = time shift for sine waves of stress and strain
Δt ω = δ, phase angle shift
ω = frequency in radian s^{-1}
ω = 2 π ν

Perfectly elasic solid	δ = 0
Perfectly viscous liquid	δ = 90°
Viscoelastic system	0 < δ < 90°

Fig. 13.14: Strain and stress sine waves for a viscoelastic system.

The frequency ω is in rad s^{-1} and the time shift between strain and stress sine waves is Δt. The phase angle shift δ is given by (in dimensionless units of radians)

$$\delta = \omega\Delta t. \tag{13.10}$$

For a perfectly elastic solid $\delta = 0$; for a perfectly viscous liquid $\delta = 90°$; for a viscoelastic system $0 < \delta < 90°$

The ratio of the maximum stress σ_0 to the maximum strain γ_0 gives the complex modulus $|G^*|$

$$|G^*| = \frac{\sigma_0}{\gamma_0}. \tag{13.11}$$

$|G^*|$ can be resolved into two components: Storage (elastic) modulus G'; the real component of the complex modulus. Loss (viscous) modulus G''; the imaginary component of the complex modulus,

$$|G^*| = G' + \mathrm{i}G'', \tag{13.12}$$

where i is the imaginary number that is equal to $(-1)^{1/2}$.

The complex modulus can be resolved into G' and G'' using vector analysis and the phase angle shift,

$$G' = |G^*| \cos \delta, \tag{13.13}$$

$$G'' = |G^*| \sin \delta, \tag{13.14}$$

$$\tan \delta = \frac{G''}{G'}. \tag{13.15}$$

Dynamic viscosity η'

$$\eta' = \frac{G''}{\omega}. \tag{13.16}$$

Note that $\eta \to \eta(0)$ as $\omega \to 0$.

Both G' and G'' can be expressed in terms of frequency ω and Maxwell relaxation time τ_m by,

$$G'(\omega) = G\frac{(\omega\tau_\mathrm{m})^2}{1 + (\omega\tau_\mathrm{m})^2}, \tag{13.17}$$

$$G''(\omega) = G\frac{\omega\tau_\mathrm{m}}{1 + (\omega\tau_\mathrm{m})^2}, \tag{13.18}$$

where G is the plateau (high frequency) modulus.

In oscillatory techniques one has to carry two types of experiments: Strain sweep, the frequency ω is kept constant and G^*, G' and G'' are measured as a function of strain amplitude. Frequency sweep; the strain is kept constant (in the linear viscoelastic region) and G^*, G' and G'' are measured as a function of frequency.

In the strain sweep experiments, the frequency is fixed say at 1 Hz (or 6.28 rad s^{-1}) and G^*, G' and G'' are measured as a function of strain amplitude γ_0. This is illustrated in Fig. 13.15.

G^*, G' and G'' remain constant up to a critical strain γ_cr. This is the linear viscoelastic region where the moduli are independent of the applied strain. Above γ_cr, G^* and G' start to decrease whereas G'' starts to increase with any further increase in γ_0. This is the nonlinear region. γ_cr may be identified with the critical strain above which the structure starts to "break down". It can also be shown that above another

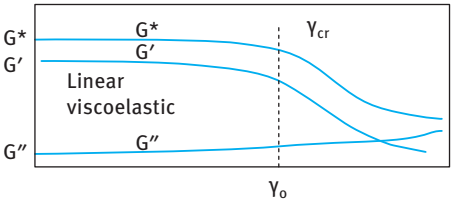

Linear viscoelastic region
G*, G′ and G″ are independent of strain amplitude
γ_{cr} is the critical strain above which systems shows non-linear response (break down of structure)

Fig. 13.15: Schematic representation of strain sweep.

critical strain, G'' becomes higher than G'. This is sometimes referred to as the "melting strain" at which the system becomes more viscous than elastic.

In the oscillatory sweep experiments, the strain γ_0 is fixed in the linear region (taking a midpoint, i.e. not too low a strain where the results may show some "noise" and far from γ_{cr}). G^*, G' and G'' are then measured as a function of frequency (a range of 10^{-3}–10^2 rad s^{-1} may be chosen depending on the instrument and operator patience). This is illustrated in Fig. 13.16. One can identify a characteristic frequency ω^* at which $G' = G''$ (the "crossover point") which can be used to obtain the Maxwell relaxation time τ_m

$$\tau_m = \frac{1}{\omega^*}. \tag{13.19}$$

In the low frequency regime, i.e. $\omega < \omega^*$, $G'' > G'$. This corresponds to a long time experiment (time is reciprocal of frequency) and hence the system can dissipate energy as viscous flow. In the high frequency regime, i.e. $\omega > \omega^*$, $G' > G''$. This corresponds to a short time experiment where energy dissipation is reduced. At sufficiently high frequency, $G' \gg G''$. At such high frequency, $G'' \to 0$ and $G' \approx G^*$. The high frequency modulus $G'(\infty)$ is sometimes referred to as the "rigidity modulus" where the response is mainly elastic. For a viscoelastic solid, G' does not become zero at low frequency. G'' still shows a maximum at intermediate frequency.

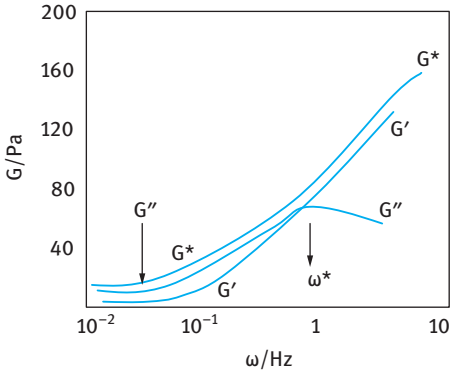

Fig. 13.16: Schematic representation of oscillatory measurements for a viscoelastic liquid.

The cohesive energy density, which is an important parameter for identifying the "strength" of the structure in a dispersion can be obtained from the change of G' with γ_0

$$E_c = \int_0^{\gamma_{cr}} \sigma \, d\gamma, \tag{13.20}$$

where σ is the stress in the sample that is given by,

$$\sigma = G'\gamma \tag{13.21}$$

$$E_c = \int_0^{\gamma_{cr}} G'\gamma_{cr} \, d\gamma = \frac{1}{2}\gamma_{cr}^2 G'. \tag{13.22}$$

Note that E_c is given in J m^{-3}.

13.2.2.5 Normal force

Normal stresses may be responsible for the flow behaviour of some paint formulations. The most well-known and certainly the most dramatic effect is the rod-climbing phenomenon, referred to as the "Weissenberg effect". It is observed when a rotating rod is dipped into a squat vessel containing an elastic liquid. Whereas a Newtonian liquid would be forced to the rim of the vessel by inertia, and thus produce a free surface that is higher at the rim than near the rod, the elastic liquid produces a free surface that is much higher near the rod. The Weissenberg effect may be viewed as a direct consequence of normal stress which acts like a hoop stress around the rod. This stress causes the liquid to "strangle" the rod and hence move along it.

Consider for example a material possessing both elasticity and viscosity is placed in the gap between parallel plates. If the upper plate is moved at a constant velocity v (or shear rate $\dot{\gamma}$), then due to the presence of elasticity (resistance to continuous deformation exerted by the material) the total force exerted on the moving plate is at an angle to the direction of motion. This total force can be resolved into its components, which include a force parallel to and in the same plane as the plate, as well as a component in a plane vertical to the plane of motion and at right angles to the direction of motion. The latter is the normal force. In practical terms, the normal force tries to push the plates apart while there is motion. In practical instruments, the moving plate must be either held rigidly in the vertical plane, or it can be allowed to move and kept in position by applying an equal and opposite restoring force to counteract the normal force. This approach allows one to measure the normal force.

13.2.2.6 Extensional (elongational) viscosity

The importance of measuring viscosity under extensional conditions is well known in the area of fibre formation, i.e. strongly spinnable materials. However, it has been rec-

ognized that measuring extensional viscosity is of direct relevance in many other areas such as ink jet printers, roll mills, blade coating, curtain coating, emulsions, suspensions, etc. Thus, measurement of extensional viscosity of paint systems could be important for several applications. With many polymer solutions, the extensional viscosity can be several orders of magnitude higher than the shear viscosity. The same may apply to some paint systems which contain high molecular weight polymers (rheology modifiers). Unfortunately, measuring extensional viscosity is not easy, although recently some manufacturers have designed special instruments for such experiments.

13.3 Application of rheological techniques to paint formulations

Any change in the physical or chemical characteristics of a paint formulation is directly reflected in its flow characteristics or rheology. These changes can occur as a result of aging, temperature changes, application of shear, type of dispersion, extent of grinding and mixing as well as addition of special surfactants for some applications.

The aging of a paint (during storage) can cause an increase or decrease in consistency. This change in consistency could be due to flocculation that may result from desorption of the dispersant during storage or simply by temperature fluctuations. Some chemical changes may also occur as a result of the reaction between the solid and liquid phases [1].

The change in consistency can be followed by measuring the flow curves at various intervals of time as illustrated in Fig. 13.17. This presentation illustrates that the consistency of the paint increases on storage, which is most likely due to flocculation. The flow curves can be analysed using the models described above. Using these models one can calculate the yield value and the viscosity as a function of storage time. Both parameters show an increase with increasing storage time.

Another important investigation is to follow the thixotropic behaviour of the paint during storage. As mentioned above, thixotropy can be investigated using the thixotropic loop or the step change method. Any flocculation will also be accompa-

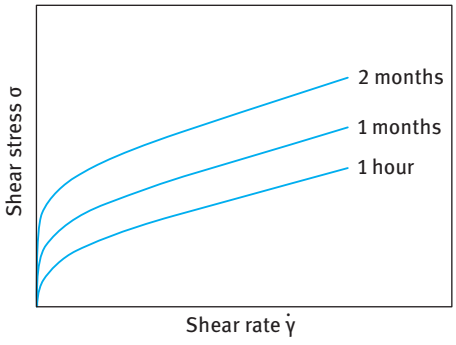

Fig. 13.17: Schematic representation of the change in the flow curve of a paint system at various times.

nied by a change in the thixotropic behaviour. Clearly, a physically stable paint should show no change in its rheological behaviour on storage for at least 6 months and also at various temperatures to which the paint system will be subjected. A more sensitive method for following the change in consistency on storage is constant stress or creep measurements. As discussed above, these measurements allows one to obtain the residual (or zero shear) viscosity $\eta(0)$ as well as the critical stress σ_{cr} above which the structure breaks down. Any increase in $\eta(0)$ and σ_{cr} indicate flocculation of the paint on storage. A third and sensitive method to follow the change of consistency on storage is the dynamic (oscillatory) method that was described above. By following the change of elastic modulus and cohesive energy during storage one can obtain information on the flocculation of the paint.

The consistency or the viscosity η of most paint formulations decrease with increasing temperature. However, in some cases the viscosity may show an increase with increasing temperature when this reaches a critical value. In most cases this is due to sudden flocculation of the paint above a critical temperature (referred to as the critical flocculation temperature, CFT). This flocculation may result from a decreased solvency of the chains to worse than θ-solvent above a critical temperature. Alternatively, the flocculation may occur as a result of desorption of the dispersant at high temperature due to the sudden increase in its solubility.

Due to the above changes in the state of the paint with changing temperature, the viscosity–temperature relationship seldom follows an Arrhenius plot (which shows a linear relationship between log η versus $(1/T)$, where T is the absolute temperature).

A rapid technique to study the effect of temperature changes on the flocculation of a paint formulation is to carry out temperature sweep experiments, running the samples from say 5–50 °C. The trend in the variation of σ_β and η_{pl} with temperature can quickly give an indication of the temperature range at which a paint remains stable (during that temperature range σ_β and η_{pl} remain constant).

13.4 Dispersion and ingredients

Most paint formulations consist of a mixture of suspension particles (pigments) and emulsion droplets (latex particles that are liquid-like at room temperature) referred to as suspoemulsions. The continuous medium with viscosity η_0 may be simply an aqueous phase in which several ingredients are dissolved or could be nonaqueous (oil) that may consist of two or more miscible oils. For non-Newtonian systems (which is the case with paint systems) some empirical equations can be established to relate the plastic viscosity η_{pl} and yield value σ_β to the volume fraction of the disperse phase ϕ [1],

$$\eta_{pl} = (\eta_0 + A)\exp(B\phi) \tag{13.23}$$

$$\sigma_\beta = M\exp(n\phi) \tag{13.24}$$

B, M and n are related to particle size, shape and surface. A is independent of particle size but may depend on particle shape and surface. A may be related to particle-particle interaction in the dispersion.

Equations (13.23) and (13.24) predict a linear relationship between log η_{pl} or log σ_β and ϕ. This is illustrated in Fig. 13.18 and 13.19 which also show the effect of average particle diameter (volume to surface ratio d_{32}) of the pigment [1]. The smaller the size, the higher the slope. This is illustrated in Fig. 13.20, which shows the variation of the exponents B and n with particle diameter. As is clear, both B and n increase with decreasing d_{32}.

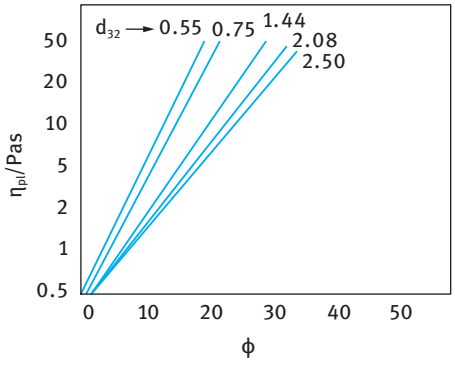

Fig. 13.18: Variation of log η_{pl} with ϕ for leaded ZnO suspensions with different particle diameters d_{32}.

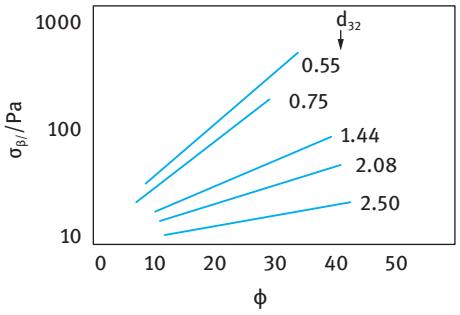

Fig. 13.19: Variation of yield value σ_β with volume fraction ϕ for ZnO suspensions at various particle diameters d_{32}.

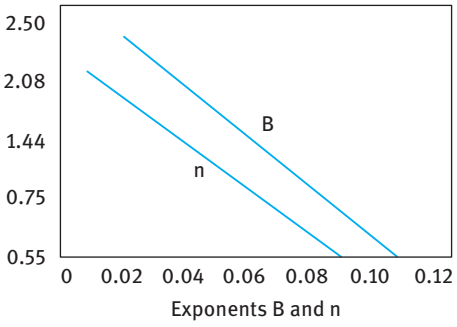

Fig. 13.20: Variation of exponents B and n with average particle diameter d_{32}.

Surface active agents are added to aid the wetting of the pigment powder. Dispersing agents (mostly polymeric surfactants) are also added to stabilize the particles against aggregation. Both materials affect the viscosity and yield value of the final paint dispersion by adsorption at the solid/liquid interface. The main purpose of wetters and dispersants is to produce "better dispersion" by causing deaggregation and deflocculation. Deaggregation is a mechanical or chemical separation of single particles in an aggregate. The aggregate consisting of these unit particles is "glued" together, thus preventing the liquid from penetrating into the aggregated mass and thus surrounding each unit particle. Deflocculation, on the other hand, can only be affected by the use of a dispersing agent. The mechanical force does not change the state of flocculation. A flocculate is a "loose" but connected structure of particles, whereby the particles are far enough apart to permit the liquid to surround them. However, the particles are sufficiently close to each other with strong van der Waals attraction. Thus, the dispersion will not flow until enough shearing stress is applied to overcome these attractive forces. This shearing stress is proportional to the yield value. A dispersant that is strongly adsorbed to the particle surface and provides sufficient repulsive forces can overcome the van der Waals attraction, thus causing a marked reduction in the yield value.

It should be mentioned that controlled flocculation of a pigment dispersion can be desirable to prevent settling and formation of hard sediments and to control the surface finish of a coating. For pigments dispersed in oil, small quantities of a polar liquid such as alcohol, glycerol and butanol are used as flocculating agents. For hydrophilic pigments suspended in aqueous media, oils and oil-soluble agents, such as lecithin can induce flocculation.

13.5 Grinding and mixing

In general increase in the viscosity of a dispersion results in an increase in the efficiency of milling. This is schematically represented in Fig. 13.21 for a three-roller mill, which shows the variation of milling time with the plastic viscosity of the dispersions measured using a rotational viscometer [1].

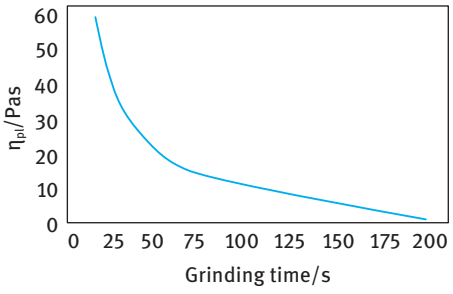

Fig. 13.21: Schematic representation of the effect of dispersion viscosity on grinding time.

It should be mentioned that the trend shown in Fig. 13.21 gives only an indication since the operational viscosity in the three-roller mill is not the same as the plastic viscosity measured using a rotational viscosity. Apparently, the yield value does not affect the grinding efficiency, as long as it is low enough that the material flows readily from the feed rollers.

In ball milling, the viscosity of the dispersion also plays an important role. A practical viscosity for good operation depends on the nature of the balls. When using steel ball mills, a high viscosity (up to 20 Pa s) can be used. With pebble and porcelain ball mills, a lower viscosity is required since the weight of the grinding medium is lower. It should also be mentioned that the viscosity measured before mixing is substantially different from that existing during the mixing operation. The flow properties of the dispersion during the process of grinding change as a result of increasing temperature, increasing wetting, increased degree of aggregation and improved interaction between the solid and liquid phases.

Microscopic investigations showed an increase in deaggregation during milling and this is accompanied by an increase in colour strength [21]. This is schematically illustrated in Fig. 13.22, which shows the change of plastic viscosity, yield value and colour strength for a carbon black dispersion in mineral oil.

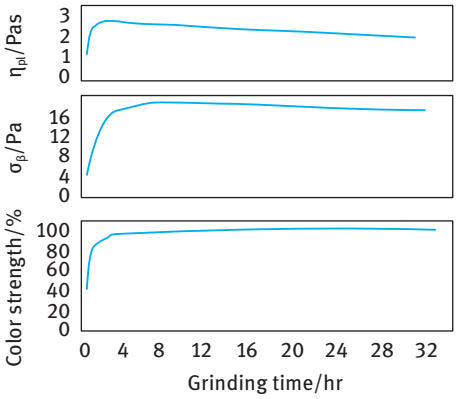

Fig. 13.22: Change in flow properties and colour strength of carbon black suspensions in mineral oil as a function of ball milling time.

Because the shear rate is much higher during milling than the maximum value measured in a rotational viscometer (usually of the order of 1000 s^{-1}), the viscosity of a pseudoplastic plastic material will decrease substantially, while its yield value may increase during milling. The viscosity of a thixotropic dispersion will decrease substantially, while its yield value may increase during milling. Thus, to evaluate the grinding performance, the consistency of the dispersion at the operational grinding conditions and at different steps of processing has to be determined. This may require measuring the viscosity at a much higher shear rate than that encountered with rotational viscometers, as for example determined using capillary viscometers (which can operate at much higher shear rates).

13.6 Application of rheology for paint evaluation

Rheology is perhaps one of the most powerful techniques for paint evaluation during its formulation as well as in its manufacture. Before a paint is manufactured, its application is known and it is essential to control its flow properties for best operation and application. To control the flow properties of the paint, a rheometer must be selected to make flow measurements that will permit good interpretation of the flow properties of the paint. This allows the manufacturer to decide whether two batches of the same material or of different materials will have equal flow behaviour under all conditions of operational application. The manufacturer could also predict from these flow measurements whether there is any difference in physical properties on paint application. In the preoperational stage, physical effects which occur in manufacturing and storing, such as temperature effects, evaporation, mixing procedures and shelf life must be studied. These physical effects can be correlated to the flow characteristics of the paint formulation. This allows one to achieve a more efficient and better controlled operation in manufacture and application.

To date, many paint manufacturers use one-point measurements for measuring the consistency. This can, for example, be carried out using a simple Brookfield viscometer using one spindle at a given rpm. This one-point measurement can be misleading [20]. To illustrate this point let us consider three systems, namely Newtonian, Bingham plastic and pseudoplastic with thixotropy as illustrated in Fig. 13.23. At a specific shear rate, all the three systems show the same apparent viscosity although their flow behaviour (using the full shear-stress curves) are significantly different [1]. These systems will show entirely different behaviour on application at the shear rate at which the apparent viscosity is the same. A study of the flow curves indicates that the Newtonian system will flow at extremely low shear rates, whereas the plastic and

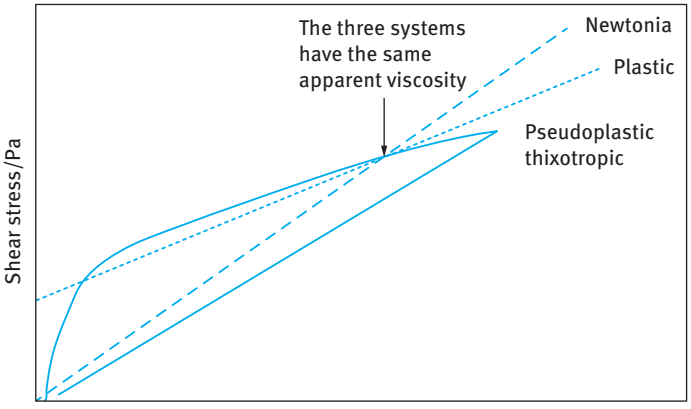

Fig. 13.23: Schematic representation of the flow behaviour of a Newtonian, a plastic and a pseudoplastic (thixotropic) system.

thixotropic systems will show reluctance to do so because of their yield values. This is clearly reflected in the final film properties. Once the yield value is overcome, the viscosity of the paint may become even lower than that of a Newtonian system. At the operational high shear rates all the three systems show different viscosities.

13.7 Flow in pipes

Since most paints are pumped through pipes during manufacture and in application, it is essential to analyse their flow behaviour in pipes. Two types of flow behaviour must be considered:

(i) Laminar flow, where distinct layers of material would pass each other;
(ii) turbulent flow, where no distinct layers are observed and all layers mix with one another forming eddy currents, swirls and vortices.

Whether the flow is laminar or turbulent depends on the dimensionless Reynolds number Re that is given by the following equation,

$$Re = \frac{vl\rho}{\eta}, \tag{13.25}$$

where v is the mean velocity, l is an instrument length parameter, ρ is the density and η is the viscosity. For laminar flow, $Re \leq 2000$, whereas for turbulent flow, $Re \geq 2000$. Thus when the shear rate exceeds a critical value, laminar flow changes to turbulent flow. This is reflected in the flow curve, which shows an apparent increase in shear stress above a critical shear rate. This does not mean that the viscosity of the material increases with increasing shear rate (as is the case with dilatant systems) but it indicates that with increasing shear rate the degree of turbulence increases, since part of the increased stress is used to increase the number of eddy currents rather than to increase the flow of the bulk material.

Turbulent flow in pipes, where l is replaced by the mean pipe diameter D, can occur when the Reynolds number exceeds 2000. Empirical equations have been established for turbulent flow of Newtonian materials [22, 23]. For smooth pipes,

$$\frac{1}{\sqrt{f}} = 2\log\left(\frac{Re}{\sqrt{f}}\right) - 0.8. \tag{13.26}$$

For rough pipes,

$$\frac{1}{\sqrt{f}} = 2\log\left(\frac{D}{2k}\right), \tag{13.27}$$

where f is the friction factor that is given by,

$$f = \frac{2DP}{\rho L v^2} = \frac{64}{Re}, \tag{13.28}$$

where k is the grain diameter that indicates surface roughness, P is the pressure in the pipe and L is the entire length of the pipe.

Thus for turbulent flow in smooth pipes, the flow velocity depends on the Reynolds number and hence on the viscosity.

The pressure that is necessary to pump a material through a pipeline system at a given flow rate depends on the pressure loss in the total pipeline system. Pressure losses are incurred by the viscous resistance of the material in the straight pipeline and in the pipeline transitions such as bends, valves, elbows, pipe expansions and contractions. The viscous losses in straight pipelines are frequently large compared to the pipeline transitions, so that the latter can sometimes be neglected.

The pressure loss for an entire pipeline system is given by [22, 23],

$$\Delta P = \rho \frac{v^2}{2}\left[\frac{L}{D}f + C_{\mathrm{L}}\right], \tag{13.29}$$

where C_{L} is the sum of all pressure loss coefficients obtained from all pipeline transitions in the pipeline system.

The flow of Newtonian materials in pipelines under laminar flow is well understood and is given by Poiseulle's equation,

$$\eta = \frac{\pi R^4 P}{8QL}, \tag{13.30}$$

where Q is the volumetric flow ($\mathrm{m^3\,s^{-1}}$) and R is the pipe radius.

In turbulent flow, the flow for Newtonian systems is given by equations (13.26) and (13.27).

The flow of non-Newtonian materials (as is the case with paints) in pipelines is not as well understood. However, Buckingham [24] derived the following equation for evaluating the plastic viscosity of a Bingham plastic system from the flow curve in a capillary viscometer (assuming end effects, kinetic energy effects and slippage flow are absent),

$$\eta_{\mathrm{pl}} = \frac{\pi P R^4}{8QL}\left[1 - \frac{8L\sigma_\beta}{3RP} + \frac{1}{3}\left(\frac{2L\sigma_\beta}{RP}\right)^4\right]. \tag{13.31}$$

Equation (13.31) can be used to determine the laminar flow of plastic materials in pipelines with R being the pipe radius. For pseudoplastic and dilatant materials, the power law equation can be used,

$$\eta = k\dot{\gamma}^{n-1}, \tag{13.32}$$

where k is the consistency index and n is the shear thinning index ($n < 1$ for pseudoplastic materials).

For a Bingham plastic in laminar flow the friction factor f is given by,

$$f = \frac{64}{Re}\frac{Pl}{8s}, \tag{13.33}$$

where Pl is the plasticity number that is given by,

$$Pl = \frac{\sigma_\beta D}{Uv}, \tag{13.34}$$

where U is the coefficient of plastic viscosity and v is the velocity.

s is the ratio of yield value to the shear stress at the wall. Since s is a function of Pl, the friction factor for Bingham plastics is fully determined from Re and Pl.

For pseudoplastic materials in laminar flow, the friction factor is given by [22, 23],

$$f = \frac{64}{Re}\left(\frac{3+N}{4}\right), \tag{13.35}$$

where $N = 1/n$. Thus the friction factor for pseudoplastic materials is fully determined from Re and N.

The shear rate in the pipeline for the flow of pseudoplastic materials is given by [22, 23],

$$\dot{\gamma} = \frac{2v(N+3)}{D}. \tag{13.36}$$

The apparent viscosity that is to be used in the Reynolds number has to be measured in the viscometer at the pipeline shear rate. This can be obtained by fitting the flow curve to the power law relationship given by equation (13.32).

In turbulent non-Newtonian flow the friction factor is a unique function of the Reynold's number. For Bingham plastic systems, the Reynold's number is calculated by using the plastic viscosity since it remains constant with increasing shear rates. For pseudoplastic flow, the Reynold's number is calculated by using an estimated apparent viscosity that is obtained by extrapolation to infinite shear rate.

13.8 Examples of the flow properties of some commercial paints

Most commercial paints have flow characteristics similar to thixotropic plastic materials [1]. Typical examples of the flow characteristics of some paints are given in Tab. 13.1.

The above results were obtained at the same shear rate (using a Stormer-type concentric cylinder) and they clearly show similar flow characteristics with viscosities of less than 0.4 Pa s and yield values not exceeding 12 Pa.

The rheological behaviour of a paint and a lacquer during and after application determines the smoothness and perfection of the resulting film surface. Paints are applied by brushing, dipping, flow coating and spraying. In all cases the flow-out of the

Tab. 13.1: Flow properties of some commercial paints.

Product	η (Pa s)	σ_β (Pa)	Degree of thixotropy
Enamels, gloss	0.14–0.39	0–3	Nil to slight
Enamels, semi-gloss	0.10–0.35	5–12	slight
Flat or matt paints	0.06–0.10	2–10	Slight to marked
Wall water-dispersible	0.02–0.14	1–10	Slight to marked
Primers, metal	0.03–0.12	0–10	Nil to marked
Varnishes	0.09–0.29	0	Nil

Tab. 13.2: Approximate time of levelling of oil films on a non-porous substrate as a function of viscosity and film thickness.

η (Pa s)	Levelling time (minutes)	Film thickness (mm)
< 0.05	< 1	0.5–5.0
0.20	5	0.5
0.20	< 0.5	≫ 0.5
1.0	> 120	0.5
1.0	10	≫ 0.5

material between the time of application and drying determines the characteristics of the finished surface. The time required for flow-out of oils of different viscosities on a non-porous surface depends on the layer thickness, as illustrated in Tab. 13.2.

The above results show that levelling to a smoother film takes less time with lower viscosity paints and for films with larger thickness. However, one should remember that the film viscosity continues to increase while drying and levelling proceed. Generally speaking, flow-out is usually complete in about 1 minute if the viscosity does not exceed 0.1 Pa s. Most paints require longer flow-out time since the viscosity is higher than 0.1 Pa s at 1 minute after deposition.

The shear rate produced by brushing paints on a surface was estimated to range from 130 to 260 s^{-1}. This value can be obtained by determining the shear rate at which the order of apparent viscosities of thyrotrophic paints exhibiting entirely different flow behaviour coincide with the order of ease of flow indicated by practical brushing. Alternatively, the shear rate can be calculated by assuming that the brushing velocity is 0.2 m s^{-1} for a distance between the substrate and the brush of about 0.001 m (this gives a shear rate of 200 s^{-1}). However, other authors assumed much higher shear rates (about 100 times higher). Various other investigators tried to correlate the flow behaviour of paints with their brushing behaviour. In general, paints have good brushing properties if the plastic viscosity ranges from 0.2 to 0.5 Pa s and the yield value from 40 to 140 Pa. Both the plastic viscosity and yield value increase with increasing solvent evaporation (particularly for nonaqueous paints based on volatile solvents). This is illustrated in Tab. 13.3 for brushed black enamel paint [25].

Tab. 13.3: Change in flow properties of a brushed black enamel.

Time (minutes)	η_{pl} (Pa s)	σ_β (Pa)	Type of flow
0	0.19	0	Newtonian
2.5	1.4	2.4	Plastic
5.0	3.0	52.0	Thyrotrophic plastic
7.5	16.7	620.0	Thixotropic plastic

A paint is considered to have good brushing properties when all brush marks disappear during the drying process. This might be achieved by rapid flow-out caused by low viscosity and low yield value or by taking advantage of the thixotropic behaviour of the paint. Low viscosity and low yield value often lead to sag marks and "curtains", since the low consistency causes the paint to continue to flow after application until drying is sufficiently advanced. Sagging can also appear if the film is applied in a layer that is too thick. The thixotropic properties have the advantage of giving the paint the low operational consistency needed for initial flow-out in order to prevent brush marks and to obtain good levelling. At the same time, they provide the paint with a mechanism to increase the consistency by means of the thixotropic build-up of the structure that can be effective immediately after application. However, a too rapid thixotropic build-up can be detrimental because levelling and flow-out are not instantaneous. It has been shown [26, 27] that thixotropic paints which decrease in consistency rapidly with increasing shear rate but rebuild the structure slowly exhibit the best levelling characteristics. A too rapid increase in thixotropic structure can produce poor levelling.

The viscosity of paints and lacquers that are applied by spraying (using for example a spray-gun) range from 0.04 to 0.12 Pa s. For hot sprays that are applied at about 75 °C, the viscosity should be adjusted to about 0.2 Pa s at room temperature, so that it will be less than 0.1 Pa s at the spraying temperature. The viscosity of hot plastic paints that are sprayed at temperatures around 150 °C should be less than 0.15 Pa s. The viscosity of the paint is usually adjusted by addition of solvent. The viscosity of the bulk paint has to be so low for spray operations, since it will substantially increase on evaporation of the solvent during the spraying process (from the time it leaves the spray nozzle to the time when it hits the substrate which is to be coated). The increase in viscosity depends on the solvent volatility.

When applying a paint by spraying, the droplet size of the spray will greatly influence the appearance of the finished surface. A fine spray will produce a glossy surface, whereas a coarse spray will gave a matt finish, unless levelling occurs before drying is completed. The drop size of the spray depends on the physical properties of the paint such as its surface tension, its viscosity and density. Other parameters such as the flow rate, the relative velocities of the liquid and air also affect the spray droplet spectrum.

References

[1] Strivens TA. In: Lambourne R, editor. Paint and surface coatings. Chicester: Horwood; 1987.
[2] Glass JE. Coatings Technol. 1978;50:56.
[3] Patton TC. Paint flow and pigment dispersion. New York: Wiley-Interscience; 1979.
[4] Kuge Y. Coating Technol. 1983;55:59.
[5] Smith NDP, Orchard SE, Rhind-Tutt A. J Oil and Colloid Chemistry Assoc. 1961;44:618.
[6] Pearson JAR. J Fluid Mech. 1960;7:481.
[7] Savage MD. J Fluid Mech. 1977;80:473.

[8] Glass JE. Oil Col Chem Assoc. 1975;58:169.
[9] Dodge JS. J Paint Technol. 1972;44:72.
[10] Snow CI. Official Digest 1957;392:907.
[11] Myers RR. J Polym Science C. 1971;35:3.
[12] Tadros T. Rheology of dispersions. Weinheim: Wiley-VCH; 2010.
[13] Whorlow RW. Rheological Techniques. Chichester: Ellis Horwood; 1980.
[14] Barnes HA, Hutton JF, Walters K. An introduction to rheology. Amsterdam: Elsevier; 1989.
[15] Goodwin JW, Hughes RW. Rheology for Chemists. Cambridge: Royal Society of Chemistry Publication; 2000.
[16] Herschel WH, Bulkley R. Proc. Amer. Soc. Test Materials. 1926;26:621; Kolloid Z. 1926;39:291.
[17] Casson N. In: Mill CC, editor. Rheology of disperse systems. New York: Pergamon Press; 1959. p. 84–104.
[18] Cross MM. J Colloid Interface Sci. 1965;20:417.
[19] Weltman RN. In: Eirich FR, editor. Rheology, Vol. 3. London: Academic Press; 1960. Chapter 6.
[20] Ferry JD. Viscoelastic properties of polymers. New York: John Wiley & Sons; 1980.
[21] Fischer EK. Ind Eng Chem. 1941;33:1465.
[22] Rouse H, Howe JW. Basic mechanics of fluids. New York: Wiley; 1953.
[23] da C. Andrade EN. Viscosity and plasticity. New York: Chemica Publishing; 1952.
[24] Buckingham E. Proc Am Soc Testing Materials. 1921;21:1154.
[25] Fischer EK. J Colloid Sci. 1950;5:271.
[26] Saunders B. J Oil Colour Chemists. 1948;31:95.
[27] Jarret MED. J Oil Colour Chemists. 1948;31:337.

Part III: **Colloid and interface science in food colloids**

14 Interaction between food-grade surfactants and water

14.1 Introduction

Many foods are colloidal systems, containing particles of various kinds that are stabilized by surfactants. The interfacial properties of these surfactant films are very important in formulating such systems and maintaining their long-term physical stability. Naturally occurring surfactants such as lecithin from egg yolk and various proteins from milk are used for the preparation of many food products such as mayonnaise, salad creams, dressings, desserts, etc. Later, polar lipids such as monoglycerides have been introduced as emulsifiers for food products. More recently, synthetic surfactants such as sorbitan esters and their ethoxylates and sucrose esters have been used in food emulsions. For example, esters of monostearate or monooleate with organic carboxylic acids, e.g. citric acid are used as antispattering agents in margarine for frying. The particles may remain as individual units suspended in the medium, but in most cases aggregation of these particles takes place forming three-dimensional structures, generally referred to as "gels". These aggregation structures are determined by the interfacial properties of the surfactant films and the interaction forces between the particles that are controlled by the relative magnitudes of attractive (van der Waals forces) and repulsive forces. The latter can be electrostatic or steric in nature depending on the composition of the food formulation. It is clear that the repulsive interactions will be determined by the nature of the surfactant present in the formulation. Such surfactants can be ionic or polar in nature, or they may be polymeric in nature. The latter are sometimes added not only to control the interaction between particles or droplets in the food formulation, but also to control the consistency (rheology) of the system. Many food formulations contain mixtures of surfactants (emulsifiers) and hydrocolloids. The interaction between the surfactant and polymer molecule plays a major role in the overall interaction between the particles or droplets, as well as the bulk rheology of the whole system. Such interactions are complex and require fundamental studies of their colloidal properties. Many food products contain proteins that are used as emulsifiers. The interaction between proteins and hydrocolloids is also very important in determining the interfacial properties and bulk rheology of the system. In addition, the proteins can also interact with the emulsifiers present in the system and this interaction requires particular attention.

In this chapter, the interaction between food-grade surfactants and water will be described with some highlights on the structure of the liquid crystalline phases. Some examples of the phase diagrams of the monoglyceride-water systems will be given [1]. Chapter 15 will deal with proteins, which are used in many food emulsions [2]. A brief description of the structure of casein micelles and their primary and secondary structures will be given. These systems are widely used in many food products. A section

https://doi.org/10.1515/9783110578997-015

will be devoted to the interfacial phenomena in food colloids, in particular their dynamic properties and the competitive adsorption of the various components at the interface. The interaction between proteins and polysaccharides in food colloids will be briefly described. This is followed by a section on the interaction between polysaccharides and surfactants. Chapter 16 will deal with surfactant association structures, microemulsions and emulsions in food [3]. Chapter 17 will describe the effect of food surfactants on the interfacial and bulk rheology of food emulsions. The formation of aggregation networks and the application of fractal concepts are then considered. The last chapter will discuss the application of rheology in studying food texture and mouth feel.

It should be mentioned that the structures of many food emulsions is complex and in many cases several phases may exist. Such structures may exist under non-equilibrium conditions and the state of the system may depend to a large extent on the process used for preparing the system, its prehistory and the conditions to which it is subjected. It is not surprising, therefore, that fundamental studies on such systems are not easy to carry out and in many cases one is content with some qualitative observations. However, due to the great demand for producing consistent food products and introduction of new recipes, a great deal of fundamental understanding of the physical chemistry of such complex systems is required.

14.2 Interaction between food-grade surfactants and water

14.2.1 Liquid crystalline structures

A review on this subject has been published by Krog et al. [1], to which the reader should refer to for more details. As discussed by these authors, food-grade surfactants are, in general, not soluble in water, but they can form association structures in aqueous media that are liquid crystalline in nature. Three main liquid crystalline structures may be distinguished, namely the lamellar phase, the hexagonal phase and the cubic phase. Fig. 14.1 shows a model of the crystalline state of a surfactant which forms a lamellar phase (Fig. 14.1 (a)).

When dispersed in water above its Krafft temperature (T_c) it produces a lamellar mesophase (Fig. 14.1 (b)) with a thickness d_a of the bilayer, a thickness d_w of the water layer. The lamellar layer thickness d is simply $d_a + d_w$. These thicknesses can be determined using low angle X-ray diffraction. The surface area per molecule of surfactant is denoted by S. The lamellar mesophase can be diluted with water and it has almost infinite swelling capacity provided the lipid bilayers contain charged molecules and the water phase has a low ion concentration [4]. These diluted lamellar phases may form liposomes (multilamellar vesicles), which are spherical aggregates with internal lamellar structures [5]. Under the polarizing microscope, the lamellar structures show an “oil-streaky” texture.

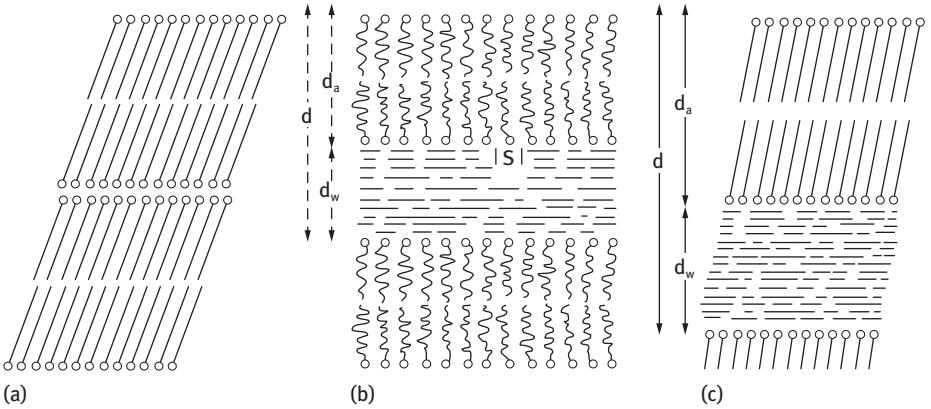

Fig. 14.1: Schematic representation of lamellar liquid crystalline structures.

When the surfactant solution containing the lamellar phase is cooled below the Krafft temperature of the surfactant, a gel phase is formed as schematically shown in Fig. 14.1 (c). The crystalline structure of the bilayer is now similar to that of the pure surfactant and the aqueous layer with thickness d_w is the continuous phase of the gel.

The hexagonal mesophase structure is periodic in two dimensions and it exists in two modifications, hexagonal I and hexagonal II. The structure of the hexagonal I phase consists of cylindrical aggregates of surfactant molecules with the polar head groups oriented towards the outer (continuous) water phase and the surfactant hydrocarbon chains filling out the core of the cylinders. These structures show a fan-like or angular texture under the polarizing microscope. The hexagonal II phase consists of cylindrical aggregates of water in a continuous medium of surfactant molecules with the polar head groups oriented towards the water phase and the hydrocarbon chains filling out the exterior between the water cylinders. This phase shows the same angular texture, under the polarizing microscope, as the hexagonal I phase. Whereas the hexagonal I phase can be diluted with water to produce micellar (spherical) solutions, the hexagonal II phase has a limited swelling capacity (usually not more than 40 % water in the cylindrical aggregates).

The viscous isotropic cubic phase, which is periodic in three dimensions, is produced with monoglyceride-water systems at chain lengths above C_{14}. This isotropic phase was shown to consist of a bicontinuous structure, consisting of a lamellar bilayer, which separates two water channel systems [6, 7]. The cubic phase behaves as a very viscous liquid phase, which can accommodate up to ≈ 40 % water.

Of the above liquid crystalline structures, the lamellar phase is the most important for food applications. As we will see later, these lamellar structures are very good stabilizers for food emulsions. In addition, they can be diluted with water forming liposome dispersions which are easy to handle (pumpable liquids) and they interact with water-soluble components such as amylose in starch particles. The hexagonal

and cubic phases, in contrast, when formed give problems in food processing due to their highly viscous nature (viscous particles may block filters).

14.2.2 Binary phase diagrams

Typical binary (surfactant + water) phase diagrams of monoglycerides are shown in Fig. 14.2 for three molecules with decreasing Krafft temperature (1-monopalmitin, 1-monoelaidin and 1-mono-olein). With 1-monopalmitin, the dominant mesophase is the lamellar (neat) phase, which swells to a maximum water layer thickness, d_w, of 2.1 nm at 40 % water. At higher water content (> 60 %) a disperse phase is produced in the temperature range 55–68 °C, whereas above 68 °C, a cubic phase in equilibrium with water is formed. With the monoelaidin-water phase diagram (Fig. 14.2 (b)), the lamellar region becomes smaller, whereas the cubic phase region becomes larger, when compared with the monopalmitin-water phase diagram. The temperature at which the lamellar phase is formed (Krafft point) is decreased from 55 to 33 °C.

At higher water concentration (> 40 %), the monoelaidin forms a cubic phase in equilibrium with bulk water. The mono-olein-water phase diagram shows the formation of a lamellar liquid crystalline structure at room temperature (20 °C) at water content between 2 and 20 %. At higher water concentration, a cubic phase is formed which above 40 % water exists in equilibrium with water. If the temperature of the cubic phase is increased above 90 °C, a hexagonal II phase is produced, which may contain up to 25 % water in the cylindrical aggregates.

Commercial distilled monoglycerides from edible fats (lard, tallow or vegetable oils) shows similar mesophase formation to that of the pure monoglycerides. This is illustrated in Fig. 14.3, which shows the binary phase diagram of saturated, distilled monoglycerides based on hydrogenated lard (monopalmitin/monostearin ratio 30 : 65) (Fig. 14.3 (a)) and unsaturated, distilled monoglycerides based on sunflower oil containing 21 % mono-olein, 68 % monolinolein and 11 % saturated (C_{16}/C_{18}) monoglycerides.

The phase regions may differ in size depending on the purity and fatty acid composition of the commercial monoglycerides. As mentioned above, the continuous swelling of the lamellar phase in the water-rich region of the phase diagram is controlled by the charge of the lipid, which can be obtained by neutralization of the free fatty acid in the monoglyceride (by adding sodium bicarbonate or sodium hydroxide). The formation of charged RCOO– molecules in the lipid bilayer of the lamellar phase increases swelling by water, owing to the electric repulsion effect. This has been confirmed using low angle X-ray diffraction methods to measure the water thickness. This is illustrated in Fig. 14.4, which shows the X-ray data of lamellar phases on fully hydrogenated lard (C_{16}/C_{18} 35 : 65) in distilled water at 60 °C; (A) without neutralization and (B) with neutralization of the free fatty acids present (0.8 %).

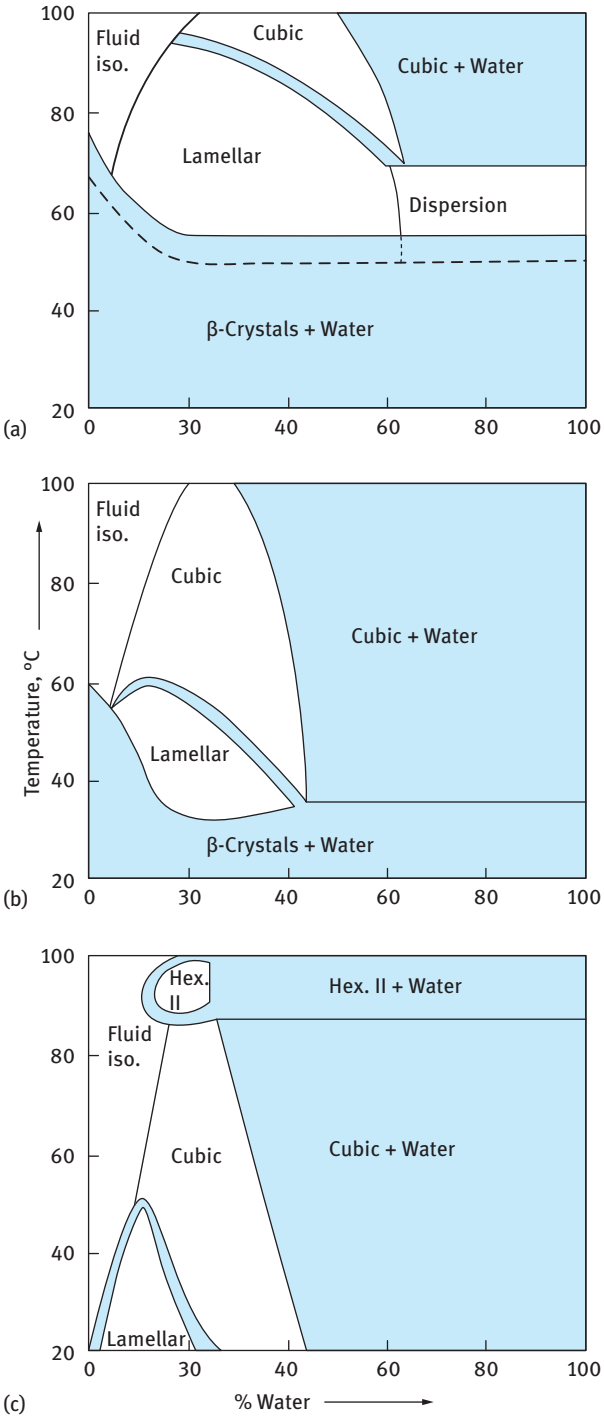

Fig. 14.2: Binary phase diagrams of pure 1-monoglycerides in water: (a) 1-monopalmitin; (b) monoelaidin; (c) mono-olein.

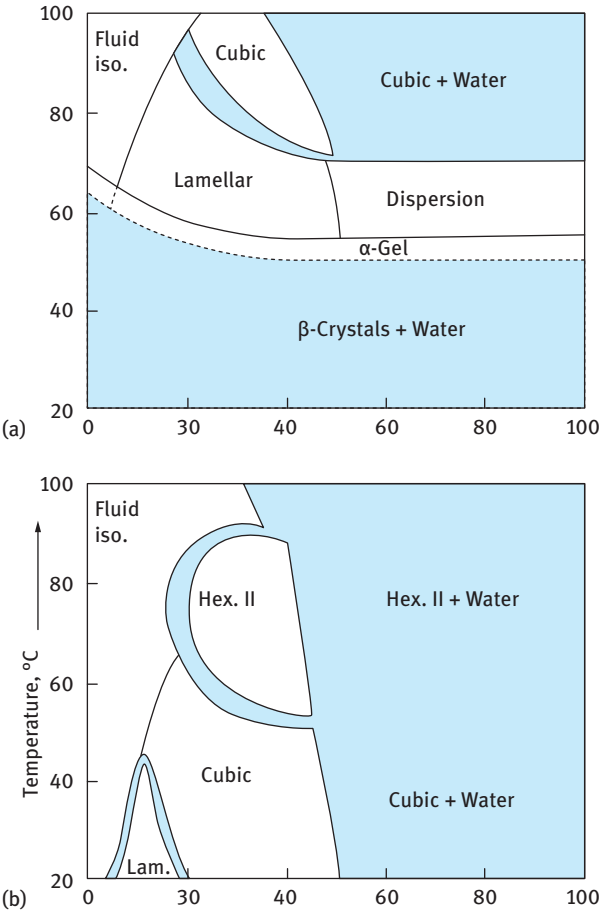

Fig. 14.3: Binary phase diagrams of commercial, distilled saturated monoglycerides (a) and unsaturated monoglycerides (b).

It can be seen from Fig. 14.4 that without neutralization, maximum swelling occurs at 30 % water corresponding to a water layer thickness (d_w) of 1.6 nm. After neutralization of the free fatty acid with 1 mol dm^{-3} NaOH, the swelling is strongly increased. At a water concentration of 75 %, the lamellar phase has a water layer thickness (d_w) of 11.6 nm between the lipid layers. At higher water concentrations (> 95 %), these neutralized monoglycerides form transparent dispersions (liposomes).

The phase diagram of a pure soybean lecithin-water system is shown in Fig. 14.5. The excess water region, relevant to emulsions based on this surfactant, consists of a dispersion of the lamellar liquid crystalline phase in the form of liposomes.

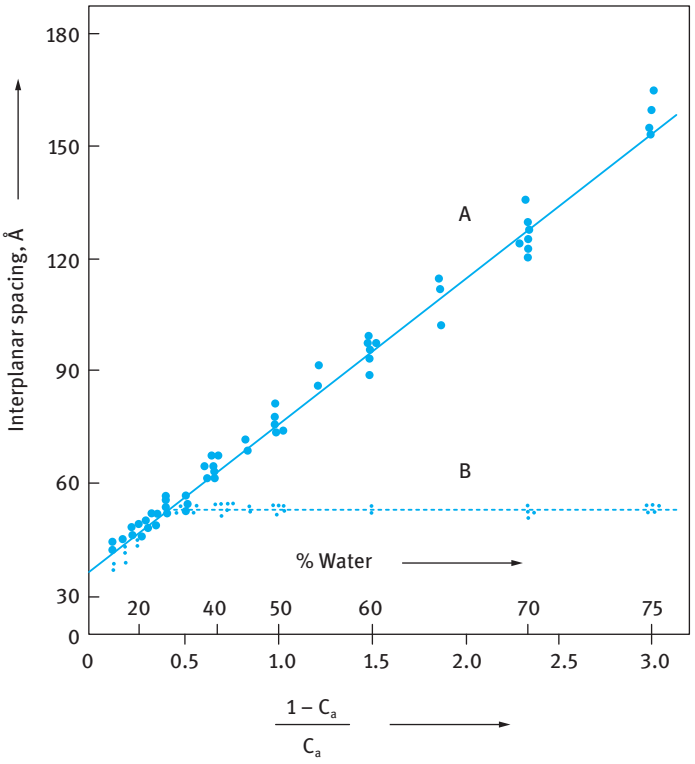

Fig. 14.4: X-ray data of monoglyceride-water lamellar phases at 60 °C; (A) with neutralized free fatty acid, (B) without neutralization.

When a liquid-crystalline mesophase of a surfactant-water system is cooled below the Krafft point, a gel is formed. In the gel state, the lipid bilayers are separated by alternating water layers as in the lamellar phase. The hydrocarbon bilayers are solidified into an α-crystal form with a hexagonal subcell backing (short spacing 0.415 nm) and they are tilted 54° toward the water layer. A gel of distilled monoglycerides containing 75 % w/w water and approximately 0.5 % neutralized fatty acids shows X-ray diffraction Bragg spacings of about 23 nm corresponding of a water layer thickness (d_w) of 17.5 nm and a lipid bilayer thickness (d_a) of 5.5 nm. The specific surface in contact with water is 2.2 nm in the gel phase. Fig. 14.6 shows the X-ray data of a gel phase.

The gel phase is very sensitive to electrolytes in water; 0.05 % w/w NaCl is enough to prevent swelling of the monoglyceride gel containing 70 % water which corresponds to a decrease in the water thickness (d_w) from 13.6 nm to about 0.9 nm. Gel phases of monoglycerides with other surfactants, such as propylene glycol monostearate or polysorbate 60 containing 50–70 % water, are used as aerating agents in cakes and other food products.

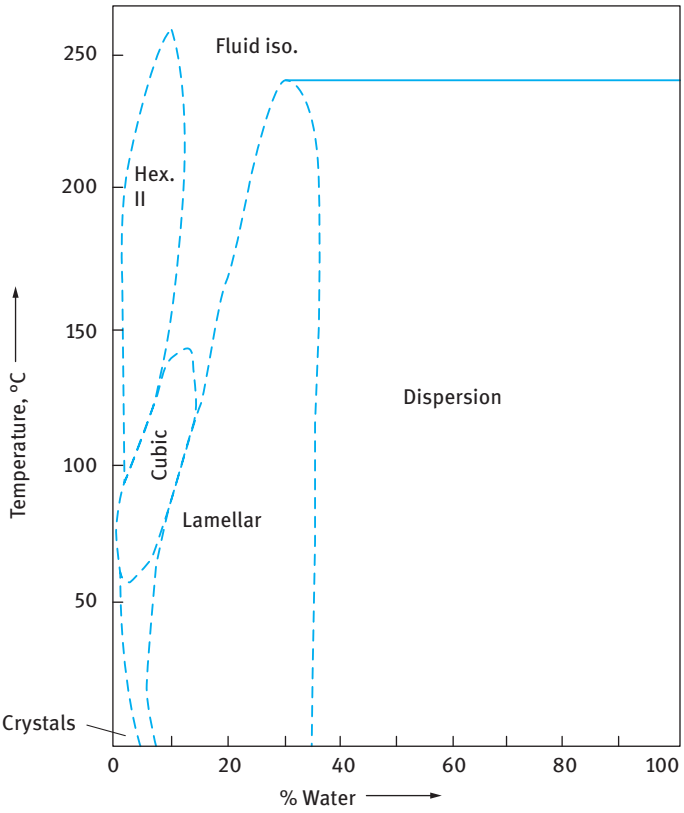

Fig. 14.5: Binary phase diagram of soybean lecithin–water system.

14.2.3 Ternary phase diagrams

A typical ternary phase diagram of soybean oil (triglyceride), sunflower oil monoglyceride and water at 25 °C [8] is shown in Fig. 14.7. It clearly shows the L_C phase and the inverse micellar (L_2) phase. This inverse micellar phase is relevant to the formation of water-in-oil emulsions. The interfacial tension between the micellar L_2 phase and water is about 1–2 mN m^{-1} and that between the L_2 and is even lower. It is proposed that the L_2 phase forms an interfacial film during emulsification, and the droplet size distribution should then be expected to be related mainly to the interfacial and rheological properties of the L_2 phase.

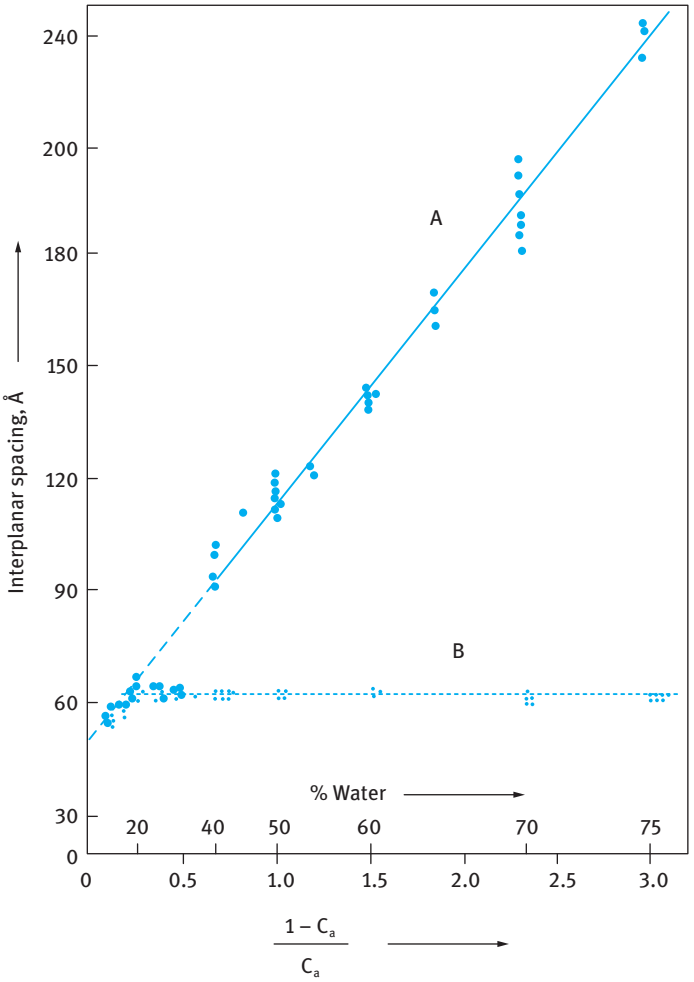

Fig. 14.6: X-ray data of monoglyceride-water gel phases at 25 °C. (A) With neutralized free fatty acid; (B) without neutralization.

14.3 Monolayer formation

The formation of a monomolecular film of the emulsifier at the oil/water (O/W) interface is a crucial factor in the emulsification process. Experimentally, it is easier to study lipid monolayers at the air/water (A/W) interface compared to the O/W interface. However, recently studies at the O/W interface became possible using drop profile techniques. The results showed similar trends as observed at the A/W interface. As an illustration, Fig. 14.8 shows the variation of the film pressure π with concentration of pure 1-mono-olein spread on the water surface at 20 °C.

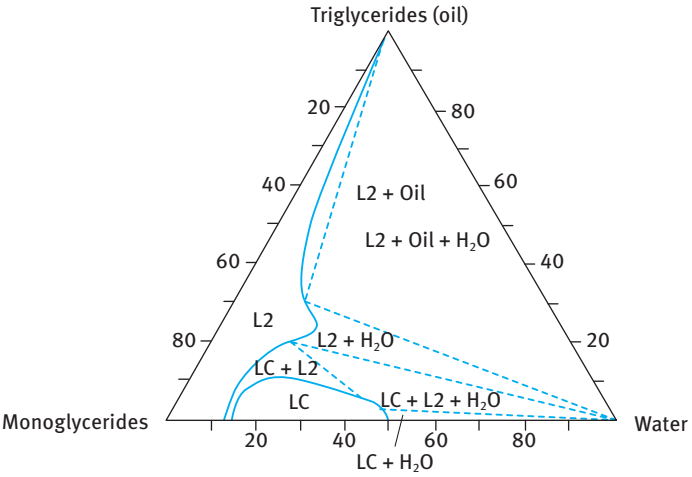

Fig. 14.7: Ternary phase diagram of soybean oil, sunflower oil monoglyceride and water.

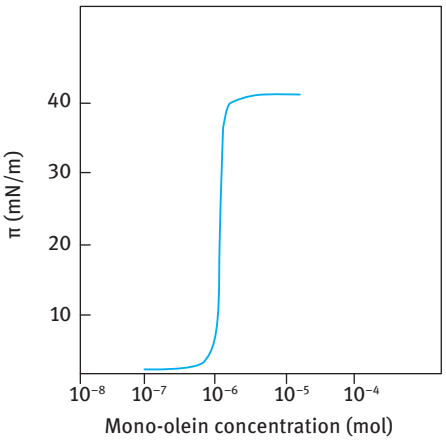

Fig. 14.8: Surface film pressure (π) versus concentration of pure 1-mono-olein spread on the water surface at 20 °C.

The results of Fig. 14.8 show a steep rise of surface pressure at a critical surfactant concentration ($\approx 10^{-6}$ mol dm^{-3}) and this concentration corresponds to the highest monomer concentration in bulk solution. Above 10^{-6} mol dm^{-3} the lipid monomers begin to associate. Surface pressure measurements at the air-water interface showed that the lipid molecules begin to associate to form a cubic structure. Monoglycerides of saturated fatty acids associate to form lamellar liquid crystalline phase or the gel phase at low concentrations. These condensed layers form at the oil-water interface at and above the critical temperature T_c, which is the temperature used for emulsification. These liquid crystalline phases play a major role in emulsion stabilization. It is necessary to have enough polar lipids to form a stabilizing film at the O/W interface,

and this is not possible until the maximum of monomer concentration in the bulk is exceeded.

Hydrophilic emulsifiers, which in bulk form micellar solutions, exhibit a different monolayer behaviour. The interfacial tension γ shows a linear decrease with log concentration until the critical micelle concentration is reached, after which γ remains virtually constant with any further increase in surfactant concentration. However, most surfactants used in food emulsions do not form micellar solutions.

One of the most informative techniques for studying monolayer formation relevant to emulsification is to measure the surface pressure as a function of molecular area using a surface balance (Langmuir trough). In this method, the surfactant film is spread at the A/W or O/W interface between two barriers placed in the Langmuir trough. One of the barriers is fixed whereas the second can be moved to reduce the area occupied by the film. The surface or interfacial tension γ is monitored using the Wilhelmy plate that could be attached to a microbalance, thus measuring the force and hence calculating γ. In this way, surface pressure (π)–area/molecule (A) isotherms can be established. As an illustration, Fig. 14.9 shows the π–A isotherms (at 25 °C) for pure 1-monomyristin at the A/W interface. It can be seen that π shows a gradual increase with decreasing A, reaching a plateau at $\approx 27\,\mathrm{mN\,m^{-1}}$ where a monolayer with liquid hydrocarbon chains, referred to as form I, can coexist with a monolayer with liquid crystalline chains, referred to as form II. The cross-sectional area per molecule at this pressure of form I is $2.85\,\mathrm{nm^2}$ ($28.5\,A^2$), which is in good agreement with that of the lamellar liquid crystalline phase. The molecular surface area at this transition of form II is $2.25\,\mathrm{nm^2}$, which is identical to that of the liquid crystalline structure in the gel phase.

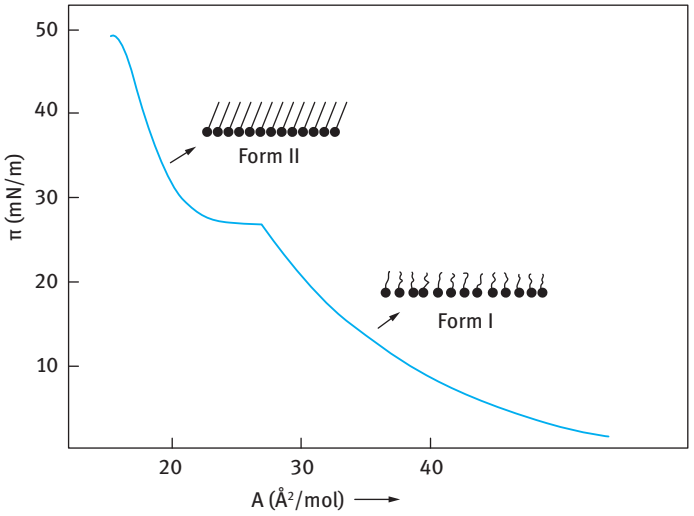

Fig. 14.9: π–A isotherm of pure 1-monomyristin at 25 °C.

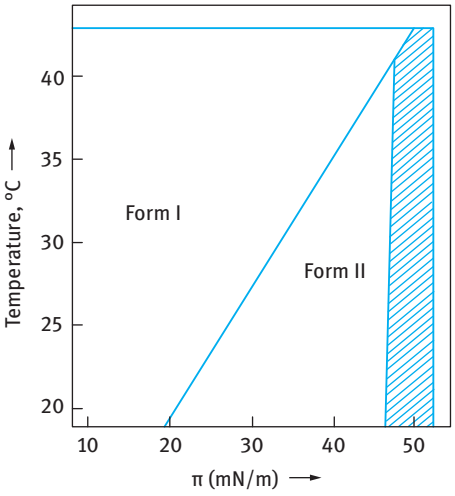

Fig. 14.10: Phase changes of 1-monomyristin monolayers at the A/W interface as a function of temperature. The shaded area shows the region above the collapse of the monolayer.

The variation of the transition between form I and form II with temperature is shown in Fig. 14.10. The pressure of the transition plateau increases with temperature, and above a temperature of 42 °C no solid condensed monolayer (form II) is formed. This temperature is also in good agreement with the temperature of transition from the crystalline state to the lamellar liquid crystalline state in the aqueous system of monomyristin.

The corresponding relations between temperature and monolayer film pressure of forms I and II in the case of monoelaidin is shown in Fig. 14.11. Monoelaidin, having a trans double bond, exhibits monolayers with liquid crystalline chains (form II) up to about 30 °C. The relation between the monolayer transitions and the corresponding bulk phase transition in the binary phase diagram of monoelaidin/water (Fig. 14.2 (b)) is thus very close. Mono-olein shows only monolayers with liquid chains (form I) at all

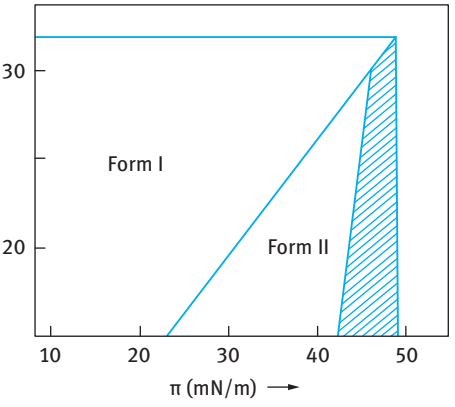

Fig. 14.11: Phase changes of 1-monoelaidin at the A/W interface as a function of temperature. The shaded area shows the region above collapse of the monolayer.

temperatures between 0 and 100 °C, which is in agreement with the phase diagram of mono-olein/water shown in Fig. 14.2 (c).

The equilibrium surface pressure of the α-crystal form of monomyristin was also followed as a function of temperature, and it was found to have the same value as the plateau pressure at the transition from form I to form II. One can then assume that the monolayer formed when excess of the α-crystal form is present has the structure illustrated as form II in Fig. 14.9. The agreement between molecular areas and transition temperatures indicates that the hydrocarbon chain structure of monolayer forms I and II is identical to that of the liquid crystalline phases and the α-crystalline gel phase respectively.

The liquid crystalline state of the monolayer, which is always formed at a temperature above the existence of the crystalline monolayer, possesses ideal rheological properties. The monolayer with liquid hydrocarbon chains (form I) can thus vary its curvature and cross-sectional area per molecule over wide ranges. Under certain conditions, however, it is possible to crystallize the monolayer after the emulsion has been formed.

14.4 Liquid crystalline phases and emulsion stability

A maximum in emulsion stability is obtained when three phases exist in equilibrium, and it was therefore proposed that the lamellar liquid crystalline phase stabilizes the emulsion by forming a film at the O/W interface. This film provides a barrier against coalescence. This is illustrated in Fig. 14.12, which shows that the lamellar liquid crystalline phase exhibits a hydrophobic surface towards the oil and a hydrophilic surface towards the water. These multilayers cause a significant reduction in the attraction potential and they also produce a viscoelastic film with much higher viscosity than that of the oil droplet. In other words, the multilayers produce a form of "mechanical barrier" against coalescence.

The rheological properties of monolayers of binary surfactant mixtures has been related to emulsion stability as will be discussed in Chapter 17 and to the structural

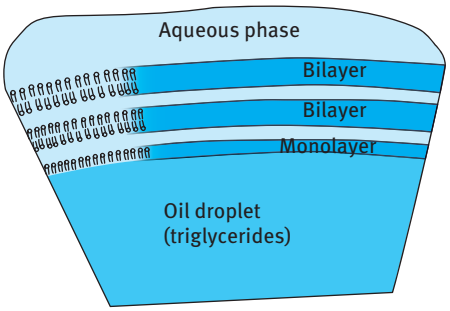

Fig. 14.12: Schematic representation of the lamellar liquid crystalline structure at the oil/water interface.

properties of the lamellar liquid crystalline phases formed by the surfactant in water. It was suggested that the emulsifier molecules adsorbed at the O/W interface will adopt the same hydrocarbon chain structure as they have in the bimolecular lipid layer of lamellar mesophases. Other liquid crystalline phases than the lamellar phase can also occur at the O/W interface. Fluctuations of interfacial tension at the dodecane/water interface with a sodium sulphonate surfactant have been observed and this was attributed to the formation of a liquid crystalline phase of the hexagonal type at the interface. As mentioned above, the enhanced emulsion stability in the presence of lipid multilayers at the interface is related to the reduced attraction potential. In addition, the multilayer viscosity is considerably higher than that of the oil phase. Also the lamellar liquid crystalline phase results in a repulsive force that is usually referred to as hydration force (see below).

Another important repulsive force that occurs when the surfactant film contains charged molecules, e.g. on addition of sodium stearate to lecithin, is the double layer repulsion arising from these ionogenic groups. An obvious consequence of the presence of charged chains is the increased distance between the surfactant bilayers.

The transition between the lamellar liquid crystalline phase and the gel phase can be utilized to stabilize the emulsion, provided the actual gel phase is stable. If an aqueous dispersion of the emulsifier is first formed, and emulsification is then performed under cooling, an emulsion is formed with the gel phase forming the O/W interface. Such an emulsion has a much higher stability when compared with that produced with the lamellar phase at the O/W interface. This is probably due to the higher mechanical stability of the crystalline lipid bilayers compared to bilayers with liquid chain conformation.

Another repulsive force between the lipid bilayers in water is the hydration force which is a short-range force with exponential falloff. This is related to repulsion between dipoles and induced dipoles. It is quite obvious that the hydration force will tend to inhibit coalescence of emulsion droplets with a multilayer structure as schematically shown in Fig. 14.12.

References

[1] Krog NJ, Riisom TH. In: Becher P, editor. Encyclopedia of emulsion technology, Vol. 2. New York: Marcel Dekker; 1985. p. 321–365.
[2] Jaynes EN. In: Becher P, editor. Encyclopedia of emulsion technology, Vol. 2. New York: Marcel Dekker; 1985. p. 367–384.
[3] Friberg SE, Kayali I. In: El-Nokaly M, Cornell D, editors. Microemulsions and emulsions in food. ACS Symposium Series 448. 1991. p. 7.
[4] Luzzati V. In: Chapman D, editor. Biological membranes. New York: Academic Press; 1968. p. 71.
[5] Krog N, Borup AP. J Sci Food Agric. 1973;24:691.
[6] Lindblom G, Larsson K, Johansson L, Fontell K, Forsen S. J Amer Chem Soc. 1979;101:5465.
[7] Larsson K, Fontell K, Krog N. Chem Phys Lipids. 1980;27:321.
[8] Pilman E, Tonberg E, Lartsson K. J Dispersion Sci Technol. 1980;3:335.

15 Proteins as emulsifiers and their interaction with polysaccharides

15.1 Protein structure

A protein is a linear chain of amino acids that assumes a three-dimensional shape dictated by the primary sequence of the amino acids in the chain. The side chains of the amino acids play an important role in directing the way in which the protein folds in solution. The hydrophobic (nonpolar) side chains avoid interaction with water, while the hydrophilic (polar) side chains seek such interaction. This results in a folded globular structure with the hydrophobic side chains inside and the hydrophilic side chains outside [1]. The final shape of the protein (helix, planar or "random coil") is a product of many interactions which form a delicate balance [2, 3]. These interactions and structural organizations are briefly discussed below.

Three levels of structural organization have been suggested:

(i) Primary structure, referring to the amino acid sequence.
(ii) Secondary structure, denoting the regular arrangement of the polypeptide backbone.
(iii) Tertiary structure as the three-dimensional organization of globular proteins.

A quaternary structure consisting of the arrangement of aggregates of the globular proteins may also be distinguished. The regular arrangement of the protein polypeptide chain in the secondary structure is determined by the structural restrictions. The C–N bonds in the peptide amide groups have a partial double bond character that restricts the free rotation about the C–N bond. This influences the formation of secondary structures. The polypeptide backbone forms a linear group if successive peptide units assume identical relative orientations. The secondary structures are stabilized by hydrogen bonds between peptide amide and carbonyl groups. In the α-helix, the C=O bond is parallel to the helix axis and a straight hydrogen bond is formed with the N–H group and this is the most stable geometrical arrangement. The interaction of all constituent atoms of the main chain, which are closely packed together, allows the van der Waals attraction to stabilize the helix. This shows that the α-helix is the most abundant secondary structure in proteins. Several other structures may be identified and these are designated as π-helix, β-sheet, etc.

The classification of proteins is based on the secondary structures: α-proteins with α-helix only, e.g. myoglobin; β-proteins mainly with β-sheets, e.g. immunoglobin; α + β proteins with α-helix and β-sheet region that exist apart in the sequence, e.g. lysozome. The protein structure is stabilized by covalent disulphide bonds and a complexity of non-covalent forces, e.g. electrostatic interactions, hydrogen bonds, hydrophobic interactions and van der Waals forces. Both the average hydrophobicity and the charge frequency (parameter of hydrophobicity) are important in determining the

https://doi.org/10.1515/9783110578997-016

physical properties such as solubility of the protein. The solubility can be expressed as the equilibrium between hydrophilic (protein–solvent) and hydrophobic (protein–protein) interactions. Protein denaturation can be defined as the change in the native conformation (i.e. in the region of secondary, tertiary and quaternary structure) which takes place without change of the primary structure, i.e. without splitting of the peptide bonds. Complete denaturation may correspond to totally unfolded protein. When the protein is formed, the structure produced adopts the conformation with the least energy. This structure is referred to as the native or naturated form of the protein. Modification of the amino side chains or their hydrolysis may lead to different conformations. Similarly, addition of molecules that interact with the amino acids may cause conformational changes (denaturation of the protein). Proteins can be denaturated by adsorption at interfaces, as a result of hydrophobic interaction between the internal hydrophobic core and the nonpolar surfaces.

Many examples of proteins that have been used in interfacial adsorption studies may be quoted: Small and medium size globular proteins, e.g. those present in milk such as β-lactoglobulin, α-lactoalbumin and serum albumin, and in egg white, e.g. lysozyme and ovalalbumin. At pH values below the isoelectric point (4.2–4.5), these proteins associate to form dimers, trimers and higher aggregates. α-lactoalbumin is stabilized by Ca^{+} against thermal unfolding. X-ray analysis of lysozyme showed that all charged and polar groups are located at the surface, whereas the hydrophobic groups are buried in the interior. Bovine serum albumin (which represents about 5 % of whey proteins in bovine milk) forms a triple domain structure which includes three very similar structural domains, each consisting of two large double loops and one small double loop. Below pH 4, the molecule becomes fully uncoiled within the limits of its disulphide bonds. Ovalbumin, the major component of egg white, is a monomeric phosphoglycoprotein with a molecular weight of 43 kDa. During storage of eggs, even at low temperatures, ovalbumin is modified by SH/SS exchange into a variant with greater heat stability, called s-ovalbumin.

Among the protein-forming micelles, casein is the major protein fraction in bovine milk (about 80 % of the total milk protein). Several components may be identified, namely $\alpha_{s,1}$- and $\alpha_{s,2}$-caseins, β-casein and κ-casein. A protolytic breakdown product of β-casein is γ -casein. Similar to ovalbumin, caseins are phosphoproteins. Large spherical casein micelles are formed by association of α_s-, β- and κ-casein in the presence of free phosphate and calcium ions. The molecules are held together by electrostatic and hydrophobic interactions. The α_s- and β-caseins are surrounded by the flexible hydrophilic κ-casein which forms the surface layer of the micelle. The high negative charge of the κ-casein prevents collapse of the micelle by electrostatic repulsion. The micelle diameter varies between 50 and 300 nm.

Several oligomeric plant storage proteins can be identified. They are classified according to their sedimentation behaviour in the analytical ultracentrifuge, namely 11 S, 7 S and 2 S proteins. Both 11 S and 7 S proteins are oligomeric globular proteins. The 11 S globulins are composed of 6 non-covalently linked subunits, each

of which contains a disulphide bridged pair of a rather hydrophilic acidic 30–40 kDa α-polypeptide chain and a more hydrophilic basic 20 kDa β-polypeptide chain. The molar mass and size of the protein as well as its shape depend on the nature of the plant from which it is extracted. These plant proteins can be used as emulsifying and foaming agents.

15.2 Interfacial properties of proteins at the liquid/liquid interface

Since proteins are used as emulsifying agents for oil-in-water emulsions, it is important to understand their interfacial properties, in particular the structural change that may occur on adsorption. The properties of protein adsorption layers differ significantly from those of simple surfactant molecules. In the first place, surface denaturation of the protein molecule may take place, resulting in unfolding of the molecule, at least at low surface pressures. Secondly, the partial molar surface area of proteins is large and can vary depending on the conditions for adsorption. The number of configurations of the protein molecule at the interface exceeds that in bulk solution, resulting in a significant increase in the non-ideality of the surface entropy. Thus, one cannot apply thermodynamic analysis, e.g. Langmuir adsorption isotherm, for protein adsorption. The question of reversibility versus irreversibility of protein adsorption at the liquid interface is still subject to a great deal of controversy. For that reason protein adsorption is usually described using statistical mechanical models. Scaling theories proposed by de Gennes [4] could also be applied.

One of the most important investigations of protein surface layers is to measure their interfacial rheological properties (e.g. viscoelastic behaviour). Several techniques can be applied to study the rheological properties of protein layers, e.g. using constant stress (creep) or stress relaxation measurements. At very low protein concentrations, the interfacial layer exhibits Newtonian behaviour, independent of pH and ionic strength. At higher protein concentrations, the extent of surface coverage increases and the interfacial layers exhibit viscoelastic behaviour, revealing features of solid-like phases. Above a critical protein concentration, protein–protein interactions become significant, resulting in a "two-dimensional" structure formation. The dynamics of formation of protein layers at the liquid-liquid interface should be considered in detail when one employs protein molecules as stabilizers for emulsions. Several kinetic processes must be considered: solubilization of nonpolar molecules resulting in the formation of associates in the aqueous phase; diffusion of solutes from bulk solution to the interface; adsorption of the molecules at the interface; orientation of the molecules at the liquid/liquid interface; formation of aggregation structures, etc.

15.3 Proteins as emulsifiers

When a protein is used as an emulsifier, it may adopt various conformations depending on the interaction forces involved. The protein may adopt a folded or unfolded conformation at the oil/water interface. In addition, the protein molecule may interpenetrate the lipid phase to various degrees. Several layers of proteins may also exist. The protein molecule may bridge one drop interface to another. The actual structure of the protein interfacial layer may be complex, combining any or all of the above possibilities. For these reasons, the measurement of protein conformations at various interfaces still remains a difficult task, even when using several techniques such as UV, IR and NMR spectroscopy as well as circular dichroism [5]. At an oil/water interface, the assumption is usually made that the protein molecule undergoes some unfolding and this accounts for the lowering of the interfacial tension on protein adsorption. As mentioned above, multilayers of protein molecules may be produced and one should take into account the intermolecular interactions as well as the interaction with the lipid (oil) phase. Proteins act in a similar way to polymeric stabilizers (steric stabilization). However, the molecules with compact structures may precipitate to form small particles which accumulate at the oil/water interface. These particles stabilize the emulsions (sometimes referred to as Pickering emulsions) by a different mechanism. As a result of the partial wetting of the particles by the water and the oil, they remain at the interface. The equilibrium location at the interface provides the stability since their displacement into the dispersed phase (during coalescence) results in an increase in the wetting energy.

From the above discussion, it is clear that proteins act as stabilizers for emulsions by different mechanisms depending on their state at the interface. If the protein molecules unfold and form loops and tails, they provide stabilization in a similar way to synthetic macromolecules. On the other hand, if the protein molecules form globular structures, they may provide a mechanical barrier that prevents coalescence. Finally, precipitated protein particles that are located at the oil/water interface provide stability as a result of the unfavourable increase in the wetting energy on their displacement. It is clear that in all cases, the rheological behaviour of the film plays an important role in the stability of the emulsions.

15.4 Protein–polysaccharide interactions in food colloids

Proteins and polysaccharides are present in nearly all food colloids [6]. Proteins are used as emulsion and foam stabilizers, whereas polysaccharides act as a thickener and also for water-holding. Both proteins and polysaccharides contribute to the structural and textural characteristics of many food colloids through their aggregation and gelation behaviour. Several interactions between proteins and polysaccharides may be distinguished, ranging from repulsive to attractive interactions. The repulsive in-

teractions may arise from excluded volume effects and/or electrostatic interaction. These repulsive interactions tend to be weak, except at very low ionic strength (expanded double layers) or with anionic polysaccharides at pH values above the isoelectric point of the protein (negatively charged molecules). The attractive interaction can be weak or strong, and either specific or nonspecific. A covalent linkage between protein and polysaccharide represents one specific strong interaction. A nonspecific protein–polysaccharide interaction may occur as a result of ionic, dipolar, hydrophobic or hydrogen bonding interaction between groups on the biopolymers. Strong attractive interaction may occur between a positively charged protein (at a pH below its isoelectric point) and an anionic polysaccharide. In any particular system, the protein–polysaccharide interaction may change from repulsive to attractive as the temperature or solvent conditions (e.g. pH and ionic strength) change.

Aqueous solutions of proteins and polysaccharides may exhibit phase separation at finite concentrations. Two types of behaviour may be recognized, namely coacervation and incompatibility. Complex coacervation involves spontaneous separation into solvent-rich and solvent-depleted phases. The latter contains the protein–polysaccharide complex which is caused by nonspecific attractive protein–polysaccharide interaction, e.g. opposite charge interaction. Incompatibility is caused by spontaneous separation into two solvent-rich phases, one composed of predominantly protein and the other predominantly of polysaccharide. Depending on the interactions, a gel formed from a mixture of two biopolymers may contain a coupled network, an interpenetrating network or a phase-separated network. In food colloids, the two most important proteinaceous gelling systems are gelatin and casein micelles. An example of a covalent protein–polysaccharide interaction is that produced when gelatin reacts with propylene glycol alginate under mildly alkaline conditions. Noncovalent nonspecific interaction occurs in mixed gels of gelatin with sodium alginate or low-methoxy pectin. In food emulsions containing protein and polysaccharide, any of the mentioned interactions may take place in the aqueous phase of the system. This results in specific structures with desirable rheological characteristics and enhanced stability. The nature of the protein–polysaccharide interaction affects the surface behaviour of the biopolymers and the aggregation properties of the dispersed droplets.

Weak protein–polysaccharide interactions may be exemplified by a mixture of milk protein (sodium casinate) and a hydrocolloid such as xanthan gum. Sodium casinate acts as the emulsifier and xanthan gum (with a molecular weight in the region of 2×10^6 Daltons) is widely used as a thickening agent and a synergistic gelling agent (with locust bean gum). In solution, xanthan gum exhibits pseudoplastic behaviour that is maintained over a wide range of temperature, pH and ionic strength. Xanthan gum at concentrations exceeding 0.1 % inhibits creaming of emulsion droplets by producing a gel-like network with a high residual viscosity. At lower xanthan gum concentrations (< 0.1 %) creaming is enhanced as a result of depletion flocculation. Other hydrocolloids such as carboxymethyl cellulose (with a lower molecular weight than xanthan gum) are less effective in reducing creaming of emulsions.

Covalent protein–polysaccharide conjugates are sometimes used to avoid any flocculation and phase separation that is produced with weak nonspecific protein–polysaccharide interactions. An example of such conjugates is that produced with globulin-dextran or bovine serum albumin-dextran. These conjugates produce emulsions with smaller droplets and narrower size distribution and they stabilize the emulsion against creaming and coalescence.

15.5 Polysaccharide–surfactant interactions

One of the most important aspects of polymer–surfactant systems is their ability to control stability and rheology over a wide range of compositions [6]. Surfactant molecules that bind to a polymer chain generally do so in clusters that closely resemble the micelles formed in the absence of polymer [7]. If the polymer is less polar or contains hydrophobic regions or sites, there is an intimate contact between the micelles and polymer chain. In such a situation, the contact between one surfactant micelle and two polymer segments will be favourable. The two segments can be in the same polymer chain or in two different chains, depending on the polymer concentration. For a dilute solution, the two segments can be in the same polymer chain, whereas in more concentrated solutions the two segments can be in two polymer chains with significant chain overlap. The crosslinking of two or more polymer chains can lead to network formation and dramatic rheological effects.

Surfactant–polymer interaction can be treated in different ways, depending on the nature of the polymer. A useful approach is to consider the binding of surfactant to a polymer chain as a cooperative process. The onset of binding is well defined and can be characterized by a critical association concentration (CAC). The CAC decreases with increasing alkyl chain length of the surfactant. This implies an effect of the polymer on surfactant micellization. The polymer is considered to stabilize the micelle by short- or long-range (electrostatic) interaction. The main driving force for surfactant self-assembly in polymer–surfactant mixtures is generally the hydrophobic interaction between the alkyl chains of the surfactant molecules. Ionic surfactants often interact significantly with both nonionic and ionic polymers. This can be attributed to the unfavourable contribution to the energetics of micelle formation from the electrostatic effects and their partial elimination due to charge neutralization or lowering of charge density. For nonionic surfactants, there is little to gain in forming micelles in the presence of a polymer and hence the interaction between nonionic surfactants and polymers is relatively weak. However, if the polymer chain contains hydrophobic segments or groups, e.g. with block copolymers, the hydrophobic polymer–surfactant interaction will be significant.

For hydrophobically modified polymers (such as hydrophobically modified hydroxyethyl cellulose or polyethylene oxide), the interaction between the surfactant micelles and the hydrophobic chains on the polymer can result in the formation of

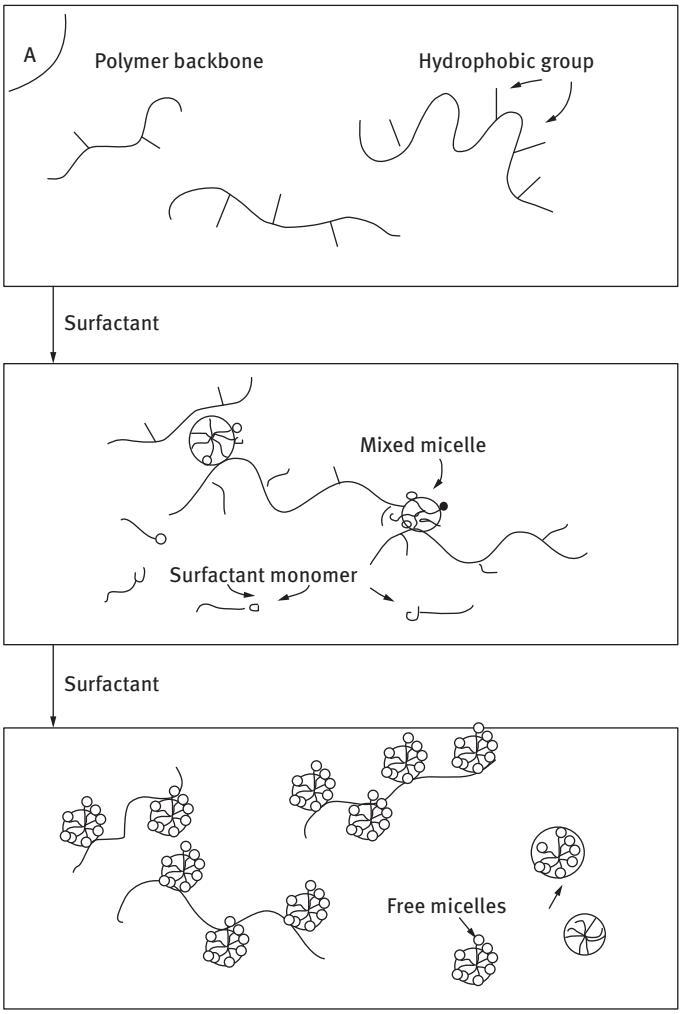

Fig. 15.1: Schematic representation of interaction between hydrophobically modified polymer chains and surfactant micelles.

crosslinks, i.e. gel formation. This is schematically represented in Fig. 15.1. However, at high surfactant concentrations, there will be more micelles that can interact with the individual polymer chains and the crosslinks are broken.

The above interactions are manifested in the variation of viscosity with surfactant concentration. Initially, the viscosity shows an increase with increasing surfactant concentration, reaching a maximum and then decreases with any further increase in surfactant concentration. The maximum is consistent with the formation of crosslinks and the decrease after that indicates destruction these crosslinks (see Fig. 15.1).

References

[1] Mierovitch H, Scheraga HA. Macromolecules. 1980;13:1406.
[2] Tanford C. Adv Protein Chem. 1970;24:1.
[3] Mobius D, Miller R, editors. Proteins at liquid interfaces. Amsterdam: Elsevier; 1998.
[4] de Gennes PG. Scaling concepts of polymer physics. Ithaca: Cornell University Press; 1979.
[5] Larsson K. J Dispersion Sci Technol. 1980;1:267.
[6] Dickinson E, Walstra P, editors. Food colloids and polymers: Stability and mechanical properties. Royal Society of Chemistry Publication; 1993.
[7] Goddard ED, Ananthapadmanqabhan KP, editors. Polymer-surfactant interaction. Boca Raton: CRC Press; 1992.

16 Surfactant association structures, microemulsions and emulsions in food

A typical phase diagram of a ternary system of water, ionic surfactant and long chain alcohol (cosurfactant) is shown in Fig. 16.1. The aqueous micellar solution A solubilizes some alcohol (spherical normal micelles), whereas the alcohol solution dissolves huge amounts of water-forming inverse micelles, B. These two phases are not in equilibrium with each other, but are separated by a third region, namely the lamellar liquid crystalline phase. These lamellar structures and their equilibrium with the aqueous micellar solution (A) and the inverse micellar solution (B) are the essential elements for both microemulsion and emulsion stability [1, 2].

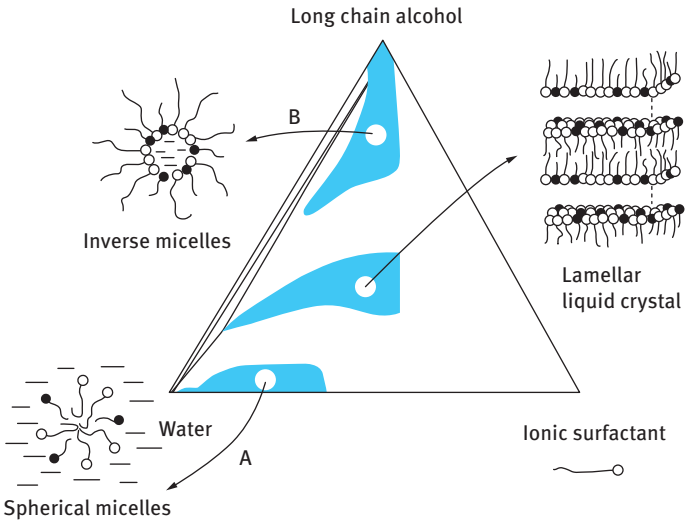

Fig. 16.1: Ternary phase diagram of water, an anionic surfactant and long chain alcohol (cosurfactant).

Microemulsions are thermodynamically stable and they form spontaneously (primary droplets few nms in size), whereas emulsions are not thermodynamically stable since the interfacial free energy is positive and dominant in the total free energy. This difference can be related to the difference in bending energy between the two systems [3]. With microemulsions, containing very small droplets, the bending energy (negative contribution) is comparable to the stretching energy (positive contribution) and hence the total surface free energy is extremely small ($\approx 10^{-3}$ mN m^{-1}). With macroemulsions, on the other hand, the bending energy is negligible (small curvature of the large emulsion drops) and hence the stretching energy dominates the total sur-

https://doi.org/10.1515/9783110578997-017

face free energy, which is now large and positive (few mN m^{-1}). The microemulsion may be related to the micellar solutions A and B shown in Fig. 16.1. A W/O microemulsion is obtained by adding a hydrocarbon to the inverse micellar solution B, whereas an O/W microemulsion emanates from the aqueous micellar solution A. These microemulsion regions are in equilibrium with the lamellar liquid crystalline structure. To maximize the microemulsion region, the lamellar phase has to be destabilized, as for example by the addition of a relatively short chain alcohol such as pentanol. In contrast for a macroemulsion, with its large radius, the parallel packing of the surfactant/cosurfactant is optimal and hence the cosurfactant should be of chain length similar to that of the surfactant.

From the above discussion, it is clear that a surfactant/cosurfactant combination for a microemulsion is of little use to stabilize an emulsion. This is a disadvantage when a multiple emulsion of the W/O/W type is to be formulated and the W/O system is a microemulsion. This problem has been resolved by Larsson et al. [4], who used a surfactant combination to stabilize the microemulsion and a polymer to stabilize the emulsion.

The formulation of food systems as microemulsions is not easy, since addition of triglycerides to inverse micellar systems results in a phase change to a lamellar liquid crystalline phase. The latter has to be destabilized by other means than adding cosurfactants, which are normally toxic. An alternative approach to destabilizing the lamellar phase is to use a hydrotrope, a number of which are allowed in food products.

As discussed in Chapter 14, for emulsion stabilization in food systems lamellar liquid crystalline structures are ideal. Friberg and co-workers [5, 6] attributed the enhanced stability of emulsions formed with mixtures of surfactants to the formation of three-dimensional structures, namely, liquid crystals. These structures can form, for example, in a three-component system of surfactant, alcohol and water, as illustrated in Fig. 16.2. The lamellar liquid crystalline phase, denoted by N (neat phase) in the phase diagram, is particularly important for stabilizing the emulsion against coalescence. In this case, the liquid crystals "wrap" around the droplets in several layers as will be illustrated below. These multilayers form a barrier against coalescence as will be discussed below. Friberg et al. [5] have given an explanation in terms of the reduced attractive potential energy between two emulsion droplets, each surrounded by a layer of liquid crystalline phase. They have also considered changes in the hydrodynamic interactions in the interdroplet region; this affects the aggregation kinetics.

Friberg et al. [5] have calculated the effect on the van der Waals attraction of the presence of a liquid crystalline phase surrounding the droplets. A schematic representation of the flocculation and coalescence of droplets with and without a liquid crystalline layer is shown in Fig. 16.3.

The upper part of Fig. 16.3 (A to F) represents the flocculation process when the emulsifier is adsorbed as a monomolecular layer. The distance d between the water droplets decreases to a distance m at which the film ruptures and the droplets coalesce; m is chosen to correspond to the thickness of the hydrophilic layers in the

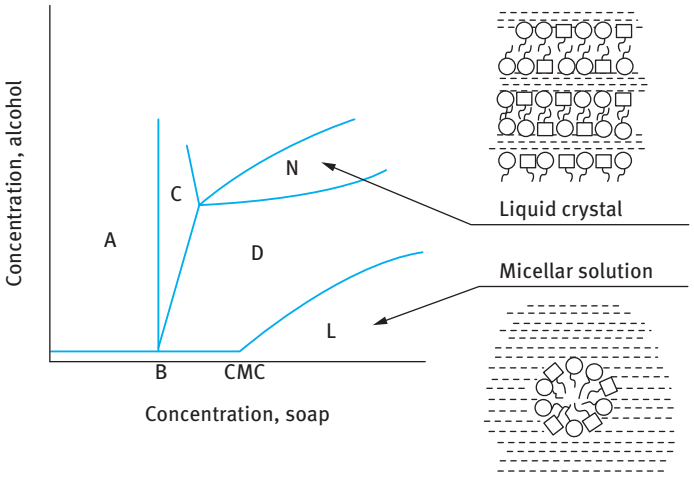

Fig. 16.2: Phase diagram of surfactant–alcohol–water system.

liquid crystalline phase. This simplifies the calculations and facilitates comparison with the case in which the liquid crystalline layer is adsorbed around the droplets.

The flocculation process for the case of droplets covered with liquid crystalline layers is illustrated in the lower part of Fig. 16.3 (B to M). The oil layer between the droplets thins to thickness *m*. The coalescence process which follows involves the removal of successive layers between the droplets until a thickness of one layer is reached (F); the final coalescence step occurs in a similar manner to the case for a monomolecular layer of adsorbed surfactant.

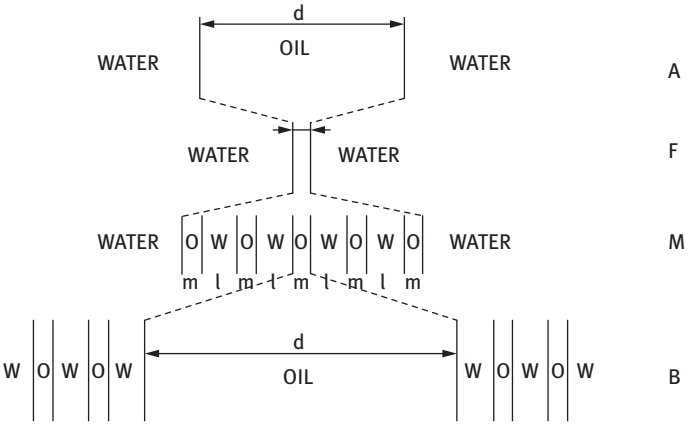

Fig. 16.3: Schematic representation of flocculation and coalescence in the presence and absence of liquid crystalline phases.

For case A, the van der Waals attraction is given by the expression,

$$G_A = -\frac{A}{12\pi d^2}, \tag{16.1}$$

where A is the effective Hamaker constant,

$$A = (A_{11}^{1/2} - A_{22}^{1/2})^2, \tag{16.2}$$

where A_{11} and A_{22} are the Hamaker constants of the two phases.

For case B, G_B can be obtained from the algebraic summation of this expression for the aqueous layer on each side of the central layer. The ratio G_B/G_A is then given by,

$$\frac{G_B}{G_A} = d^2 \left\{ \sum_{p=0}^{n} \sum_{q=0}^{n} [d + (p+q)(l+m)]^{-2} + \sum_{p=0}^{n-1} \sum_{q=0}^{n-1} [d + 2l + (p+q)(l+m)]^{-2} - \sum_{p=0}^{n} \sum_{q=0}^{n-1} [2(d+l) + (p+q)(l+m)]^{-2} \right\}, \tag{16.3}$$

where l and m are the thicknesses of the water and oil layers, n is the number of water layers (which is equal to the number of oil layers), and p and q are integers.

The free energy change associated with coalescence (i.e., M → F) is calculated from the variation of the van der Waals interaction across the droplet walls. This treatment reflects the energy change associated with the layers squeezed out from the interdroplet region. The problem is circumvented by assuming that these displaced layers adhere to the enlarged droplets so that their free energy is not significantly changed in the process. In this manner, the ratio of the interaction energies in the states F and M is obtained from summation of the van der Waals interactions from the individual layers on the water parts, i.e.,

$$\frac{G_M}{G_F} = m^2 \left\{ \sum_{p=0}^{n} [(m+p)(m+l)]^{-2} - \sum_{p=0}^{n} [(p+l)(m+l)]^{-2} \right\}. \tag{16.4}$$

To illustrate the relative importance of the van de Waals attraction energy, calculations were made using the above expressions, for the case of flocculation (i.e. A and B) and for the case of coalescence (i.e. F and M). The results are given in Fig. 16.4 (a) and 16.4 (b), respectively.

Fig. 16.4 (a) shows that the influence on the flocculation process of liquid crystalline layers around the droplets is insignificant. In contrast, the effect on the free energy change is quite significant. For example, with nine layers on each droplet and a layer thickness of reasonable magnitude ($l = m = 5$ nm), the total van der Waals interaction is reduced to only 10 % of its original value for the coalescence process in

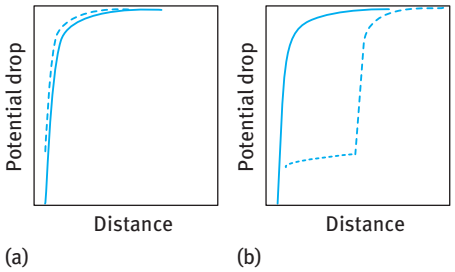

Fig. 16.4: Van der Waals potential energy–distance curves for flocculation (a) and coalescence (b) in the presence (---) and absence (—) of liquid crystalline phases.

the case of the layer structure. This is to be compared with 98 % in the case of two droplets at the same distance, but separated by the oil phase instead of the liquid crystalline phase. Even more important are the extremely small changes in attraction energy after removal of the first layers. The first layers give a drop corresponding to 1.5 % of the total van der Waals interaction energy (A to F). The last layer, before the state F is reached, corresponds to 78 % of the total van der Waals energy. It seems, therefore, that the presence of a liquid crystalline phase has a pronounced influence on the distance dependence of the van der Waals energy, leading to a drastic reduction in the force of attraction between the emulsion droplets.

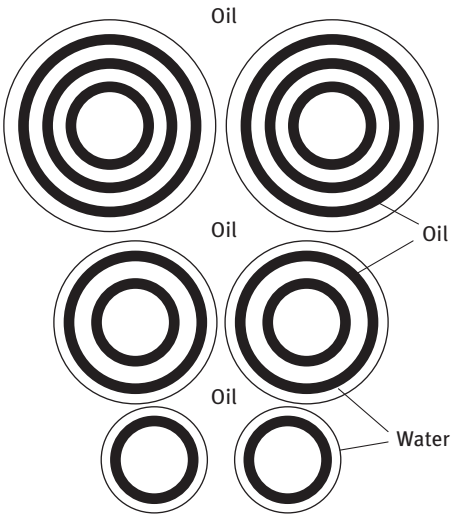

Fig. 16.5: Schematic representation of emulsions containing liquid crystalline structures.

A schematic representation of the role of liquid crystalline phases in reducing emulsion coalescence is shown in Fig. 16.5.

The process of coalescence occurs in two stages: first the layers of liquid crystals are removed two by two and the terminal stage is the disruption of the final bilayer of the structure. The initiation of the flocculation process leads to very small energy changes and good stability is assumed as long as the liquid crystal remains adsorbed.

This adsorption is the result of its structure. At the interface, the final layer towards the aqueous phase terminates with the polar group, while the layer towards the oil finishes with the methyl layer. In this manner, the interfacial free energy is a minimum.

References

[1] Tadros T. Emulsions. Berlin: De Gruyter; 2016.
[2] Tadros T. Applied surfactants. Weinheim: Wiley-VCH; 2005.
[3] Friberg SE, Kayali I. In: El-Nokaly M, Cornell D, editors. Microemulsions and emulsions in food. ACS Symposium Series 448; 1991. p. 7.
[4] Larsson K. J Dispersion Sci Technol. 1980;1:267.
[5] Friberg S, Jansson PO, Cederberg E. J Colloid Interface Sci. 1976;55:614.
[6] Jansson PO, Friberg SE. Mol Cryst Liq Cryst. 1976;34:75.

17 Rheology of food emulsions

17.1 Interfacial rheology

It has long been argued that interfacial rheology, namely interfacial viscosity and elasticity, plays an important role in emulsion stability. This is particularly the case with mixed surfactant films (which may also form liquid crystalline phases) and polymers such as hydrocolloids and proteins that are commonly used in food emulsions.

A fluid interface in equilibrium exhibits an intrinsic state of tension that is characterized by its interfacial tension γ, which is given by the change in free energy with area of the interface, at constant composition n_i and temperature T,

$$\gamma = \left(\frac{\partial G}{\partial A}\right)_{n_i,T} \tag{17.1}$$

The unit for γ is energy per unit area (mJ m^{-1}) or force per unit length (mN m^{-1}), which are dimensionally equivalent. Adsorption of surfactants or polymers lowers the interfacial tension and this produces a two-dimensional surface pressure π that is given by,

$$\pi = \gamma_0 - \gamma, \tag{17.2}$$

where γ_0 is the interfacial tension of the "clean" interface (before adsorption) and γ that after adsorption.

The interface is considered to be a macroscopically planer, dynamic fluid interface. Thus, the interface is regarded as a two-dimensional entity independent of the surrounding three-dimensional fluid. The interface is considered to correspond to a highly viscous insoluble monolayer and the interfacial stress, σ_s, acting within such a monolayer is sufficiently large compared to the bulk-fluid stress acting across the interface and in this way one can define an interfacial shear viscosity η_s,

$$\sigma_s = \eta_s \dot{\gamma}, \tag{17.3}$$

where γ is the shear rate. η_s is given in surface Pa s (N m^{-1} s) or surface poise (dyne cm^{-1} s). It should be mentioned that the surface viscosity of a surfactant-free interface is negligible and it can reach high values for adsorbed rigid molecules such as proteins.

Many surface viscometers utilize torsional stress measurements upon a rotating ring, disk or knife edge (shown schematically in Fig. 17.1) within or near to the liquid/liquid interface [1]. This type of viscometer is moderately sensitive; for a disk viscometer the interfacial shear viscosity can be measured in the range $\eta_s \geq 10^{-2}$ surface Pa s. The disk is rotated within the plane of the interface with angular velocity ω. A torque is exerted upon the disk of radius R by both the surfactant film with surface viscosity η_s and the viscous liquid (with bulk viscosity η) that is given by the expression,

$$M = (8/3)R^3\eta\omega + 4\pi R^2\eta_s\omega. \tag{17.4}$$

https://doi.org/10.1515/9783110578997-018

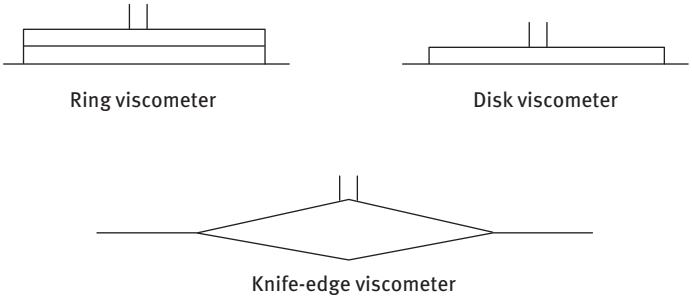

Fig. 17.1: Schematic representation of surface viscometers.

The interfacial dilational (Gibbs) elasticity ε, which is an important parameter in determining emulsion stability (reduction of coalescence during formation), is given by the following equation,

$$\varepsilon = \frac{\mathrm{d}\gamma}{\mathrm{d}\ln A}, \tag{17.5}$$

where $\mathrm{d}\gamma$ is the change in interfacial tension during expansion of the interface by an amount $\mathrm{d}A$ (referred to as interfacial tension gradient resulting from nonuniform surfactant adsorption on expansion of the interface). One of the most convenient methods for measuring ε is to use a Langmuir trough with two moving barriers for expansion and compression of the interface. Another method for measuring ε is to use the oscillating bubble technique for which instruments are commercially available.

A useful method for measuring ε is the pulsed drop method [2]. Rapid expansion of a droplet at the end of a capillary from a radius r_1 to r_2 is obtained by application of pressure. The pressure drop within the droplet is measured as a function of time using a sensitive pressure transducer. From the pressure drop one can obtain the interfacial tension as a function of time. The Gibbs dilational elasticity is determined from values of the time-dependent interfacial tension. Measurements can be made as a function of frequency as illustrated in Fig. 17.2 for stearic acid at the decane-water interface at pH = 2.5.

Measuring the dilational viscosity is more difficult than measuring the interfacial shear viscosity. This is due to the coupling between dilational viscous and elastic components. The most convenient method for measuring dilational viscosity is the maximum bubble pressure technique that can only be applied at the air/water interface. According to this technique, the pressure drop across the bubble surface at the instant when the bubble possesses a hemispherical shape (corresponding to the maximum pressure) is due to a combination of bulk viscous, surface tension and surface dilational viscosity effects and this allows one to obtain the interfacial dilational viscosity.

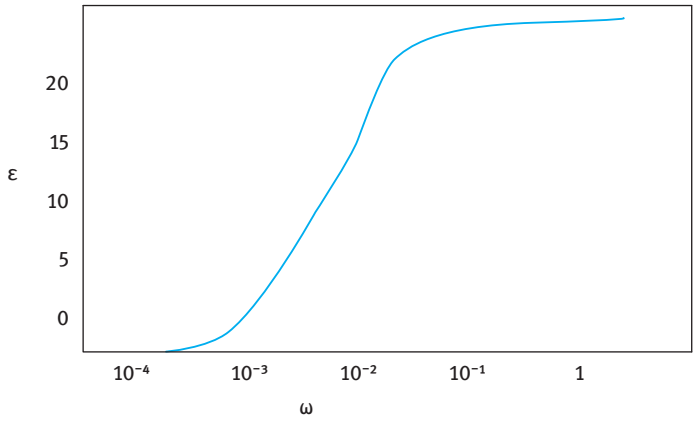

Fig. 17.2: Gibbs dilational elasticity versus frequency.

Most adsorbed surfactant and polymer coils at the oil/water (O/W) interface show non-Newtonian rheological behaviour. The surface shear viscosity η_s depends on the applied shear rate, showing shear thinning at high shear rates. Some films also show Bingham plastic behaviour with a measurable yield stress. Many adsorbed polymers and proteins show viscoelastic behaviour and one can measure viscous and elastic components using sinusoidally oscillating surface dilation. For example, the complex dilational modulus ε^* obtained can be split into an "in-phase" (the elastic component ε') and "out-of-phase" (the viscous component ε'') components. Creep and stress relaxation methods can be applied to study viscoelasticity.

17.2 Correlation of emulsion stability with interfacial rheology

17.2.1 Mixed surfactant films

Prins et al. [3] found that a mixture of sodium dodecyl sulphate (SDS) and dodecyl alcohol give a more stable O/W emulsion when compared to emulsions prepared using SDS alone. This enhanced stability is due to the higher interfacial dilational elasticity ε for the mixture when compared to that of SDS alone. Interfacial dilational viscosity did not play a major role since the emulsions are stable at high temperature at which the interfacial viscosity becomes lower. This correlation is not general for all surfactant films since other factors such as thinning of the film between emulsion droplets (which depends on other factors such as repulsive forces) can also play a major role.

17.2.2 Protein films

Biswas and Haydon [4] found some correlation between the viscoelastic properties of protein (albumin or arabinic acid) films at the O/W interface and the stability of emulsion drops against coalescence. Viscoelastic measurements were carried out using creep and stress relaxation measurements (using a specially designed interfacial rheometer). A constant torque or stress σ (mN m^{-1}) was applied and the deformation γ was measured as a function of time for 30 minutes. After this period, the torque was removed and γ (which changes sign) was measured as a function of time to obtain the recovery curve. The results are illustrated in Fig. 17.3. From the creep curves one can obtain the instantaneous modulus G_0 ($\sigma/\gamma_{\text{int}}$) and the surface viscosity η_s from the slope of the straight line (which gives the shear rate) and the applied stress. G_0 and η_s are plotted versus pH as shown in Fig. 17.4. Both show an increase with increasing pH, reaching a maximum at pH $\approx$ 6 (the isoelectric point of the protein) at which the protein molecules show maximum rigidity at the interface. The stability of the emulsion was assessed by measuring the residence time t of several oil droplets at a planer O/W interface containing the adsorbed protein. Fig. 17.4 shows the variation of $t_{1/2}$ (time taken for half the number of oil droplets to coalesce with the oil at the O/W interface) with pH. Good correlation between $t_{1/2}$ and G_0 and η_s is obtained.

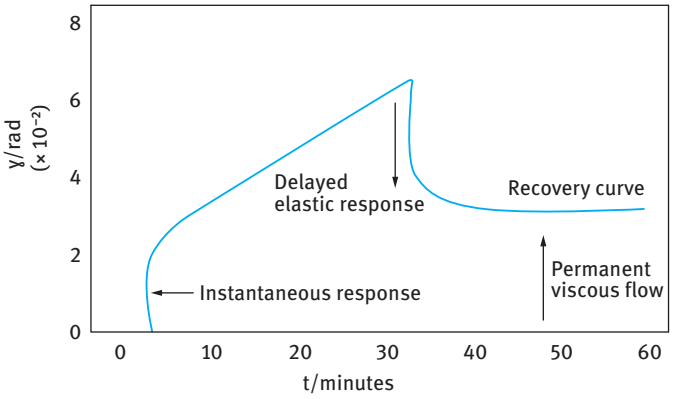

Fig. 17.3: Creep curve for protein film at the O/W interface.

Biswas and Haydon [4] derived a relationship between coalescence time τ and surface viscosity η_s, instantaneous modulus G_0 and adsorbed film thickness h,

$$\tau = \eta_s \left[3C' \frac{h^2}{A} - \frac{1}{G_0} - \phi(t) \right], \tag{17.6}$$

where $3C'$ is a critical deformation factor, A is the Hamaker constant and $\phi(t)$ is the elastic deformation per unit stress.

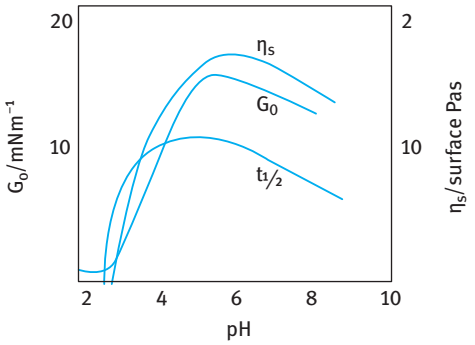

Fig. 17.4: Variation of $t_{1/2}$, G_0 and η_s with pH.

Equation (17.6) shows that τ increases with increasing η_s, but most importantly it is directly proportional to h^2. These results show that viscoelasticity is necessary but not sufficient to ensure stability against coalescence. To ensure stability of an emulsion one must make sure that h is large enough and film drainage is prevented.

17.3 Bulk rheology of emulsions

For rigid (highly viscous) oil droplets dispersed in a medium of low viscosity such as water, the relative viscosity η_r of a dilute (volume fraction $\phi \leq 0.01$) O/W emulsion of non-interacting droplets behaves as "hard spheres" (similar to suspensions). In this case, η_r is given by the Einstein equation [5],

$$\eta_r = 1 + [\eta]\phi, \tag{17.7}$$

where $[\eta]$ is the intrinsic viscosity that is equal to 2.5 for hard spheres.

For droplets with low viscosity (comparable to that of the medium), the transmission of tangential stress across the O/W interface, from the continuous phase to the dispersed phase, causes liquid circulation in the droplets. Energy dissipation is less than that for hard spheres and the relative viscosity is lower than that predicted by the Einstein equation. For an emulsion with viscosity η_i for the disperse phase and η_0 for the continuous phase,

$$[\eta] = 2.5\left(\frac{\eta_i + 0.4\eta_0}{\eta_i + \eta_0}\right). \tag{17.8}$$

Clearly when $\eta_i \gg \eta_0$, the droplets behave as rigid spheres and $[\eta]$ approaches the Einstein limit of 2.5. In contrast, if $\eta_i \ll \eta_0$ (as is the case for foams), $[\eta] = 1$. In the presence of viscous interfacial layers, equation (17.8) is modified to take into account the surface shear viscosity η_s and surface dilational viscosity μ_s

$$[\eta] = 2.5\left(\frac{\eta_i + 0.4\eta_0 + \xi}{\eta_i + \eta_0 + \xi}\right), \tag{17.9}$$

$$\xi = \frac{(2\eta_s + 3\mu_s)}{R}, \tag{17.10}$$

where R is the droplet radius.

When the volume fraction of droplets exceeds the Einstein limit, i.e. $\phi > 0.01$, one must take into account the effect of Brownian motion and interparticle interactions. The smaller the emulsion droplets, the more important the contribution of Brownian motion and colloidal interactions. Brownian diffusion tends to randomize the position of colloidal particles, leading to the formation of temporary doublets, triplets, etc. The hydrodynamic interactions are of longer range than the colloidal interactions and they come into play at relatively low volume fractions ($\phi > 0.01$), resulting in ordering of the particles into layers and tending to destroy the temporary aggregates caused by Brownian diffusion. This explains the shear thinning behaviour of emulsions at high shear rates.

For the volume fraction range $0.01 < \phi < 0.2$, Batchelor [6] derived the following expression for a dispersion of hydrodynamically interacting hard spheres,

$$\eta_r = 1 + 2.5\phi + 6.2\phi^2 + \vartheta\phi^3 \tag{17.11}$$

The second term in equation (17.11) is the Einstein limit, the third term accounts for hydrodynamic (two-body) interaction while the fourth term relates to multi-body interaction.

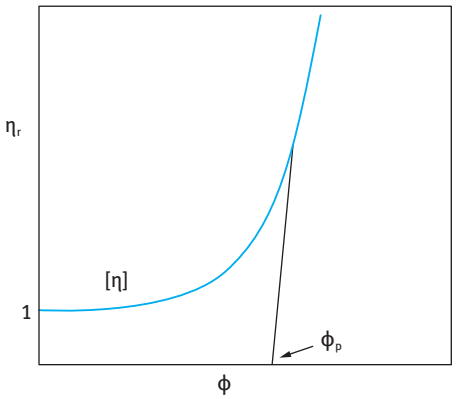

Fig. 17.5: η_r–ϕ curve.

At higher volume fractions ($\phi > 0.2$), η_r is a complex function of ϕ and the η_r–ϕ curve is schematically shown in Fig. 17.5. This curve is characterized by two asymptotes, $[\eta]$ the intrinsic viscosity and ϕ_p the maximum packing fraction.

A good semi-empirical equation that fits the curve is given by Dougherty and Krieger [7, 8],

$$\eta_r = \left(1 - \frac{\phi}{\phi_p}\right)^{-[\eta]\phi_p}. \tag{17.12}$$

17.4 Formation of networks

One of the important factors that affect the rheology of food emulsions is the presence of "networks" that are produced by the droplets or by the thickeners. These "networks" or "gels" control the consistency of the product and hence its acceptability by the customer. This can be illustrated from the work of van den Tempel [9] and Papenhuizen [10] who studied "gels" consisting of 25 % glyceryl stearate in paraffin oil (a model system for margarine). Creep experiments at various stress values showed an increase in strain (shear) γ, under constant stress τ, with time t. The data could be fitted empirically to an equation of the form,

$$\gamma = \frac{\tau}{G_1} + \frac{\tau}{G_2} \log t, \tag{17.13}$$

where G_1 and G_2 are the "rapid" and "retarded" elastic moduli respectively. The results could be explained by postulating two types of bonds between the particles in a network. The primary bonds (crystal bridges) were assumed to remain unbroken, whereas the secondary bonds (assumed to be due to van der Waals bonds) were broken under the influence of a stress and will reform in another relaxed position. The latter process gives rise to a retarded elastic behaviour. The relaxation of the reversible bonds causes an increasing part of the stress to be carried out by the irreversible bonds. Steady state stress–strain measurements, carried out at low shear rates, showed a rapid increase in stress, reaching a maximum that was followed by a decrease, reaching an equilibrium value at large deformation. This is schematically illustrated in Fig. 17.6. This behaviour was explained by assuming that the network structure was destroyed to such an extent that only non-interacting aggregates of particles remained. The only effect of the agglomerates was immobilization of the liquid.

The above behaviour at low and larger deformation has been analysed using a network model, in which the particles were assumed to be connected by van der Waals forces. The network was considered to consist of agglomerates of particles connected by chains. This is illustrated in Fig. 17.7, in which the network structure is subdivided

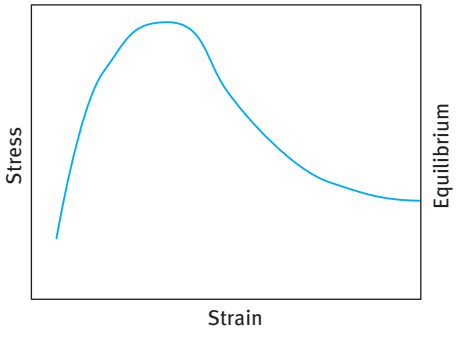

Fig. 17.6: Steady state stress–strain relationship (at low shear rate).

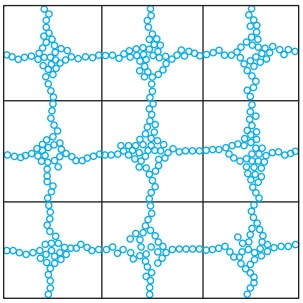

Fig. 17.7: Model of a network structure of a flocculated structure.

into small volume elements of characteristic size L, each consisting of one agglomerate. During the deformation process, stretching or tensile forces are applied to the network chain. Such forces will increase the distance between the rheological units (agglomerate or single particle). If this force reaches a critical value, the bond may break, depending on the time available. However, in large deformation, reformation of the bonds may also occur. This is due to compression, i.e. deformation in the lateral direction.

Using the above model, Papenhuizen [10] derived an expression for the viscosity coefficient, η_{I}, resulting from purely hydrodynamic effects, i.e.,

$$\eta_{\mathrm{I}} = \frac{\eta_0 \phi a}{H}, \tag{17.14}$$

where η_0 is the viscosity of the medium, ϕ is the volume fraction, a is the radius of the particles (assumed to be spherical) and H is the distance between two spheres.

Papenhuizen [10] derived an expression for the viscosity coefficient, η_{II}, resulting from the presence of an agglomerate. He considered the force required to move an agglomerate consisting of a large number of particles through a stationary viscous medium at a certain speed. Such a flow problem is similar to determining the velocity of a viscous liquid flowing through a stationary porous plug under the influence of a pressure gradient, e.g. using Darcy's law [11] and the Kozney–Carman equation [12]. Proceeding in this manner, the following expression for η_{II} was derived,

$$\eta_{\mathrm{II}} = \frac{CS^2}{2^{1/2}} \left(\frac{\phi}{1-\phi} \right)^2 \eta_0 L^2, \tag{17.15}$$

where C is a constant, that is equal to 5 for spheres, S is the surface area that is equal to $3/a$ for spheres. Equation (17.15) shows that η_{II} depends on S and hence on particle size. Large particles have small S resulting in a low value for η_{II}, whereas small particles give rise to a large value of η_{II}. The latter is also proportional to the square of the volume fraction of the disperse phase. This shows the importance of particle size and volume fraction in controlling the viscosity (consistency) of a food emulsion system.

17.5 Rheology of microgel dispersions

Many food colloids are thickened with elastic micro-networks of polymeric materials, eg. gelatinized starch granules. The rheology of these systems is determined by particle swelling and deformability. Evans and Lips [13] developed a theory for the elasticity of microgel dispersions and this theory was tested using dispersions of Sephadex particles (spherical crosslinked dextran moieties). However, when using non-retrograded starch dispersions, deviation from theoretical predictions was obtained. This was attributed to the presence of solubilized amylose. The effect of addition of dextran on the elasticity of Sephadex dispersions was also investigated. The results could be explained by polymer particle bridging or depletion flocculation. However, it could be concluded that bridging is unlikely since Sephadex and dextran are chemically similar. Thus, addition of dextran to the dispersion was assumed to cause depletion flocculation which provides an attractive component to the pair potential.

17.6 Fractal nature of the aggregated network

Considerable progress in describing the structure of aggregated particles has been made using the concept of fractals [14]. The complex structure of the aggregates is characterized by a single fractal dimension D, which describes a relation between the number N of particles in the aggregate and its typical radius R: $N \approx R^D$; the higher the value of D, the more compact is the aggregate structure. Fractal growth models have been successfully studies for two limited regimes of fractal aggregation:

(i) Diffusion-limited (or fast) aggregation characterized by $D = 1.7–1.8$.
(ii) Reaction limited (or slow) aggregation characterized by $D = 2.0–2.1$.

The fractal nature of the aggregates has important consequences for the rheology of dispersions. For example the fractal theory predicts a scaling law for the elastic modulus G' versus volume fraction ϕ in the form $G' \approx \phi^n$ with $n = (3 + x)/(3 - D)$, where x is the backbone fractal dimension that varies between 1 and 1.3. This concept has been applied by Vreeker et al. [15] for dispersions containing 0.5 % glycerol stearate in olive or paraffin oil. The fat crystals were obtained by rapid cooling of the melt from 90 °C to 2 °C, after which the dispersion temperature was increased to 25 °C. At this temperature rapid aggregation of the fat crystals was observed. The scattered light intensity $I(q)$ for the glycerol tristearate aggregates in olive or paraffin oil was measured as a function of the scattering vector q. Plots of $I(q)$ versus q gave a straight line, indicating the fractal nature of the fat aggregates. The fractal dimension D was calculated from the slope of the line and this was found to be 1.7; $I(q) \approx q - D$. This low value is characteristic of aggregates with a very open structure. This is consistent with a diffusion-limited aggregation dominated by attractive forces. However, aggregates with a low fractal dimension are sensitive to spontaneous restructuring or ageing

effects. D was found to increase from 1.7 to 2.0 over several days of storage. Measurements of the elastic modulus G' versus (% w/w) solid fat content (for glycerol tristearate in paraffin oil) also showed a straight line when log G' was plotted versus log(% w/w) and this gave $D = 2.0$, which compares well with the value obtained from light scattering for dilute dispersions. Log-log plots of yield value σ_β versus solid fat content (% w/w) also gave a straight line and this gave $D = 1.9$.

References

[1] Criddle DW. The viscosity and viscoelasticity of interfaces. In: Eirich FR, editor. Rheology. Vol. 3. New York: Academic Press; 1960. Chapter 11.
[2] Edwards DA, Brenner H, Wasan DT. Interfacial transport processes and rheology. Boston, London: Butterworth-Heinemann; 1991.
[3] Prins A, Arcuri C, van den Tempel M. J Colloid and Interface Sci. 1967;24:811.
[4] Biswas B, Haydon DA. Proc Roy Soc. 1963;A271:296. 1963;A2:317. Kolloid Z. 1962;185:31. 1962;186:57.
[5] Einstein A. Ann Physik. 1906;19:289. 1911;34:591.
[6] Bachelor GK. J Fluid Mech. 1977;83:97.
[7] Krieger IM, Dougherty TJ. Trans Soc Rheol. 1959;3:137.
[8] Krieger IM. Advances Colloid and Interface Sci. 1972;3:111.
[9] van den Tempel M. Rheol Acta. 1958;1:115. J Colloid Sci. 1961;16:284.
[10] Papenhuizen JMP. Rheol Acta. 1972;11:73.
[11] D'Archy H. Les Fantaines Publique de la Vill de Dijon. Paris; 1961.
[12] Carmen PC. Trans Inst Chem Eng. 1937;15:150.
[13] Evans ID, Lipps A. In: Dickinson E, Walstra P, editors. Food colloids and polymers: Stability and mechanical properties. Cambridge: Royal Society of Chemistry; 1993. p. 214.
[14] Meakin P. Advances Colloid Interface Sci. 1988;28:249.
[15] Vreeker R, Hoekstra LL, den Boer DC, Agterof WG. In: Dickinson E, Walstra P, editors. Food colloids and polymers: Stability and mechanical properties. Cambridge: Royal Society of Chemistry; 1993.

18 Food rheology and mouth feel

18.1 Introduction

As mentioned in Chapter 14, food systems are complex multiphase products that may contain dispersed components such as solid particles, liquid droplets or gas bubbles. The continuous phase may also contain colloidally dispersed macromolecules such as polysaccharides, proteins and lipids. These systems are non-Newtonian, showing complex rheology and usually plastic or pseudoplastic (shear thinning). Complex structural units are produced as a result of the interaction between the particles of the disperse phase as well as interaction with the polymers that are added to control the properties of the system, such as its creaming or sedimentation, as well as the flow characteristics. The control of rheology is important not only during processing but also for control of texture and sensory perception.

18.2 Rheological measurements

For adequate investigations of food rheology, it is essential to carry out well-defined rheological experiments. These experiments fall into two main categories, namely steady state shear stress–shear rate measurements and the possible time effects (thixotropy); and low deformation measurements of constant stress (creep) and dynamic (oscillatory) measurements. During the flow process, both viscous (shear and normal) and inertial stresses act on the fluid matrix. The flow stresses tend to impede or influence the interactions of the structural components. Above a critical stress, flow-induced structuring may occur. The structural states may be of a reversible or irreversible nature. These structural changes influence the rheological behaviour of the fluid system and consequently the flow process itself is affected.

The above structural changes can have a significant effect on the technical performance of the food product. Problems of creaming or sedimentation and phase separation are directly related to the product's rheological characteristics. It is, therefore, crucial to control the rheology of the food product to avoid problems during manufacture, during storage and with the sensory perception of the product.

The sensory perception of food texture is significantly dependent on the structure of the system (e.g. the nature of the three-dimensional units produced and the nature of the "gel" produced in the system) as well as its rheological behaviour. In a multiphase food product, such as an oil-in-water emulsion that contains surfactants for emulsification and polysaccharides that are added to reduce creaming, it is essential to relate the structure of the system to its rheology. This allows one to define the quality of the product in terms of its sensorial function (texture and consistency) as well as its technical function such as flow, dosing and storage stability.

https://doi.org/10.1515/9783110578997-019

To achieve the above objectives, it is essential to understand the colloid-chemical properties of the system as well as its flow characteristics under various conditions. Many food products (e.g. yoghurt) can be compared with the microstructure of particulate gels. The structure is formed from a continuous colloidal network, which holds the product together and gives rise to its characteristic properties. A colloidal network can be formed from particles linked together forming strands, enveloping pores and/or droplets, inclusions, etc. The size and shape of the particles, strands and pores may vary, thus creating different product properties.

During mastication, the structure breaks down and the sensory perception of the texture reflects such breakdown processes. Various subjective tests for sensory evaluation are used, e.g. manual texture (touching) by a light pressure with the forefinger, visual texture, mouth feel during manipulation of the sample in the mouth. In order to relate the rheological characteristics of the product to the above sensory evaluation, it is essential to carry out experiments under various deformation conditions.

Two main types of measurements are required:

(i) Steady state measurements of shear stress versus shear rate relationship to distinguish between the various responses: Newtonian, plastic, pseudoplastic and dilatant. Particular attention is given to time effects during flow (thixotropy and negative thixotropy).
(ii) Viscoelastic behaviour, stress relaxation, constant stress (creep) and oscillatory measurements.

In steady state measurements, one applies a constant and increasing shear rate, γ (s^{-1}), on the sample (which may be placed in a concentric cylinder, cone and plate or parallel plate platens) and the stress σ (Pa) is simultaneously measured. For Newtonian systems, the stress increases linearly with increasing shear rate and the slope of the shear stress–shear rate curve gives the Newtonian viscosity η (which is independent of the applied shear rate),

$$\sigma = \eta\gamma. \tag{18.1}$$

For a non-Newtonian system, as is the case with most food colloids, the stress–shear rate gives a pseudoplastic curve and the system is shear thinning, i.e. the viscosity decreases with increasing shear rate. In most cases the shear stress–shear rate curve can be fitted with the Herschel–Bulkley equation,

$$\sigma = \sigma_\beta + k\gamma^n, \tag{18.2}$$

where σ_β is the yield stress (that gives a measure of the "structure" in the system, e.g. its gel strength), k is the consistency index and n is the shear thinning index.

By fitting the experimental data to the above equation, one can obtain σ_β, k and n. The viscosity at any shear rate can then be calculated,

$$\eta = \frac{\sigma}{\gamma} = \frac{\sigma_\beta + k\gamma^n}{\gamma}. \tag{18.3}$$

Most food colloids show reversible time dependency of viscosity, i.e. thixotropy. If the system is sheared at any constant shear rate for a certain period of time, the viscosity shows a gradual decrease with increasing time. When the shear is removed, the viscosity returns to its initial value. This phenomenon can be understood from a consideration of the structure of the multiphase food colloid that contains particles and/or droplets, surfactants, hydrocolloids, etc. On shearing the sample, this structure is "broken down". When the shear is removed, the structure recovers within a certain timescale that depends on the sample. Thixotropy is investigated by applying sequences of shear stress–shear rates within well-defined time periods. If the shear rate is applied within a short period, e.g. increasing from 0 to 500 s^{-1} in one minute, then when reducing the shear rate from 500 to 0 s^{-1}, the structure of the sample cannot be recovered within this timescale. In this case, the shear stress–shear rate curves (the up and down curves) show large hysteresis, i.e. a large thixotropic loop is produced. By increasing the time of shear (say 5 minutes for the up curve and 5 minutes for the down curve), the loop closes. In this way one can investigate the thixotropy of the sample.

In constant stress (creep) measurements, one applies the stress (that is kept constant at each measurement) in small increasing increments. If the stress applied is below the yield stress, the system behaves as a viscoelastic solid. In this case, the strain shows a small increase at zero time and this strain remains virtually constant over the duration of the experiment (near zero shear rate). When the stress is removed, the strain returns back to zero. This behaviour will be the same at increasing stress values, provided the applied stress is still below the yield stress. Any increase in stress will be accompanied by an increase in strain at zero time. However, when the stress exceeds the yield stress, the system behaves as a viscoelastic liquid. In this case, the strain rapidly increases at zero time, giving a rapid elastic response characterized by an instantaneous compliance J_0 (the compliance is simply the ratio between the strain and applied stress, Pa^{-1}). At time larger than zero, the strain shows a gradual and slow increase with time. This is the region of retarded response (bonds are broken and reformed at different rates). Ultimately, the system shows a steady state (with constant shear rate), in which the compliance increases linearly with increasing time. The slope of this linear portion gives the reciprocal viscosity at the applied shear stress (slope = J/t = Pa^{-1}/s = $1/Pa\,s$ = $1/\eta_\sigma$). After the steady state is reached, the stress is then removed and the system shows partial recovery, i.e. the strain changes sign and decreases with time, reaching an equilibrium value. The creep curves are analysed to obtain the residual (zero shear) viscosity, i.e. the plateau value at low stresses (below the yield stress) and the critical stress, σ_{cr}, above which the viscosity shows a rapid decrease with any further decrease in stress. This critical stress may be denoted as the "true yield value". In addition, by fitting the compliance time curves to models, one can also obtain the relaxation time of the sample.

In dynamic (oscillatory) measurements, one applies a sinusoidal strain or stress (with amplitudes γ_0 or σ_0 and frequency ω in rad s^{-1}) and the stress or strain are mea-

sured simultaneously. For a viscoelastic system, the stress oscillates with the same frequency as the strain, but out of phase. From the time shift of stress and strain, one can calculate the phase angle shift δ. This allows one to obtain the various viscoelastic parameters: G^* (the complex modulus), G' (the storage modulus, i.e. the elastic component of the complex modulus) and G'' (the loss modulus or the viscous component of the complex modulus). These viscoelastic parameters are measured as a function of strain amplitude (at constant frequency) to obtain the linear viscoelastic region. G^*, G' and G'' are independent of the applied strain until a critical strain, γ_{cr}, above which G^* and G' begin to decrease with any further increase in strain, whereas G'' shows an increase. Below γ_{cr}, the structure of the system is not broken down, whereas above γ_{cr} the structure begins to break. From G' and γ_{cr} one can obtain the cohesive energy density of the structure E_c. The viscoelastic parameters are then measured as a function of frequency at constant strain (that is kept within the linear viscoelastic region). For a viscoelastic liquid, G^* and G' increase with increasing frequency and ultimately both values reach a plateau that becomes independent of frequency. G'' shows an increase with increasing frequency, reaching a maximum at a characteristic frequency ω^* and then it decreases with a further increase in frequency, reaching almost zero at high frequency (in the region of the plateau region of G'). From ω^* one can calculate the relaxation time of the sample ($t_{relaxation} = 1/\omega^*$).

The above measurements are essential before one can go into detail of relating rheology to sensory evaluation, e.g. mouth feel which will be discussed below.

18.3 Mouth feel of foods – the role of rheology

Food products are generally designed with an optimum "consistency" for application in cutting, slicing, spreading or mixing. During eating and mastication, the food loses its initial "consistency", at least partially. The mouth feel of food products may be related to the loss of this initial "consistency". During the first stage of this mastication process, the food is comminuted by the action of the teeth into particles (few mm in size). At this stage, the food is close to its initial "consistency".

Thus, in the first stages of mastication, the mouth feel may be related to its rheological characteristics. It is, therefore, possible to relate the mouth feel during the first stages of mastication to the rheological parameters such as "yield value", "creep compliance", "storage modulus", etc. After the initial stages of comminution, the food particles "soften" as a result of temperature rise and moisture uptake in the oral cavity. This results in significant reduction in "consistency", which may reach values of stresses comparable to the level encountered by the saliva flow in the oral cavity. When these stresses are reached, the food particles will be broken down to much smaller size which is determined by the hydrodynamics of the "flowing" saliva. The flow of saliva is rather complex and calculating the shear stresses is not straightforward.

When the above stage is reached, the food product will form a "homogeneous" mix with the saliva and the mouth feel will appear smooth. It is clear that if the "consistency" of the product does not decrease to a sufficient degree (such that the stresses are comparable to those encountered by the saliva flow), the masticated food will remain "thicker" and the mouth feel becomes unacceptable to the consumer (feel of "graininess", "stickiness" or "waxiness"). Controlling the "consistency" (rheological characteristics) of food products is essential for consumer acceptability and this may require sophisticated measurements and interpretation of the results obtained.

The size reduction of the food products during mastication controls the flavour release. Assuming the particles produced to be spherical, the time required for release is directly proportional to the square of the radius of the particles R (which is a measure of the surface area),

$$t \approx \frac{R^2}{D}, \tag{18.4}$$

where D is the diffusion coefficient of the flavour molecule that is inversely proportional to the viscosity of the medium (D is of the order of 10^{-9} m^2 s^{-1} in dilute aqueous foods and can be as low as 10^{-11} m^2 s^{-1} in fat foods).

For achieving adequate release of food flavours, R has to be reduced to $\approx 70\,\mu$m for aqueous foods and much smaller sizes for fat continuous foods. The break-up of food products in the saliva is determined by the balance of two forces:

(i) Hydrodynamic forces exerted by the saliva flow, which will deform the food product;
(ii) interfacial forces and rheological properties of the food product that resist the deformation.

To investigate the break-up of food products during mastication one needs to know the following parameters:

(i) The stress exerted by the saliva flow.
(ii) The interfacial tension between the food material and saliva, relevant to both non-aqueous and fat continuous products.
(iii) The rheological properties of the food products.

The relationship between the above forces and the droplets size of the product is exactly known for Newtonian liquids (e.g., oils). The break-up of Newtonian fluids in purely elongational flow is the most simple to analyse. Each element of volume is stretched without rotation of the direction of stretching. If the direction of stretching is not fixed, but it rotates, then in simple "shear flow" the rate of rotation of the axis of stretching and the rate of stretching are equal.

Using the above assumptions it is possible to predict the droplet diameter of Newtonian oils during break-up by the flow in the saliva. In elongational flow, the stress σ_c acting on each drop is approximately equal to the stress in the continuous phase

($\eta_c\gamma$, where η_c is the fluid viscosity and γ is the shear rate),

$$\sigma_c = \eta_c\dot{\gamma}. \tag{18.5}$$

The interfacial tension γ resists the deformation (i.e. it tries to keep spherical symmetry of the drops) and this effect can be accounted for by means of a "Young's modulus", E, equivalent to the Laplace pressure,

$$E = \frac{2\gamma}{R}. \tag{18.6}$$

The degree of deformation of the drop, ε_d, is the ratio between σ_c and E, i.e.,

$$\varepsilon_d = \frac{\sigma_c}{E} = \frac{\eta_c\dot{\gamma}R}{2\gamma}. \tag{18.7}$$

When drop elongation exceeds a certain value, the drop breaks up into smaller drops. ε_d is related to the capillary number Ω,

$$\Omega = \frac{\eta_c\dot{\gamma}d}{\gamma}, \tag{18.8}$$

where d is the droplet diameter. Note that $\Omega = 4\varepsilon_d$.

Using equations (18.7) and (18.8) one can obtain the droplet diameter from a knowledge of the stress acting on each drop (in elongational flow) and the interfacial tension at the oil/saliva interface. Alternatively, one can measure the droplet diameter of the oil drops produced in the saliva and from a knowledge of the viscosity of the saliva and of the interfacial tension of the oil/saliva interface one can estimate the stress in the flowing saliva. This is illustrated below.

18.3.1 Break-up of Newtonian liquids

The break-up of Newtonian liquids with various viscosities η_d can be investigated by mastication of small oil samples and measuring the resulting droplet size distribution, using a Coulter Counter or a Mastersizer. The samples are expectorated into a suitable surfactant solution, e.g. Tween (to prevent any coalescence during the measurements). η_d can be measured at 37 °C (body temperature) using a suitable rheometer (e.g. Haake-Rotovisco). The interfacial tension γ at the oil/saliva interface can be measured using the Wilhelmy plate method. A typical result for the oil/saliva interface is $\approx 15\,\mathrm{mN\,m^{-1}}$. The interfacial tension between oil and saliva can be systematically reduced by dissolving various amounts of lecithin in the oil phase. To calculate the capillary number, one needs to know σ_c. Initially, σ_c may be given an assumed value, say 1 Pa. The viscosity of saliva can be measured using the Haake and this is about 50 mPa s.

The experimental results using the above assumed value of σ_c are compared with the literature value for elongational flow. The measured d values were found to be

≈ 50 times lower than the literature value and this means that the actual saliva stress in the mastication process is ≈ 50 Pa. Under shear flow, there is a rapid increase in capillary number when $\eta_d/\eta_c > 1$.

18.3.2 Break-up of non-Newtonian liquids

Food products are usually non-Newtonian and they may be approximated by Bingham fluids,

$$\sigma = 2\sigma_\beta + \eta_{pl}\dot{\gamma}, \tag{18.9}$$

where $2\sigma_\beta$ is the yield stress in elongation (assumed to twice the yield stress in shear flow) and η_{pl} is the Bingham plastic viscosity.

"Soft" foods, e.g. salad dressing and yoghurt, show a Bingham-like consistency at room temperature. More "solid" foods, e.g. fat spreads, cheese and puddings become more liquid-like during mastication (melting and moisture uptake). The "yield stress" may decrease by several orders of magnitude during mastication. A "Bingham fluid" will only break-up when the stress exerted in the saliva (≈ 50 Pa) exceeds the yield stress of the food product. This means that the break-up of food products with a "yield stress" greater than ≈ 50 Pa is difficult in the oral cavity.

An example of a "model" food product with varying "yield stress" is a W/O emulsion that can be prepared by emulsification of water in an oil, such as ricinoleic acid or soya oil, using an emulsifier with low HLB number, such as polyglycerol ester. The yield stress of the resulting W/O emulsion can be systematically increased by increasing the water phase volume fraction, ϕ. The ratio of water to emulsifier should be kept constant in the above system. When $\phi = 0.6$, the emulsion is nearly Newtonian ($\sigma_\beta = 0$) and it becomes gradually more non-Newtonian as the water volume fraction increases, i.e. σ_β increases with increasing ϕ and may exceed 50 Pa when $\phi > 0.6$. During mastication, all emulsions show large drops, but the "Newtonian" emulsions with $\phi < 0.6$ showed a much larger number of small drops when compared with the non-Newtonian emulsions.

The above investigations, using droplet size analysis and microscopy investigations, can be used to study the effect of rheology on the "break-up" of non-Newtonian food products. They allow one also to study the mouth feel using panels and some correlations between rheology and mouth feel may be obtained.

18.4 Complexity of flow in the oral cavity

The flow in the oral cavity is not a "steady" flow and hence the break-up process is not simple. Break-up in the oral cavity can only occur when this flow is maintained long enough, longer than the relaxation time of the drops. For most viscous oils ($\eta_d \approx 6$ Pa s) and $\eta \approx 15$ mN m^{-2}, the drop relaxation time is $\approx 5 \times 10^{-3}$ s, giving an ultimate drop

size of ≈ 20 μm. A range of 200–2000 μm is initially produced with relaxation time of 5×10^{-2}–5×10^{-1} s respectively. Since these large drops break-up, the elongational flow remains steady for such periods of time. When one considers how the jaws and the tongue drive the saliva flow, one must conclude that the flow cannot be kept steady for much longer times. The limited duration of elongational flow in the oral cavity is more important for food products showing viscoelastic behaviour at large degrees of deformation, e.g. for products containing thickeners such as hydrocolloids. Many food products contain hydrocolloids such as xanthan gum which is added for physical stability reasons and also for the control of the consistency of the product. In the presence of other food materials that increase the hydrodynamic stresses on the material of interest (e.g. bread), the drops produced could be much smaller.

18.5 Rheology-texture relationship

During any flow process, whether during manufacture or during mastication of the food product, the flow stress affects the "structure" of the system, which in turn affects its rheological characteristics. The sensory perception and the mouth feel depend to a large extent on the structure of the system (e.g. its "gel" behaviour) as well as its response to the stresses exerted by flowing saliva in the oral cavity. Using colloid and interfacial methods to study the "structure" and various rheological methods to assess the response of the food material to various shear regimes allows one to obtain a "texture"-rheology relationship.

A good example to consider is oil-in-water (O/W) emulsions such as mayonnaise or sauces, which can be prepared using an industrial dispersing process. By controlling the energy input one can control the droplet size of the emulsion. These emulsions are usually "structured" by addition of emulsifier/"thickener" combinations such as proteins/polysaccharides. In laminar flow, the stresses acting in the gap of a dispersing process device are dominated by the viscous shear stress σ (viscosity × shear rate). For turbulent flow (which is the case for most dispersing devices), the so-called Reynold stress σ_R is the dominant factor. A critical shear stress σ_{crit} has to be exceeded for droplet break-up, i.e.,

$$\sigma_{\text{cr}} = \frac{We\,\gamma}{d}, \tag{18.10}$$

where *We* is the critical Weber number that is a function of the ratio of the viscosity of the disperse phase and that of the continuous medium,

$$We = f\left(\frac{\eta_{\text{d}}}{\eta_{\text{c}}}\right), \tag{18.11}$$

where η_{d} is the viscosity of the disperse phase, η_{c} is the viscosity of the continuous medium, γ is the interfacial tension and d is the droplet diameter.

An O/W emulsion of mayonnaise (using for example sunflower oil) can be prepared at various oil weight fractions, e.g. 0.14, 0.65 and 0.85, using an emulsifier such as modified starch. The droplet size distribution of the resulting emulsions could be measured using a Coulter Counter or Malvern Mastersizer (based on measurement of the light diffraction by the droplets). The texture of the mayonnaise could be assessed according to "spoonability" and mouth feel (using panels). Various rheological methods may be applied as discussed above.

Using the above emulsion systems, it was shown that in many cases the mean droplet size decreased with increasing the volume energy input E_v ($J\,m^{-3}$). In some cases, the mean droplet size showed an increase, after the initial increase, with increasing E_v. This could be due to emulsion droplet coalescence when E_v exceeded a critical value. Comparing the various rheological results showed that the "structural" changes produced are determined by the value of the elastic modulus G'. G' was measured at low strains (in the linear viscoelastic region) and at a frequency of 1 Hz. G' is an elastic parameter and hence it reflects the interdroplet interaction as well as any interaction with the thickener. Since G' is measured at low deformation, it causes "minimum" change in the structure of the system during the measurement. An increase in G' reflects an increase in interaction. For example, for O/W emulsions without any thickener, a decrease in droplet size increases the number of "contact" points between the emulsion droplets and this leads to an increase in G'. Any reduction in G' with increasing E_v (that leads to a decrease in droplet size) implies a reduction in the "networking" properties (produced for example by the emulsifier). When G' increases with increasing E_v (particularly for high oil phase volume fraction) this implies an increase in the "network" stability.

There seems to be a correlation between the sensorial texture parameter ("thickness" as measured by the spoon test) and the rheological parameters, G' (the storage modulus, the elastic component) and G'' (the loss modulus, the viscous component). One of the most useful parameters to measure is $\tan\delta$,

$$\tan\delta = \frac{G''}{G'}. \tag{18.12}$$

The reciprocal of $\tan\delta$ is referred to as the dynamic Weissenberg number Wi',

$$Wi' = \frac{1}{\tan\delta} = \frac{G'}{G''}. \tag{18.13}$$

Wi' is a measure of the relative magnitudes of the elastic to the viscous moduli. Many food products such as yoghurt, egg products, etc. can be compared with the microstructure of particulate gels. The structure is formed from a continuous colloidal network, which holds the product together and gives rise to its characteristic properties. A gel network structure can be formed from particles linked together forming strands, enveloping pores and/or droplets. During mastication the gel structure breaks down and the new "structure" formed is perceived as "texture". An example

of a gel network is protein gels formed for example from lactoglobulin. Several physical methods may be applied to characterize the gel produced. Image analysis and transmission electron microscopy could be applied to obtain the average pore size and particle size of the gel formed. Several rheological methods may be applied to study the properties of these gels:

(i) Large deformation measurements, for example tensile tested by fracturing the sample using an Instron.
(ii) Viscoelastic measurements (low deformation measurements) to obtain the storage and the loss modulus as well as the phase angle shift δ.

The low deformation measurements can be used to obtain quantitative information on the structure of the gel formed, for example the number of "crosslinks", the gel rigidity and its behaviour under low deformation.

The sensory tests which are carried out by panels (subjective tests) include manual texture measurement using light pressure with the forefinger, visual evaluation of the texture produced in a newly-cut surface and oral texture (mouth feel):

(i) Manual texture, soft, resistance to light pressure by finger; springy, recovery of shape after light pressure.
(ii) Visual texture, surface moisture – water released from a newly-cut surface; graininess of a newly-cut surface.
(iii) Oral texture, gritty during chewing; sticky, adherence to teeth after chewing; falling apart during chewing.

The perceived texture shows nonlinear dependence on the "microstructure". Gels formed at faster heating rates (12 °C/min) were more difficult to fracture when compared with gels formed at slower heating rates (1 °C/min). The gels formed at high heating rates have smaller pores; higher resistance to falling apart. The perception of "soft" and "springy" is related to the strand characteristic of the gel. Gels formed at slower heating rates (1 °C/min) have higher G' values when compared with those produced at higher heating rates (12 °C/min). Gels formed at 1 °C/minute have stiff strands formed of many particles joined together (resulting in higher G'). Gels formed of flexible strands have lower G' values. The strand characteristics can explain the gel texture as assessed by viscoelastic measurements.

For analysing the texture of gels one can perform two tests:

(i) Destructive (Instron test). This gives a measure of the overall network dimensions.
(ii) Non-destructive (viscoelastic measurements). The measured G' values are sensitive to the strand characteristics which can be evaluated using microscopy.

These measurements are carried out on gels produced under various conditions, such as heating rates, in order to arrive at the desired properties.

It can be concluded from the above discussion that a combination of microscopy, sensory analysis and rheological properties (obtained under high and low deforma-

tion) using statistical evaluation methods can provide a correlation between sensory perception (as evaluated by expert panels) and the various characteristics of the gel. The relationship between microstructure and texture is important in optimizing the properties of food products as well as in the development of new products with the desirable properties. Modern techniques of microscopy (such as freeze fracture) can be applied to study the microstructure of gels. The viscoelastic properties of gels, which can be studied using oscillatory techniques (under various conditions of applied strain and frequency) can be correlated to the microstructure.

18.6 Practical applications of food colloids

Processed foods are often colloidal systems such as suspensions, emulsions and foams. Examples of food emulsions, which are the most commonly used products, are milk, cream, butter, ice cream, margarine, mayonnaise and salad dressings. Emulsions are also prepared as an intermediate step in processing many foods, e.g. powdered toppings, coffee whiteners and cake mixes. These systems are dried emulsions that are re-formed into emulsion state by the consumer.

Milk and cream are oil-in-water (O/W) emulsions consisting of fat droplets (triglycerides partially crystalline and liquid oils) typically in the size range 1–10 μm. The fat content of milk is 3–4 % by volume, and that of cream is 10–30 % by volume. The aqueous disperse medium contain milk proteins, salts and minerals. The fat droplets are stabilized by lipoprotein, phospholipids and adsorbed casein. This produces a very stable system against coalescence, as a result of steric stabilization and the presence of a viscoelastic film at the O/W interface. The only instability process in milk is creaming, since the gravity force exerted by the droplets exceeds Brownian diffusion. This problem of creaming is eliminated by homogenizing the milk using a high pressure homogenizer. This reduces the droplet size to submicron range and the gravity force becomes smaller than the Brownian diffusion.

Ice cream is an O/W emulsion that is aerated to form a foam. The disperse phase consists of butterfat (cream) or vegetable fat, partially crystallized fat. The volume fraction of air in the foam is approximately 50 %. The continuous phase consists of water and ice crystals, milk protein and carbohydrates, e.g. sucrose or corn syrup. Approximately 85 % of the water content is frozen at −20 °C. The foam structure is stabilized by agglomerated fat globules forming the surface of air cells in the foam. The added surfactants act as “destabilizers”, controlling the agglomeration of the fat globules. The continuous phase is semi-solid and its structure is complex.

Both butter and margarine are W/O emulsions with the water droplets dispersed in a semi-solid fat phase containing fat crystals and liquid oil. With butter, the fat is partially crystallized triglycerides and liquid oil. Genuine milk fat globules are also present. The water droplets are distributed in a semi-solid plastic continuous fat phase. With margarine the continuous phase consists of edible fats and oils, partially

hydrogenated, of animal or vegetable origin. The dispersed water droplets are fixed in a semi-solid matrix of fat crystals. Surfactants are added to reduce the interfacial tension in order to promote emulsification during processing. The preparation of the W/O emulsion requires considerable energy to reduce the size of the dispersed phase droplets. Once the emulsion is produced, the whole system is chilled to enable the final emulsification and crystallization of the fat phase. The initial emulsion need not be very stable, since on cooling the water droplets become fixed in a semi-solid fat phase.

In the early development of margarine, egg yolk was first used as the emulsifier, since this contains lecithin and other phospholipids. Later, lipophilic emulsifiers such as monodiglycerides of long chain fatty acids (C_{16}–C_{18}) were used in combination with soybean lecithin. The emulsifiers produce water droplets in the size range 2–4 μm. The consistency of margarine is strongly related to the amount of crystalline fat (solid fat content, SFC) which can be determined using dilatometry or low-resolution NMR spectroscopy. The solid fat content of margarine is in the range 5–25 % at 20 °C. It is desirable to use fat blends that form small needle-shaped β′ crystals (about 1 μm long) which imparts good plasticity. One should avoid transformation of these small needle-shaped β′ crystals to the large β crystals during storage. This results in an undesirable grainy consistency ("sandiness"). The crystal morphology may be controlled by using sorbitan esters and their ethoxylates, ethoxylated fatty alcohols, citric acid esters of monoglycerides, diacetyl tartaric acid esters of monoglycerides, sucrose monostearate, sodium stearoyl lactylate and polyglycerol esters of fatty acids. It was found that sorbitan monostearate and citric acid esters of monoglycerides were most effective in preventing the crystallization of tristearin from the α to the β form. However, when used in emulsions, the surfactants become adsorbed at the O/W interface and only lipophilic surfactants with high oil solubility can act as crystal growth inhibitors.

Low calorie margarine contains at least 50 % water, 40 % fat and the balance being protein milks, salts, flavour, vitamins and emulsifiers (mainly monoglycerides and soybean lecithin). Some products are based on milk fat alone or in combination with vegetable fats. With such high water content, a stable interfacial film is required. It has been shown that saturated monoglycerides are superior to unsaturated monoglycerides in stabilizing the water droplets. This is due to the formation of liquid crystalline films at the W/O interface.

An important class of O/W emulsions in the food industry is mayonnaise and salad dressings. Mayonnaise is a semisolid O/W emulsion made from a minimum of 65 % edible vegetable oil, acidifying ingredients, e.g. vinegar, and egg yolk phosphatides as the emulsifying agent. The high volume fraction of oil does not favour the formation of an O/W emulsion and it is necessary to disperse the egg yolk in the water phase before addition of the oil phase. Colloid mills and other homogenizers must be used with care in order not to produce too small oil droplets (with high surface area), since then the emulsifier content would not be sufficient to cover the whole interface.

The main difference between mayonnaise and salad dressing is the oil content, which is lower with salad dressings. Thickening agents such as starch, cereal flour or hydrocolloids may be used. Egg yolk is the main emulsifying agent, but other food-grade surfactants may also be used, e.g. polysorbates or esters of monoglycerides. Addition of salt can enhance the emulsion stability as a result of its effect on protein conformation.

Several other food emulsions can be quoted such as coffee whiteners and cake emulsions. Coffee whiteners are O/W emulsions containing vegetable oils and fats covering the size range 1–5 μm and an oil volume fraction of 10–15 %. The aqueous continuous phase contains proteins, e.g. sodium casinate, carbohydrates, e.g. maltodextrin, salts and hydrocolloids. The emulsifying system consists of blends of non-ionic and anionic surfactant with adsorbed protein.

Cake emulsions are very complex systems of fats or oil in an aqueous phase containing flour, sugar, eggs and micro-ingredients. The mix is aerated during the mixing process and then further processed by baking. In many cake emulsions the air bubbles formed during mixing are located in the fat phase instead of the water phase. This is the case with high-ratio cakes that may contain 15–25 % plastic shortenings or margarine based on total batter weight. Fat-free cakes or high-ratio cakes made with liquid vegetable oils are aerated in the aqueous phase and the foam stability is provided by egg yolk and added surfactants. To obtain a satisfactory appearance, volume and texture, the shortening or margarine must have special properties with regard to the solid fat content and plasticity. Shortening containing fat crystals in the β′ form are ideal for entrapping and stabilizing the air cells. Unless egg yolk is present in the batter, the air cells in a fat particle tend to coalesce within the fat particles rather than be transferred as individual air cells in the aqueous phase. By heating during the baking process, the air cells are greatly enlarged by thermal expansion and by uptake of carbon dioxide from leavening agents and generated water vapour. At this point, the surface elasticity properties of the layers surrounding the air cells are very important. At the end of the baking process, the air cells become connected in an open network and the liquid fat droplets coalesce into a film which covers the inner surface of the air channels.

Surfactants play a major role in both fatless and fat-containing cakes. The types of surfactants commonly used are monoglycerides, polyglycerol esters, propylene glycol esters of fatty acids and polysorbates. These surfactants act as emulsifiers for the fat by reducing the interfacial tension, thus aiding the dispersion of the fat phase. Plastic shortenings may contain 6–10 % lipophilic surfactants such as monoglycerides, or propylene glycol esters of fatty acids. These surfactants have no influence on the air/fat surface tension. The fat-based aeration is, therefore, highly dependent on the plasticity of the fat phase, which is controlled by the type of fats and surfactants used.

Surfactants such as monoglycerides may also interact with the starch fraction of the batter and form an insoluble amylose complex. This reduces gelatinization in the cakes, resulting in a better cake structure with improved tenderness. In fat-free cakes,

special surfactant preparations in gel form or α-crystalline powder forms are often used as aerating agents. Monoglycerides of palmitic and stearic acids have been found to form liquid crystalline mesophases in cakes containing corn oil. These monoglycerides were found to encapsulate oil droplets at 94 °C by multilayer sheets. At higher temperatures, transition of monoglycerides from lamellar to cubic phases enhances the viscosity and this plays an important role in stabilizing the sponge cake batter during baking.

References

[1] de Bruijne DW, Hendrickx HACM, Alderliesten L, de Looff J. In: Dickinson E, Walstra P, editors. Food colloids and polymers: Stability and mechanical properties. Cambridge: Royal Society of Chemistry; 1993. p. 2014.

Index